Utah State University

DigitalCommons@USU

All Graduate Theses and Dissertations | Graduate Studies

5-2010

Investigating Characteristics of Lightning-Induced Transient Luminous Events Over South America

Matthew A. Bailey
Utah State University

Follow this and additional works at: https://digitalcommons.usu.edu/etd

 Part of the Physics Commons

Recommended Citation

Bailey, Matthew A., "Investigating Characteristics of Lightning-Induced Transient Luminous Events Over South America" (2010). *All Graduate Theses and Dissertations*. 972.
https://digitalcommons.usu.edu/etd/972

This Dissertation is brought to you for free and open access by the Graduate Studies at DigitalCommons@USU. It has been accepted for inclusion in All Graduate Theses and Dissertations by an authorized administrator of DigitalCommons@USU. For more information, please contact digitalcommons@usu.edu.



INVESTIGATING CHARACTERISTICS OF LIGHTNING-INDUCED TRANSIENT LUMINOUS EVENTS OVER SOUTH AMERICA

by

Matthew A. Bailey

A dissertation submitted in partial fulfillment
of the requirements for the degree

of

DOCTOR OF PHILOSOPHY

in

Physics

Approved:

_____	_____
Michael J. Taylor Major Professor	Jan J. Sojka Committee Member
_____	_____
Lawrence E. Hipps Committee Member	Bela G. Fejer Committee Member
_____	_____
W. Farrell Edwards Committee Member	Byron R. Burnham Dean of Graduate Studies

UTAH STATE UNIVERSITY
Logan, Utah

2010

Copyright © Matthew A. Bailey 2010
All Rights Reserved

ABSTRACT

Investigating Characteristics of Lightning-Induced Transient Luminous Events over South America

by

Matthew A. Bailey, Doctor of Philosophy

Utah State University, 2010

Major Professor: Dr. Michael J. Taylor
Department: Physics

Sprites, halos, and elves are members of a family of short-lived, luminous phenomena known as Transient Luminous Events (TLEs), which occur in the middle atmosphere. Sprites are vertical glows occurring at altitudes typically ranging from ~40 to 90 km. In video imagery they exhibit a red color at their top, with blue tendril-like structure at low altitudes. Elves are disk-like glows that occur at the base of the ionosphere, with diameters of ~100-300 km, and have very short lifetimes (~2-3 ms). Halos are diffuse glows that occur at low altitudes, have diameters <100 km, and have a duration that may last up to 10s of ms.

A majority of the studies of TLEs have taken place over the Midwestern U.S. where they were first discovered. This area produces large thunderstorms, which in turn generate large lightning discharges that have been associated with the formation of TLEs. Studies have used the low frequency radiation that initiates with these strokes to study

characteristics of these events. This low frequency radiation has been used to determine where large numbers of TLEs may occur. Extreme southern Brazil is a region of the globe believed to have many TLEs, but few studies on these phenomena.

Two collaborative campaigns involving Utah State University proceeded in 2002-2003, and in 2006. Multiple TLE images were made, proving this is, indeed, a region of the globe where these types of events are prominent. In particular, one storm in February 2003 produced over 440 TLEs imaged by USU video cameras. Of these events, over 100 of them had associated halos. Statistical studies for halos previously had been performed in the U.S., but never abroad. Also, several events from the February storm have been associated with negative cloud to ground lightning, a surprising occurrence, as to date, less than a handful of such events have ever been witnessed or published.

In analyzing the TLEs from this campaign, we have shown the halos are similar to those seen in the U.S., even though the storms may be somewhat different. Also, detailed analyses of the negative events show both temporal and spatial morphology heretofore never reported on.

(245 pages)

ACKNOWLEDGMENTS

In the game of baseball perfect games by a pitcher are extremely rare. In fact, only 18 pitchers have completed this remarkable feat in the history of Major League Baseball (as of 2009). Their names are immortalized in the history books. However, those pitchers were not alone on the baseball fields when they pitched their memorable games. There were shortstops, catchers, center fielders, etc., not to mention the coaches sitting in the dugout. There were also the little league, Pop-Warner, and high school coaches who helped that pitcher throughout the years. These people are not remembered by the masses, but they definitely had an influence on the outcome of those games.

When writing a dissertation, it is a similar process. Although it is my name on the cover, I could not have done it alone. I would like to thank a few of those who helped me along the way.

First and foremost, I must thank my advisor, Michael Taylor. He took me on as a graduate research student, and immediately started me with data analysis, traveling to different parts of the world on field campaigns, presenting at scientific conferences, and generally letting me feel my way into the scientific community. He has been extremely patient, gracious, and kind toward me, helping me to find my own path. He has done everything in his power to help me. I will be forever grateful.

Secondly, I am grateful to Dominique Pautet. "The Boss" is a master at resolving computer and software issues, has a keen understanding of data analysis, and is not bad company on a field campaign.

I also thank YuCheng Zhao, and Visjna Taylor. They were always behind the scenes fixing software issues, helping me with data analysis, and facilitating the research that I needed to finish this dissertation. I will always count them as great friends.

I need to thank my collaborators throughout the globe. In particular, I wish to thank Dr. Steven Cummer at Duke University, Jeremy Thomas, formerly of the University of Washington, and Walt Lyons, of FMA research in Fort Collins, CO. My research would not have been as successful without the coordination of data and collaboration with these colleagues. They have always been gracious in answering my questions, and still help me to learn more about this area of research. I would also like to acknowledge my Brazilian colleagues, both at INPE and at the University of Santa Maria, for providing logistical support for this study. This research was supported under NSF grants ATM 0355190 and ATM 0221968.

I also send my thanks to the physics department at Utah State University. I am grateful for the classes, the discussions, the knowledge, and the friendship. I was given many opportunities to teach and learn there for which I will always be grateful. I wish to particularly mention the “physics ladies”: Deborah, Karalee, Shelley, Sharon, Shawna, and Melanie. You were always so willing in helping me with whatever I needed.

Lastly, I wish to thank my family. My wife and parents have always been so supportive of my studies, even when it seemed as if I would be in school forever. My wife, Heather, has sacrificed so much allowing me the opportunity to continue my education, and I just want to say that I am thankful, and I love you.

Matthew Bailey

CONTENTS

Page

ABSTRACT……..…. iii

ACKNOWLEDGMENTS……..……..…….. v

LIST OF TABLES……...…… ix

LIST OF FIGURES…….…….. x

CHAPTER

I. INTRODUCTION…… 1

1.1. Preface ……..... 2
1.2. The Earth's Atmosphere…… 5
1.3. Thunderstorms and Lightning…..…… 10
1.4. Early TLE Observations……..... 18
1.5. Summary……... 33
1.6. Objectives of This Study……..... 34
1.7. Content of This Dissertation……36
1.8. Epigraphs……. 37

II. TLE THEORY……..… 38

2.1. Introduction……..... 39
2.2. Lightning-Driven Electric Fields…….. 39
2.3. Sprite Models……... 44
2.4. Elve Theories……... 49
2.5. Halo Theories…….. 51
2.6. Blue Jet Theories……. 54
2.7. VLF/ELF Monitoring and Charge Moments…….…..…… 55
2.8. Summary…….. 57

III. BRAZIL 1 CAMPAIGN……...…….. 61

3.1. Introduction……..... 62
3.2. Instrumentation…….. 67
3.3. First Sprite Observations…..…….. 73
3.4. Phase 2 Sprite Measurements ……..... 77
3.5. Results……..... 78
3.6. Brazil 1 Campaign Summary..……..... 83

IV. BRAZIL 2 CAMPAIGN……..……. 85

4.1. Introduction……. 86
4.2. Instrumentation……..... 88
4.3. Storm 1…… 94
4.4. Storm 2……..……..101
4.5. Summary……..…….. 103

V. HALO STUDY……...……..…….…... 106

5.1. Introduction……..……..... 107
5.2. South American Halo Data……..……..…… 111
5.3. Halo Analysis Method..……. 112
5.4. Halo and Storm Comparison. ……... 115
5.5. Halo Statistical Results……..……... 120
5.6. Summary……..…….……..……... 124

VI. INVESTIGATING NEGATIVE CG EVENTS……...……. 126

6.1. Introduction……... 127
6.2. The First Negative Event..……..... 130
6.3. Other Negative Events…….. 139
6.4. Summary..…….. 154

VII. SUMMARY AND FUTURE WORK……... 156

7.1. Summary……..… 157
7.2. Future Research……..... 161

VIII. REFERENCES……..... 163

IX. APPENDICES…….……. 177

APPENDIX A: LIGHTNING DETECTION NETWORKS……... 178
APPENDIX B: CHARGE MOMENT CALCULATION…… 186
APPENDIX C: PERMISSION FOR PUBLICATION FORMS…….. 197

CURRICULUM VITAE……..……..…..…… 225

LIST OF TABLES

Table Page

3.1. Summary of all Brazil 1 TLE events, including peak current (from the Brazilian Lightning Detection Network), and impulsive charge moment changes (from ELF/VLF measurements, Tohoku University, Japan)……. 81

6.1. Table showing a summary of case studies of sprite parent lightning polarity……...…… 128

6.2. Summary of TLE events associated with negative CGs observed on February 23, 2006…… 154

LIST OF FIGURES

Figure		Page
1.1.	Remarkable image of the first sprite captured on video……..	3
1.2.	The main layers of the atmosphere, including approximate altitudes and temperatures of these regions.……..	7
1.3.	A simple illustration showing Wilson's thunderstorm hypothesis for the global electric circuit……..	10
1.4.	An isolated thundercloud over central New Mexico, with superposed electric charge distribution, inside and around the cloud……...	13
1.5.	Illustration showing stepped leader propagation, attachment to ground leader, and first return stroke……..	15
1.6.	Examples of cloud-to-ground lightning……..…	16
1.7.	Image of a sprite above an illuminated thunder cloud taken from the space shuttle on April 28, 1990 over the Gulf of Guinea…….	20
1.8.	First color image of a sprite, showing a red emission from the upper part of the sprite, while the lower tendrils have a blue signature……...	21
1.9.	(A) Sprite observed on June 19, 1995, 07:24:20 UT, showing the orientation of the spectrograph slit (dotted line), and (B) observed sprite spectrum ……	22
1.10.	Two examples of sprites captured by Utah State University cameras……..…	24
1.11.	High resolution image showing complex tendril structures constituting a sprite body, with scale-sizes of 10s of meters…….	25
1.12.	High speed sprite sequence from August 13, 2005 at 03:12:32.0 UT, each labeled from the lightning return stroke initiation.…….	26
1.13.	(a) Photometric data of an elve followed ~10 ms by a sprite event. (b) Image of a diffuse elve emission, and sketch showing relative locations of the elve and sprite……	27
1.14.	Elve imaged over Europe in 1999……...	28

Figure Page

1.15. ISUAL image showing an elve as observed above the Earth from orbit …….. 29

1.16. Video image (17 ms resolution) of a halo with a sprite (sprite-halo) recorded over the Midwestern U.S ……..... 30

1.17. High speed (1 ms resolution) images of the development of a halo with a following sprite, showing streamer initiation and branching, as the halo fades …… 31

1.18. Photo taken from the ground over Reunion Island, showing a blue jet emanating from a cloud top……..... 32

1.19. False-color images showing development of a gigantic jet captured over Puerto Rico……. 34

1.20. Sketch showing approximate altitudes and scale-sizes of different TLEs……... 35

2.1. Mechanism showing QSF model, showing sprite formation after +CG stroke……. 47

2.2. A sketch showing the electrical field, and subsequent sprite formation formed above a thundercloud after, in this case, a +CG lightning discharge, due to the runaway breakdown model……..….. 48

2.3. Electron ionization for a vertical discharge centered over a source……. 50

2.4. Simulation results for emissions from the 1^{st} (left panel) and 2^{nd} (right panel) positive bands of N_2 at 0.501 ms after lightning discharge……. 52

2.5. Comparison of observations (false colored), along with modeled QE and EMP fields……. 53

2.6. The ELF/VLF azimuthal magnetic field Bphi associated with a positive lightning stroke……. 58

2.7. Mechanism of ELVEs, sprites, halos, and blue jets……...……. 58

2.8. (a) High-speed image of a sprite-halo, captured from a ground station in Wyoming on August 18, 1999; (b) associated array photometer data plot and VLF sferics waveform……... 59

Figure Page

2.9. Global map of TLE occurrence in fall and winter of the northern hemisphere…….. 60

3.1. Map showing the locations of several TLEs detected by nadir pointing cameras on the International Space Station (ISS) ……..... 63

3.2. University of Washington balloon payload, under testing in INPE hangar at Cachoeira Paulista……..... 68

3.3. (a) View of the hangar and the dirt runway used for the balloon launch at Cachoeria Paulista, and conveys well the nature of these field measurements; (b) a photograph of a test payload shortly after launch from Oregon…….……... 68

3.4. Xybion ISG – 780 Intensified CCD camera……..... 69

3.5. Research aircraft provided by INPE for Brazil 1 campaign…..…….…. 70

3.6. M. Bailey (foreground) taking a well earned rest during camera integration, while Dr. Michael Taylor and Fernanda São Sabbas finalize adjustments to instrumentation...…….. 71

3.7. A map showing the state of Sao Paulo, Brazil, indicating the two ground sites of the Brazil 1 campaign, Cachoeira Paulista and Santa Rita do Passo Quatro.……... 72

3.8. First ground-based observation of a sprite from Cahcoeira Paulista, Brazil.…. 74

3.9. Satellite image showing locations of the two sprite events captured from ground-based cameras on November 25, 2002, as well as the observation site at Cachoeira Paulista.…… 74

3.10. Carrot sprites imaged from the INPE provided aircraft on November 26th at 03:09:50.630 UT..……..……. 75

3.11. Map showing location of the three events captured on the night of November 26, 2002, along with the corresponding satellite image showing the cold front at 2:40 UT…… 76

3.12. Map showing location of eleven TLE events (events 7-10, 12-18, Table 3.1), imaged on March 21, 2003, and correlated with positive lightning discharges recorded from the Brazilian lightning network……. 78

Figure Page

3.13. Images of 16 sprite events seen during the Brazil 1 campaign (excluding events 12 and 13) ……..……..……..……. 79

3.14. Probability of sprite initiation vs. charge moment change for positive CG discharges…….…….…... 81

3.15. Plot showing all lightning flashes >26 kA peak current within ground cameras fields of view, for March 21, 2003…..…….. 82

4.1. Map showing the location of Santa Maria, in Rio Grande do Sul, which was the center for the Brazil 2 campaign ……..…..... 87

4.2. Wide field image from the ground site (29.4˚S, 53.8˚W) at the Southern Space Observatory (SSO) showing excellent viewing conditions at low elevations over a broad westward azimuth range..... 87

4.3. (a) WATEC 120N Camera, fitted with a Fujinon all-sky (180˚) lens. (b) Close-up showing WATEC camera mounted on top of the balloon payload.……... 89

4.4. UW and USU researchers moving the balloon payload from the integration facility at the University of Santa Maria to the launch site in an adjacent field.……..... 91

4.5. Preparations for a test balloon and payload launched from Santa Maria on Feb. 15, 2006…..……..…….…. 92

4.6. (a) Photo showing balloon launch configuration. (b) Video image taken from USU WATEC camera mounted on top of the balloon payload……. 93

4.7. (a) Duke University electromagnetic sensors, used to measure lightning sferics, and (b) system deployment at SSO…… 95

4.8. GOES 12 infrared image of a TLE producing thunderstorm to the west and southwest of SSO…….....…. 96

4.9. Distribution of sprite top altitudes, as determined using WWLLN lightning locations, which resulted in a mean sprite top altitude of 85 km……... 99

4.10. Three snapshot images depicting a complex sequence of TLEs imaged over Northern Argentina during the night of February 23…….... 100

Figure Page

4.11. An array of GOES 12 infrared images of a TLE producing thunderstorm to the north-northwest of SSO……..……...…… 103

4.12. Map showing relationship between observing site at SSO and all of the TLEs observed during storm 2 on the night of March 3–4, 2006……..……. 104

5.1. Video image of a well-defined sprite halo recorded from Bear Mountain, South Dakota on August 18, 1999 ……...…..... 109

5.2. Map showing triangulation of three sprites (solid circles) and estimated size and location of coincident halo together with positions of their parent +CGs..... 109

5.3. Coordinated high-speed photometer and video data taken from Yucca Ridge, CO, on July 21, 1996, showing both elve and halo optical signatures, as well as VLF data by a Stanford University sensor.…….……...…... 110

5.4. (Left) Two sequenced images showing a sprite-halo, with the halo and a faint streamer seen in the top panel, followed 17 ms later by multiple vertical structures, as the halo fades; (Right) Two halos imaged almost four hours apart on February 23, 2006..……..... 112

5.5. Halo imaged over Northern Argentina at 06:57:02.682 UT on Feb. 23.…..……...…….…...…. 114

5.6. Geographic projections of the halo event of Figure 5.5, for different assume altitudes of 77, 82, 87, and 91 km. …….…..…. 115

5.7. Plot showing the location of all halo events imaged between 02:30 UT and 04:00 UT…….… 117

5.8. Plot showing the location of all halo events imaged between 04:00 UT and 06:30 UT……...……..… 118

5.9. Plot showing the location of all halo events imaged between 06:30 UT and 08:30 UT……...……. 119

5.10. Altitude distribution (mean of 82.7 ± 1 km) of halos and sprite-halos, determined from 85 WWLLN lightning detections……..… 121

Figure Page

5.11. Distribution of diameters (mean of 58 ± 5 km) for halos and sprite-halos that were correlated with WWLLN lightning data……..……...… 122

5.12. Impulsive (2 ms) charge moment distribution (mean 255C.km) for all 185 halo and sprite-halo events observed on Feb. 22-23……. 124

6.1. Sprite captured over the Gulf of California by low light level cameras operating at 60 Hz ……...……..... 129

6.2. Map showing locations of 81 TLEs observed from 05-06:00 UT…….…….... 131

6.3. GOES 12 infrared satellite image showing the storm at 06:30 UT…….…… 132

6.4. (a) Enlarged (6° x 4°) video image of the negative event imaged at 05:29:33.522 UT (azimuth ~257.9° N, range ~944 km) showing a well developed sprite-halo with streamers; (b) Same event with same camera 17 ms later, showing further streamer development as the halo slowly fades; (c) Same negative event imaged by the second camera with larger field of view and higher electronic gain...……..... 133

6.5. (a) The ELF/VLF azimuthal magnetic field (Bφ) waveform corresponding to Figure 6.3. The large positive pulse unambiguously identifies this TLE with a negative CG stroke. (b) The Bφ waveform of a sprite-halo (Figure 6.5c) produced by a positive CG of similar ΔM_{Qv} …….……..……. 134

6.6. Images (a, b) showing the downward development of the negative event over two video fields (duration 33 ms). …….……..... 138

6.7. A sprite-halo associated with a negative event at 06:32:06:085 UT...…..…... 141

6.8. Map showing the locations of all TLEs associated with –CGs imaged on February 22-23.……...……..……..... 141

6.9. A sprite halo associated with a –CG at 07:17:17.131 UT….……...……..... 142

6.10. A sprite halo associated with a +CG occurring at 07:17:16.264, 867 ms just before the halo shown in Figure 6.9……...…….…….. 143

6.11. Map showing the locations of the positive and negative sprite-halos imaged at ~07:17:17 (within 1 second of each other)…….……..……..... 144

Figure Page

6.12. Composite image showing a positive sprite-halo (upper panel) and a nearby negative (bottom panel) event that occurred within 1 s of each other…….. 146

6.13. Horizontal scans across the TLE images shown in Figure 6.12 centered on the peak of the halo signatures……..…….…….…….. 147

6.14. Two simultaneous images of a negative halo (event 4) imaged at 05:59:43 UT by separate cameras, each with different electronic gain settings. ……..…….…… 148

6.15. A negative halo captured at 07:00:10 UT on Feb. 22-23...…..…….…... 149

6.16. The ELF/VLF azimuthal magnetic field Bphi associated with a negative halo (event 5)…….…… 150

6.17. Contrast stretched difference image of a faint halo (event 6) that occurred at 04:35:43.955 UT on February 23, 2006…….…… 151

A.1. Illustration showing the Earth-Ionosphere wave guide, which allows VLF (3-30 kHz) sferics to propagate over large distances (100s – 1000s km) through reflection off the ionosphere……..... 181

A.2. Map of South America, with overlaying WWLLN lightning stroke locations.……...…….... 185

B.1. Calculated ELF sferic spectra for propagation distances of 1000, 2000, and 3000 km under nighttime and daytime ionospheres …….……..... 192

B.2. Calculated ELF B_y waveforms for the ELF sferic spectra of Figure 1.…….... 194

CHAPTER 1

INTRODUCTION

"Many years ago, while a lowly student assistant supporting the National Hail Research Experiment on the Pawnee National Grassland of NE Colorado – A research associate from Texas A&M, John Marrs and I were out late at night watching thunderstorms in the distance 15 to 20 miles, with the purpose of catching rattlesnakes, we both observed a very active storm and on one occasion saw a red spike go out of the top of that storm. We questioned each other and made sure we were not seeing things. We definitely saw the red spike. WOW!! The next day, we told the research scientists from the National Center for Atmospheric Research about the sighting. They laughed it off and joked about us smoking too much dope.

I am sure we saw what is now classified as a red sprite, based on the images I have seen."

—Hans Jensen, amateur observer



A beautiful false-color image of a sprite cluster observed from Yucca Ridge, CO looking out over the Great Plains during the Sprites'95 campaign. This image shows a mixture of carrot and column-type sprites captured by a USU CCD camera filtered to observe the nitrogen first positive band emission.

1.1. Preface

As long ago as 1925, Scottish scientist, and Nobel Prize winner C. T. R. Wilson postulated the existence of brief flashes of light high above large thunderstorms. Over thirty years later in a paper entitled "A theory of thundercloud electricity," Wilson again stated that "…it is quite possible that a discharge between the top of the cloud and the ionosphere is a normal accompaniment of a lightning discharge to Earth…and many years ago I observed what appeared to be discharges of this kind from a thundercloud below the horizon…." [*Wilson*, 1956]. The wide use of commercial and military aircraft during the 20th and 21st centuries has subsequently led to many eye witness accounts by pilots of transient optical events, similar to those described by Wilson. A summary of these interesting, but often anecdotal accounts was compiled by *Vaughan and Vonnegut* [1989] in an article focusing on recent observations of lightning discharges from thundercloud tops into the clear air above.

The first confirmed evidence of such optical phenomena was obtained serendipitously on July 6, 1989, by John Winkler who was testing an intensified low-light-level TV camera at O'Brien Observatory (45.18° N, -92.77° E), operated by the University of Minnesota. The camera was being calibrated for coordinated observations for a sounding rocket campaign, and was aimed out of a low elevation window looking at the night sky. Remarkably, the camera captured a transient flash of light, which on inspection, revealed two bright vertically structured emissions, which we now term sprites. Figure 1.1 is an image showing this first event, which established the existence of sprites. In their initial report of this remarkable event, it is described as a "discharge [that] began at the cloud tops at 14 km and extended into the clear air 20 km or higher"

[*Franz et al.,* 1990]. These altitude estimations would eventually be shown to be far too low, due to an underestimation of the horizontal range. This extraordinary observation stimulated a number of researchers to look for evidence of such phenomena, with immediate success using video archive data obtained by TV cameras on the Space Shuttle [*Vaughan et al.,* 1992; *Boeck et al.,* 1995].



Figure 1.1. Remarkable image of the first sprite captured on video [*Franz et al.,* 1990, Fig. 1]. Reprinted with permission from the American Association for the Advancement of Science (AAAS).

These early findings have sparked many observation campaigns during the past 15 years, initially focusing on the Midwestern U.S., and later, as more was learned about their origins, from various sites around the world. In 1993, Dr. Walter Lyons of FMA Research, Colorado, as well as Dr. Davis Sentman of the University of Alaska Fairbanks (UAF), set up two independent searches for these optical events. Within a day of each other, the two research teams had witnessed and documented a multitude of sprites, which have subsequently turned out to be a common occurrence at mesospheric heights

[*Sentman and Wescott*, 1993; *Lyons*, 1994]. These early sprite observations were followed by detections of other distinct luminous events, which now comprise a family of Transient Luminous Events (TLEs). Included in the TLE family are sprites (or red sprites), elves, blue jets, and halos. Sprites appear as vertically structured columns of luminosity that extend from the mesosphere down to the lower stratosphere (see section 1.2), and are now known to be associated with positive lightning strikes. In contrast, elves appear as horizontal, cylindrical or doughnut-shaped discs of luminosity, which occur at the base of the ionosphere in association with the lightning induced electromagnetic pulse. Blue jets are enigmatic lightning-like discharges that originate at the top of thunderclouds, and extend upwards toward the ionosphere. The most recently discovered member of the TLE family, termed halos, is similar in morphology to elves, in that they appear as horizontal discs of light, but they have longer temporal lifetimes, and often occur in close association with sprites. At this point it is important to note that many researchers in the scientific community use the generic term sprites when referring to any type of TLE. As such, the terms TLEs and sprites are often used interchangeably in this dissertation.

TLEs are studied for many reasons. It has been postulated that sprites and other TLEs may be significant driving mechanisms for the global electric circuit (see section 1.2.1), or they may be viable producers of NO_x in the middle atmosphere [e.g., *Hiraki et al.*, 2002; *Enell et al.*, 2008]. High-altitude discharges (such as TLEs) may also adversely affect radio communications systems and aircraft, while some suggest that the gap between the inner and outer radiation belts of the Earth may result from lightning-driven electron precipitation [*Voss et al.*, 1998; *Cliverd et al.*, 2004], including TLEs.

Although discharges in the middle atmosphere have yet to be directly correlated with aircraft or spacecraft failure, the Atlas-Centaur 67 rocket failure in 1997 was attributed to a lighting discharge which damaged the rocket-guidance circuitry, causing it to destruct. Importantly, NASA now has criteria in place at Cape Canaveral that restricts launches when tropospheric lightning and/or high altitude (sprite-type) electrical discharges are possible [*Thomas*, 2005]. In fact, one of the first campaigns to study TLEs was funded by NASA, which was concerned about the potential of lightning-induced sprites as a launch hazard.

Scientifically, TLEs are fascinating new phenomena, and those who observe them are often captivated by their intricate structure and beauty. This introductory chapter reviews some of the basic meteorological knowledge of thunderstorms and lightning responsible for sprite phenomena, as well summarizing the known properties of TLEs.

1.2. The Earth's Atmosphere

The Earth's atmosphere consists of a thin ocean of well-mixed gases which sustain a habitable environment for living organisms, and provides a protective shield from harmful extraterrestrial radiation. Up to the turbopause (~100 km altitude) these gases occur in almost constant proportions: 78.1% nitrogen (N_2), 20.1% Oxygen (O_2) and 0.9% argon (Ar). In addition, other minor constituent gases are present that can have variable concentrations over time, but are geographically well mixed. These variable gases include carbon dioxide (CO_2), methane (CH_4), nitrous oxide (N_2O), ozone (O_3), water vapor (H_20), as well as aerosols and other chlorofluorocarbons [*Mayes and Hughes*,

2004]. The Earth's atmospheric density decreases exponentially with altitude, with over half of all atmospheric mass residing below an altitude of 6 km.

Figure 1.2 is an illustration of a vertical cross section of the Earth's atmosphere, including the main layers of the atmosphere. Each of these layers is defined by its environmental lapse rate, which is determined by how it absorbs solar radiation. The atmospheric region closest to the Earth's surface is the troposphere (from the Greek word *tropos*, which means mixing), the depth of which extends in altitude from ~ 8 – 18 km, depending upon the latitude. This region is characterized by large concentrations of water vapor, which absorb solar radiation, the cause of our weather, which is driven by the development and decomposition of clouds and associated weather systems. Weather prediction depends upon understanding what is happening in this moisture-rich zone, particularly the formation of clouds and rainfall due to condensation. In the troposphere, air is heated by solar absorption at low elevations (near the Earth's surface), the temperature decreases with altitude, and buoyancy causes warm air to rise generating convective activity. This process is important for thunderstorm formation and is discussed in more detail in section 1.3.

The tropopause is the boundary between the troposphere and the stratosphere and is characterized by a change in the environmental lapse rate. The stratosphere (from the Greek word *strato* meaning layered) is a region that is thermodynamically stable (temperature increasing with altitude), and has little cloud cover or water vapor that is so prevalent in the troposphere. The stratosphere's environmental lapse rate is due to the strong absorption of ultra-violet solar radiation by molecular oxygen (O_2), leading to the disassociation of this molecules and subsequent recombining of atomic oxygen with

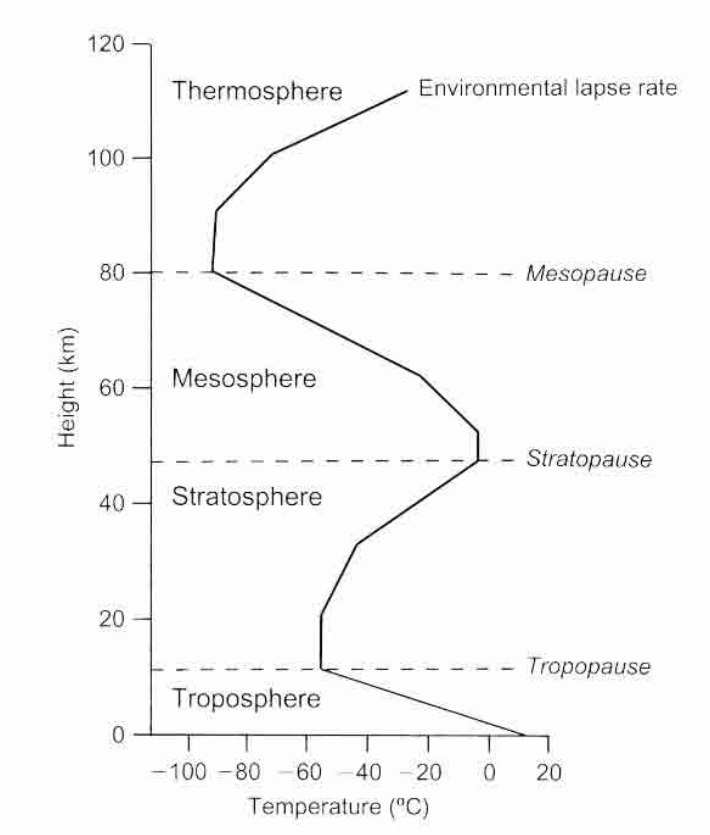


Figure 1.2. The main layers of the atmosphere, including approximate altitudes and temperatures of these regions [*Mayes and Hughes*, 2004, Fig.1.1]. Reproduced with permission of Oxford University Press.

molecular oxygen to form stratospheric ozone (O_3). Kinetic energy released in the formation of the ozone layer leads to warming of the stratosphere. The stratosphere extends to nearly 50 km in altitude.

The mesosphere (from the Greek word *mesos* meaning middle) is the atmospheric layer directly above the stratopause (upper boundary of the stratosphere), and extends upwards to ~ 80-90 km in altitude (depending on latitude and season). In this region, the disassociation of molecular oxygen decreases, and cooling by CO_2 radiative emission increases. The main dynamic features in this region are atmospheric tides, internal atmospheric gravity waves, and planetary waves. Most of these waves and

tides are excited in the troposphere and lower stratosphere, and propagate upwards into the mesosphere, where wave amplitudes can become so large that the waves may become unstable and dissipate, depositing momentum and energy into the mesosphere. Noctilucent clouds (consisting of microscopic ice particles) are sometimes observed near the upper boundary of the mesosphere, known as the mesopause. The mesosphere and stratosphere are sometimes referred to as the middle atmosphere, and are the regions where many types of TLEs occur. It should be noted that the electron density in the mesosphere varies from 10^4 to 10^7 electrons/cm^3, increasing with altitude. These existing (or ambient) electrons are instrumental in the formation of TLEs (see Chapter 2).

Above the mesopause, the atmosphere's temperature increases with height, with temperatures varying between 600 – 2000 K at an altitude of 500 km [*Fleagle and Businger*, 1980]. This area is known as the thermosphere, the name being derived from the Greek word for heat (*thermos*). In this region, temperatures increase due to absorption of highly energetic (solar extreme ultra-violet) radiation by the small amount of residual molecular oxygen still present, creating atomic oxygen. The character of the thermosphere is different from atmospheric layers below it due to: (1) ionization of air molecules and atoms, (2) disassociation of molecular oxygen and other constituents, and (3) the fact that diffusion is more important than mixing in this region, resulting in relatively high concentrations of light gases in exosphere (altitude ~ 1000 km). Within the thermosphere the ionization of air molecules and atoms creates the ionosphere. This area is of practical importance, as it influences radio wave propagation and GPS navigation systems, and is also the home of the auroras which occur primarily at high latitudes during solar magnetic storms.

There is no definite boundary between the atmosphere and outer space, and the region above the thermosphere is known as the exosphere. The exosphere extends outwards to 10,000 km above the Earth's surface, and is characterized by very low density, which decreases at high altitudes, and by free particles which move in and out of the magnetosphere, a region where the Earth's magnetic field interacts with the solar wind.

1.2.1. The Global Electric Circuit

The idea of a global electric circuit was suggested by C.T.R. Wilson in the 1920s, and is the name given to describe the flow of charged particles within the Earth's atmosphere. Scientific measurements near the Earth's surface have shown that a downward electric field of ~ 100 V/m exists in this region during good (or fair) weather. In a way, the Earth's atmosphere can be modeled as a spherical capacitor, with one surface being the conducting shell of the ionosphere (with an electric potential of ~ 250 kV). The ionosphere discharges by sending charged particles downward to land or oceans, which form the other surface of this capacitor. Mathematically, it can be shown that to maintain the measured electric field near the Earth's surface, the ionospheric charge reservoir would be drained in ~ 1 hr if there were no mechanism to replenish electric charges to the ionosphere. Wilson predicted that thunderstorms provided this mechanism, as shown in Figure 1.3.

A simple charge separation model for a thunderstorm (see section 1.3.2) where a positive charge reservoir remains at a higher altitude than its negative counterpart would theoretically provide this driving mechanism. Experimental studies have shown that

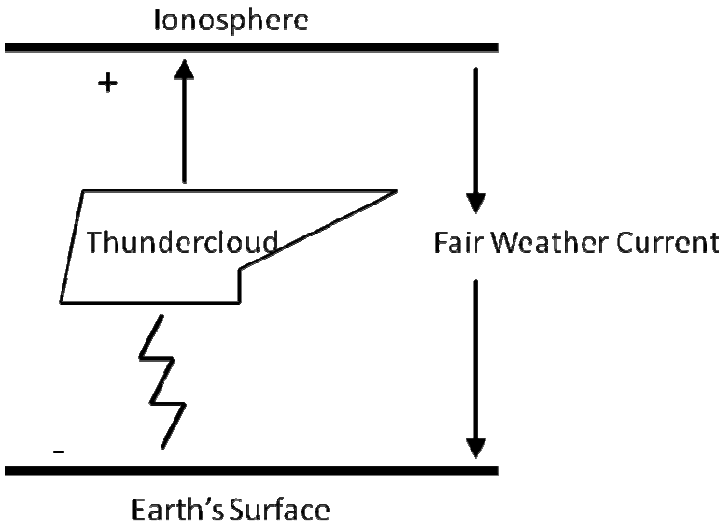


Figure 1.3. A simple illustration showing Wilson's thunderstorm hypothesis for the global electric circuit.

thunderstorms do indeed provide this type of charge movement within the atmosphere, although it is unclear whether these storms provide enough of a driving force to maintain the ionosphere's electric potential [*Thomas*, 2005].

1.3. Thunderstorms and Lightning

1.3.1. Thunderstorm Development

When one thinks of thunderstorms, a picture of large, dark cumulonimbus clouds rolling in on a summer day comes to mind. These large storms usually form from small, highly convective regions that typically develop from fair-weather clouds known as cumuli. To understand how these clouds form and grow, consider a warm parcel of air, which expands and cools adiabatically. When the humidity within the parcel of air reaches saturation (at the dew point temperature), water droplets begin to develop, and a cloud becomes visible. In this process, latent heat is released inside the rising air parcel,

which partially offsets the cooling due to expansion. If the rate at which the air temperature decreases with height, termed the lapse rate of the surrounding atmosphere, is greater than the moist-adiabatic lapse rate of the expanding air parcel (0.6° C /100 m), the air parcel will remain warmer than the surrounding air, and it will continue to rise. Under these conditions, the atmosphere is said to be unstable and this process will efficiently form cumuli clouds, which, under very unstable humid conditions, can then develop into thunderstorms [*Ahrens,* 2003].

Thunderstorms develop within the troposphere, where temperature decreases with height until reaching the tropopause, where it encounters the stable stratospheric air above, and vertical motion decays (see section 1.2). The height of the tropopause can vary from ~8 km at high latitudes in the wintertime to ~18 km at tropical latitudes, due to differential solar heating. Thunderstorms typically occur where surface air is warm and humid (and thus buoyant in an unstable atmosphere). However, they may also form at high latitudes during the summer, as well as during winter where the temperature may be no more than 10°C due to strong frontal activity (such as occurs off the west coast of North America).

Typical thunderstorms are inclined to develop in regions where there is limited wind shear, and to grow primarily due to the abundance of warm, moist air near the Earth's surface, which starts the convection process. There are many other factors which can contribute to their development, such as differential heating (e.g., water and land, mountains and valleys), or by orographic effects, where horizontal winds are directed upward after colliding with a mountain [*Rakov and Uman,* 2003]. A cluster of medium to large-scale thunderstorms that develop due to widespread instability is known as a

Mesoscale Convective System (MCS), which can further develop into a singular large-scale storm known as a Mesoscale Convective Complex (MCC). These complexes can be 1000 times larger than typical thunderstorms. MCSs and MCCs are defined as having a large horizontal extent (~250 -2500 km) and lifetimes in excess of a few to several hours. They are typically associated with strong frontal activity, and often develop when a large mass of cool air travels southward over the United States, and moves beneath a region of warmer, moist air, causing a massive instability. Importantly, MCSs and MCCs have been shown as prolific producers of TLEs.

1.3.2. Cloud Electrification

When a rising air parcel's temperature falls below 0°C, some of the water droplets freeze, while other (typically smaller) particles remain in their liquid state, and are known as super-cooled water. If an air parcel reaches - 40° C, all moisture will turn to ice. Between these two temperatures, a mixed-phase region exists, which then permits electrification to occur within the cloud [*Rakov and Uman*, 2003]. A very common model of cloud charge distribution is a tri-pole, with positive charge reservoirs near the top and bottom of the cloud, and a negative charge reservoir in the central region of the cloud, as inferred by many in-situ balloon observations. This situation is depicted in Figure 1.4. Other balloon measurements have found that the charge distribution may be significantly more complex [e.g., *Stolzenburg et al.,* 1998].

How charge layers are formed is still not well understood. The most well accepted theory at this time is the graupel-ice mechanism [e.g., *Jayaratne*, 1998]. In this mechanism, the electrification of individual particles is caused by collisions between

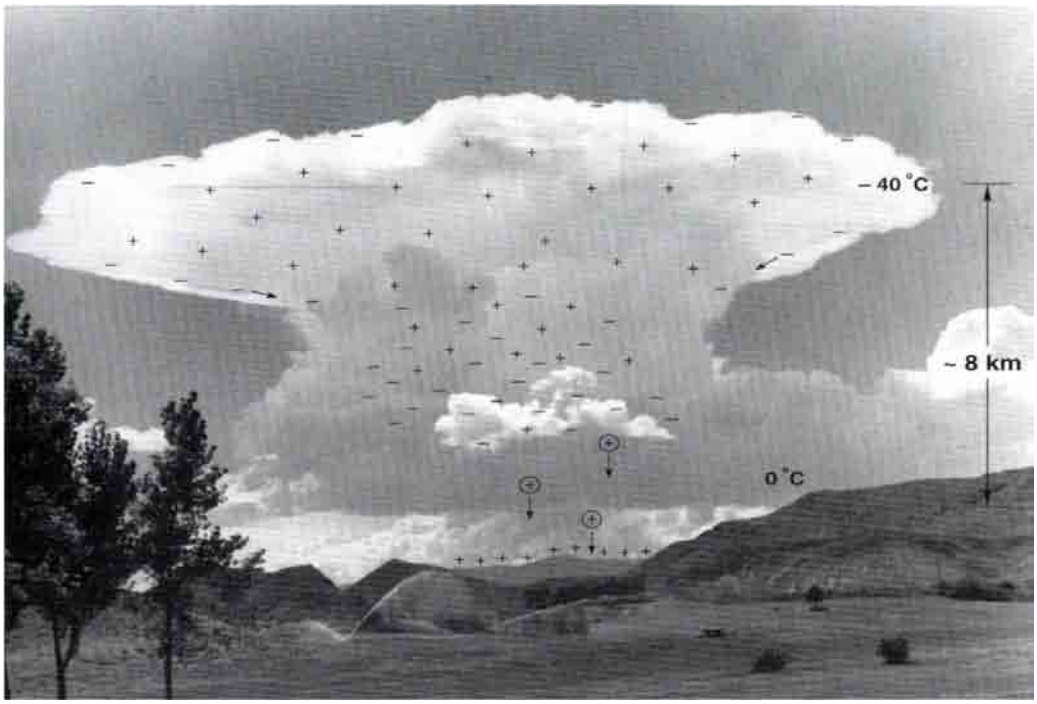


Figure 1.4. An isolated thundercloud over central New Mexico, with superposed electric charge distribution, inside and around the cloud [*Rakov and Uman*, 2003, Figure 3.1]. Reprinted with the permission of Cambridge University Press.

particles of icy matter (graupel or snow pellets) and cloud particles (small ice crystals) in the presence of water droplets. The heavy graupel particles fall colliding with cloud particles and super cooled water droplets. Laboratory experiments have shown that when the temperature is below a critical value (known as the reversal temperature, T_R), the graupel particles acquire a negative charge by colliding with the ice crystals. Above this temperature, they gain a positive charge due to the collisions. T_R has been measured in laboratory experiments, and is estimated to be between -10° C and -20° C [e.g., *Jayaratne et al.*, 1983]. The amount of charge separated within a cloud, as well as the polarity, therefore, depends on several factors such as cloud water content, ice crystal size, relative velocity of collisions, and contaminants in the water [*Rakov and Uman*, 2003]. The lighter, positively charged cloud particles (which gave their electrons to the

graupel), are then carried to the upper regions of the clouds by strong updrafts. The larger, negatively charged graupel particles, fall toward the mid-to-bottom of the cloud. A region of positive charge tends to form at the very bottom of the cloud, located in the falling precipitation near the melting level [*Ahrens*, 2003]. This is believed to be due to graupel particles, at lower levels in the clouds (and at temperatures higher than T_R) acquiring positive charge. Thus, the graupel-ice mechanism has been used to explain the tri-pole charge distribution in a thundercloud.

1.3.3. Lightning Characteristics

1.3.3.1. Negative Lightning

Each lightning flash consists of two main parts, a leader, and a return stroke. In a typical negative cloud-to-ground (-CG) lightning flash, a stepped leader (a plasma channel) initiates within the cloud, and moves downward at about 2×10^5 m/s [*Rakov and Uman*, 2003], forming a conducting path between the cloud and the ground. Several coulombs (C) of negative charge are distributed along its path during this process, which includes significant downward branching. The average stepped-leader current is between 100 and 1000 amperes (A). The electric field caused by the leader as it nears the Earth initiates an upward moving leader from the ground. The leaders tend to connect tens of meters above the ground (called the attachment process), and a strong return stroke then follows, which serves to neutralize the stepped leader charge. Figure 1.5 illustrates this process. The first return stroke current measured at the ground rises rapidly to an initial peak of about 30 kA (the median value) in several microseconds (μs), and subsequently decays to half-peak value over tens of μs [*Rakov and Uman*, 2003].

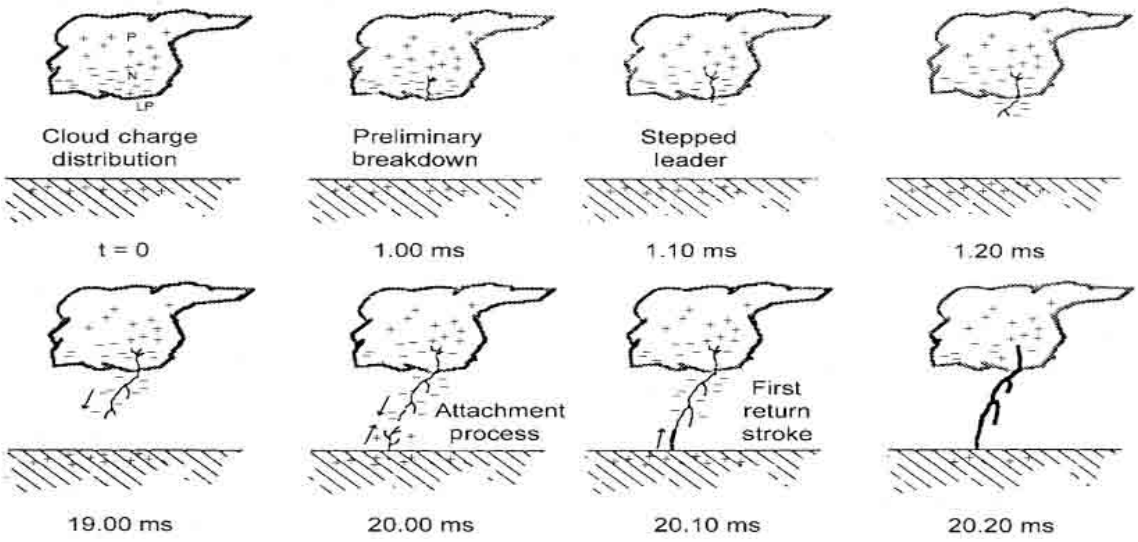


Figure 1.5. Illustration showing stepped leader propagation, attachment to ground leader, and first return stroke [Adapted from *Rakov and Uman*, 2003, Figure 4.2]. Reprinted with the permission of Cambridge University Press.

A few tens of milliseconds (ms) later, a second leader, often termed a dart leader, may travel along the same path as the stepped leader (typically without branching) with a much larger speed of ~10^7 m/s. As it travels, it deposits approximately 1 C of charge along the channel. Following attachment process near the ground, a second upward stroke follows, which may have peak currents of up to 10 – 15 kA. This process may be repeated many times, and accounts for the repeated flashing that one sometimes observes when witnessing a lightning strike. Approximately 90% of all cloud-to-ground lightning flashes are -CG.

1.3.3.2. Positive Lightning

Positive cloud-to-ground (+CG) lightning discharges are similar in morphology to – CG flashes, but differ from their negative counterparts with typically larger peak currents, and initially developing from the positive charge reservoir near the top of the

cloud. They also differ from their negative counterparts in that +CG flashes are usually composed of only one return lightning stroke, followed by long continuing currents (lasting for tens to hundreds of ms). Furthermore, the return stroke appears to be preceded by significant intra-cloud discharge activity connecting large horizontal channels within the cloud, and enabling much larger charge removal to the ground. This is a key factor for sprite production, and is discussed further in Chapter 2. In fact, the highest directly measured lightning currents (near 300 kA), and the largest charge transfers (hundreds of coulombs or more), are thought to be associated with positive lightning [*Rakov and Uman*, 2003]. Figure 1.6 compares positive and negative CGs. Positive events are much less frequent, contributing 10% or less of the total cloud-to-ground discharges.

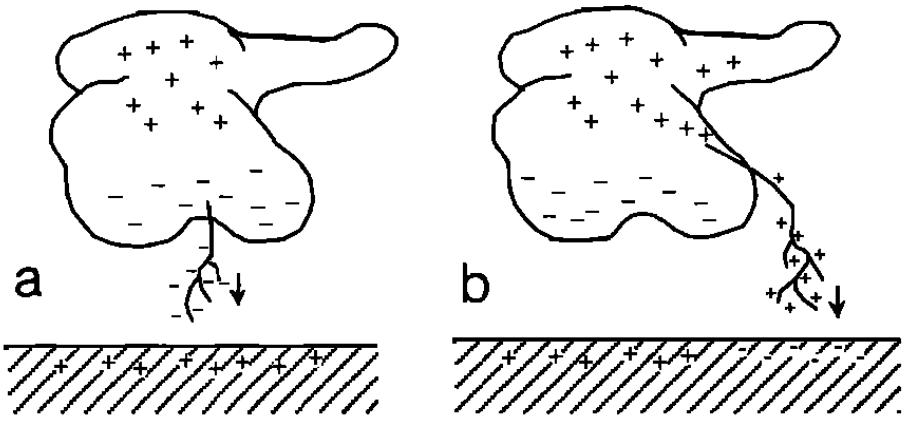


Figure 1.6. Examples of cloud-to-ground lightning. (a) negative cloud-to-ground discharge (-CG) and (b) positive cloud-to-ground discharge (+CG) [*Rodger*, 1999, Fig. 7]. Reproduced by Permission of the American Geophysical Union (AGU).

Positive CG leaders can either travel as stepped leaders, as with – CG discharges, but also are able to propagate with no branching in virgin air, similar to a dart leader. Special meteorological conditions are conducive to +CG flashes, such as the dissipating

state of an individual thunderstorm [*Orville et al.*, 1983], winter thunderstorms [e.g., *Mikaye et al.*, 1992], shallow clouds such as the trailing stratiform regions of MCSs [e.g., *Engholm et al.*, 1990], severe storms [e.g., *MacGorman and Burgess*, 1994], and thunderclouds formed over forest fires or contaminated by smoke [e.g., *Lyons et al*., 1998]. Positive CG discharges are of special interest in this study because of the correlation between + CG strokes and many TLEs.

1.3.3.3. Spider Lightning

Discharges within clouds, termed intra-cloud lightning or spider lightning, are the most common type of lightning on Earth. These discharges are most likely to begin near the upper and lower boundaries of the main negative charge region and often bridge the main negative and positive regions within the cloud. It is thought that a cloud discharge begins as a bidirectional leader, the positive section of this leader infiltrating the negative charge region, and providing substantial negative charge along the path between the negative and positive charge reservoirs. This initial leader is similar to the stepped leader of typical CG lightning, and travels at ~10^5 m/s with currents on the order of 10s – 100s of Amperes. These leaders are associated with the largest changes in the electric field recorded to date using balloon-borne measurements over Brazil [$E_z \sim 43$ V/m, $E_x \sim 15$ V/m, *Thomas et al*., 2005], as discussed in Chapter 3.

How initial breakdown occurs for all types of lightning is still poorly understood. Balloon-borne measurements have measured electric fields up to a few hundreds of kV/m, but never surpassing the conventional breakdown for air [e.g., *Stolzenburg et al.*, 1998]. This suggests that there may be other processes involved in initial breakdown,

such as microscale fields or relativistic breakdown [*Marshall et al.,* 1995]. It also has been theorized that ionization by micro-meteors may be an important initiation mechanism [*Gurevich et al.,* 1999].

1.3.3.4. Ball Lightning

There are many eyewitness reports of a phenomenon known as ball lightning, yet there is little, if any, scientific documentation of these enigmatic events. A common description of the event is an orange to grapefruit size sphere (reports vary both larger and smaller), and is usually red, orange, or yellow in color, and is about as bright as a 60 watt light bulb [*Rakov and Uman*, 2003]. Reports claim that the sphere tends to move horizontally, and decays either silently and slowly, or results in an abrupt explosion. It is most often seen close to and after a cloud to ground flash.

There have been many theories devised to explain ball lightning, but none are completely satisfactory, as some violate the accepted laws of physics [*Finkelstein and Rubinstein,* 1964]. Ball lightning has apparently not been generated in the lab to date. At minimum, it is fair to say that any generation in the lab has not been well documented in the literature, nor reproduced by other scientists.

1.4. Early TLE Observations

This section reviews early optical observations and studies of TLEs, and summarizes their known properties.

1.4.1. Sprites

A century has now elapsed since the first published sightings of TLEs. Since 1886, dozens of eyewitness accounts of TLEs have been reported, many as minor publications, accompanied by articles describing meteorological anomalies, such as toads falling from the sky [*Lyons et al.*, 2000]. Since science advances at a guarded pace, such reports were largely ignored by the atmospheric electricity community [*Williams*, 2001]. This all changed with Winkler's chance observation of a sprite, which was originally dubbed a large upward electrical discharge, as shown in Figure 1.1.

Following Winkler's first observation, Bernard Vonnegut of SUNY Albany realized that these types of events may be present in video imagery of Earth's upper atmosphere recorded by Space Shuttle astronauts. He encouraged lightning researchers at NASA's Marshal Space Flight Center lightning researchers to look for such luminous events using a camera on the Space Shuttle. During an observational campaign in October 1989, their imagers captured several strange upward lightning-like events. These observations established that sprites, which did not look anything like normal lightning, originated above the anvils of large, very active thunderstorm complexes. An example image of a sprite recorded from the Space Shuttle is shown in Figure 1.7.

Most descriptions of sprites in early reports attempted to include physical characteristics in their names which were assumed, and later would prove to be at least partially misleading. Examples of such names include large upward electrical discharge [*Franz et al.*, 1990], cloud to space lightning [*Vaughan et al.*, 1992], cloud-to-stratosphere electrical discharges [e.g., *Lyons and Williams*, 1993], luminous structures in the stratosphere [*Lyons*, 1994], stratospheric flash or lightning in the stratosphere [*Boeck*

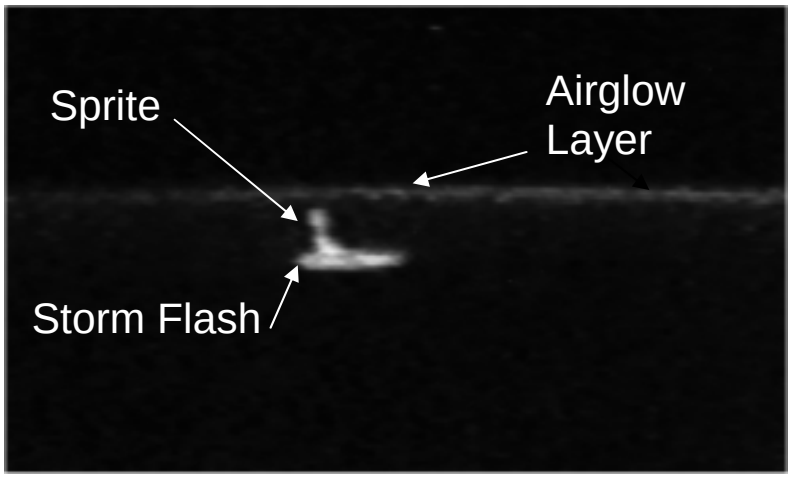


Figure 1.7. Image of a sprite above an illuminated thunder cloud taken from the space shuttle on April 28, 1990 over the Gulf of Guinea [Adapted from *Boeck et al.,* 1995, Figure 1.g]. Reproduced by permission of the AGU.

et al., 1995], and cloud–ionosphere electrical discharges [*Winckler*, 1995]. Following altitude measurements by *Sentman and Wescott* [1993], sprites were determined to occur at much higher altitudes, extending well into the mesosphere. Due to the lack of knowledge concerning the physical mechanisms that cause these strange events, the term sprite was used by D. Sentman, University of Alaska, Fairbanks (UAF), to capture the elusive, transient nature of these optical emissions (some reports say the name was also inspired by Shakespeare's The Tempest). Sprites or red sprites is the term typically now accepted in the scientific community, although terms such as High Altitude Lightning [*Valdivia*, 1997], glow phenomena [*Gomes and Cooray*, 1998], ionospheric lightning [*Boeck et al.,* 1998], and upward lightning discharges, as well as mesospheric electrical discharges [*Winckler*, 1998], are still occasionally used in the literature.

In 1994, a University of Alaska Fairbanks airborne program conducted over the Midwestern U.S. captured the first color images of sprites. The campaign, consisting of two airplanes equipped with color video cameras, allowed for triangulation of the

captured video images, and thus enabled analysis of the size and vertical extent of these events. Figure 1.8 shows an example of the first color image data. This image shows that sprites have a red main body, extending over the altitude range of ~50-90 km, and lateral dimensions of 5-30 km. Faint bluish tendrils are seen to extend downward from the main body of the sprite toward the cloud tops [*Sentman et al.*, 1995].

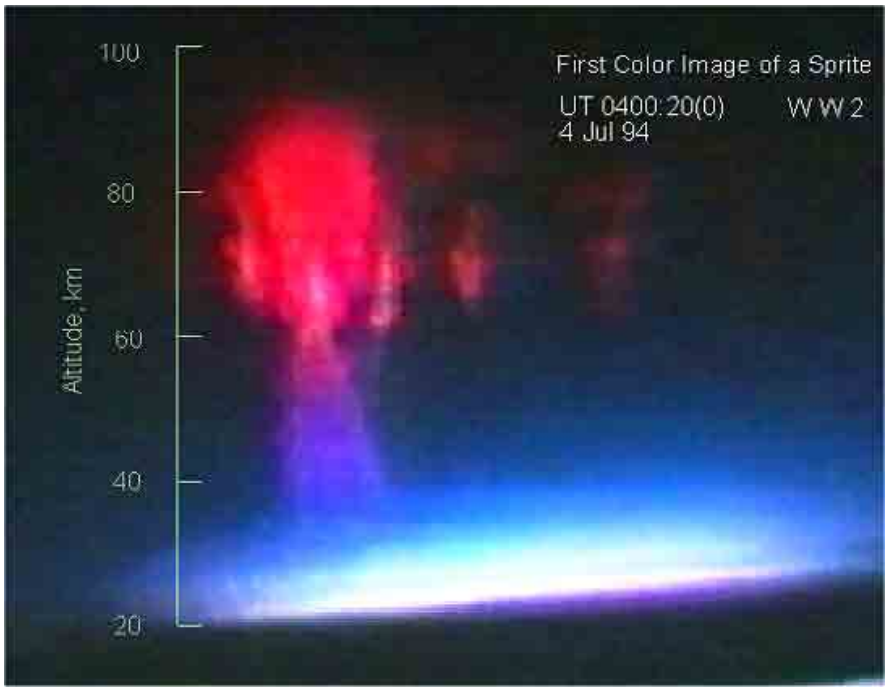


Figure 1.8. First color image of a sprite, showing a red emission from the upper part of the sprite, while the lower tendrils have a blue signature. Triangulation shows the altitude extends from typically 40 – 90 km [Adapted, *Sentman et al.*, 1995, Fig. 1b]. Reproduced by permission of the AGU.

In order to determine the origin, or cause of the red emissions recorded by these color cameras, new ground-based measurements were made from Mt. Evans, Colorado, during the summer of 1995, using coordinated imager and spectrograph instrumentation [*Heavner*, 2000]. The Mt. Evans observatory was selected because of its high altitude, which provided reduced Rayleigh scattering and atmospheric absorption, as well as its

prime location for observing TLEs over the U.S. Great Plains. Using a spectrograph, which measured in the wavelength range from 540 to 840 nm, the first optical spectra were obtained on June 19, 1995, and revealed the primary emission of sprites to originate from the first positive bands of N_2 [N_2(1PG)]. A surprising result was that there was no evidence of the Meinel bands of N_2^+, indicating that the mechanism responsible for sprites produces little, or no ionization at 70 km altitude [*Hampton et al.*, 1996]. Figure 1.9 shows a sprite captured at the same time as corresponding data from the spectrograph. Independent confirmation of these findings came three weeks later from Yucca Ridge, CO (on July 16, 1995), using a slit grating spectrograph system with an intensified CCD camera, initially developed to study space shuttle glow [*Mende et al.,* 1995].

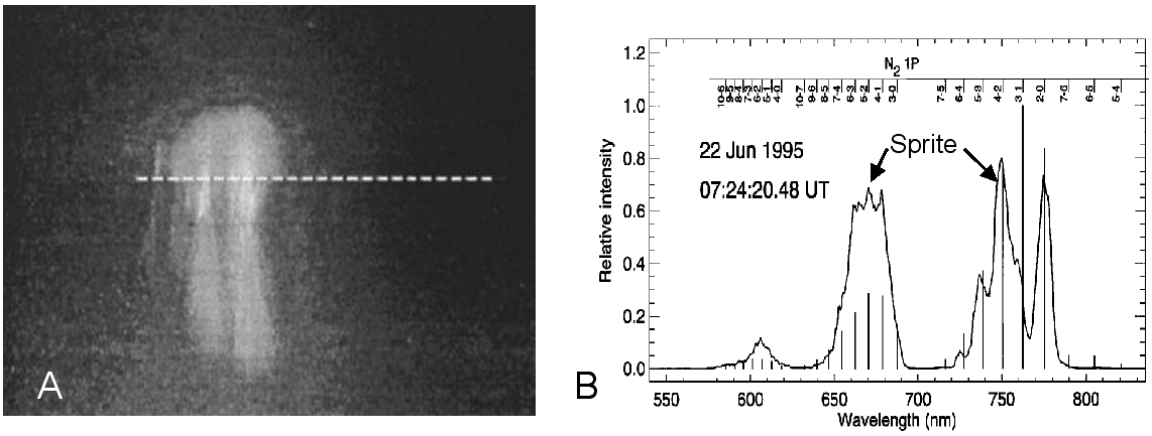


Figure 1.9. (A) Sprite observed on June 19, 1995, 07:24:20 UT, showing the orientation of the spectrograph slit (dotted line), and (B) observed sprite spectrum. The spectrum has many fine scale structures within the sprites, including so called "fireworks" [*Sentman et al.*, 1996], downward branching [*Taylor and Clark*, 1996], and upward branching shapes [e.g., *Stanley et al.*, 1999].

Subsequently, *Armstrong et al*. [1998] obtained the first blue photometric measurements of the N_2 second positive band (399.8 nm) and the N_2^+ first negative

(427.8 nm) emissions using a high-speed photometer with narrow band filters, establishing that ionization is present, at least in some of the large sprite events.

Two types of sprites were readily identified in video data. The first is known as a carrot sprite, which exhibits the classic sprite structure of a broad main body topped by diffuse hair and multiple downward root-like tendrils. An example of a carrot sprite is shown in Figure 1.10A, which was obtained using a USU CCD camera operated at Yucca Ridge, CO, during the summer of 1996. This type of sprite exhibits significant spreading away from the vertical axis at both high and low altitudes [*Sentman et al*., 1995]. The other type of sprite was identified later, and is now known as column sprite, often abbreviated to c-sprite [*Wescott et al.,* 1998b]. A cluster of c-sprites is shown in Figure 1.10B. They are characterized by thin vertical structures, with a bright main upper body sometimes accompanied by long streamers at lower altitudes. Meteorology may play a major role in what type of sprite is produced. Typically, storms in the United States produce a majority of classic sprites, and a lower percentage of c-sprites. However, this is not always the case, as on June 21, 1995, a storm over New Mexico produced almost exclusively c-sprites [*Wescott et al*., 1998b]. It has also been suggested that c-sprites tend to be produced over open water (H. Fukunishi, Tohoku University, private communication), while some high speed video observations indicate that all sprites may begin as c-sprites, and then develop more structured forms [e.g., *Stanley et al.*, 1999].

High resolution telescopic image measurements have revealed very fine structures within a sprite with lateral extents ranging from tens to a few hundred meters. An example high resolution image is shown in Figure 1.11, revealing thousands of fine

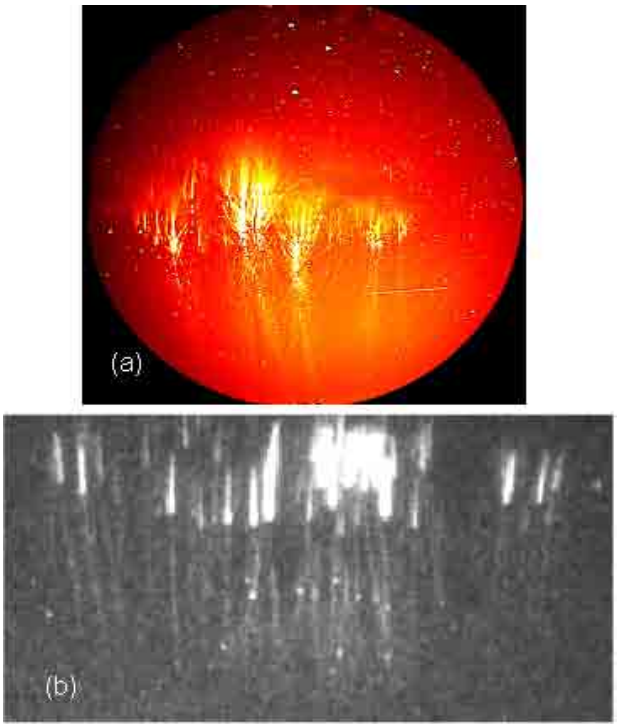


Figure 1.10. Two examples of sprites captured by Utah State University cameras: (a) a false color image of a cluster of carrot sprites obtained from Yucca Ridge, CO, in July 1996, using a N_2 first positive band filter at 865 nm; (b) unfiltered, black and white image of a c-sprite cluster imaged over Argentina in February 2006, using an intensified CCD camera.

streamer structures (transverse extents of 20-50 m) within the main sprite body observed in the altitude range of 76-80 km [*Gerken et al.*, 2000].

In contrast, high speed video observations have provided details of the development of these fine-scale structures, such as upward and downward branching with moving beads [e.g., *Stanley et al.*, 1999; *Stenbaek-Nielsen et al.*, 2000; *Cummer et al.*, 2006; *McHarg et al.*, 2007]. Figure 1.12 shows a high-speed time series of sprite development. In this time sequence, the sprite initially appears as a diffuse emission near 80 km (known as a halo) and develops vertically upwards and downwards with streamer ends resembling luminous beads traveling in both directions. These streamers branch as

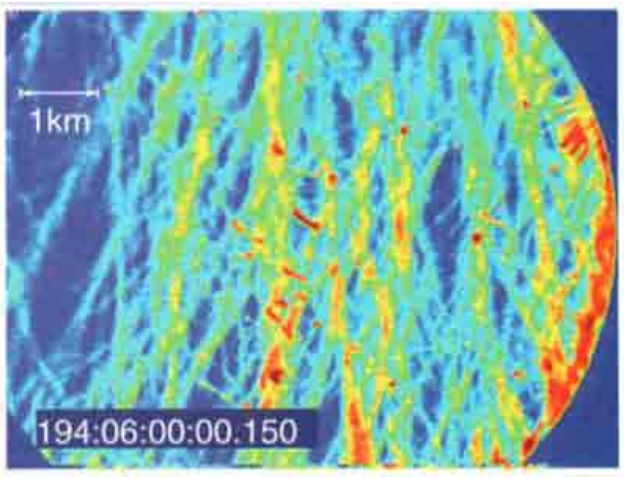


Figure 1.11. High resolution image showing complex tendril structures constituting a sprite body, with scale-sizes of 10s of meters [*Gerken et al.,* 2000, Fig. 1]. Reproduced by permission of the AGU.

they propagate, with the lower part of the upward streamers being very bright (and forming the main body of the sprite), while at higher altitudes, the upward traveling streamers terminate in diffuse emissions. Downward streamers penetrate deep into the stratosphere, and appear to be attracted to other downward propagating streamer channels, even colliding with them, forming long lasting bright sprite beads [*Cummer et al.,* 2006]. Most recently, very high speed cameras (10,000 frames per second) have shown that downward streamers initiate first, with the upward streamers starting a few ms afterwards. At this high temporal resolution, these streamers appear simply as small beads of light [*McHarg et al.,* 2007]. Although not always detected with sprites, electrical currents within extremely bright sprite bodies have been experimentally measured [e.g., *Cummer et al*., 1998], with typical currents ranging from 1.6 – 3.3 kA.

In 2004, the Imager of Sprites and Upper Atmospheric Lightning (ISUAL) instrument was launched into orbit, on board the Formosat-2 satellite (formerly known as

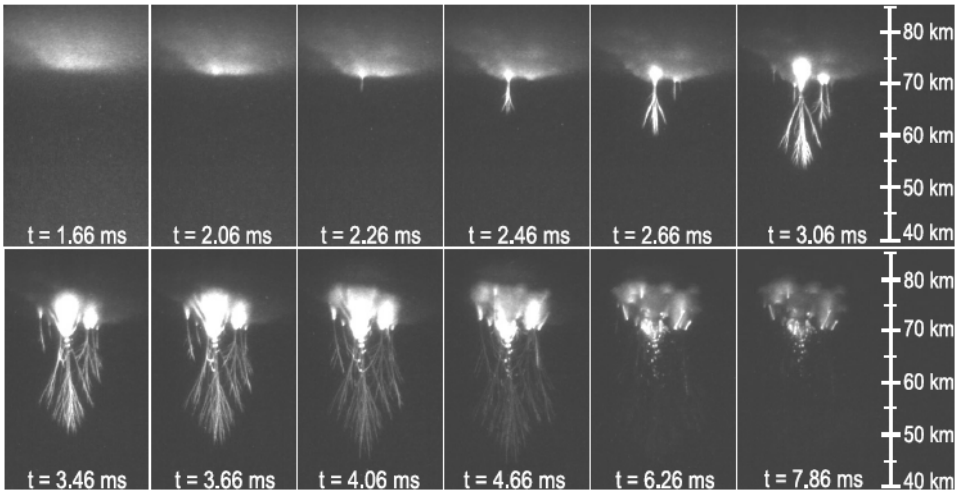


Figure 1.12. High speed sprite sequence from August 13, 2005 at 03:12:32.0 UT, each labeled from the lightning return stroke initiation. These images were taken from Yucca Ridge, CO, using a camera operating at 5000 frames/sec [*Cummer et al.*, 2006, Fig. 2]. Reproduced by permission of the AGU.

Roscat-2). This imager is the first instrument dedicated to observe TLEs from space. As of March 2007, it has recorded nearly 5000 TLEs, including many sprites. ISUAL views sprites in the earth's limb, and provides data on the TLE together with the in-cloud scattered luminosity due to the parent lightning. It is therefore possible to investigate both the temporal evolution of the TLE and the spatial properties of its parent lightning, if both signals are able to be separated. This instrument has also been used to study the electric field in sprites [*Kuo et al.*, 2005, *Adachi et al.*, 2006].

1.4.2. Elves

During the summer of 1995, Japanese researchers at Yucca Ridge Field Station (40.7° N, 105° W) near Fort Collins, CO, recorded several very brief red emissions that appeared to originate near the base of the nighttime ionosphere at altitudes of ~95 km [*Fukunishi et al.*, 1995]. These diffuse optical flashes were subsequently named ELVEs

(Emission of Light and VLF perturbations due to EMP sources [*Lyons and Nelson*, 1995; *Fukunishi et al.*, 1996]. Elves have characteristics similar to horizontal airglow enhancements associated with lightning, previously observed by space shuttle imagers [*Boeck et al*., 1992] and also possibly from sounding rockets [*Li et al.*, 1991]. The Yucca Ridge observations were made with video cameras co-aligned with high-speed photometers, and often preceded structured sprites. Figure 1.13 shows both photometric and video data of an elve and a sprite recorded from Yucca Ridge, together with an illustration depicting the relative locations of the elve and sprite [*Fukunishi et al*., 1996].

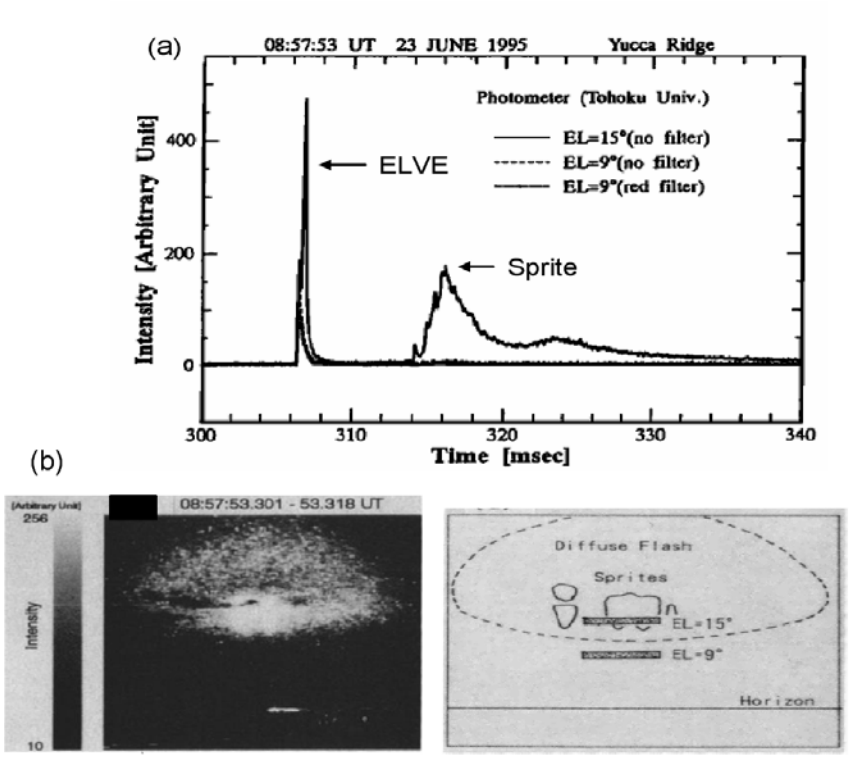


Figure 1.13. (a) Photometric data of an elve followed ~10 ms by a sprite event. (b) Image of diffuse elve emission, and sketch showing relative locations of the elve and sprite [*Fukunishi et al*., 1996, Figs. 1a, 2a, 2d]. Reproduced by permission of the AGU.

In 1997, Stanford University studied this new type of TLE with a recently developed photometer array, known as a Fly's Eye that was bore-sighted with a low-

light-level video camera providing the first measurements of the rapid expansion of elves [*Inan et al.*, 1997]. They conclude that elves typically have a duration of less than 1 ms, and appear to propagate outwards at 3 times the speed of light, achieving horizontal scale-sizes of ~100 to 300 km. Since elves are so transient in nature, they are difficult, but not impossible, to capture with cameras operating at typical video rates. For example, Figure 1.14 shows an image of an elve recorded by a USU CCD video camera onboard a NASA airplane flying over the southern Mediterranean during the Leonids Meteor Storm campaign during November 1999. The camera was aimed at low elevations observing thunderstorm activity over Bosnia, and captured multiple images of elves as well as sprites. This figure clearly shows the diffuse doughnut shaped disk with a characteristic central hole (the mechanism is discussed further in Chapter 2). Modeling studies have shown that elves are quite distinct from sprites, as they are caused by the absorption of the electro-magnetic pulse (EMP) at the base of the ionosphere. This EMP is due to terrestrial lightning strokes.



Figure 1.14. Elve imaged over Europe in 1999 (Courtesy M.J. Taylor, Utah State University).

Fly's-eye measurements of elves indicate that they are associated with both positive and negative CGs [*Barrington-Leigh and Inan*, 1999]. Most recently, elves have been observed by the ISUAL instrument on the Formosat-2 satellite. Since its launch in 2004, a large number of elves have been imaged, and their potential effects on the ionosphere have been studied [*Mende et al.*, 2005]. Figure 1.15 shows an elve imaged by the ISUAL instrument. Due to the satellite viewing geometry, the elve appears as a very thin disk above the Earth's limb with a dark central region.

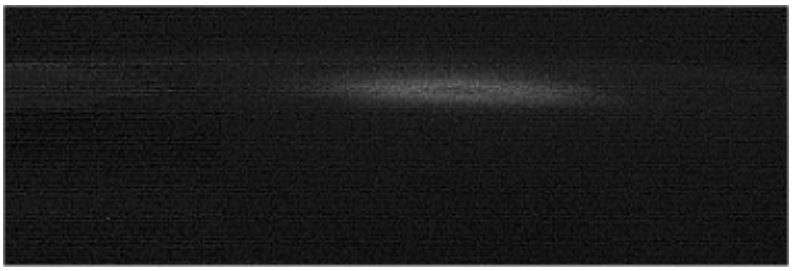


Figure 1.15. ISUAL image showing an elve as observed above the Earth from orbit [*Mende et al.*, 2005, Fig. 4]. Reproduced by permission of the AGU.

1.4.3. Halos

Astute image analysis by *Barrington-Leigh et al*. [2001] led to the discovery of a new type of TLE commonly termed a halo. For several years, video imagery of halos was misinterpreted as signatures of elves. However, using fast (3000 frames per second) video cameras together with the Fly's Eye high-speed photometer array, Barrington-Leigh showed that a diffuse flash, similar in shape to elves, but originating at lower altitudes, sometimes preceded sprite formation. These halo events also exhibited longer durations (10-20 ms) and significantly smaller diameters (typically < 100 km) than elves. *Barrington-Leigh et al.* [2001] dubbed these flashes sprite halos, but the scientific

community has since simplified this to halos. An image of a diffuse halo disk, along with a structured sprite is shown in Figure 1.16.

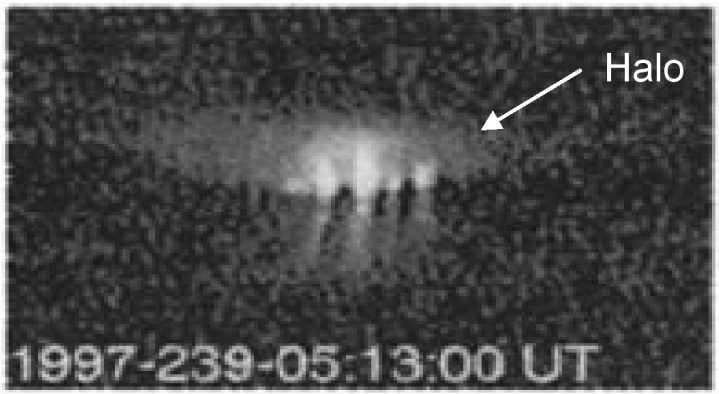


Figure 1.16. Video image (17 ms resolution) of a halo with a sprite (sprite-halo) recorded over the Midwestern U.S. [Adapted from *Barrington-Leigh et al.*, 2001]. Reproduced by permission of the AGU.

There are relatively few studies that have focused on halos. Using high-speed video cameras with a 1 ms temporal resolution, *Stenbaek-Nielsen et al*. [2000], showed that sprite structures tend to develop from the lower boundary of halos. Figure 1.17 shows an example of this phenomena illustrated by their data. *Wescott et al.* [2001] performed triangulation of several elves, halos, and sprite streamers using cameras at two sites, one in Wyoming and the other in South Dakota. Of the four halo events studied, they were found to originate at a mean altitude of ~78 km, exhibit an apparent thickness of ~4 km, and a mean diameter of ~66 km. *Barrington-Leigh et al*. [2001] also showed that halos occurred over the altitude range of ~70-85 km, and with horizontal extents from ~40-70 km. Their modeling studies and high speed image data also showed that halos exhibit a concave shape, with the middle of the halo moving downward following initiation at speeds of typically ~ 4.3 x 10^7 m/s [*Barrington-Leigh et al*., 2001].

Miyasato et al. [2002] also investigated the characteristics of halos using high-speed multi-anode array photometers. In conjunction with the photometers, USU video cameras operated from Colorado and a University of Alaska high speed camera operated from Wyoming. They were able to clearly show the temporal development from elves, to halos, to structured sprites. They also determined halos exhibited a mean altitude of ~80 km, and a mean diameter of ~86 km. These results together with new measurements of halos over Brazil will be discussed further in Chapter 5.

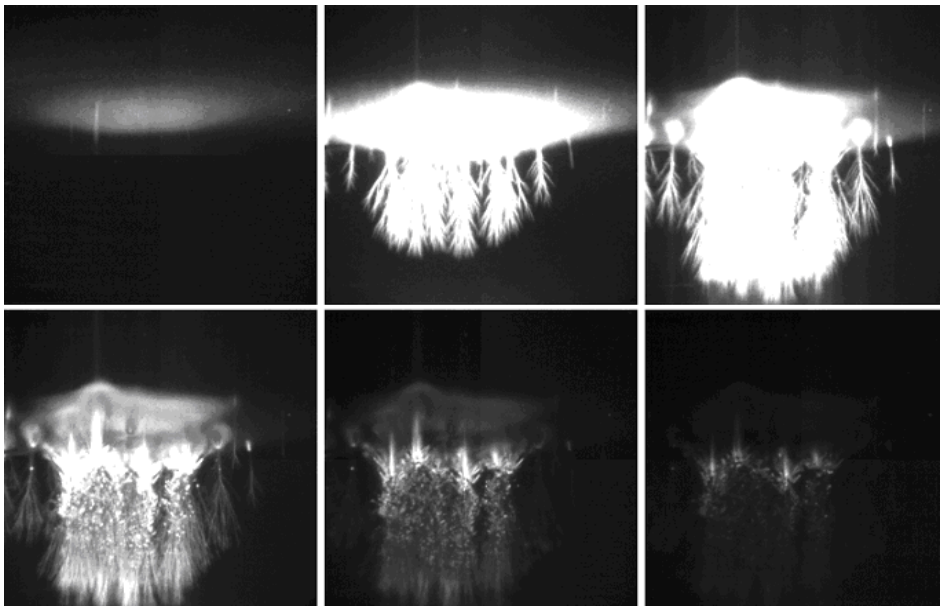


Figure 1.17. High speed (1 ms resolution) images of the development of a halo with a following sprite, showing streamer initiation and branching, as the halo fades [*Stenbaek-Nielsen et al.*, 2000, Fig. 1]. Reproduced by permission of the AGU.

1.4.4. Blue Jets and Blue Starters

These enigmatic events were first captured on video during an airborne campaign over an extremely active thunderstorm in Arkansas on July 1, 1994. Only a few sprites were measured during this night, but a large number of upward propagating jets of light

were observed. Remarkably, a total of 56 jet-like events occurred in a 22-minute interval. These new events were clearly different from sprites in two aspects: (1) color video cameras showed that the emissions were blue and, (2) movement of these events was upward from the cloud tops at relatively low speeds of ~100 km/s. Due to their signature, these new events were dubbed blue jets [*Wescott et al*., 1995]. Triangulation of a subset of events observed from both aircraft revealed an upper altitude of ~37 km, and a maximum upward velocity of ~112 km/s [*Wescott et al.,* 1998a]. Airborne measurements of the base of the jets were obscured by cloud. Figure 1.18 shows an example of a blue jet captured on photographic film from Reunion Island in the Indian Ocean. The jet appears as an upward bolt of lightning originating close to the cloud tops, which fans out and appears blue in color with increasing altitude.



Figure 1.18. Photo taken from the ground over Reunion Island, showing a blue jet emanating from a cloud top (Adapted from an image taken by Patrice Huet).

During the same airborne campaign where blue jets were first observed, video imagery was also obtained of a related phenomena coined blue starters. These events are similar to blue jets, propagating up from the top of the thunderstorm, but only reaching heights of ~26 km, with an average speed of ~120 km/s [*Wescott et al.*, 1998a]. Intensified color video cameras show that blue starters have the same apparent color as blue jets. They have since been observed in blue filtered images [*Wescott et al.*, 1998b].

More recently, several gigantic jets have been captured on video. These events are similar in morphology to blue jets, but are able to penetrate to much higher altitudes in the atmosphere, extending from the cloud tops to ionospheric heights (between 70 -100 km), and they exhibit more branching than blue jets [*Pasko et al.*, 2002]. Figure 1.19 shows a sequence of images taken of a gigantic jet recorded from Puerto Rico. Similar events have been captured over the South China Seas from a ground station in Taiwan [*Su et al.*, 2003]. The Taiwanese gigantic jet events extended up to 90 km in altitude, and occurred over the open ocean, near the Philippines. Studies of the meteorological conditions of this event show that the gigantic jet originated from the convective core of a thunderstorm. However, *Wescott et al*. [1998a] has shown that blue jets are not coincident with positive or negative ground flashes, but that they occurred in the same general area as -CG and large hail. This result was later confirmed by *Su et al*. [2003].

1.5. Summary

Figure 1.20 illustrates the relative sizes and locations of TLEs (notable exception are jets and starters), in association with a parent thunderstorm. Sprites, elves, and halos have all been shown to be associated with terrestrial CG lightning, with elves occurring

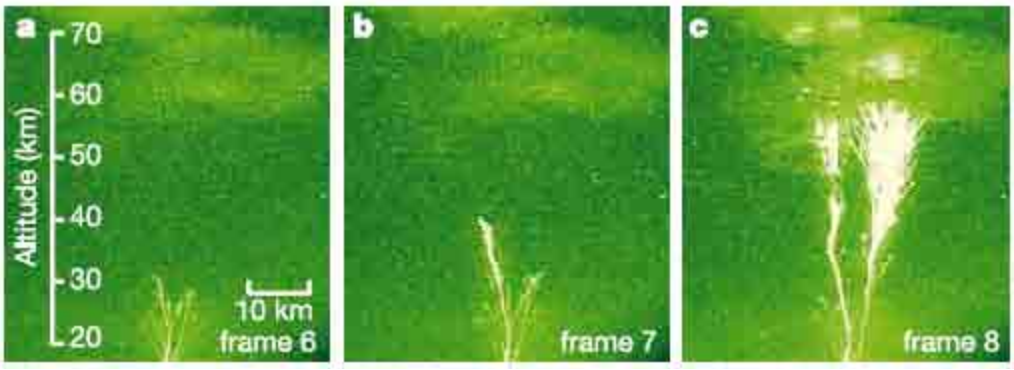


Figure 1.19. False-color images showing development of a gigantic jet captured over Puerto Rico [*Pasko et al*., 2002, Fig. 2]. Reproduced by permission of the Nature Publishing Group. Each field has a 33 ms resolution.

first, followed by halos and/or then sprites. Elves originate at the base of the ionosphere (90-100 km altitude), and have a characteristic doughnut shape and horizontal diameters of up to 300 km. They are the most fleeting of the TLE family, and occur in association with positive and negative lightning. Halos are similar disk shape emissions that occur at lower altitudes (~80 km) and exhibit smaller horizontal extents, typically 50-100 km. They occur several ms after an elve, and may be associated with sprite formation, or may occur independently. Sprites are vertical structured emissions that extend in altitude from 40-90 km. They are the brightest of the TLE emissions, and have lifetimes of up to several tens of milliseconds. Although there have been many studies of TLEs in several different parts of the world, new campaigns, new instrumentation, and new techniques are continuing to build our knowledge of these magnificent events.

1.6. Objectives of This Study

Our knowledge about TLEs is rapidly changing, but is still somewhat restricted due to number of experimental studies performed since their discovery two decades ago.

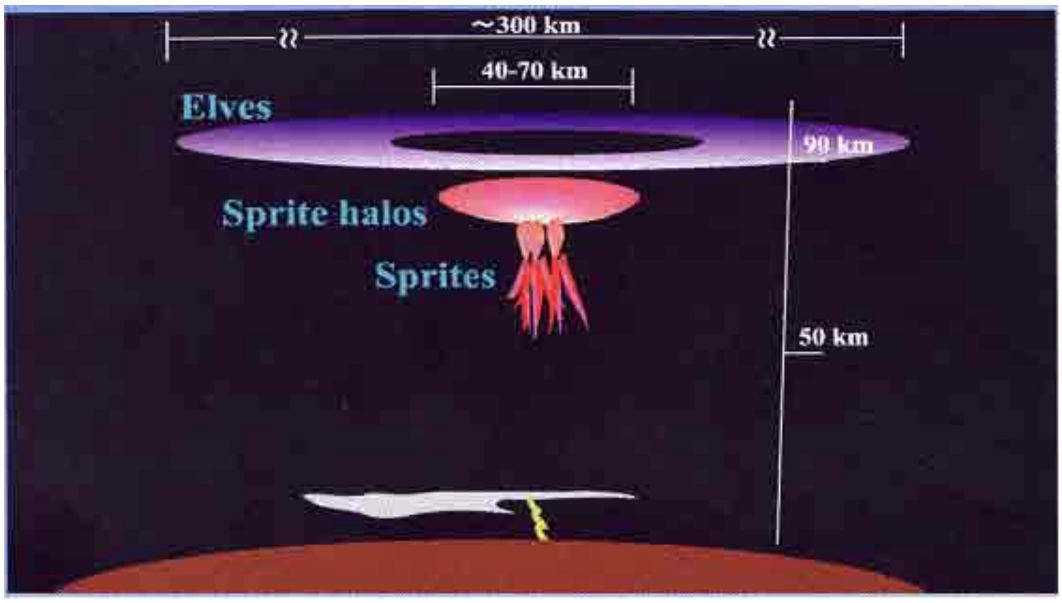


Figure 1.20. Sketch showing approximate altitudes and scale-sizes of different TLEs. (Courtesy R. Miyasato).

Importantly, the concentration of measurements over the Midwestern United States, with only a small number of studies in other parts of the world, have provided quantitative information about the temporal and spatial morphology of TLEs (mainly of sprites) to compare with current models. In addition, new, high-speed cameras and high-resolution cameras are giving us deeper insight into what is actually occurring within the TLE during its formation, including the individual streamer dynamics of these events. Coordinated measurements using new techniques which analyze the electromagnetic signatures of both causative lightning and the following TLE, and these techniques are being used to quantify the occurrence of TLEs in different parts of the world, giving new information on the dynamics of these events (see section 2.7).

The objectives of this study include:

- Analysis of TLEs observed in South America over two separate campaigns. This area of the world was expected to be a prolific producer of TLEs but had not previously been studied.
- Statistical analysis of a large number of halo and sprite-halo events, which were recorded during a large storm complex over Argentina in February, 2006. Halo studies are few, and this investigation is the most comprehensive one to date.
- Detection and measurement of several halo and sprite-halo events caused by negative lightning, and detailed comparison with similar type events caused by positive lightning. To date, only two (possibly three) negative events have been confirmed out of the several thousand positive events reported in the literature. These novel measurements clearly establish their optical and ELF/VLF characteristics.

1.7. Content of This Dissertation

Chapter 2 presents a theoretical discussion of electric field changes above thunderclouds due to cloud to ground lightning, as well as reviewing models that explain TLE characteristics. Chapter 3 outlines our first TLE observation campaign (Brazil 1) conducted in South America, in coordination with the Brazilian National Institute for Space Research (INPE), and the University of Washington. This campaign established the prevalence of sprites over Brazil. Chapter 4 describes a second TLE observation campaign (Brazil 2) that took place in Southern Brazil, where we witnessed one of the largest TLE producing storms was ever recorded. Chapter 5 contains a detailed study on

halo statistics using data from two large storms observed during the Brazil 2 campaign. This is followed by Chapter 6, which presents observations and analysis of extremely rare sprite and halo events associated with –CG lightning. Chapter 7 summarizes the dissertation results, and presents ideas for future research.

1.8. Epigraphs

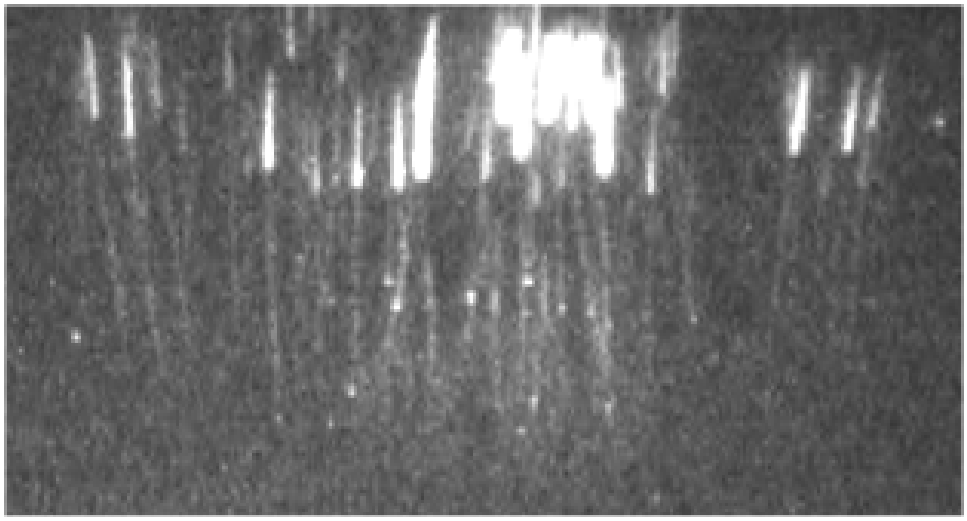
At the beginning of each chapter, an epigraph of a TLE observation is presented. These were taken from a public outreach program based at the Geophysical Institute at the University of Alaska Fairbanks (http://elf.gi.alaska.edu/) that describes observations and ongoing experiments in the sprite community. A link on this website solicits reports of similar observations from the public. The epigraphs at the beginning of each chapter are selected reports from these amateur observers. The epigraphs are accompanied by images of TLEs were captured by USU cameras during campaigns in the USA and in Brazil.

CHAPTER 2

TLE THEORY

"*Over the course of the past few nights, I have observed four sprites over eastern Arizona and southwestern New Mexico from two different observing locations. I was on Mt. Lemmon (about 9000' elevation) in the Catalinas (just north of Tucson) and looking almost due north at a line of storms about 80 to 100 miles away. Lightning activity was moderately active to sometimes very active. The sprites were difficult to see because of an intervening cloud layer and I suspect that there were more than two I saw that night. I saw two more under more favorable conditions the following night from Chiracahua Mountains in the southeastern corner of Arizona…….I tune my AM radio to a band with no station (typically 1710 kHz) to 'listen' to the lightning (and sprites?). I initially did this because it was a bit odd to watch lightning and not hear any thunder. My girlfriend and I even thought that there may be a difference in the static sound created by cloud-to-ground and cloud-to-cloud lightning. I should also like to note that distant station reception was enhanced compared with other recent nights when it was clear and I was stargazing…*"

— Jason Fields, amateur observer



A cluster of c-sprites, imaged over Northern Argentina at 08:20:46 UT by a USU imager on February 23, 2006.

2.1. Introduction

Within a few years of the first video capture of sprites, several campaigns were conducted [e.g., *Sentman and Wescott*, 1993: *Lyons*, 1994], and many new types of luminous events were discovered, named, and characterized. It soon became apparent that most of the new phenomena were closely associated with lightning, most probably driven from below by individual lightning strokes [*Winckler*, 1995].

Coordinated studies over the Midwestern U.S. (where a majority of early observations were carried out) showed that, in particular, sprites, elves, and halos were almost always associated with fairly large lightning strokes [average 81 kilo-Amperes (kA), *Lyons*, 1996]. One emerging anomaly was the fact that although elves were produced by both positive and negative CGs [*Barrington-Leigh and Inan, 1999*], sprites were almost exclusively correlated only with +CGs. Recent studies have shown that halos may be associated with either positive or negative CGs [e.g., *Frey et al.*, 2007].

Several different models have been proposed to explain each of these luminous events, and throughout the past decade, advancements in observation techniques have stimulated refinements in these theories. This chapter discusses the electric field above a thunderstorm immediately following a lightning stroke, and summarizes the currently accepted theories of TLEs.

2.2. Lightning-Driven Electric Fields

Electric fields form above lightning storms during the slow buildup of charge before a lightning flash and through currents associated with the lightning return stroke

and redistribution of charge by the currents. The return stroke drives the radiation fields while the continuing flow of the current forms quasi-static, near field radiation [*Rowland*, 1998].

Prior to initiation of lightning discharges, a thunderstorm usually develops a complicated, multilayered charge distribution within the clouds (see Chapter 1). The initial charges in the clouds build up over timescales of several seconds or longer. Because the atmosphere surrounding the cloud is conducting, even down to 10 km in altitude, any electric field above the thundercloud due to intra-cloud charges will be small, due to shielding of these charges by atmospheric conductivity. Lightning caused electromagnetic pulses (EMPs) have a much shorter time scale (microseconds), but atmospheric conductivity is small enough that EMPs do not affect electric fields until they reach the ionosphere. However, quasi-static electric (QE) fields can change on the orders of ms, so they are also weakly shielded by the atmosphere.

For simplicity, we assume that the positive charge reservoir at the bottom of a typical thundercloud is small, and deal with the large positive charge reservoirs (positive at the top of the cloud, and negative towards the middle) to form an electric dipole within the cloud. In the following discussion we closely follow derivations by *Rowland* [1998].

A lightning return stroke can be modeled as a uniform line charge and current flowing along a vertical axis z at a constant speed v (using cylindrical coordinates ρ, z φ,):

$$I(\rho, z, t) = vQ_z(\rho, z, t) = I_0\delta(\rho)H(z)H(t - z/v), \qquad (1)$$

where I is the current of the return stroke, Q_z is the distributed charge, δ is the Dirac delta function (included to localize the current to an infinitely thin channel at zero radius), and

H is the Heaviside function (to only include $z > 0$), and *t* is time. To conserve charge, an additional charge is placed at the origin:

$$Q(\rho, z, t) = -I_0 H(t)\delta(\rho)\delta(z)\,. \qquad (2)$$

If the lightning return stroke propagates at a normalized speed of ½ the speed of light, or $v = c/2$, it would take 70μs to travel a lightning channel 10 km long. This time would determine the duration of the electromagnetic pulse that is emitted by the return stroke.

2.2.1. Electromagnetic pulse (EMP)

One can solve equations 1 and 2 for the vector and scalar potentials. In the far field (using spherical coordinates) the electric field *E* is transverse [*Le Vine and Willet,* 1992]:

$$E_\theta = \frac{BI_0}{rc}\frac{\sin\theta}{1-\frac{v}{c}\cos\theta}\,. \qquad (3)$$

Here we assume a constant $\partial I / \partial t$ so *E* has constant amplitude during the pulse. The field is no longer equivalent to that of a standard dipole. We must also include image currents and charges. Assuming the Earth as a perfect conductor, for a –CG stroke, the return stroke is upward. The image ground field then has $I_0 \to -I_0$ and $\theta \to \theta - \pi$ in equation (3). If we sum the source and image fields, it gives the total radiation field [*Krider*, 1992]:

$$E_\theta = \frac{2BI_0}{rc}\frac{\sin\theta}{1-\frac{v^2}{c^2}\cos^2\theta}. \quad (4)$$

Substituting $z = r\cos\theta$, and using a trigonometric identity:

$$E_\theta = \frac{BI_0}{zc}\frac{\sin 2\theta}{1-\frac{v^2}{c^2}\cos^2\theta}. \quad (5)$$

For a fixed *r* (assuming $v/c < 0.7$) the maximum field is at the horizon. Now, taking some fixed altitude *h*, the field peaks at:

$$\theta_{\max} = \frac{1}{2}\cos^{-1}\left[\frac{(v/c)^2}{2-(v/c)^2}\right]. \quad (6)$$

If $v = 0$, which would be a typical dipole, $\theta = 45°$. As *v* increases, the angle θ will decrease. For example, if $v/c = 0.7$, $\theta \sim 36°$. Thus, given a vertical lightning discharge, the EMP will be maximum in a ring found around the lightning channel. The radius of the ring will be roughly equal to *h*, though relativistic effects will tend to reduce the radius [*Rowland*, 1998]. The maximum electric field will be:

$$E_{\max}(h) = 30\frac{(v/c)\gamma I_0}{h}, \quad (7)$$

where the units of the electric field *E* is in V/m, I_0 is in kA, and *h* is in km. The electric field has a null directly above the discharge.

2.2.2. Quasi-Static Fields

The current associated with the lightning return stroke will enhance existing charge differences inside the parent thunderstorm, or between the cloud and the ground. If a current continues long enough, and is large enough, the quasi-static field becomes stronger than the field due to the EMP. In the absence of shielding, the quasi-static electric (QE) field from a vertical current is:

$$E = -\nabla\Phi\,, \tag{8}$$

where the potential Φ is given by

$$\Phi = I_0 t\left[\frac{1}{\sqrt{\rho^2 + (z - z_d)^2}} + \frac{1}{\rho^2 + z^2}\right]. \tag{9}$$

Assuming $z_d << r = \sqrt{(\rho^2 + z^2)}$ where z_d is the discharge length, and substituting $Q(t) = I_0 t$, equation (9) may be reduced to

$$\Phi = \frac{Q(t) z_d}{r^3}\cos\theta\,. \tag{10}$$

The far fields solutions are:

$$E_\rho = \frac{2Q(t) z_d}{r_3}\cos\theta\,, \tag{11}$$

and

$$E_\theta = \frac{2Q(t)z_d}{r_3}\sin\theta\,. \qquad (12)$$

For a vertical discharge, the EMP is weakest above a discharge where the QE field is strongest. The ground image doubles this field strength. Thus for the EMP, the field strength is determined by vI_0/c while for the QE field, it is determined by Qz_d, which is known as the charge moment (M_{Qv}). This latter term is very important in the study of TLEs.

With a –CG, the lightning effectively removes negative charge from the cloud to the ground, and the positive charge reservoir will have a greater influence on the electric field above the cloud temporarily, producing an upward electric field. This field causes ambient electrons in the atmosphere to move toward the cloud. In the case of a +CG flash, the negative charge reservoir becomes, in a sense, unshielded, and creates a temporary electric field above the charge reservoir, which points vertically upwards. In this case, the atmospheric electrons would be accelerated upwards.

Both the EMP and QE fields due to lightning discharge are important in TLE formation, with EMP being primarily responsible for elve production, and QE fields being the main factor for sprite and halo production. Detailed models of these events follow in the next sections.

2.3. Sprite Models

Since the first confirmed observations in 1998, numerous sprite theories have been developed and subsequently published. For example, sprite models are given by

Pasko et al. [1995, 1996a,b, 1997a,b, 1998], *Milikh et al*. [1995, 1998a,b], *Fernsler and Rowland* [1996*], Taranenko and Roussel-Dupre* [1996], *Lehtinen et al*. [1997], *Roussel-Dupre and Gurevich* [1996], *Valdivia et al*. [1997, 1998], *Cho and Rycroft* [1998], *Rycroft and Cho* [1998], *Raizer et al.* [1998], *Yukhimuk et al*. [1998, 1999], *Veronis et al*. [1999] *and Barrington-Leigh et al.* [2001] among others. Theories of sprite generation begin with the production of electric fields, typically by one of two mechanisms: (1) the quasi-static electric field produced when a CG lightning stoke occurs (typically a +CG stroke) [e.g., *Pasko et al.,* 1995, *Roussell-Doupre and Gurevich* 1996], or (2) a radiation field generated by a horizontal cloud discharge [e.g., *Milikh et al.,* 1995; *Valdivia et al.,* 1997, 1998]. Since almost all sprites have been positively associated with +CG strokes, I will not discuss the second mechanism further here, and will focus on the quasi-static field theory.

These sudden electric fields accelerate electrons high in the atmosphere. If the electrons reach a high enough velocity, collisions with neutral air molecules can cause heating, and molecular excitation leading to optical emissions. Two processes have been proposed to explain the optical emission from sprites. One method assumes acceleration of low energy electrons to energies where they can collide with neutral atmospheric molecules, causing excitation, or even ionization, of these molecules. The other method involves high energy electrons which accelerate to the MeV energies. During collision with neutral molecules, if more of these runaway electrons are formed, a chain reaction may occur, possibly leading to breakdown [*Roussell-Dupre and Gurevich,* 1996].

2.3.1. Quasi-Static Heating and Ionization

Pasko et al. [1995] studied the effects of the QE field using a two-dimensional, cylindrical, Poisson solver to calculate the electric field. The model considered thermal breakdown based upon ionization rates calculated by *Papadopoulos et al.* [1996]. This ionization then modified the conductivity. Excitation rates from *Taranenko et al.* [1993a] were used to calculate the resulting optical emissions. Changes in electron mobility due to the electric field were specified from experimental data [*Rowland,* 1998].

With a typical (large) charge of Q = 300 C, they showed ionization down to 65 km in altitude. The first positive band of nitrogen ($N_2$1P), which emits in the red part of the visible spectrum, dominates the second positive band (blue emissions) by an order of magnitude. The authors pointed out that the emissions are a strongly non-linear function of charge Q. The *Pasko et al.* [1996a] study of quasi-static fields showed breakdown occurring below 50 km. After the CG discharge, a current must continue to build up to obtain a large enough charge Q; this could delay the appearance of the optical emissions for 1 to 20 ms. The model also predicted that the glow would be greater on the outside of the sprite, and that above 50 km, the $N_2$1P radiation is dominant, whereas below this altitude, the $N_2$2P emission may become stronger. This model is not dependant on the direction of the electric field, but predicts that optical emissions would start high in the atmosphere, where the mean free path of the electrons between collisions would be sufficient to accelerate electrons to sufficient velocities. The high-speed observations of *Stanley et al.* [1999] of upward and downward corona-like streamers from a starting point near 75 km would appear to support this model prediction. Figure 2.1 sketches the sequence of events which would cause this heating and ionization.

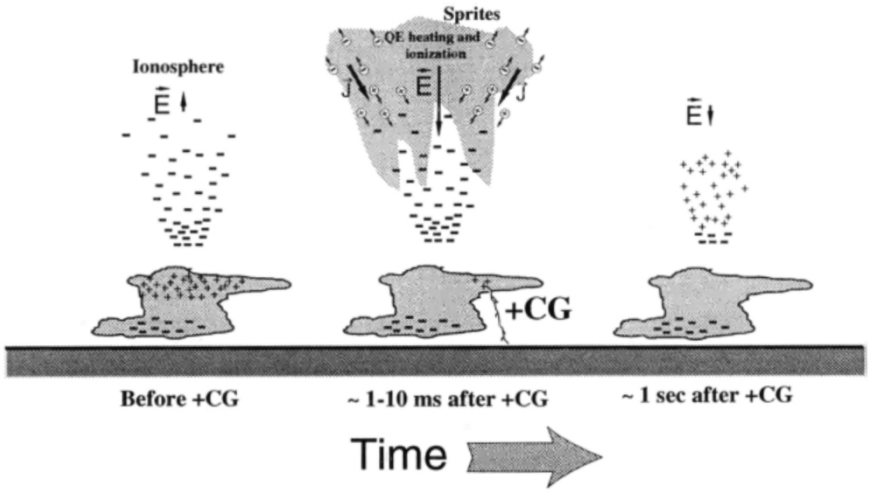


Figure 2.1. Mechanism showing QSF model, showing sprite formation after +CG stroke [*Pasko et al.* 1997a, Fig.2]. Reproduced by permission of the AGU.

It has also been proposed that intra-cloud lightning may play an important role in TLE production. Although not producing the QE fields necessary for sprites, this spider lightning may be important in transferring charge from one part of a cloud to another, thus enabling large charge and electric field buildup resulting in powerful CG discharges associated with sprites [for more details, see *São Sabbas and Sentman*, 2003].

2.3.2. Runaway Ionization

Gurevich et al. [1992] were the first to model air breakdown in lightning storms, and *Roussel-Dupre and Gurevich* [1996] extended this work to model sprite events. Their theoretical runaway model uses naturally occurring high-energy (MeV) seed electrons to initiate sprites and blue jets, producing gamma rays and RF bursts in the process. These high energy starter electrons cause ionization of the neutral atmosphere, producing and accelerating more electrons that continue the ionization process. This breakdown occurs when an electron reaches a kinetic energy in the range of 20 keV to 20

MeV. These seed electrons are given high velocities due to collisions with cosmic rays [*Rousell-Dupre et al.*, 1994]. Figure 2.2 shows a sketch of the electric fields involved. *Bell et al.* [1995] showed that increased conductivity reduces the E field and stops the runaway process after ~1ms. Above 80 km, the neutral density is so low that the runaways escape, and there is no additional ionization.

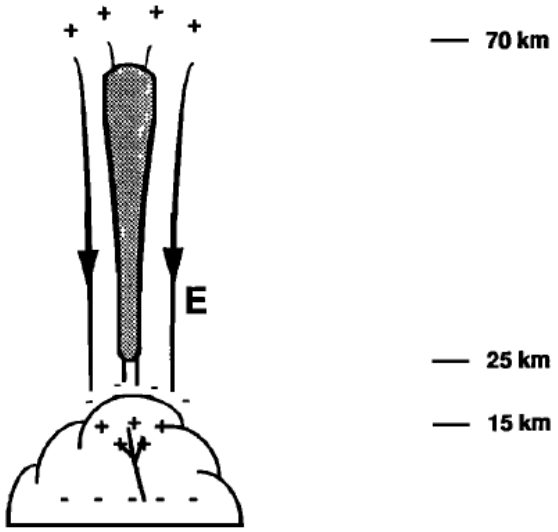


Figure 2.2. A sketch showing the electrical field, and subsequent sprite formation formed above a thundercloud after, in this case, a +CG lightning discharge, due to the runaway breakdown model [*Roussel-Dupre and Gurevich*, 1996, Fig. 7]. Reproduced by permission of the AGU.

This model requires a downward electric field, and thus a +CG lightning stroke for initiation. This model does show a breakdown process that starts with relativistic runaway electrons can produce a diffuse blue light from dissipation of the relativistic electron beam in the air, resulting in a trail of secondary, low energy electrons in the atmosphere that facilitate further breakdown in a lower electric field than for conventional breakdown [*Lehtinen et al.*, 1997]. Thus, it was originally thought that this model could characterize the blue tendrils seen in sprites [*Rakov and Uman*, 2003].

Recent high speed and high resolution observations have now shown that these lower altitude sprite components are individual streamers, and not diffuse glows. Thus, the runaway model is unable to explain the blue streamers of sprites [*Lehtinen et al.*, 1999, 2001]. The runaway-breakdown model also predicts the formation of x-rays and gamma rays with TLE production, although to date, this result has not yet been confirmed.

Pasko et al. [1997a] when forming their QE model did not attempt to explain the lower altitude sprite features, such as blue tendrils. This was due, mainly, to the lack of observations and understanding as to the morphology of sprite mechanisms at these lower altitudes. In retrospect, it is believed that the original QE model is unable to spatially resolve streamers. However, *Lehtinen et al*. [1997] did allow that both the conventional breakdown mechanism and the runaway mechanism might operate simultaneously in sprite formation. This finding was in essence, the precursor to the discovery of halos, which were unidentified at that time.

2.4. Elve Theories

The atmospheric density at the bottom of the ionosphere, near 90 km, is such that both transient radiation fields associated with return strokes, and other impulsive lightning processes, as well as QE fields, can accelerate electrons to sufficient energies to result in optical emission, via collisions with neutral molecules. *Inan et al.* [1991] investigated the effects of lightning on the lower ionosphere, as an explanation for absorption and phase changes of VLF sferics. A one-dimensional model was used to study the EMP and thermal heating of the lower ionosphere, as it related to VLF

propagation (this is discussed further in Section 2.7). They also pointed out that ionization of N_2 molecules around 90 km level could cause airglow emissions. *Rodriguez et al.* [1992] used this same model and looked at the EMP and thermal ionization at the lower boundary of the ionosphere. By using ray tracing, they showed that a vertical discharge would form an ellipsoid shaped region, creating a donut-shaped region of heating with the hole centered directly over the discharge. This model compared three different density models of the ionosphere, and varied the power of the lightning discharge, and did not consider refraction or reflection of power. Figure 2.3 shows a sketch of the electron ionization based on this model.

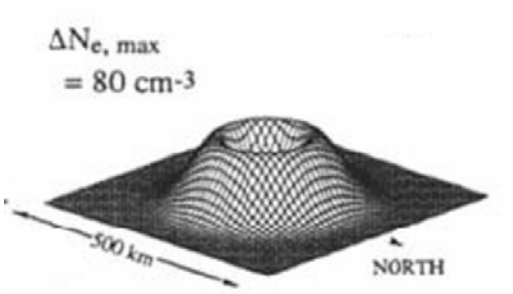


Figure 2.3. Electron ionization for a vertical discharge centered over a source. This figure is for h = ~93 km, with E_{100} (Electric field normalized to 100 km range) = 40 V/m [*Rodriguez et al.,* 1992, Fig. 4b]. Reproduced by permission of the AGU.

Since these original models were reported, many variations have been published [e.g., *Taranenko et al.,* 1993a,b; *Rowland et al.,* 1995, 1996; *Milkikh et al.,* 1995; *Inan et al.*,1996; *Glukhov and Inan*, 1996; *Sukhorukov et al.,* 1996b], each of which added new information and details. Additional effects and processes include, but are not limited to, reflection of the EMP pulse off the ionosphere [*Rowland et al.,* 1995], looking at dynamics due to lightning discharge orientations [*Rowland et al.,* 1996], plasma densities at the ionospheric boundary [*Sukhorukov et al*., 1996b], and simulations taking into

account relaxation times to achieve steady states in the ionospheric plasma [*Glukhov and Inan*, 1996].

2.5. Halo Theories

Pasko et al. [1995, 1996b, 1997a] developed a two dimensional cylindrically symmetric QE field model to investigate electric fields at mesospheric altitudes following sudden removal of charges at lower altitudes due to lightning flashes. Figure 2.4 illustrates the optical luminosity of the N_2 first positive band corresponding to the removal of 100-300 C of charge from a 10 km span of altitude. Although physically unknown at the time, this luminosity corresponds to what is now referred to as a halo. The establishment of large QE fields above thunderstorms is slow (~1ms) when compared with a typical lightning return stroke (~100μs). High speed video demonstrates that halos usually occur within 1 ms of the lightning stroke. This time sequence led *Barrington-Leigh et al.* [2001] to use a two-dimensional cylindrically symmetric electromagnetic model that includes both the EMP and QE fields to study elves, sprites, and halos. This model allows effective studies of lightning-driven ionospheric variations on time scales ranging from several μs to tens of ms. Figure 2.5 shows a time sequenced high speed video image, as well as models for the quasi-static electric field, (shown as QSF in the diagram), and the model due to an EMP. This figure clearly shows that the QE fields are the most probable mechanism for generations of sprite halos.

Using this model *Barrington-Leigh et al*. [2002] suggested that ionization and optical emissions in this halo region, as well as the lower streamer region of sprites, are observed to occur both as coupled events, or may occur separately. Halos are

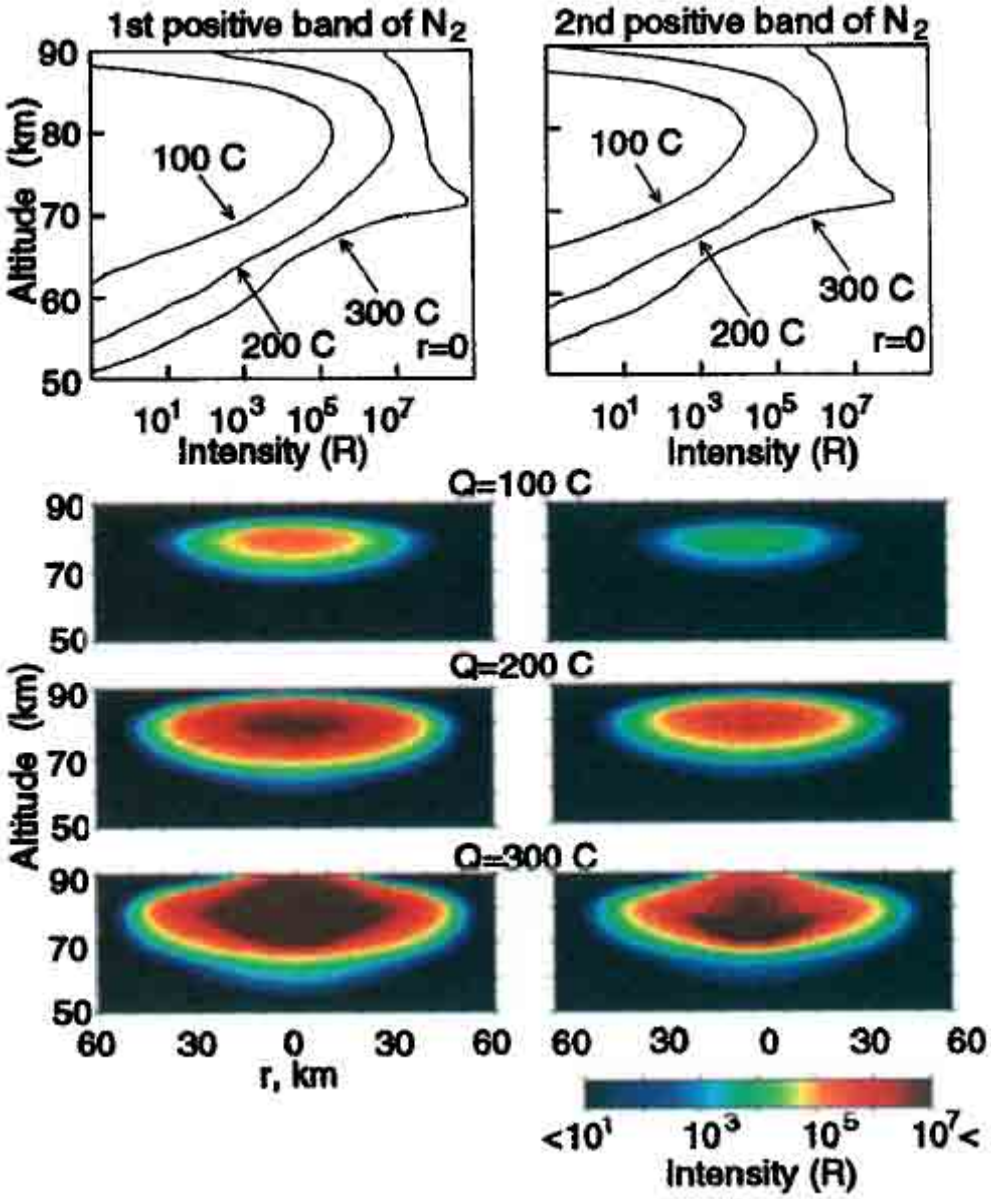


Figure 2.4. Simulation results for emissions from the 1st (left panel) and 2nd (right panel) positive bands of N_2 at 0.501 ms after lightning discharge. The top panels show the emission intensities just above the lightning discharge as a function of altitude for charges of Q = 100-300 C [*Pasko et al.*, 1995, Fig. 4]. Reproduced by permission of the AGU.

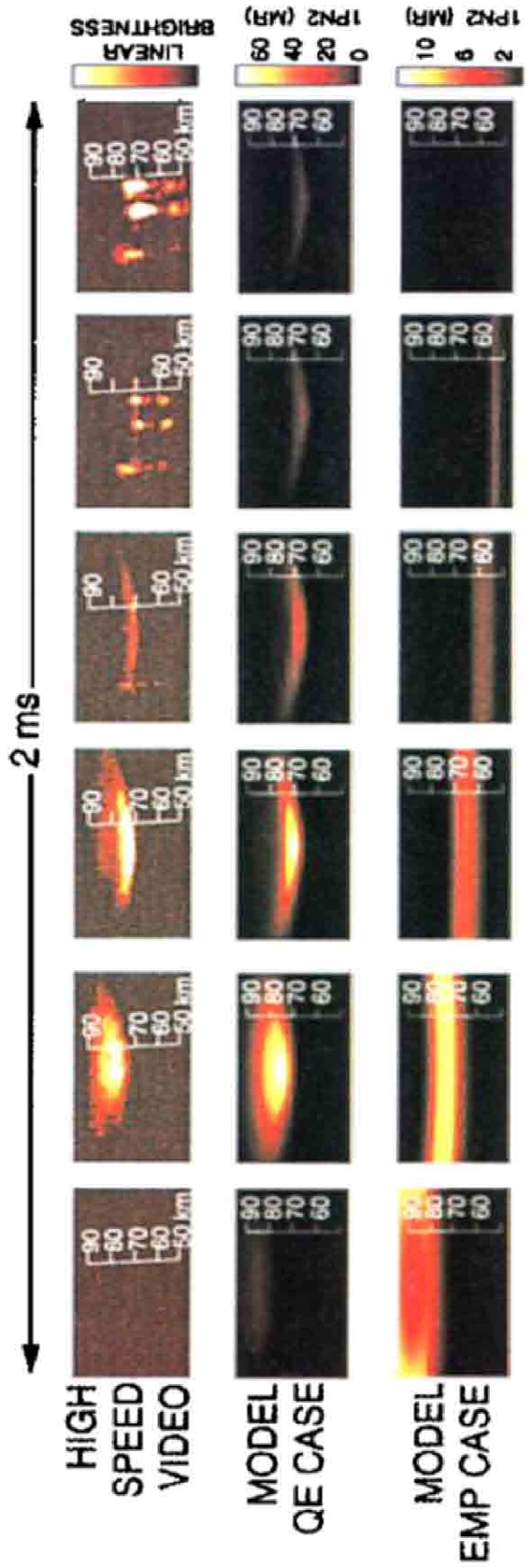


Figure 2.5. Comparison of observations (false colored), along with modeled QE and EMP fields [*Barrington-Leigh et al.*, 2001, Plate 6c]. Reproduced by permission of the AGU.

characterized by very fast relaxation of the driving electric field, owing to high conductivity at the lower edges of the ionosphere. The upward concave shape sometimes evident in sprite halos is due to enhanced ionization along the edges of the halo. They also discussed how since the timescale for electrical relaxation varies with altitude, a lightning discharge with a fast (<1ms) charge moment change may be sufficient to cause just a halo, especially if lightning currents do not continue to flow. Conversely, a sprite may occur without a halo if the lightning flash is characterized by slow currents.

2.6. Blue Jet Theories

In 1996 a model of blue jets was reported based upon positive charge streamers [*Pasko et al.*, 1996a]. When the QE field exceeds breakdown threshold at the top of the cloud, ionization occurs, and current flows into a streamer head so that the field increases, causing further breakdown. As the streamer head moves upwards, the process continues. This paper used the same process developed by *Pasko et al*. [1995] for sprite formation. Typical charges of 300-400 C are used with the charge reservoir assumed at an altitude of 20 km. Model results agreed well with limited measurements of the velocities and observed shapes of blue jets.

Sukhorukov et al. [1996a] also presented a model based upon ionization breakdown waves. In this model the streamer head is negative, and the QE field is pointed down, in contrast to Pasko's model where the streamer head is positive, and the QE field is pointed up. The Sukhorukov model requires an intra-cloud of positive polarity or a +CG discharge, moving at least 350 C of charge. Once again, modeled speeds are in good agreement with blue jet observations.

In agreement with the runaway electron model proposed by *Roussel-Dupre and Gurevich* [1996] for sprite production, Sukhorukov demonstrated that when the vertical electrical field falls below the breakdown field, the blue jets will stop propagating upwards; this usually occurs between 40 and 60 km. If *Q* is smaller than the 350 C used in the model, the terminal altitude could be much smaller, explaining blue starters [*Wescott et al.*, 1995]. Both *Sukhorukov et al.* [1996a] and *Pasko et al.* [1996a] showed that when the conductivity at the head of the blue jet matched the ambient conductivity of the atmosphere, the blue jet will stop propagating. Neither of these models have, to date, been definitively substantiated.

2.7. VLF/ELF Monitoring and Charge Moments

In 1994, during storms over the Great Plains, Walter Lyons and Dennis Boccippio compared video observations of sprites in Colorado with electromagnetic observations from a Massachusetts Institute of Technology (MIT) field station located in Rhode Island [*Boccippio et al.*, 1995]. They showed that sprite-producing lightning also excite Schumann resonances – electromagnetic wave modes in the natural Earth-ionosphere wave guide. Schuman resonances, being global, extend farther from lightning than the QE fields, which is substantial only at distances less than the height of the ionosphere [*Williams*, 2001].

Lightning causes low frequency (<20kHz) electromagnetic impulses (also known as radio atmospherics or sferics). *Boccippio et al.* [1995] showed that sprite-producing lightning strokes are very strong at the lowest frequencies (~<100 Hz). This discovery

provided a new method to study lightning-driven TLEs. The question that remained was why some lightning strokes cause TLEs while others do not.

Boccippio et al. [1995] and *Reising et al.* [1996] showed indirectly that the primary difference between lightning flashes producing sprites, and their non sprite-producing counterparts is that they contain larger charge moment changes (as introduced in section 2.2), and thus transfer more charge from the cloud to the ground. However, *Cummer and Inan* [1997] were the first to qualitatively measure the lightning charge moment change. Further methods and studies have since been conducted [e.g., *Cummer and Inan*, 2000; *Cummer and Lyons* 2005]. Measurements of these Schumann resonances and other extremely low-frequency (ELF) radiation from mesoscale convective systems (MCSs) show that for large +CGs, the changes in the charge moment may exceed 1000 C.km, which is much larger than the charge moments of negative lightning (~100 C.km) from ordinary thunderstorms, first measured by Wilson in the early 1900s. Since charge moments depend on charge transfer, as well as a displacement distance from the cloud to the ground, +CG flashes typically have larger charge moments, as the positive charge reservoirs in clouds are usually higher in altitude.

This method of studying sprites follows well established methods of studying CG flashes using remote electro-magnetic fields [e.g., *Norinder and Knudsen*, 1956] which have been used for decades. Information about different lightning parameters is embedded in the electromagnetic fields. Charge moment data is contained in sferics at frequencies below roughly 1 kHz (for a more complete description, see *Cummer and Inan* [2000]). These techniques are based on measuring the electrostatic field change resulting from a lightning stroke [e.g., *Krehbiel et al.*, 1979].

Using Schumann resonances, lightning charge moment data can only be resolved with approximately 20 ms time resolution, which is substantially longer than the typical delay between lightning and sprite formation. A new method was developed using both ELF and VLF radiation from lightning to calculate charge moment change [*Cummer and Inan*, 2000]. The chief advantage of using this band for lightning remote sensing is that the wider bandwidth enables sub-millisecond time resolution in calculating charge moments. Another advantage of this method is that ELF and VLF sferics are easily detectable many thousands of km away from the lightning stroke. An example of an ELF-VLF magnetic field waveform from a distant lightning stroke is shown in Figure 2.6. It has been theorized that to obtain TLEs above thunderstorms, there is a minimum threshold (~350-600 C.km) that must be met for initiation [*Cummer and Lyons,* 2005], with larger charge moments providing greater probability of TLE production [*Hu et al.,* 2002].

2.8. Summary

Many different models have been proposed for TLE production. However, the most accepted models agree on the following: elves are most likely caused by electro-magnetic pulses (EMPs) due to lightning discharges, where sprites and halos are due to quasi static-fields (QEs) due to similar lightning discharges. Blue jets and blue starters are quite possibly due to the same mechanism, but with different starting conditions, but are not obviously associated with cloud to ground lightning. Figure 2.7 shows the mechanisms of these events.

When multiple TLEs are formed due to the same lightning stroke, they typically

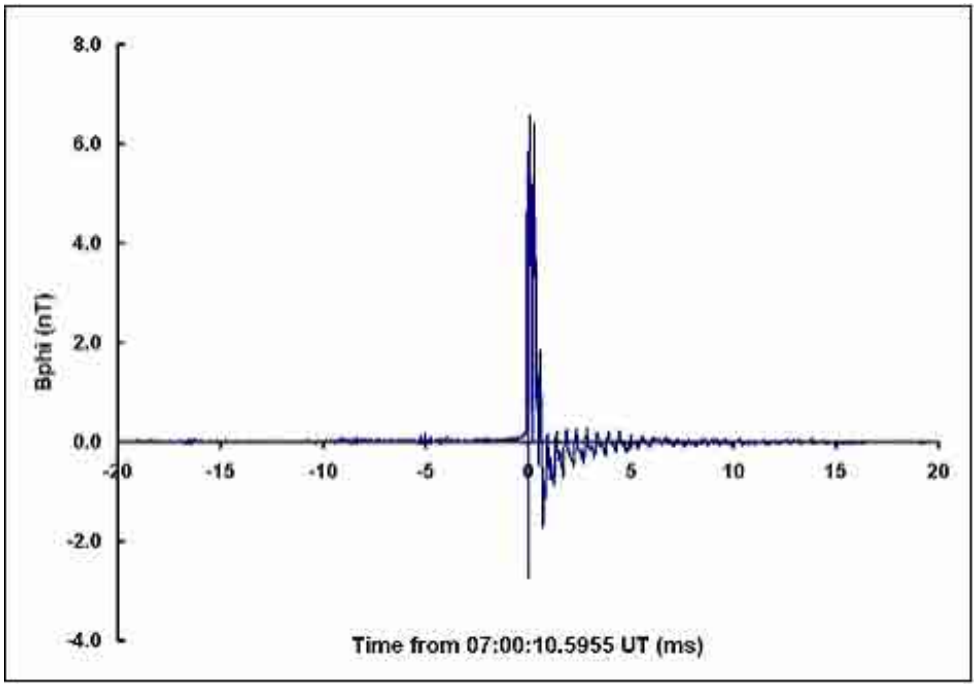


Figure 2.6. The ELF/VLF azimuthal magnetic field Bphi associated with a positive lightning stroke (Courtesy S.A. Cummer, Duke University).

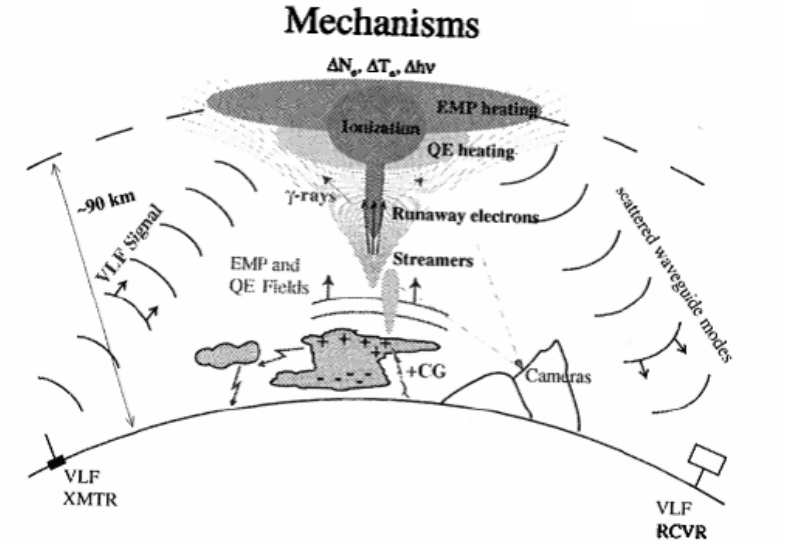


Figure 2.7. Mechanisms of ELVEs, sprites, halos, and blue jets [*Pasko et al.*, 1997a, Fig. 1]. Reproduced by permission of the AGU.

follow a specific sequence. High speed photometer and image measurements show ELVES occur first, followed within 10s of ms by a halo, which may or may not be followed by a sprite within a few ms. Figure 2.8 shows photometric data to this effect.

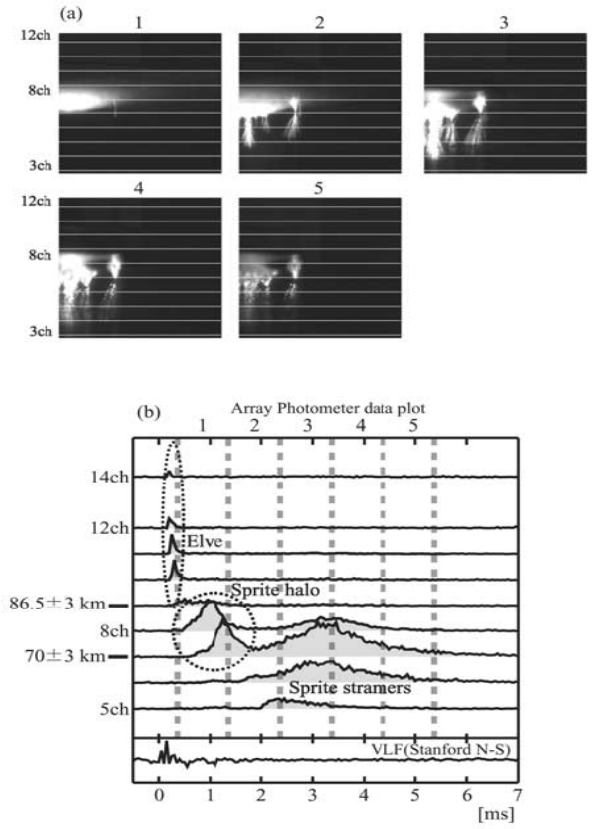


Figure 2.8. (a) High-speed image of a sprite-halo, captured from a ground station in Wyoming on August 18, 1999; (b) associated array photometer data plot and VLF sferics waveform [*Miyasato et al.*, 2002, Fig. 3]. Reproduced by permission of the AGU.

Recent global studies of ELF/VLF measurements have shown that TLEs are happening in many areas of the world. In fact, a recent study [*Sato and Fukinishi*, 2003] showed that during the fall and winter of the northern hemisphere, South America, and especially the northern Argentina/southern Brazil region, may be very active in producing TLEs. Figure 2.9 shows a global map of projected TLE occurrence based on these

ELF/VLF measurements. The two observational campaigns conducted in Brazil and discussed in Chapters 3 – 6 were stimulated by these findings.

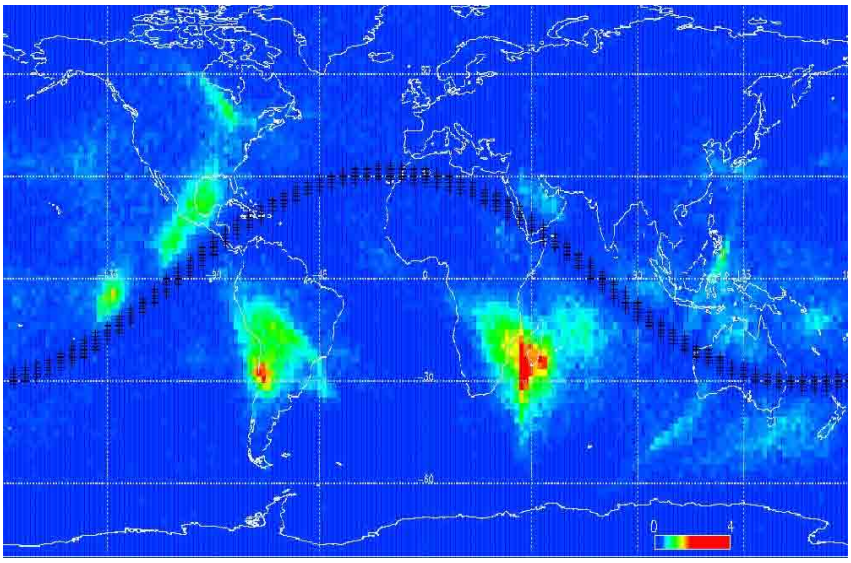


Figure 2.9. Global map of TLE occurrence in fall and winter of the northern hemisphere [*Sato and Fukunishi*, 2003, Fig. 4c]. Reproduced by permission of the AGU.

CHAPTER 3

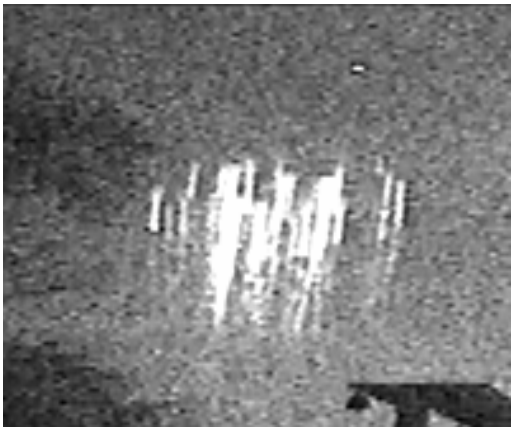
BRAZIL 1 CAMPAIGN

"I was amazed to read in New Scientist recently, that lightning coming out of the top of a thunderstorm had only recently been accepted as a real phenomenon!

I saw such an occurrence in the seventies. I was driving with my parents along the road from Umvuma to what is now Masvingo in Zimbabwe. We were on our way to spend the weekend at Kyle Dam. Ahead of us, perhaps 20 km away, was a single very tall thunderstorm. The rest of the sky was clear. The top of the storm was not flattened into an anvil, but looked rounded like the dome of a Van de Graff generator. From the top of this storm I clearly saw several 'bolts of lightning' going upwards. I seem to remember it looked like forked lightning going up from the top of the storm and dissipating in the clear air above the storm.

I remarked to my parents that there was lightning coming out of the top of the thunderstorm ahead of us, and I am sure they saw it too. All in all, I must have seen 5 or 6 occurrence of lightning above that storm before it stopped. I remember thinking that what I had seen was unusual, and I have never seen it since!"

— Richard Grant, Senior Lecturer, Department of Physics and Electronics
Rhodes University, Grahamstown, South Africa



First sprite imaged from the ground in Brazil. The data were obtained on November 25, 2002, and show a cluster of column sprites.

3.1. Introduction

In conjunction with the University of Washington and the Brazilian National Institute for Space Research (INPE), Utah State University participated in two exploratory campaigns to investigate TLE occurrence and properties over Brazil. The first campaign focused on intense thunderstorms over the state of São Paulo and was divided into two parts. The primary measurements were conducted from November 6 to December 14, 2002 during the austral spring, which was determined to have better weather conditions for our exploratory TLE observations. The second observation period was from February 22 to March 26, 2003, and was planned as a back up to gain supplemental information. Following the success of this campaign, a second observation program was conducted from Santa Maria, in the southern-most state of Brazil during austral fall, 2006. The U.S. participation in both of these campaigns was funded by the National Science Foundation (NSF). This chapter introduces measurements obtained during the first campaign.

Our first campaign in Brazil was strongly influenced by (then) recent ELF/VLF observations suggesting that South America is an important and prolific region for sprite production [*Sato and Fukunishi,* 2003]. Until this time, the only optical evidence of TLEs over South America was limited to a few chance measurements from the space shuttle in the early 1990's [*Boeck et al.,* 1995], and more recently, several TLE observations from the International Space Station (ISS) in October, 2002 [*Blanc et al.,* 2004]. Figure 3.1 shows the locations of the events imaged by the ISS. The primary goal of our first Brazil campaign was to perform exploratory ground-based and aircraft image

observations of TLEs over south-central Brazil in coordination with high-altitude, balloon-borne measurements by the University of Washington.

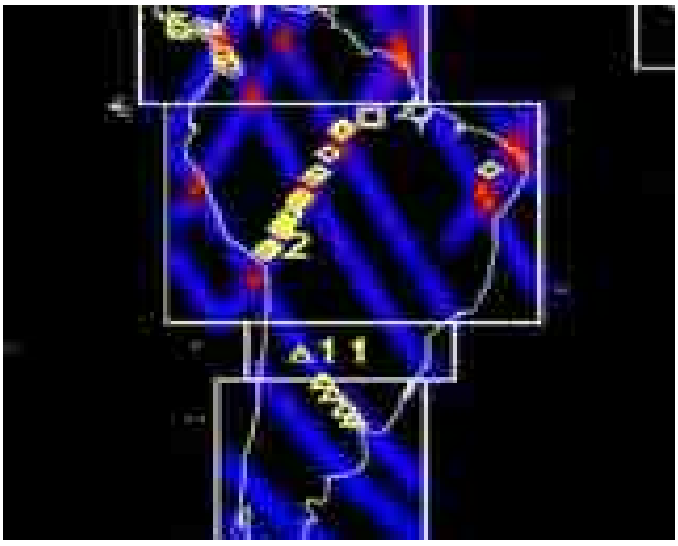


Figure 3.1. Map showing the locations of several TLEs detected by nadir pointing cameras on the International Space Station (ISS) [*Blanc et al.*, 2004]. The TLEs are indicated by the yellow diamonds, while the blue diagonal lines indicate the ISS orbital path. The numbers correspond to groups of TLEs imaged. Of particular note is #11, where five sprites were seen near the Brazil/Argentina border on October 6-7, 2002, about one month prior to our first Brazil campaign [*Blanc et al.*, 2004, Fig. 3]. Reproduced by permission from the AGU.

The two main mission objectives were:

1) To obtain novel near-field measurements of electromagnetic signatures of lightning-producing TLE events (electric and magnetic fields, their visible signatures, as well as possible x-rays), using a combination of balloon-borne payloads within the stratosphere and ground based/aircraft image observations.
2) To investigate the occurrence and morphology of TLEs produced over southern Brazil, for comparison with prior TLE observations, primarily from the U.S.A.

This program was recognized as ambitious, yet important, as up through the time of our campaign these objectives had never been accomplished in any previous experiment. TLEs have been imaged from a number of sites globally, and their characteristics have been studied remotely using their VLF signatures. Current models make discriminating predictions of electric fields and runaway electrons, but these models have yet to be substantiated, as there have been no successful in-situ measurements of the middle atmosphere electrodynamics within 100 km of TLE production.

Previous investigations of electromagnetic pulses (EMPs) produced by lightning have shown them to have an important effect on the ionosphere [e.g., *Kelley et al.,* 1985, 1990, 1997; *Li et al.,* 1991]. However, the lightning discharges studied were significantly smaller than the positive lightning discharges associated with TLE production.

Our campaign focused on the electrical coupling between the atmosphere and the ionosphere during sprite production. A similar balloon-borne program (dubbed the Sprites99 campaign) took place over the U.S. high plains in 1999 [*Bering et al.,* 2002]. During this campaign, stratospheric balloons were each equipped with a number of sensors to measure the in-situ fields and optical signatures associated with TLEs. Ground-based observations using low-light video cameras were also made from three sites (Yucca Ridge, CO, Jelm Mountain, WY, and Bear Mountain, SD) to identify the sprite signatures. The balloons reached altitudes of ~31 km, and succeeded in obtaining electric field measurements, some of which were correlated with sprites and halos imaged simultaneously from Yucca Ridge and Jelm Mountain [*Bering et al.,* 2004].

However, a key limitation of their campaign was that balloons were not allowed to fly directly over large TLE producing storms, due to safety considerations and difficulties in tracking the payloads. As a result, the measurements were performed at significant ranges from the storms, and they did not quantify the near-field signatures. It was later noted that the Sprites99 payloads utilized a low pass filter of 1 kHz, which complicated the interpretation of the mesospheric current data and their association with sprites [*Thomas,* 2005].

South-central Brazil was chosen as a location for our first Brazil (Brazil 1) campaign due to frequent and intense thunderstorm activity, and due to the limited flight restrictions for high-altitude balloon measurements. The U.S. Principal Investigator (PI) of this program (Dr. R. W. Holzworth, University of Washington) has a long-standing collaborative research program with INPE (Brazilian PI Dr. Osmar Pinto Jr.), and the INPE research site at Cachoeira Paulista (22.73° S, 44.93° W) was selected for these measurements. This research facility is located in the state of São Paulo, about halfway between the cities of São Paulo and Rio de Janeiro in south-eastern Brazil, and provided good facilities for the integration, testing and launch of the balloon payloads (supported by INPE), as well as a ground-based site for the imager measurements. This site was also in close proximity to a small airport at Guaratingueta where we outfitted an INPE aircraft with intensified cameras for our airborne sprite measurements.

Difficulties were expected in the observing conditions, so it was proposed that two ground stations and the INPE aircraft be employed in our TLE search. This required several cameras, some from USU, and some on loan from Dr. Peter Jenniskens, of the Search for Extra Terrestrial Intelligence Institute (SETI) and used previously for airborne

meteor studies. The aircraft was non-pressurized (it had a limited operational altitude of ~ 4500 meters), so it was planned for the plane to stand off from nearby storms and observe sprites emanating from them at the same time as the balloon payload performed in-situ measurements over the storms. To operate these multiple stations, the imager team consisted of Dr. Michael Taylor, Dr. Pierre-Dominique Pautet, and Matthew Bailey (all from USU), along with Fernanda São Sabbas (University of Alaska-Fairbanks).

Our efforts focused on the ground-based and aircraft image measurements to quantify the occurrence and spatial/temporal characteristics of TLEs during these two extended observing periods in the austral spring and fall. In particular, our objectives were:

1) To obtain simultaneous observations with the in situ balloon electric and magnetic field measurements to definitively correlate their association with TLEs.
2) To image TLEs on as many nights as possible to provide new evidence on the occurrence frequency of these events over South America.
3) To investigate the optical properties of the TLEs and their associated peak currents and charge moments of the causative lightning.
4) To study the relationship of TLE production with the tropospheric thunderstorms within the area.

The rest of this chapter describes the instrumentation used in the Brazil 1 campaign, our first ground-based measurements of sprites over Brazil, subsequent data analysis, and results.

3.2. Instrumentation

3.2.1. University of Washington Instrumentation

The University of Washington (UW) has considerable experience with prior balloon-borne and sounding-rocket measurements studying lightning [e.g., *Holzworth et al.,* 1985; *Holzworth and Bering*, 1998]. However, this was their first balloon program focusing on lightning associated with sprites, and as part of this campaign, UW designed a new stratospheric payload to be flown near and above thunderstorms. The payload included: (1) vector electric field sensors from DC to VLF (up to 195 V/m); (2) upward and downward looking X-ray sensors (20 keV – 1MeV); (3) vector VLF magnetic field sensors; (4) positive and negative polar ion conductivity detectors; and (5) an optical lightning detector [*Holzworth et al.*, 2005]. All of these instruments had been flown previously, except for a new electric field instrument, designed to dramatically increase the range of the vector electric field detector. This instrument was developed by Dr. Jeremy Thomas, and the Brazil 1 balloon measurements are described in his Ph.D. dissertation [*Thomas,* 2005]. All data were transmitted to ground using a new 3 megabit per second digital telemetry system [*Holzworth et al.,* 2005]. Figure 3.2 shows a photograph of one of the balloon payloads under testing in the INPE hangar. In this configuration, the insulated central payload is surrounded by deployed booms, which were used to measure the electric and magnetic fields. Figure 3.3 (a) shows a view of the hangar and the dirt runway used for the balloon launch at Cachoeira Paulista while (b) shows a photograph of a test payload shortly after launch from Tillamook, Oregon.

Unfortunately, no photographs were taken of the balloon during launch at Cachoeira Paulista due to the close proximity of a rapidly developing thunderstorm.



Figure 3.2. University of Washington balloon payload, under testing in INPE hangar at Cachoeira Paulista.

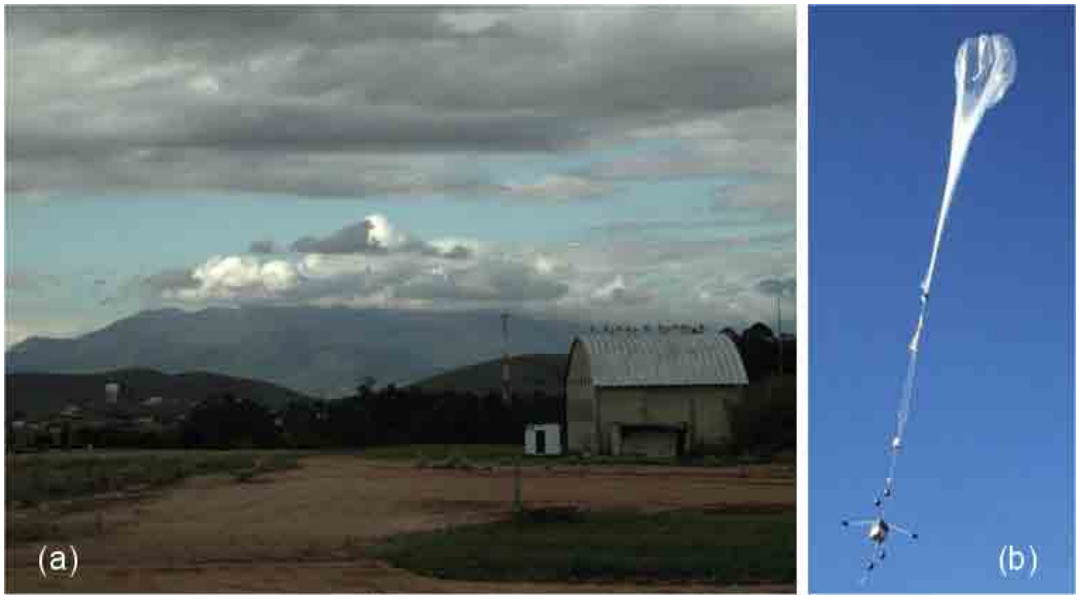


Figure 3.3. (a) View of the hangar and the dirt runway used for the balloon launch at Cachoeira Paulista, and conveys well the nature of these field measurements; (b) a photograph of a test payload shortly after launch from Oregon.

3.2.2. USU Instrumentation

The USU instrumentation consisted of two Gen III intensified Xybion ISG – 780 CCD cameras (operated at 60 Hz., field rate), and one Gen II intensified Xybion ISG – 750 CCD camera (operated at 50 Hz., field rate). In addition, three image-intensified Sony camcorders (on loan from P. Jenniskens, SETI Institute) were used to image TLEs during this campaign. Each camera was fitted with a GPS timing system (timing accurate to within 1 ms), and video data were recorded on Sony GV-D8000 digital video cassette recorders, using Hi-8 and SVHS digital video tapes. Each camera was fitted with standard lenses, providing fields of view ranging from 40 - 60°. Figure 3.4 shows a photograph of one of the Xybion ISG-780 intensified cameras. This instrument uses a GEN III intensifier, and required ITAR (International Trafficking in Arms Regulations) approval to be used in Brazil. This delayed the use of these cameras until the second phase (February/March 2003) of this program. The SETI instruments were used to make the first sprite measurements, as described below.



Figure 3.4. Xybion ISG – 780 Intensified CCD camera.

Figure 3.5 shows a photograph of the INPE aircraft used for airborne imaging of the sprites. This aircraft was based out of nearby Guaratingueta airport, a few km west of Cachoeira Paulista, and was used successfully to image sprites during both phases of the Brazil 1 campaign. As mentioned earlier, INPE provided this small aircraft to fly at night in the vicinity of thunderstorms, with the objective of capturing TLEs using our CCD video cameras mounted at low elevations looking out the windows. Figure 3.6 shows camera integration within the aircraft (the insert shows a close up of the SETI institute intensified camcorder). As the flights were limited to approximately three hours duration, after landing the cameras were removed and used for further ground-based measurements at Cachoeira Paulista.



Figure 3.5. Research aircraft provided by INPE for Brazil 1 campaign.

During the first phase (November/December 2002) of the campaign, two intensified Sony camcorders were installed on the aircraft, providing a wide overlapping field of view of (~80°). These camcorders were secured in such a way that they could be moved from one side of the aircraft to the other during flight, depending upon the



Figure 3.6. M. Bailey (foreground) taking a well-earned rest during camera integration, while Dr. Michael Taylor and Fernanda São Sabbas finalize adjustments to instrumentation. Insert shows the SETI intensified camcorder mounted on specialized moveable supports.

flight plan and the location of the target thunderstorm(s). In addition, a third intensified camcorder was stationed at Santa Rita do Passo Quatro (290 km to the north-west Cachoeira Paulista, see Figure 3.7). The choice of this second ground site was based on our expectation (using previous meteorological data) that most of the storms would develop to the southwest of Cachoeira Paulista. Having two ground sites also increased our probability of recording the TLEs during the prevailing stormy conditions, and provided the opportunity for triangulation on the sprites to precisely determine their geographic location and altitude.

During the February/March 2003 observing phase, the USU Xybion intensified imagers were available for measurements, and two were mounted within the aircraft, as well as two intensified Sony camcorders. This set up eliminated possible safety hazards



Figure 3.7. A map showing the state of Sao Paulo, Brazil, indicating the two ground sites of the Brazil 1 campaign, Cachoeira Paulista and Santa Rita do Passo Quatro.

encountered when moving imagers from one side of the aircraft to the other during flight. As measurements at Santa Rita do Passo Quatro were severely compromised by clouds during the first phase, a single ground site at Cachoeira Paulista was instrumented with the remaining camera.

3.2.3. Brazilian Lightning Network

Lightning data were obtained by a network developed at INPE (PI. Dr. Osmar Pinto) that was capable of measuring lightning parameters over a large area encompassing the southeast region and part of the south and central regions of Brazil [*Pinto et al.*, 2004]. At the time of the Brazil 1 campaign, the network composed 23 sensors (7 Impact and 16 LPATS sensors, see Appendix A for further details), and has

since been further enhanced. Data were analyzed to determine lightning location, number of strokes, peak current, and polarity. As intra-cloud lightning can contaminate the measurement of +CG strokes, a minimum event detection of 10 kA peak current was used during data analysis to help eliminate uncertainties in +CG detection by this network [*Pinto et al.,* 2004].

3.3. First Sprite Observations

On the evening of November 25, 2002, a Mesoscale Convective System (MCS) developed and moved over the state of São Paulo. After the storm passed over Cachoeira Paulista, and local cloud cover had significantly dissipated, we successfully imaged sprites from this storm located to the north near the city of Belo Horizonte, at a range of ~320km. The first image is shown in Figure 3.8, and consisted of a beautiful cluster of column sprites (occurring at 02:49:19.611 UT) that appear to be slightly tilted from the vertical. Within three minutes, a second single C-sprite was captured at the same location. These events were captured in the waning stages of the MCS, and no further TLEs were imaged. No balloon launch was attempted on this night. Nevertheless these first data demonstrated the existence and capability of measuring sprites over Brazil using ground-based stations [*Pinto et al.,* 2004]. A map showing the geographical locations of these two events, as determined by the Brazilian Lightning Network, is shown in Figure 3.9 (corresponding to events 1 and 2 in Table 3.1), together with a GOES satellite image of the storm at approximately the same time (2:40 UT).

The next night, November 26, a cold front moved over São Paulo and the neighboring state of Parana, generating strong storm activity. Although ground visibility



Figure 3.8. First ground-based observation of a sprite from Cachoeira Paulista, Brazil. The event comprised a cluster of near vertical C-sprites observed at low elevations, at a range of 320 km. A tree obscures the view to the left, and a tractor is evident in the foreground. The GPS information indicates the date and time of this event, and the latitude and longitude of the ground site.

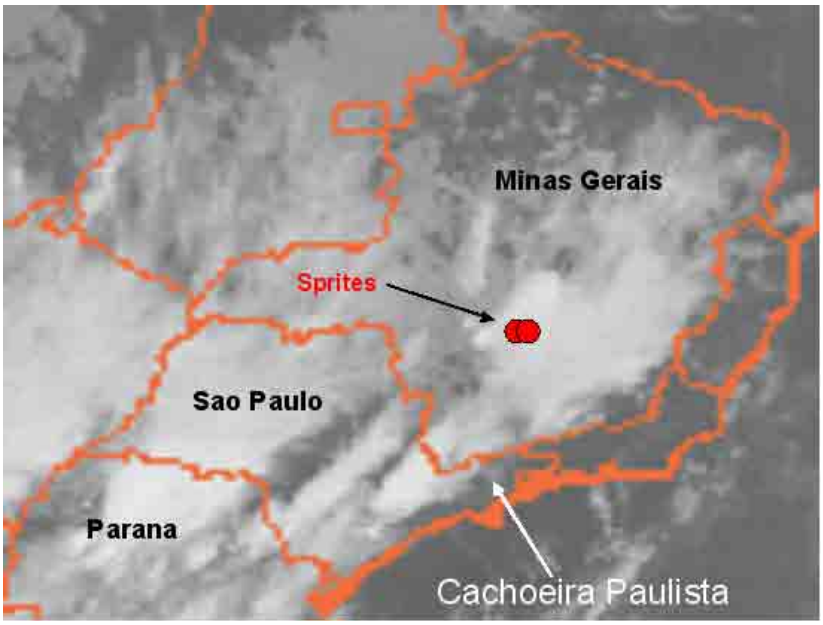


Figure 3.9. Satellite image showing locations of the two sprite events captured from ground-based cameras on November 25, 2002, as well as the observation site at Cachoeira Paulista. This image was taken at 02:40 UT.

was limited at Cachoeira Paulista, the aircraft was able to take off and fly alongside a large storm in a clear corridor (as shown in Figure 3.11). This was the first instrumented test flight of the aircraft, and four sprites were successfully imaged to the southwest of Cachoeria Paulista (corresponding to events 3 – 6 in Table 3.1) and comprised several carrots and clustered columns. An example of one of these events (#6) is given in Figure 3.10, and shows two isolated carrot sprites to the right of the field of view with lightning activity illuminating clouds at lower elevations to the left. This event was captured at 03:09:50.630 UT. Figure 3.11 maps the location of events 3, 4, and 6, as identified by the lightning network. The image data show that event 5 occurred at a similar azimuth to the other events, but was not detected by its lightning signature. The GOES map showing the location of the aircraft and the sprite events is given in Figure 3.11. All four events were recorded at ~ 300 – 350 km range from the aircraft.



Figure 3.10. Carrot sprites imaged from the INPE provided aircraft on November 26th at 03:09:50.630 UT. Note the lightning illuminated clouds below.

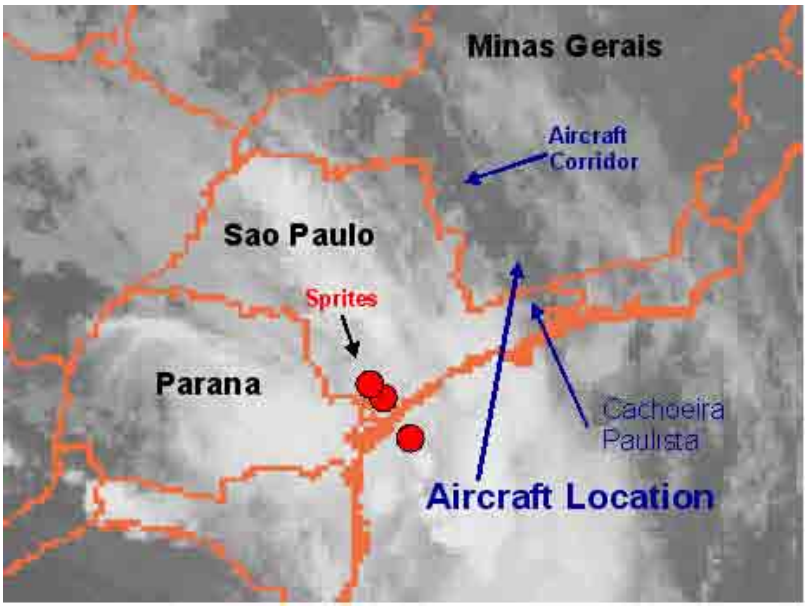


Figure 3.11. Map showing location of the three events captured on the night of November 26, 2002, along with the corresponding satellite image showing the cold front at 2:40 UT. Also shown is the approximate location of the aircraft as it captured the TLE images.

Meteorological conditions again did not allow for the launching of the balloon-borne payload on this night, and no corresponding electric or magnetic field measurements were made. Ground-based measurements were continued until Dec 14, but no further sprites were imaged due to deteriorating weather conditions. However, a balloon was successfully launched on December 6-7, and high-quality in-situ measurements were made above an intense localized storm that grew rapidly. The balloon achieved an altitude of 34 km, and detected exceptionally large vertical electric fields of 140 V/m, more than an order of magnitude higher than previous measurements taken at >30 km altitude [*Holzworth et al.,* 2005]. This electric field was clearly associated with +CG with a peak current of 53 kA, and may have been associated with a TLE. However, the onboard photometer did not register any optical signature, and from

the ground we were not able to correlate this event with a sprite, as the close proximity of the storm restricted our aircraft and ground observations on this occasion.

In summary, the first phase of this exploratory campaign was successful in detecting and measuring sprites over Brazil and in obtaining high-quality balloon-borne measurements of large lightning-generated electric fields. However, our efforts to obtain coincident balloon and ground-based measurements were thwarted by rapidly changing meteorological conditions. As a result, further measurements were planned for the following austral fall period in 2003.

3.4. Phase 2 Sprite Measurements

During the second phase of the Brazil 1 campaign (February 22 – March 26, 2003), images of TLEs were captured only on March 21, 2003, which proved to be a very active night. On this occasion, there were many storms in the area, and TLEs were imaged from four separate storms; three of which developed within a large cold front moving in from the southwest, and one of which was associated with a local air mass thunderstorm to the northeast [*Pinto et al.*, 2004]. Figure 3.12a summarizes the events imaged by our cameras, These events were successfully located by the Brazilian lightning network and the associated satellite imagery are shown at two times, 01:40 and 07:10 UT, identifying active regions in the cold front.

On this night airborne measurements were made during the early evening hours, and two sprites were detected, one from the isolated storm to the northeast (~00:40 UT), and the second (not registered by the lightning network) from an active region in the cold front near the coast to the southwest. Subsequently, ground-based observations from

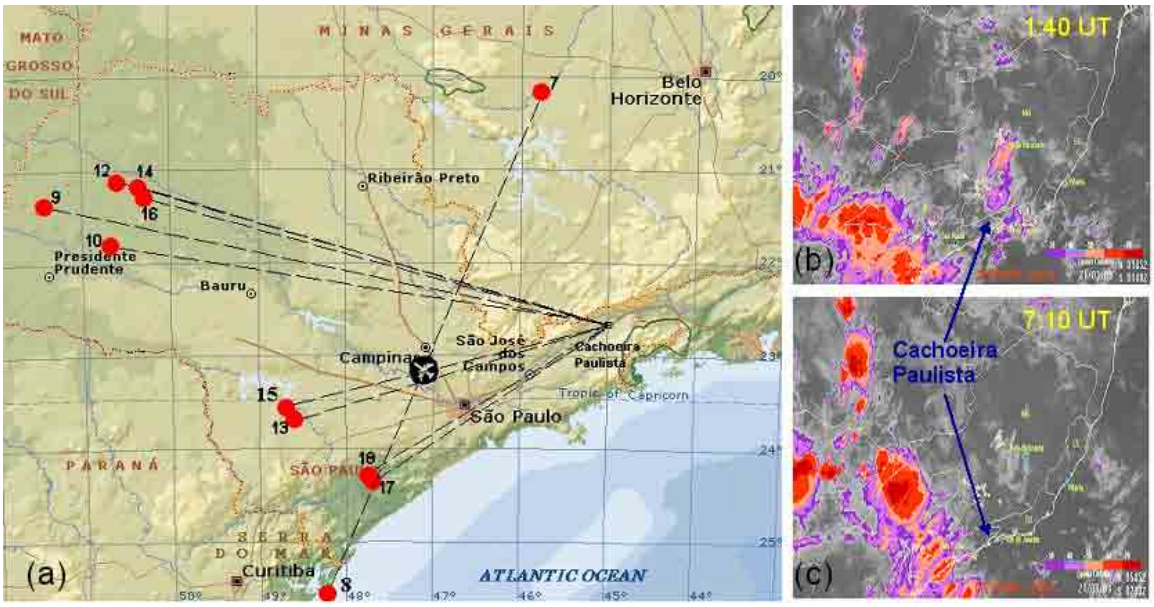


Figure 3.12. (a) Map showing locations eleven TLE events (events 7-10, 12-18, Table 3.1), imaged on March 21, 2003, and correlated with positive lightning discharges recorded from the Brazilian lightning network. These events were imaged both from the ground and the aircraft. An additional event (event 11) had no associated lightning signature; Inserts b and c show satellite infra-red images (01:40 and 07:10 UT) locating intense convective regions in the cold front where sprites were produced.

Cachoeira Paulista captured a further 10 sprites (events 9-18, as listed in Table 3.1) originating from the two main active areas to the west (around 06:15 UT) and southwest (~07:00 UT) as indicated by Figure 3.12a. Unfortunately, again no balloon measurements were possible on this night due to strong winds at Cachoeira Paulista. A collage illustrating 16 of the 18 TLEs observed during the Brazil 1 program is shown in Figure 3.13. The majority of the events were sprites, ranging from a faint unit sprite (e.g., event 2) to multiple carrots (e.g., events 6 and 16), and clustered c-sprites (e.g., events 1, 4, and 17), with only two halo/elve detections.

3.5. Results

Separately, the balloon-borne payload succeeded in capturing in situ

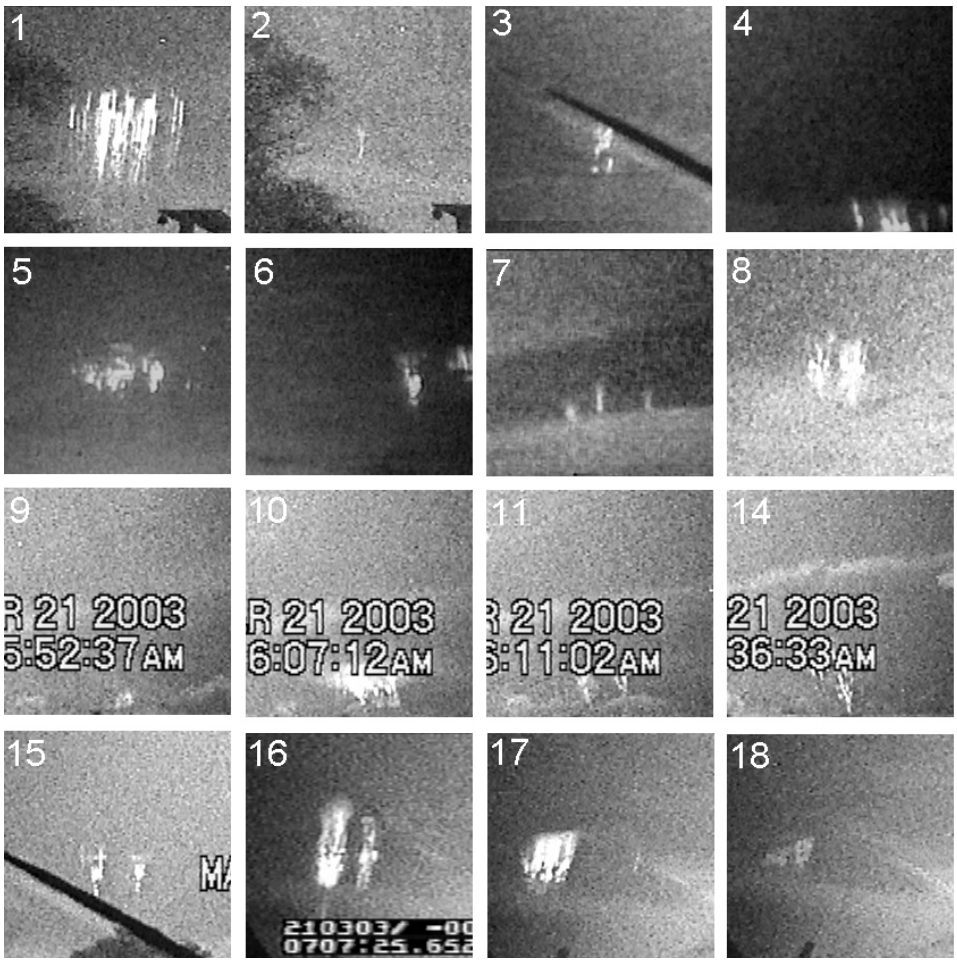


Figure 3.13. Images of 16 sprite events seen during the Brazil 1 campaign (excluding events 12 and 13).

measurements indicating very high electric fields over intense thunderstorms, while the ground-based and airborne images established the frequent presence of sprites over Brazil (they were imaged whenever observing conditions permitted), and their direct association with lightning events as determined by the lightning network. The analysis of the lightning data showed that all TLEs were correlated with +CG (as detected by the Brazilian lightning network) lightning strokes, with the possible exception of event 8, whose lightning signature was ambiguous. Peak currents ranged from 26 – 150 kA, the

lowest values of which are somewhat smaller than typical peak currents over the mid-western U.S. associated with sprite production [*Lyons*, 1996].

Table 3.1 summarizes the 18 TLEs imaged on this campaign, and compares the GPS times of the optical emission with the lightning detections (two of which had no corresponding lightning data). The peak currents are also listed together with their calculated impulsive charge moment changes (the charge moment for the first 2 ms of the lightning stroke), as discussed in Chapter 2 and Appendix B. These were determined using ELF/VLF signatures of the parent lightning strokes, as measured at Syowa Station, Antarctica by H. Fukunishi and M. Sato, Tohoku University, Japan. These independent measurements confirmed the positive polarity of the sprite CGs in each case, and revealed a broad range of impulsive (2ms) charge moments (an order of magnitude) associated with these events, varying from 153 C.km to 1497 C.km.

It is interesting to note that some (~18%) of the charge moments were less than 300 C.km, which is a surprising result since this is considered as an approximate working lower limit for TLE production, at least for spriting storms over the U.S. [*Cummer and Lyons*, 2005]. This result has been further investigated by *Hu et al*. [2002] who determined the probability of sprite initiation as a function of charge moment, for a single spriting storm over the U.S. Their results are illustrated in Figure 3.14. Of the 76 events they analyzed, the overwhelming majority were associated with large charge moments over 600 C.km, with only 18% occurring in the 200-600 C.km range, and 4% with lower charge moments. In comparison, our Brazilian observations indicate 71% below 600 C.km.

Table 3.1. Summary of all Brazil 1 TLE events, including peak current (from the Brazilian Lightning Detection Network), and impulsive charge moment changes (from ELF/VLF measurements, Tohoku University, Japan).

Event #	DATE (UT)	CAMERA TIME (UT)	LIGHTNING TIME (UT)	Peak Current (kA)	Charge Moment (C*km)
1	11/25/02	02:49:19.611	02:49:19.362	41	519
2	11/25/02	02:52:15.822	02:52:15.685	45	236
3	11/26/02	03:00:11.947	03:00:11.867	33	525
4	11/26/02	03:03:07.524	03:03:07.432	44	374
5	11/26/02	03:08:51.471	03:08:51.470	122	1087
6	11/26/02	03:09:50.630	no corresponding lightning		465
7	3/21/03	00:41:11.374	00:41:11.337	29	617
8	3/21/03	02:04:01.397	02:04:01.333	44	584
9	3/21/03	05:52:19.449	05:52:19.463	150	1497
10	3/21/03	06:06:54.790	06:06:54.691 or 6:06:54.749679	124 or 93	1090
11	3/21/03	06:10:45.130	no lightning data		
12	3/21/03	06:22:19.740	06:22:19.692	101	379
13	3/21/03	06:32:39.630	06:32:39.604	146	153
14	3/21/03	06:36:15.930	06:36:15.774	28	433
15	3/21/03	06:38:03.220	06:38:03.192	35.1	555
16	3/21/03	07:07:25.652	07:07:25.055	30	271
17	3/21/03	07:12:15.011	07:12:14.986	28	1070
18	3/21/03	07:14:41.592	07:14:41.576	26	326

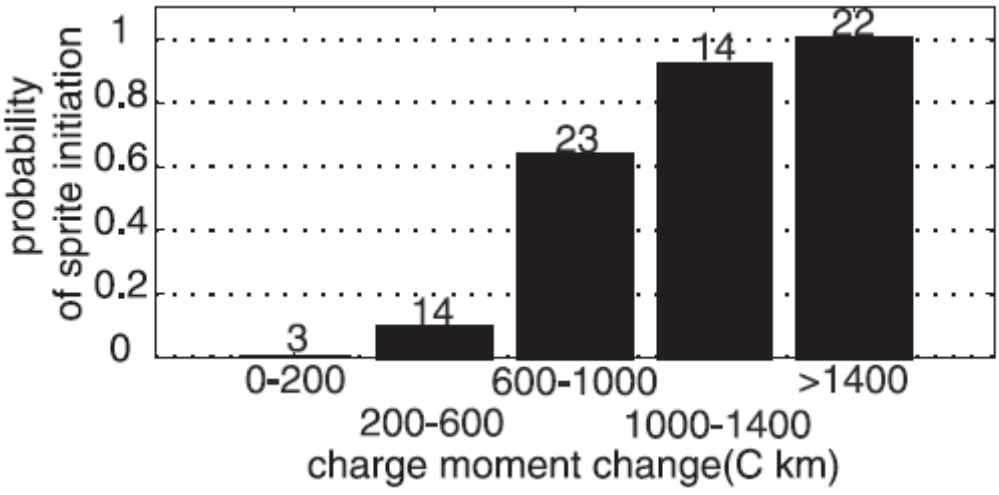


Figure 3.14. Probability of sprite initiation vs. charge moment change for positive CG discharges. The numbers labeled above each bar indicate the number of sprites (76 total) [Reproduced from *Hu et al.*, 2002, Fig. 6].

To investigate our data further, we have analyzed all lightning events with peak currents >26 kA (the lowest peak current associated with a sprite, Table 3.1) that occurred within our ground-based cameras' fields of view for March 21, 2003. Tohoku University determined the charge moments associated with each of these events (regardless of whether they produced a TLE or not). Results are plotted in Figure 3.15. Within the cameras' fields of view, a total of 125 events had peak currents of over 26 kA. The number of lightning events that did not produce TLEs decreased rapidly with increasing charge moment. Also shown on the plot are the charge moments for the +CGs associated with all 18 TLEs. This shows that as the charge moment becomes larger, it is more likely that a +CG flash will cause a TLE. This result agrees well with the study of *Hu et al.* [2002] over the Mid-western U.S.

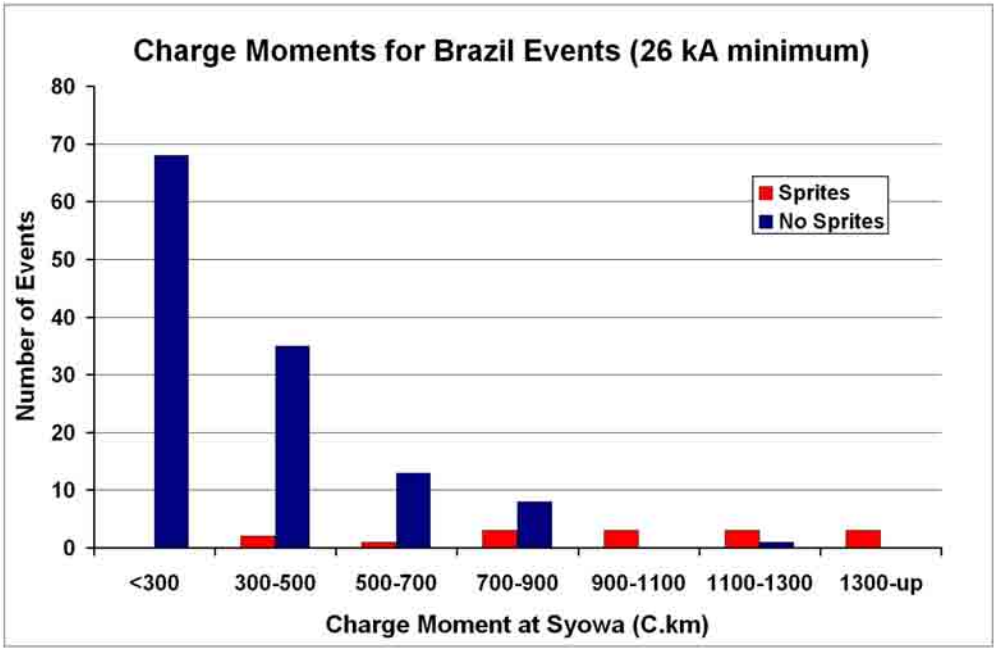


Figure 3.15. Plot showing all lightning flashes >26 kA peak current within ground cameras fields of view, for March 21, 2003. For comparison, the distribution of charge moments for the 18 TLEs is indicated.

3.6. Brazil 1 Campaign Summary

The Brazil 1 campaign was important in many ways, mainly in establishing the apparent prevalence of sprites over Brazil, an important region that had not previously been studied. These coordinated balloon and ground-based measurements also raised many questions. *Pinto et al*. [2004] showed that during the storms associated with TLE production, sprites occurred when the percentage of positive flashes in the storm was much higher than the average percentage for the whole life of the storm. All sprite events were also associated with +CG flashes with average peak currents larger than mean peak currents of the positive CG population within the same storm. Although direct correlation with image data proved to be extremely difficult, the balloon-borne instrumentation measured the largest electric field change (>140 V/m) ever observed above 30 km. However, as discussed in *Thomas et al.* [2005] this electric field change was not deemed large enough to initiate conventional breakdown, which would result in a TLE. *Thomas et al*. [2005] hypothesized that the measured electric fields support the QE model for sprite production, and suggest further measurements were needed to correlate the electric field changes with TLE imagery.

Our study of the charge moments associated with sprites observed in this campaign suggests significant differences in the storms capable of creating sprites over Brazil as compared with their U.S. counterparts. However, as research groups use different methods to determine charge moments, it is also possible that this discrepancy may lie solely in the analysis of the charge moments. As will be discussed in Chapter 4 (which details further measurements from Brazil), this led to the inclusion of ELF/VLF measurements by the Duke University group who developed a robust estimate for the

impulsive (2ms) charge moments. As a result of the Brazil 1 campaign and the questions it raised, a second sprite measurements program was planned for February-March of 2006. This campaign and its results are discussed in Chapters 4, 5, and 6.

CHAPTER 4

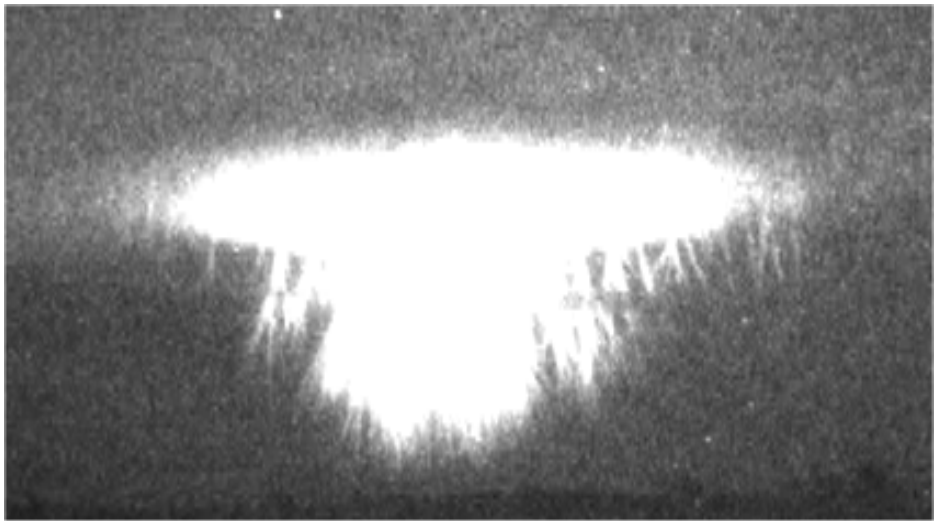
BRAZIL 2 CAMPAIGN

"In 1991, I was with my family at a KOA campground in far northeastern New Mexico. That night, a huge thunderstorm developed in the distance. I was in high school at the time, but was interested in meteorology.

The thunderstorm was huge and the lightning was very impressive. Lots of branched fingers of lightning which propagate upwards throughout the mesocyclone, illuminating the entire storm – it was probably the most beautiful storm I have ever seen. The campground was in a flat area and the storm was sufficiently far away to see it in its entirety.

During the storm, I noticed weird blue flashes above the cloud from time to time. I didn't know what they were. I figured they were some weird optical illusion, or maybe reflections off my glasses or something. Several years later I saw a report on TV and realized that I had seen blue jets. They were definitely blue jets because they "poofed" upwards in an inverted cone shape almost like a fountain. During the storm I noticed maybe 15 to 20 of these….."

—Joe Warmbrodt, amateur observer



Example of a sprite-halo imaged over Northern Argentina on February 23, 2006. The event was particularly bright, and temporarily overloaded the camera, but nevertheless it clearly shows a well-developed horizontal halo structure, with superposed vertical sprite tendrils.

4.1. Introduction

Following the first Brazil sprites campaign, which demonstrated that TLEs are an important and prominent phenomena in Brazil, a second joint NSF/INPE campaign was funded with the following main objectives: (1) to obtain new coordinated in-situ balloon and image measurements, and (2) to investigate TLEs from exceptionally large, long duration storms located over southern Brazil and northern Argentina. This campaign was somewhat different in instrumentation, field techniques, location, and results from the Brazil 1 campaign. In particular, an important technical aspect of this new program was to overcome inherent problems of obtaining coordinated imagery by including a small all-sky imager on the balloon payload.

Santa Maria is centrally located in the southernmost state of Brazil, Rio Grande do Sul, which borders Argentina and Uruguay. This site was chosen as the primary base for the Brazil 2 campaign (see Figure 4.1). In this region of Brazil, as well as neighboring Argentina and Uruguay, exceptionally large MCS storms, such as those that form over the midwestern U.S., occur frequently during the late spring and early autumn seasons. This new location in southern Brazil provided an excellent opportunity to fly a balloon-borne payload over exceptionally large TLE-producing storms.

The Federal University of Santa Maria (UFSM) and co-located INPE facilities provided housing and support for the balloon payload integration, testing, and launch. In addition, a ground-based measurement site was set up at the Southern Space Observatory (SSO), located on a plateau at São Martinho da Serra (29.4°, 53.8° W), approximately 30 km to the north of Santa Maria. This isolated facility (altitude 480 m) enabled high-quality observations at ranges of up to ~1000 km over a broad azimuth range, as there

were few viewing obstructions, and no lights from nearby cities to pollute the image data. This is illustrated in Figure 4.2, which shows a view to the south and west from SSO.



Figure 4.1. Map showing the location of Santa Maria, in Rio Grande do Sul, which was the center for the Brazil 2 campaign.



Figure 4.2. Wide field image from the ground site (29.4° S, 53.8° W) at the Southern Space Observatory (SSO) showing excellent viewing conditions at low elevations over a broad westward azimuth range.

As with the Brazil 1 program, this second campaign was a cooperative endeavor with the University of Washington, INPE, and Utah State University. In addition, Duke

University provided new ELF/VLF instrumentation at SSO to record near-field lightning sferic data to determine the impulsive charge moments of the TLEs. The University of Washington refurbished the balloon-borne payloads which were modified to include an all-sky camera provided by USU, while INPE provided the integration and balloon launching facilities and personnel. Utah State University also fielded cameras at SSO for ground-based sprite measurements alongside the Duke University ELF/VLF detectors.

This chapter describes this second campaign, including the instrumentation and detailed discussion of two MCS storms which occurred in February and March, 2006, and their associated TLEs measurements. Chapters 5 and 6 present statistical studies of halos and sprite-halos, and rare measurements of TLEs caused by –CG discharges discovered during one of these storms.

4.2. Instrumentation

4.2.1. USU Imaging Instrumentation

During the Brazil 2 campaign, image measurements were made using two Xybion ISG – 780 GEN III intensified CCD cameras for ground-based observations, and four new WATEC WAT-120N cameras, one each mounted on top of the four balloon payloads. The addition of the WATEC cameras provided a new capability for real-time measurements of TLEs from the balloon at ranges of up to several hundred km, thereby negating problems of local cloud cover that often inhibited coordinated measurements from the ground during the Brazil 1 campaign. Figure 4.3a shows a photograph of the WATEC cameras, fitted with a Fujinon YV 2.2 x 1.4 A-2 all-sky lens. The camera is small, lightweight (6.3 cm long, and 150 grams without the controller and lens), and low

power, making it ideal for balloon-borne measurements. Furthermore, WATEC cameras have been used successfully to image sprites, as well as giant jets [*Su et al.*, 2003].

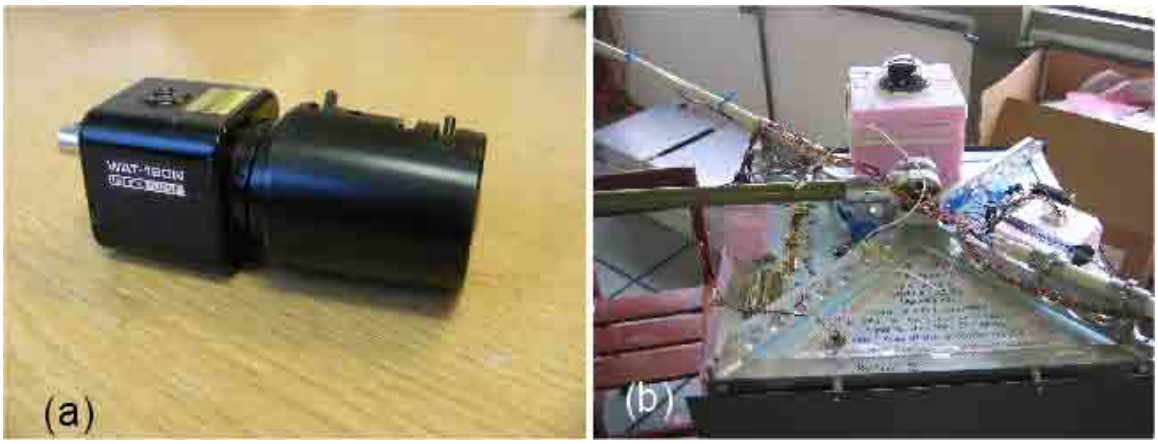


Figure 4.3. (a) WATEC 120N Camera, fitted with a Fujinon all-sky (180°) lens. (b) Close-up showing WATEC camera mounted on top of the balloon payload (in pink insulated box).

For the balloon-borne measurements, the camera was environmentally tested at the University of Washington, to simulate cold, low pressure atmospheric conditions at nominal balloon altitudes (> 30km). Our plan was to switch the camera on at launch, and to continuously transmit video data via a separate telemetry link from the balloon-borne payload during the course of each mission. Two receiving stations, one at the launch site at Santa Maria, and the second at SSO, were used to record the video data, as well as to superimpose GPS timing information on each video field (positional information was recorded onboard the balloon payload and transmitted separately with the other instrument data). Figure 4.3b shows a close-up of the camera mounted on the top of one of the balloon payloads. Each system was housed in a lightweight insulating box, fitted with a Perspex dome, enabling all-sky viewing (except in the zenith, which was blocked

by the balloon), and was purged with dry nitrogen for an extended period of time prior to each launch, to eliminate problems with condensation of the inside of the dome.

As with the Brazil 1 campaign measurements, the Xybion cameras utilized interchangeable lenses with fields of view of 48°, 30°, or 15°. Both of these cameras were operated in manual gain and field mode (60 Hz), resulting in 16.7 ms exposure time. Each camera was fitted with a GPS timing system (timing accurate to within 1 ms), and data were recorded on Sony GV-D8000 digital video cassette recorders, using Digital8 video tapes.

Since difficulties were expected with the ground-based observing conditions, it was initially proposed that two ground stations be employed, as well as the new WATEC cameras on each balloon payload. The second ground site was originally planned at Uraguaiana (near the border with Argentina and Uruguay), which was also planned to be a down-range telemetry reception site. However, due to limitations in personnel, this site was not utilized. No INPE aircraft was available for this campaign. However, it was our hope that between the ground site at SSO and the balloon-borne cameras, we would be able to see a majority of TLEs within several hundred km of the balloon flight path.

4.2.2. University of Washington Balloon-Borne Instrumentation

The University of Washington (UW) payloads were outfitted with similar instrumentation as used for the Brazil 1 campaign, with one notable exception. The new payloads included an improved electrical field sensor capable of measuring large vector fields up to about 500 V/m per axis. This modification was made as a result of the high fields observed during the Brazil 1 campaign. Figure 4.4 shows the UW balloon payload

being hand carried from the integration facility at Santa Maria to the nearby field launch site.



Figure 4.4. UW and USU researchers moving the balloon payload from the integration facility at the University of Santa Maria to the launch site in an adjacent field. The USU camera (covered) is evident on the top of the payload. (Personnel left to right, Mike McCarthy, Dominique Pautet (behind payload), Matthew Bailey, and Michael Kokorowski.)

.

Figure 4.5 shows preparations for a test launch at the University Federal de Santa Maria February 15, 2006. The balloon was launched during expected moderate storm activity from a field adjacent to the INPE integration facility in the early evening hours. Figure 4.6a shows balloon launch and (b) an all-sky video image recorded by the onboard sprite imager as the balloon ascended. At this time, the video field depicts the balloon in the center of the image together with the upward pointing boom spheres. This data,

which was taken soon after launch, illustrates the available fields of view for sprite measurements. However, on this occasion, the balloon failed to reach observation altitude, and the flight was terminated after approximately 2 hours. Nevertheless, it was successful in demonstrating the operational capability of the USU camera.



Figure 4.5. Preparations for a test balloon and payload launched from Santa Maria on Feb. 15, 2006.

4.2.3. Lightning Detection Networks

For the Brazil 2 campaign, a set of lightning sensors was deployed by INPE, providing lightning location and peak current data over most of the state of Rio Grande do Sul. Unfortunately, this network was not able to accurately characterize lightning events in neighboring northern Argentina and in Paraguay, where the storms that we observed during the campaign were located. However, the University of Washington had

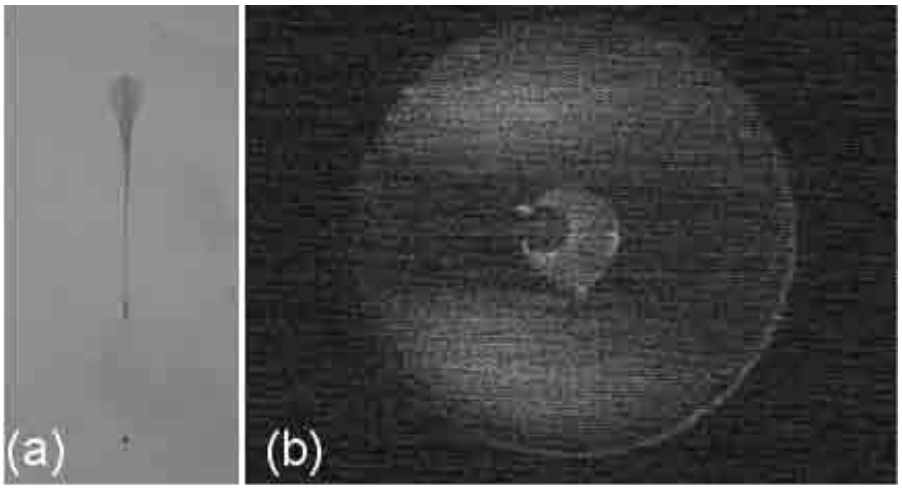


Figure 4.6. (a) Photo showing balloon launch configuration. The payload was suspended 27 meters below the balloon. (b)Video image taken from USU WATEC camera mounted on top of the balloon payload. This figure shows a 180° field of view, with the balloon and one of the spherical payload booms in the center.

real-time access to the World Wide Lightning Location Network (WWLLN, see http://wwwlln.net), which was a new global system that they had helped develop.

WWLLN data were used extensively to identify the timing and geographic location of lightning discharges by measuring very low frequency (VLF) radiation (3-30 kHz) from the lightning strokes. The timing, position, and efficiency of WWLLN have been estimated for several key geographic regions, including South America, by comparison with local ground-based lightning detection systems [e.g., *Lay et al., 2004*]. These investigations show that WWLLN is most sensitive to large lightning strokes and it is estimated that ~15-20% of all cloud-to-ground lightning discharges within South America are located with a spatial accuracy of ~10 km and a timing uncertainty of <30 μs. The WWLLN data were updated every 10 min and were used to monitor the storm conditions in near real time to aid the balloon launch and subsequently for the ground-

based TLE image measurements at SSO. These data were also used for detailed analysis of the storms as discussed in Chapters 5 and 6.

4.2.4. Duke University Instrumentation

The addition of Duke University electromagnetic sensor array provided accurate measurements of the impulsive charge moments associated with the parent lightning of the observed TLEs. This system comprised of one pair of magnetic field coils to measure the vector horizontal magnetic field and one vertical AC electric field sensor (provided by Quasar Federal Systems, Inc). Each signal was continuously sampled at 100 kHz. The magnetic and electric field sensors had flat pass bands from 2 Hz to 25 kHz, and 5 Hz to 25 kHz, respectively. Figure 4.7 shows the Duke sensor located in a nearby field at SSO. This system was operated semi-autonomously throughout the campaign. Absolute timing of lightning strokes was obtained using GPS, which was validated to better than 20μs prior to deployment in Brazil, using U.S. National Lightning Detection Network data. Cross calibration measurements were also used to ensure that the impulsive ΔM_{Qv} were directly comparable with recent measurements using permanent sensors at Duke University [e.g., *Cummer and Lyons*, 2005]. These data also yielded directional information to the lightning source with an uncertainty of ~2°, as discussed in *Taylor et al*. [2008].

4.3. Storm 1

During this campaign, TLEs were captured on two nights, February 22-23, 2006 (hereafter referred to as storm 1), and March 3-4, 2006 (storm 2). Between these two



Figure 4.7. (a) Duke University electromagnetic sensors, used to measure lightning sferics, and (b) system deployment at SSO.

storms, over 550 TLEs were imaged, mainly over Northern Argentina. On 22 February, during the late morning hours (local time), a large thunderstorm system developed over the Pampas region of northern Argentina, east of Buenos Aires. As the day progressed, this system continued to develop and strengthen while moving northwards. By the late evening (02:30 UT /23:30 LT), the storm encompassed ~300,000 km^2,as determined from the Geostationary Operational Environmental Satellite (GOES) infrared images of cloud top temperatures [*Thomas et al.*, 2007]. During most of the night the storm complex lay almost due west of SSO at a large range of ~ 500-900 km and had grown to encompass an area of about 550,000 km^2. This storm was significantly larger than most sprite-producing storms over the US High Plains [~300,000 km^2, *Lyons et al.*, 2006], but such storms are relatively common for this region of South America during the summer months. Figure 4.8 shows a GOES image of the storm at 06:30 UT (03:30 LT) over Argentina, well to the west of Santa Maria, and alas, out of range of the balloon measurements. It is interesting to note that the size of the storm is as large as the state of

Rio Grande do Sul. The site at Santa Maria (SM) is marked, as well as a scale size, showing the large size of the storm.

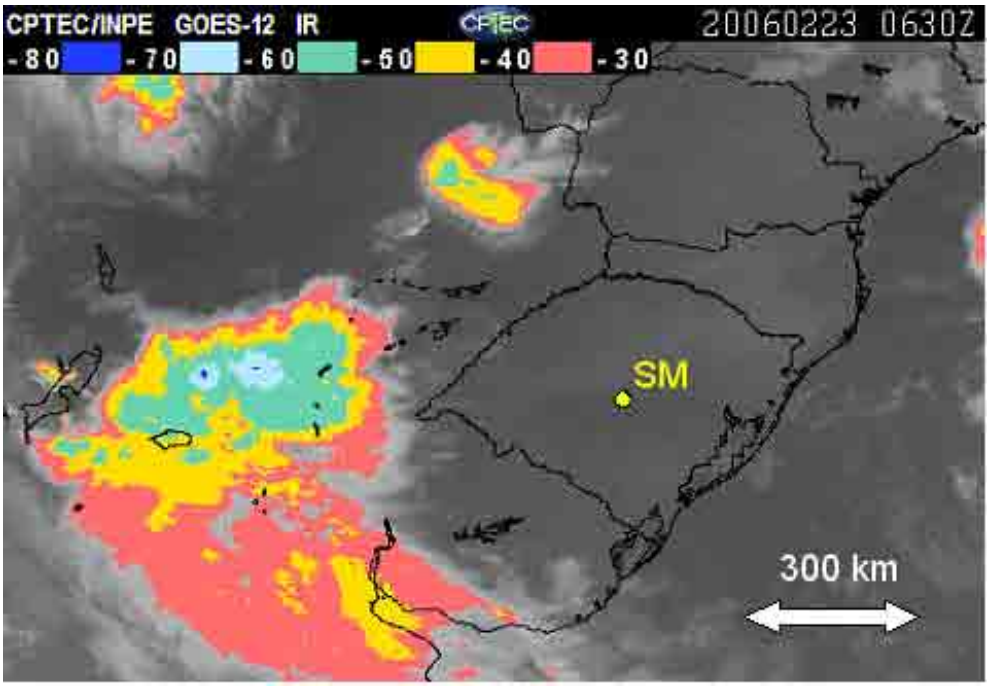


Figure 4.8. GOES 12 infrared image of a TLE producing thunderstorm to the west and southwest of SSO. The color bars shows the temperature scale within the storm.

Recently, *São Sabbas et al*. [in review][1] compared this storm with a similar size storm over the Midwestern U.S. that also produced many sprites, of which 40 were analyzed [*São Sabbas and Sentman*, 2003]. Three differences were emphasized: (1) Using satellite data, minimum cloud top temperatures of the south American storm (-70° C) were shown to be ~10° C warmer than its North American counterpart. (2) The South American storm comprised several separate convective core regions within the main storm complex, whereas the MCC over the Midwestern U.S. consisted of one main

[1] São Sabbas, F. T., M. J. Taylor, P.-D. Pautet, M. Bailey, S. Cummer, R. R. Azambuja, J. P. C. Santiago, J. N. Thomas, O. Pinto Jr., N. N. Solorzano, N. J. Schuch, S. R. Freitas, N. J. Ferreira, and J. C. Conforte (in review), Observations of prolific transient luminous event production above a mesoscale convective system in Argentina during the Sprite2006 campaign in Brazil, *J. Geophys. Res*.

convective core. These differences may or may not be significant, as U.S. storms may also have multiple convective cores (Dr. Walter Lyons, personal communication), and cloud top temperatures can vary from storm to storm by at least 10°C. (3) In the U.S. storm, the TLEs were associated with CG lightning in the trailing stratiform region of the storm, as that is where large +CG strokes tend to be located [*Lyons et al.*, 2008]. However, in the February 22-23 storm, TLEs occurred in many different areas of the storm, which may, in part, be due to the existence of multiple convective cores of the storm. Moreover, *Solorzano et al.* [2006] has shown that the maximum rate of TLEs occurred approximately one hour after the peak in lightning rates, as determined by WWLLN. This differs from the study of *São Sabbas and Sentman* [2003] which showed that TLE rates peaked at the same time as the lightning rates.

Sprites were first detected at 02:35 UT (23:35 LT), shortly after our image observations began at SSO. Observations continued until dawn (~08:30 UT), resulting in 445 TLEs captured during ~6-hrs of observations, making it the third most active TLE-producing storm on record [*Thomas et al.*, 2007]. The majority of the TLEs were imaged at large ranges (500 -1000 km), and approximately 60% comprised sprite clusters (with carrot and columnar forms). The storm was also rich in halo events, and a total of 121 sprite-halos as well as 62 unstructured halos, were observed.

To determine the geographical location of each of these TLEs, we used WWLLN lightning data which identified timing and position of the parent lightning flashes associated with these sprite and halo events. WWLLN is not able to detect polarity of CG lightning, but was able to accurately determine the location and timing of each lightning stroke with an uncertainty of approximately 10 km and 1 ms respectively.

Using the GPS timing (accurate to <30μs) encoded on our video data, TLEs matching WWLLN detection were first identified. The majority of these events were found to occur within the duration of the video field. However, we also investigated TLEs that occurred up to 30 ms after the WWLLN lightning detection to account for delayed onset of the sprite. Using the star field to calibrate each video image, these events were then projected onto a geographical grid (using an initial assumed height of 90 km for the TLE top). This enabled us to determine whether the image of the sprite occurred at the same azimuth as the one determined from the lightning data. The observed sprite clusters were typically 50-100 km wide, and located at ranges of 500-1000 km, which corresponded to an uncertainty in azimuth of typically ± 2-4°. Once the parent lightning was identified, the true altitude of the TLE was then found by adjusting the assumed altitude so that its geographic projection matched the lightning location (to within an uncertainty of 25-50 km, due to the finite size of the sprite). As sprites are known to occur over a finite altitude range of typically 80-90 km for their tops, self-consistency of the derived altitudes was then used as the final discriminating factor in their correct identification. Using this technique, a total of 141 TLEs were successfully correlated with WWLLN lightning data for storm 1 (A more detailed description of the projection method is given in Chapter 5 where the same technique was used to quantify halo events).

Of these 141 events, 56 were sprites, while the other events comprised halos and sprite-halos and are discussed in detail in chapter 5. Figure 4.9 is a histogram plot of the sprite altitudes for these 56 events, indicating a mean altitude for the top of the sprites of 85 km (± 2 km). This mean altitude was then used together with video TLE data for the remaining 204 events (not identified by WWLLN) to estimate their geographic location.

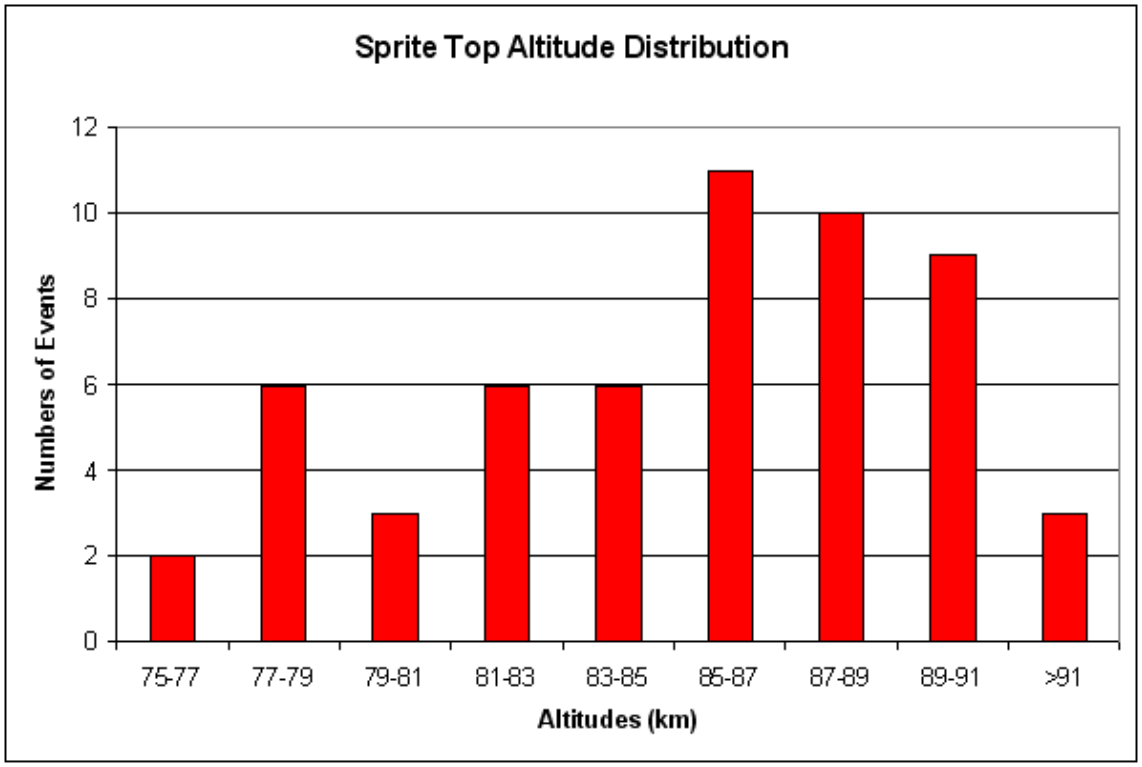


Figure 4.9. Distribution of sprite top altitudes, as determined using WWLLN lightning locations, which resulted in a mean sprite top altitude of 85 km.

4.3.1. Example Data

Figure 4.10 is a typical example of some of the TLE data recorded on this night. The data show a complex sequence of TLEs that all occurred within 0.6 seconds. Starting from left to right: a bright halo occurred at 07:30:50.473 UT, followed by a separate sprite-halo in the same location (center image) which occurred 83 ms later, followed by a separate sprite-halo in the same location (center image) which occurred 83 ms later, followed by a group of short column sprites 468 ms later, and finally an intense carrot sprite two fields later (34 ms), both of which are evident in the right hand image. All of these events, with the exception of the carrot sprite, correlated well with separate

WWLLN lightning detections, within close spatial proximity to each other. The initial halo (left frame) occurred at a range of 585 km, at a measured altitude of 80.5 km, and exhibited a visible diameter of 72 km. Using the Duke University sensors, it was found to be associated with a +CG lightning stroke with an impulsive charge moment change (ΔM_{Qv}) of 254 C.km.

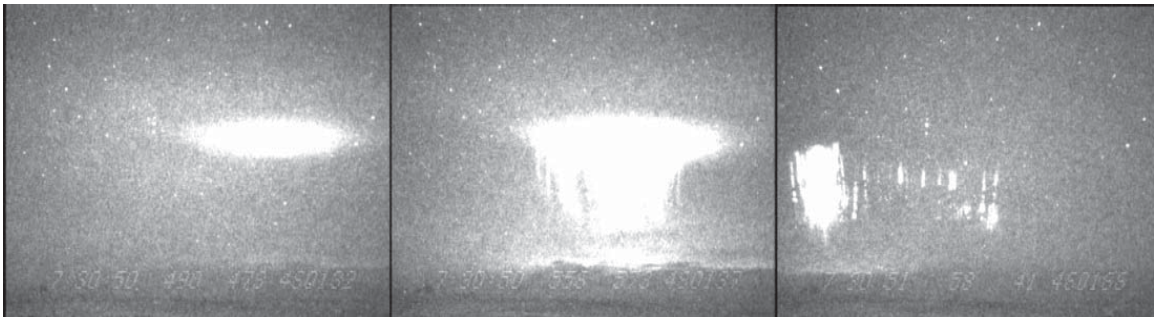


Figure 4.10. Three snapshot images depicting a complex sequence of TLEs imaged over Northern Argentina during the night of February 23. They occurred at approximately the same azimuth and all with 0.6 seconds of each other.

The sprite-halo in the middle image (recorded 83 ms later) was determined to be at a range of 578 km, at a central altitude of 79.5 km, with a halo diameter of 92 km. The impulsive ΔM_{Qv} of this event was calculated to be 368 C.km, and was also associated with a +CG. The right side image shows several short c-sprites that were rapidly followed by the carrot sprite evident on the left. These two events occurred approximately 0.5 seconds after the sprite-halo event at a range of about 610 km, and were correlated with two positive lightning events (one believed to have caused the columnar sprites, and one associated with the carrot sprite), with impulsive ΔM_{Qv}s of 157 and 194 C.km, respectively. The horizontal width of these two events was ~90 km. Very large continuing currents, which are low-level currents following lightning return strokes, were measured by Duke's ELF/VLF sensor in relation to these two events. The 194

C.km impulsive ΔM_{Qv} +CG lightning had a continuing current amplitude of about 20 kA.km that lasted for approximately 200 ms. Thus, it is likely that the total charge moment of the carrot event may have been much larger. This interesting event is discussed further in *Thomas et al*. [2007].

During this night, TLEs were imaged at horizontal distances ranging from 480 to over 1000 km. Each event has been individually analyzed to determine their ranges, widths, top heights, polarity, and impulsive charge moments. More detailed studies of specific subsets of this data set are presented in Chapters 5 and 6.

4.4. Storm 2

A second MCC was observed on March 3-4, 2006. This large thunderstorm began to develop over southern Paraguay during the day, and slowly expanded northward and moved eastward as nighttime approached. This storm had a maximum cloud shield (determined at < -40° C) of ~420,000 km^2, which is again significantly larger than a typical MCS over the Midwestern U.S. Figure 4.11 shows a series of GOES 12 satellite images of this storm after it had reached MCC status. The minimum cloud top temperatures for this storm (-80° C) were approximately 10°C colder than the storm of February 22-23, but similar to MCC event studied by *São Sabbas and Sentman* [2003]. The storm appeared to have multiple convective core regions as well, and is currently under investigation to determine more about its meteorological development.

As shown in Figure 4.11 this storm was located approximately 400-800 km due north of Santa Maria, and as such was again not accessible for our balloon measurements, but ground-based observations were successfully made from SSO. As with storm 1, the

cameras were arranged with overlapping fields of view to encompass the general area of the MCC, and sprites were first imaged at 01:40 UT (22:40 LT). In total, over 118 events were imaged over a four hour period (until 05:30 UT), consisting mainly of sprites, halos, and sprite-halos, as well as two possible elves. Figure 4.12 plots the distribution of all of the events recorded from this storm, using the method described in section 4.3. On this night, WWLLN data were successfully correlated with only 9 TLEs (2 sprites and 7 halo

the MCC, and sprites were first imaged at 01:40 UT (22:40 LT). In total, over 118 events were imaged over a four hour period (until 05:30 UT), consisting mainly of sprites, halos, and sprite-halos, as well as two possible elves. Figure 4.12 plots the distribution of all of the events recorded from this storm, using the method described in section 4.3. On this night, WWLLN data were successfully correlated with only 9 TLEs (2 sprites and 7 halo

events), with calculated altitudes of 90 km and 87 km, respectively, similar to those determined from storm 1. As the number of WWLLN identified events were limited, an average altitude of85 km (for sprite tops), and 83 km (for halo centers) determined from the storm 1 data were used to estimate the geographical locations of the remaining 108 events (total 118) plotted in Figure 4.12. The TLE locations appear to have a higher density near the coldest regions of the storm, but otherwise are dispersed throughout the storm. Charge moments for the 9 WWLLN events have been investigated, but the electrical properties (charge moment and polarity) have yet to be analyzed for all of the events. This storm is still under investigation with ongoing studies dealing with both TLE production, and relating lightning strokes to specific areas of the storm using meteorology.

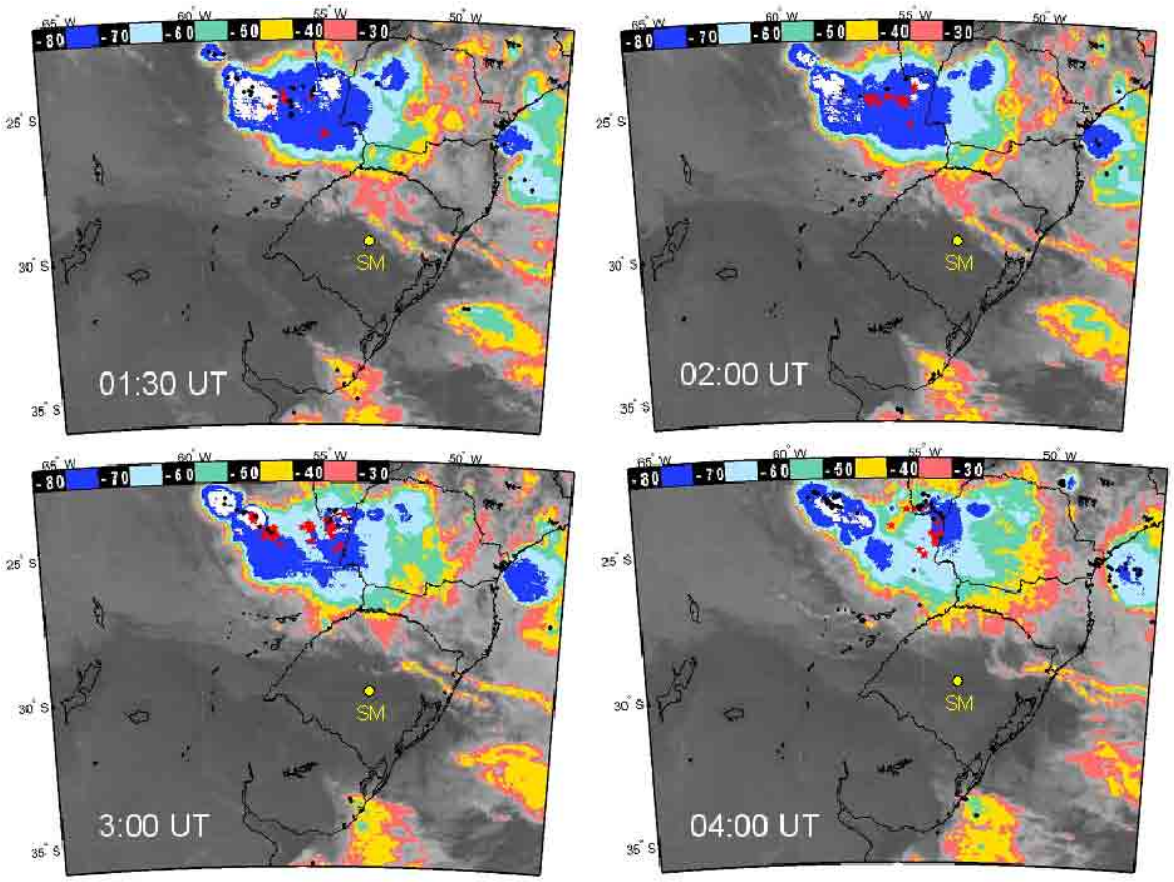


Figure 4.11. An array of GOES 12 infrared images of a TLE producing thunderstorm to the north-northwest of SSO. Also shown is a temperature scale for the figure. (Some of the TLE locations are marked (in red) on the storm complex.

4.5. Summary

Remarkably, over 550 TLEs were observed from the Southern Space Observatory in southern Brazil during these two storms. Both were Mesoscale Convective Complexes (MCCs), and were significantly larger than typical MCCs seen over the Midwestern U.S. Both storms had comparable cloud top temperatures (within 10°C) and multiple convective core regions. A singular comparison with a MCC over the Midwestern U.S. suggests some differences in temperature, size, and the relationship between peak



Figure 4.12. Map showing relationship between observing site at SSO and all of the TLEs observed during storm 2 on the night of March 3-4, 2006.

lightning rates and TLE occurrence. These differences are currently under further investigation by colleagues at the University of Washington and at INPE.

Alas, balloon-borne payloads were not able to reach either of these TLE producing storms due to their extreme ranges. Thus, we were not able to collect any in-situ measurements of the electric and magnetic fields or onboard sprite imagery associated with these two MCC storms.

However, the large number of TLEs captured by our ground-based imagers and the Duke University sensors from SSO, have clearly demonstrated that MCCs in this geographic region are prolific producers of TLEs. The following two chapters detail investigations of the TLEs measured during the February 22-23 storm. Chapter 5

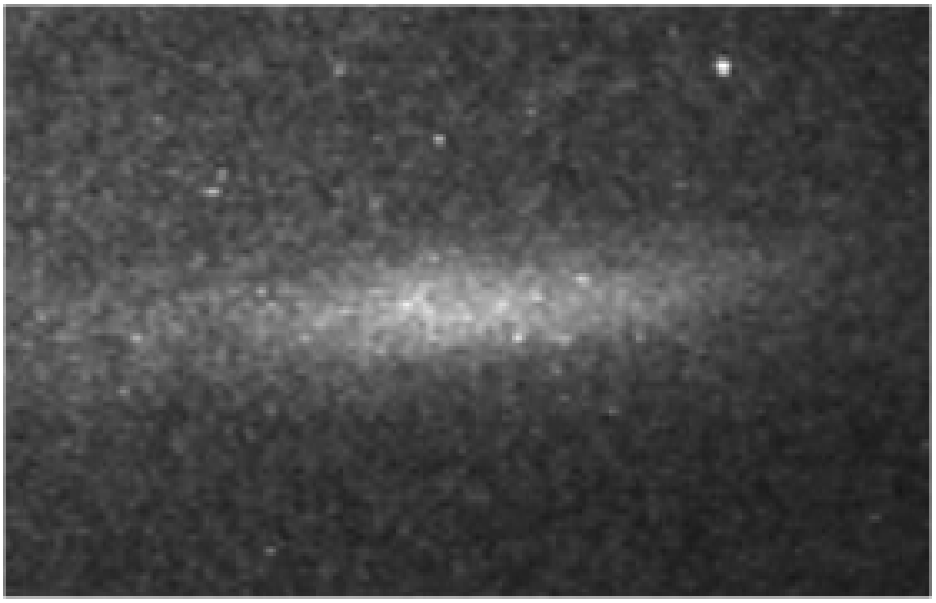
presents a statistical study of the halo events, which comprises the largest number of events ever studied from one storm. Chapter 6 focuses on rare measurements of TLE events associated with –CGs. To date, there are only two (possibly three) confirmed detections of negative sprites, yet surprisingly storm 1 was found to contain at least seven such events.

CHAPTER 5

HALO STUDY

"…en route from Denver to Louisville in our B767 at flight level 370, we paralleled an intense line of thunderstorms running from Arkansas to Indiana. Unbelievably, we witnessed around thirty or so sprites (many other airline crews witnessed them as well) and a few jets. We could not make out any particular color because the lightning activity associated with the line of thunderstorm cells (cold front in area) was extremely active and bright. We were shocked at the number of sprites – they tended to shoot out from the most intense line of cells, about 50-60 miles in depth. The whole line of cells extended several hundred miles. At first we saw a few jets, then they died off for a while and sprites replaced them. An occasional jet would pop up during the sprite show. FANTASTIC!"

— Mark E. Evans, Pilot, United Parcel Service



Example of a diffuse disk-like halo imaged over Paraguay at 3:06:52 UT on March 4, 2006. Also seen is a portion of the star field used to calibrate the image data and determine halo spatial characteristics.

5.1. Introduction

Halos, initially known as sprite halos, were only recently identified in video and photometric data by *Barrington-Leigh et al.* [2001]. As discussed earlier, they were originally confused with elves, which also appear as optically diffuse disks. *Barrington-Leigh et al.* [2001] used high speed (1000 frames per second) image intensified video systems and model results developed by *Veronis et al*. [1999], to distinguish between these two types of TLEs. Their results revealed the following properties: 1) halos are produced by quasi-static electric fields (QEs) that are also responsible for sprites, and are not due to electromagnetic pulses (EMPs) that produce elves; (2) halos ensue when the charge moment changes occur over relatively short time scales (~1ms), with longer charge moment changes producing sprites; (3) high speed halo images sometimes have a concave upward shape, which indicates significant ionization that occurs on the underside of the halos.

Somewhat surprisingly, halo studies are few in the literature. To date, they comprise four main investigations by *Barrington-Leigh et al*. [2001], *Stenbaek-Nielsen* [2000], *Wescott et al.* [2001], and *Miyasato et al.* [2002]. Each of these four studies reported characteristics of halos detected over the Midwestern U.S.

In support of NASA's Sprites '99 balloon campaign, *Wescott et al*. [2001] used cameras stationed in South Dakota and Wyoming to make two-station observations of TLEs including four halo events that were used in triangulation studies. Figure 5.1 shows an example of a sprite-halo imaged at Bear Mountain, South Dakota on August 18, 1999. The triangulated altitude was 84 km, and the center of the halo was estimated to be at approximately 7.7 km from a large +126 kA CG as detected by the National Lightning

Detection Network (NLDN). Their two-station measurements suggested that halos initiate at a mean altitude of ~78km, have an average diameter of ~66 km, and an apparent thickness of ~4 km. Importantly, they also showed that halos tend to be approximately centered over the parent lightning stroke (to within 5 km). This is very different from sprites, which have been shown to occur at horizontal distances of up to 50 km from their associated-lightning stroke. This situation is illustrated in Figure 5.2, which maps the location of three sprites (solid circles) associated with ~ +115 kA and ~ +14 kA NLDN strokes, and a 33 km radius circle centered on the triangulated location of the halo. The center of the halo was displaced from the lightning flash by 2.8 km, while the sprites were ~ 20 km away. This study, although limited in number of events, is unique to date, as the only triangulation of halos that has been published. The close centering of the halo above the lightning strike (within several km) has important implications for our single-station measurements of halos from Brazil.

Coordinated halo measurements from Yucca Ridge, CO, using USU intensified CCD video camera co-aligned with University of Tohoku, Japan, fast vertical array photometer, have helped enormously in establishing the distinction between elves and halos [*Miyasato et al.*, 2002]. In particular, the array data contained information on both the elve and the halo signatures, while the video camera clearly showed the halo. Together these data were used to investigate the altitudinal and temporal relationships of elves and halos. Figure 5.3 shows an example of their coordinated measurements.

The upper panel (a) shows the halo signature, which occurred at an altitude of ~87 km, together with the locations of the photometer array marked by the grid on their right

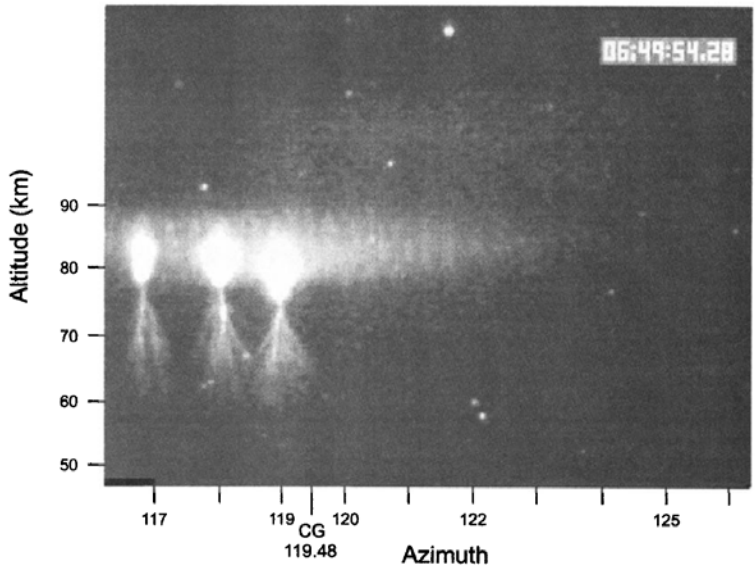


Figure 5.1. Video image of a well-defined sprite halo recorded from Bear Mountain, South Dakota on August 18, 1999. The triangulated altitude was 84 km [*Wescott et al.*, 2001, Fig. 9]. Reproduced by permission from the AGU.

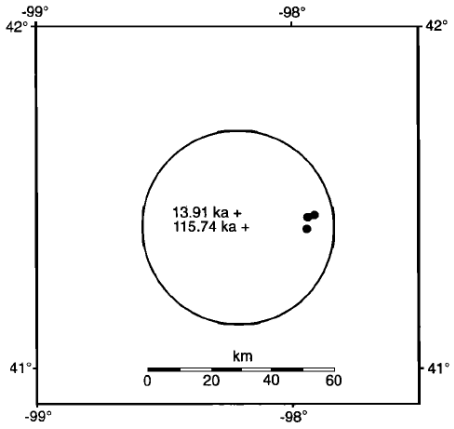


Figure 5.2. Map showing triangulation location of three sprites (solid circles) and estimated size and location of coincident halo together with positions of their parent +CGs [*Wescott et al.*, 2001, Fig. 5]. Reproduced by permission of the AGU.

hand side. The array itself spanned much of the field of view of the camera, capturing the halo signature. The lower panel (b) illustrates the photometer signal from several channels, each aimed at progressively higher elevations, as indicated in the figure. The

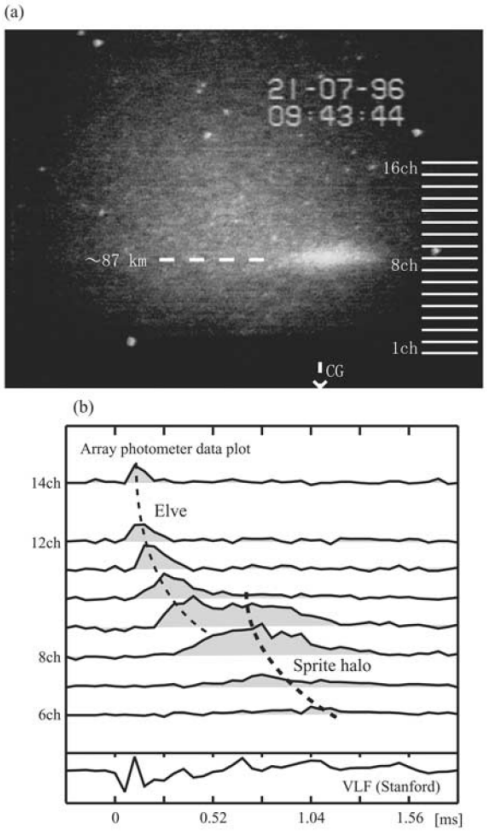


Figure 5.3. Coordinated high-speed photometer and video data taken from Yucca Ridge, CO, on July 21, 1996, showing both elve and halo optical signatures, as well as VLF data by a Stanford University sensor. The time after the VLF onset is displayed in milliseconds [Modified from *Miyasato et al.,* 2002, Fig. 1]. Reproduced by permission from the AGU.

bottom of panel (b) shows the VLF signature from Stanford University associated with the lightning strike. The elve occurs in the highest elevation data (channel 14) and appears to propagate downwards in time. The halo occurs at a lower altitude, and somewhat delayed from the elve. *Miyasato et al.* [2002] analyzed 35 such halos, determining a mean altitude of the halo centroid of 80.4 km (range 87.2 to 73.0 km), and horizontal diameters of 50-110 km, with a mean of 85.5 km. They also analyzed the temporal behavior of halos, indicating a mean time delay from the CG of 0.85 ms, and halo duration of 0.6 to 2.2 ms (mean, 1.0 ms). With the exception of one event, these

events were all associated with +CGs, with peak currents from 50-180 kA. These are the most comprehensive measurements of halos to date.

5.2. South American Halo Data

A large MCC thunderstorm formed over the Pampas region of northern Argentina on February 22-23, 2006, providing an exceptional opportunity to perform a statistical investigation of the optical and ELF/VLF signatures of halo events. This is because over 445 TLEs were imaged within a limited (~6 hr) period on this night. Of these, 182 events were determined to be associated with either isolated halos or sprite-halos. This is a very large number for one storm, which was the third largest TLE producing storm on record [*Thomas et al.*, 2007]. Examples of halo and sprite-halo data recorded during this night are shown in Figure 5.4. In this figure the two left-hand images show the development of a sprite halo event. The upper left image shows a well-formed halo imaged at low elevation, with the parent lightning flash evident near the horizon. This event which occurred at 03:12:37.355 UT, shows faint vertical sprite structures emanating from the diffuse halo. The lower left panel shows the resultant sprite image one field later (17 ms). By this time, the sprite is fully developed vertically, and the halo has faded. The two right-hand images illustrate individual examples of pure halo events. The upper right image shows a bright halo that occurred at an azimuth and elevation similar to the sprite halo, but approximately 15 minutes earlier. This event also shows some evidence of initial sprite development, but subsequent video fields revealed no sprite structures. The halo imaged in the lower right panel was obtained approximately 4 hours later and at lower elevation than the other two events, as the storm was tracked by the cameras.

These data illustrate the diversity of the halo events that we imaged, and their frequent occurrence throughout this night.

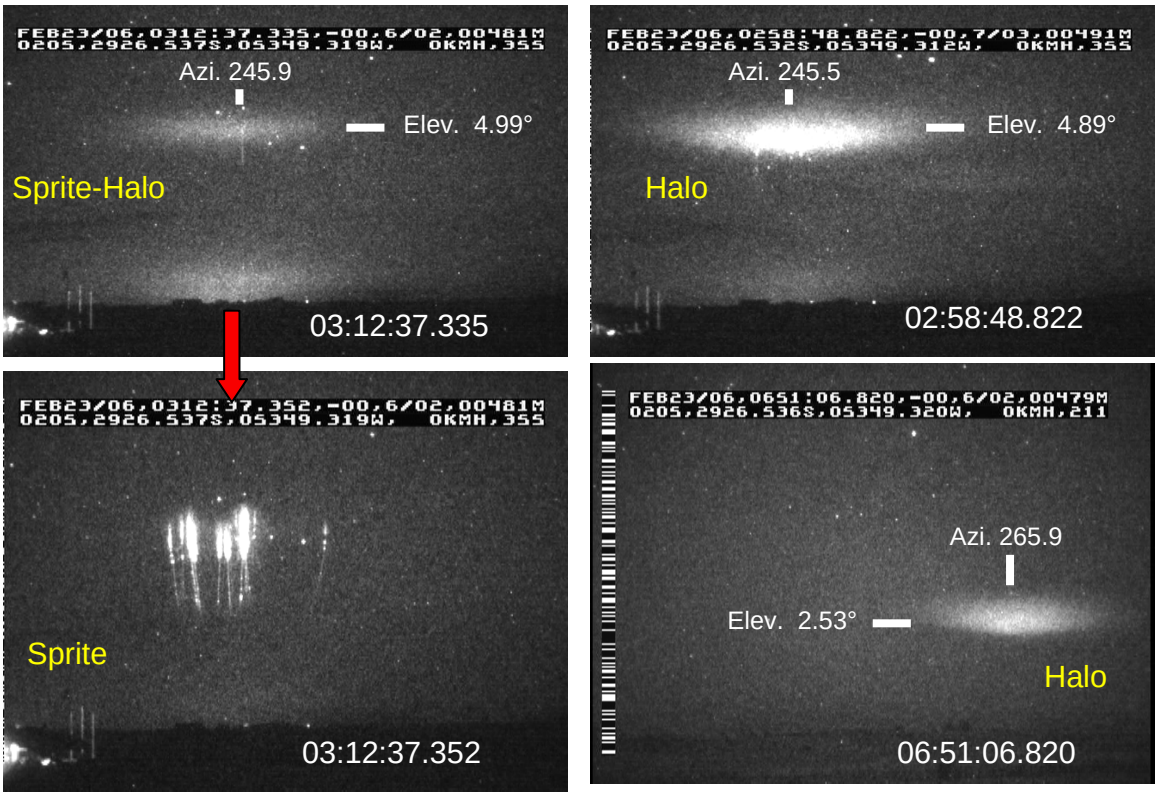


Figure 5.4. (Left) Two sequenced images showing a sprite-halo, with the halo and a faint streamer seen in the top panel, followed 17 ms later by multiple vertical structures, as the halo fades; (Right) Two halos imaged almost four hours apart on February 23, 2006. The azimuths of the camera changed during the evening, as it followed storm development.

5.3. Halo Analysis Method

To investigate the spatial properties of the halo events, it is necessary to know their altitude. Our halo measurements were made from a single station and triangulation was therefore not possible. However we can obtain good estimates of the altitude, and hence geographic location of the halos, using the findings of *Wescott et al.* [2001] who determined that halos (like elves) are formed almost centered on the parent lightning

discharge, as identified by the U.S. NLDN lighting network data. Of the 182 halo and sprite-halo events imaged from Brazil on February 22-23, 85 of these events correlated with WWLLN lightning detection, corresponding to ~ 46% of all halo related events. This number is large when compared with the number of other TLE detections by WWLLN (56 of 263 events, or 21%). This is thought to be due to the fact that WWLLN is more sensitive to large impulsive lightning signatures that are typically associated with halos than with sprite-related discharges whose signatures can last for several tens of milliseconds (Jeremy Thomas, private communication).

Using the geographical coordinates of the 85 WWLLN lightning events to identify the halo locations, the altitude and diameter of each event were then estimated. This was done using a software program developed at Utah State University for narrow angle image measurements. This program was specifically developed to study TLEs imaged at low elevations, and includes full corrections for refraction. To initiate the analysis, a halo image must first be digitized and entered into the program. At this point, the star field was used to calibrate the image in azimuth and elevation, using a catalog of known stars. The software requires the geographical location of the observer and the timing of the event, as well as the angles of view of the imager and the rotation of its optical axis (which it later corrects for). When these data are input into the program, a star field is projected onto the halo image, and may be adjusted until the projected stars match the star locations evident in the image data. An example of this can be seen in Figure 5.5.

After calibrating the image, the visible outline of the halo is traced, using the same program, which allows the user to adjust the size and shape of the halo manually.

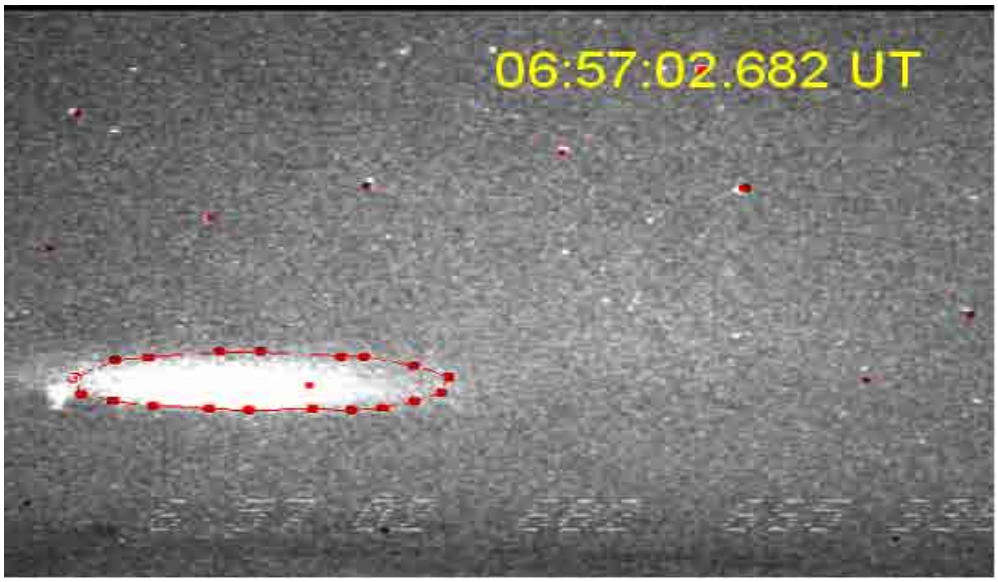


Figure 5.5. Halo imaged over Northern Argentina at 06:57:02.682 UT on Feb. 23. The superimposed stars (red dots) illustrate how the star field from our narrow angle calibration program can be matched with the actual star field. The halo outline is then traced and mapped for a range of assumed altitudes.

Once this trace is saved, the geographical projection of the halo can be plotted for a range of assumed altitudes, with an initially input value of 90 km, and altitude steps of 0.5 or 1 km. Figure 5.6 illustrates this process. Other variables that may be plotted are the lightning coordinates (in this case, from WWLLN), as well as the camera location. The figure shows four maps of the halo projection for assumed altitudes ranging from 77 - 91 km. The WWLLN lightning location is also marked on each map. Inspection of these four maps shows that the halo projection aligns well (but not perfectly) with the lightning position for an assumed altitude of 82 km. Minor adjustment on either side of this altitude indicates an estimated height for this halo of 82 ± 1 km. This is the best visual fit for this event, given the uncertainties of the WWLLN lightning location (typically ± 10 km), and our projection method. Our results using this technique agrees well with the study of *Wescott et al.* [2001], and also provides independent confirmation

of our correct association of the WWLLN lightning detection with this event. Having determined the mean height of the halo, the average diameter was estimated from spatial measurements from its traced outline, yielding ~60 km.

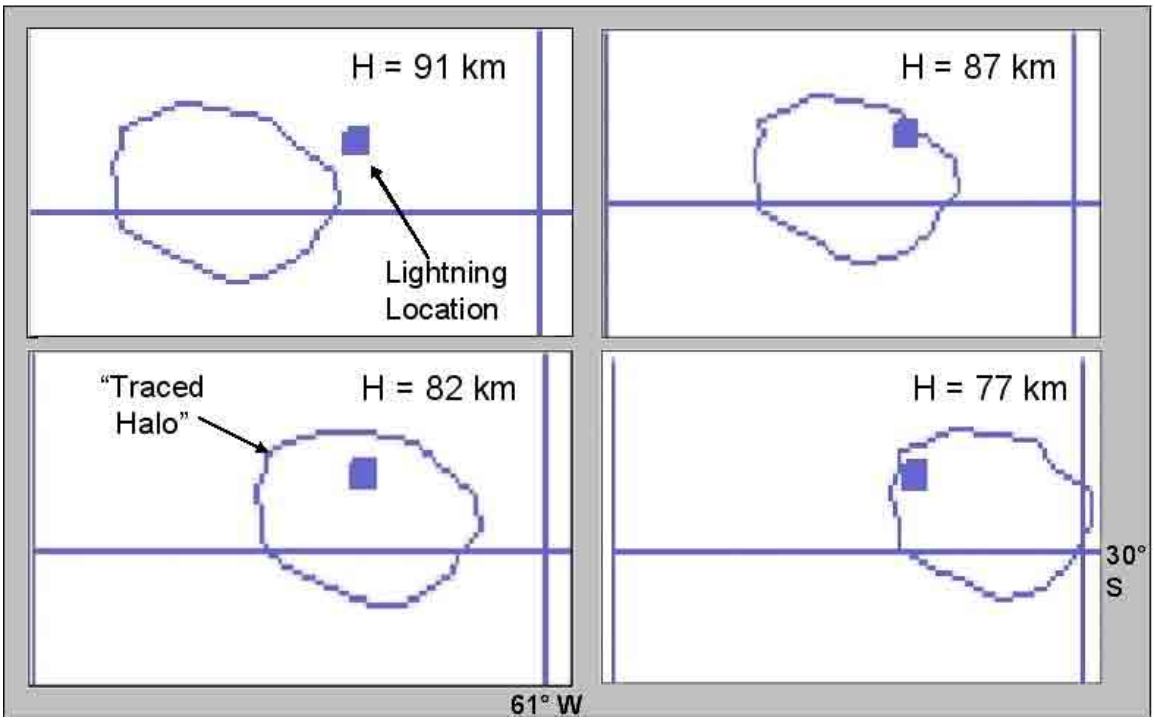


Figure 5.6. Geographic projections of the halo event of Figure 5.5, for different assumed altitudes of 77, 82, 87, and 91 km. Each plot shows the WWLLN lightning location for the parent lightning stroke. A mean altitude of 82 km is determined, and a diameter of 60 km. The ground site at SSO was directed due eastward of this event.

5.4. Halo and Storm Comparison

Before presenting statistical results of the halo analysis, it is interesting to investigate the locations of the halos within the storm during the course of the night. Of the 445 events imaged, 61 were isolated halo events, with 121 sprite-halos. The sum total of 182 events constitutes ~ 41% of all TLEs recorded, and had a similar frequency of occurrence (38%) to the storm studied by *Miyasato et al.* [2002] over the Great Plains.

In order to perform a comparison between halo locations and their relationship to the thunderstorm, the location of each halo event has been plotted on a geographic grid in two hour blocks for the duration of this night. For halo events with no associated WWLLN detection, an assumed altitude of 83 km was used to estimate their locations. This is the mean altitude of all 85 halo events mapped using WWLLN data. This analysis is described later in section 5.5. The following Figures 5.7 - 5.9 present maps of showing halo distributions, and associated GOES satellite images indicating the main activity within the storm during each two hour period. The halos are indicated by the red dots, all of which were determined to be associated with positive lightning, using combined WWLLN and ELF/VLF data.

Figure 5.7 shows the first two hour period during which 47 halos and sprite-halos were detected. They were well distributed in range from ~ 400-900 km, and the majority was captured in both the narrow and wide field cameras, as the azimuth of the storm was relatively narrow. The two GOES images show the thunderstorm location and size at 02:30 and 04:00 UT. Close comparison with the map shows that the halos were distributed throughout the storm, and were apparently not generated by prominent, individual storm cell activity within the large-scale MCC.

Figure 5.8 shows the subsequent two hour period. During this time, significantly more halos were observed (69 events), as well as the first detection of rare negative halo and sprite-halo events (indicated by the green stars), which are discussed in detail in Chapter 6. During this period the wide field camera, which was detecting relatively few events to the southwest, was modified to narrow field (~15°), and aimed due west of SSO, providing overlapping fields of view where the storm was most active. While the

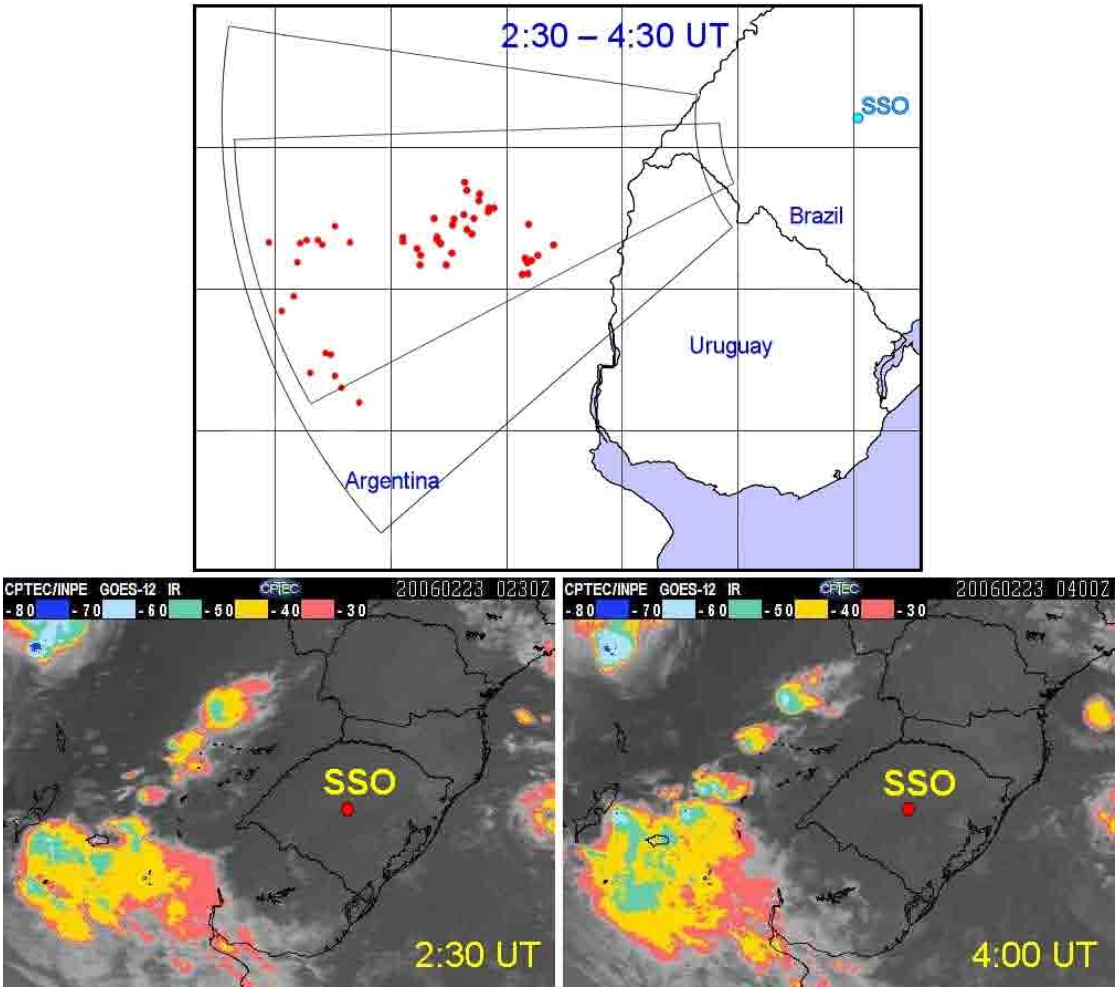


Figure 5.7. Plot showing the location of all halo events imaged between 02:30 UT and 04:00 UT. The fields of view of the two cameras are indicated. Also shown are two GOES infrared images depicting the storm at 02:30 UT and 04:00 UT. Unfortunately, there were no satellite data available at 04:30 UT.

primary halo activity was clearly associated with the main storm, a significant number of events were seen in the trailing storm region. During this time the storm intensified, as indicated by the larger region of colder cloud tops.

Figure 5.9 shows the halo locations for the last two hour period, 06:30-08:30 UT. During this time, the storm complex was almost due west of SSO, and the halo events were concentrated more towards its leading (northern) edge. During this period, three further negative halo/sprite-halo events were detected (see Chapter 6). There were 66

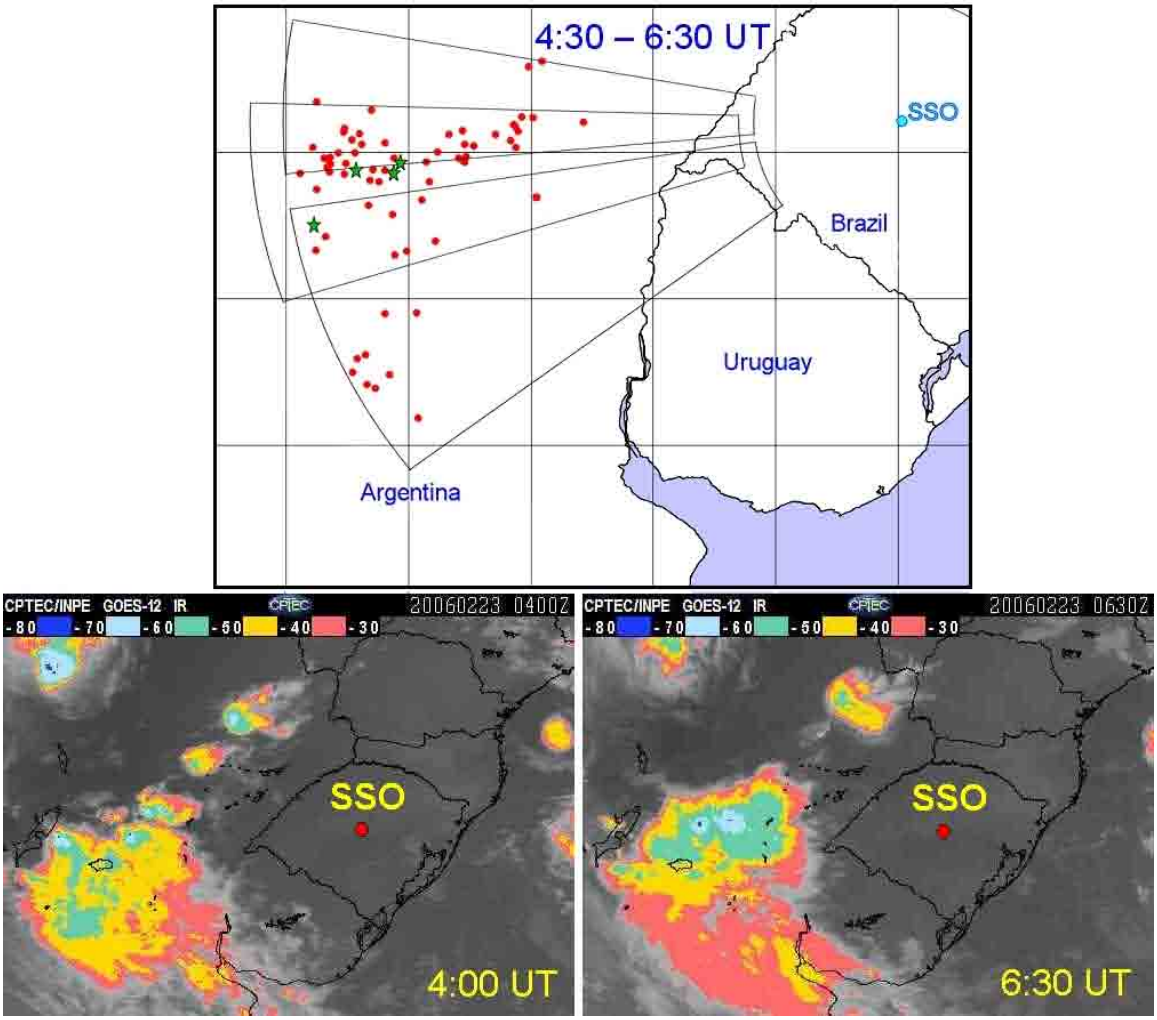


Figure 5.8. Plot showing the location of all halo events imaged between 04:00 UT and 06:30 UT. The fields of view of the two cameras are indicated. The two GOES infrared images show the storm at 04:00 UT and 06:30 UT. Unfortunately, there were no satellite images available between 04:00 – 06:30 UT.

halo events detected. Observations ceased at dawn, but it was evident that the sprite activity was continuing, albeit at a lower frequency of occurrence.

In summary, these three figures illustrate how the storm developed from several separate convective regions, which evolved and intensified as the night progressed. The maps demonstrate that halos were occurring in many parts of this storm complex. This result is somewhat surprising, as previous comparisons of sprite and storm locations over

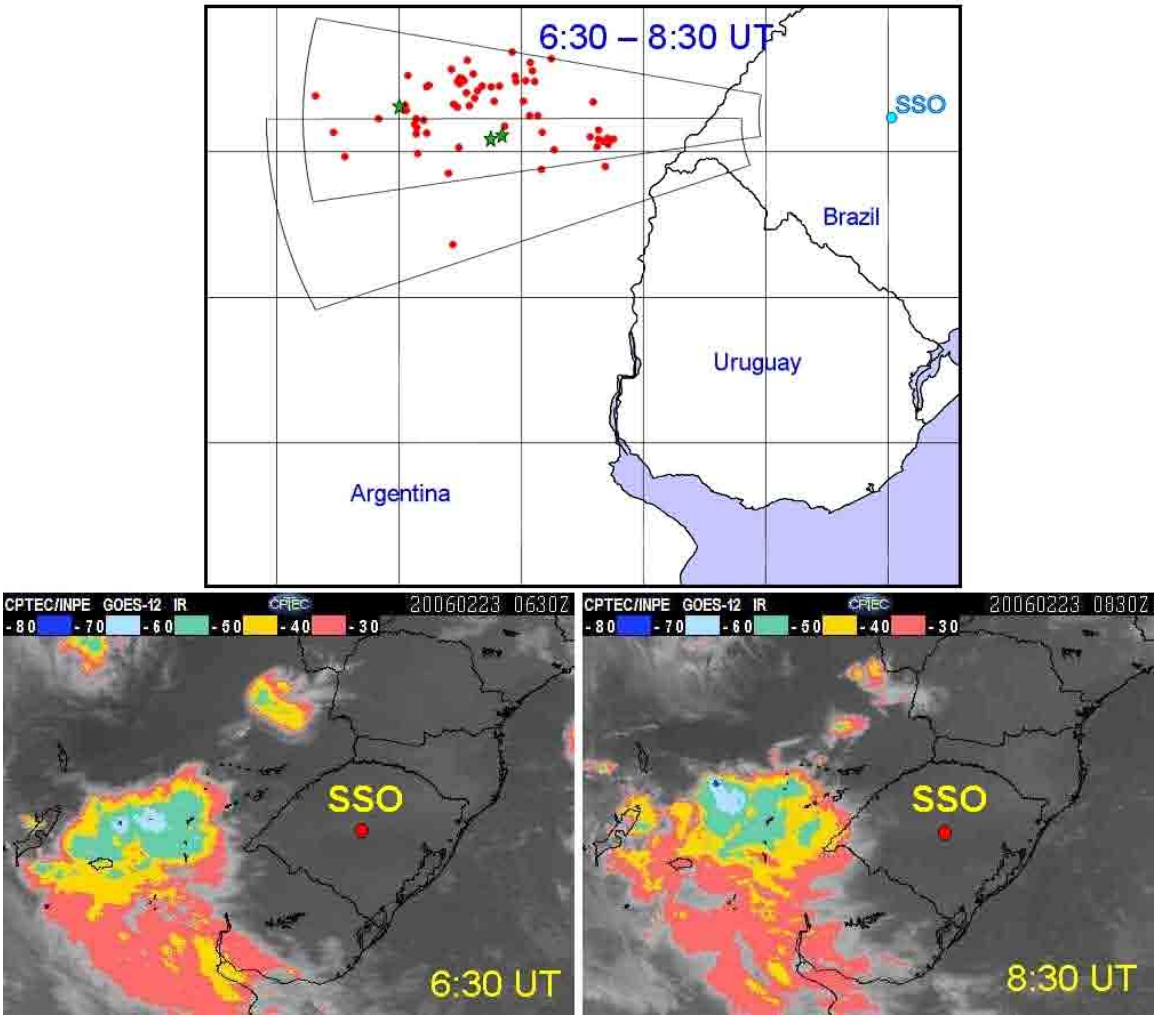


Figure 5.9. Plot showing the location of all halo events imaged between 06:30UT and 08:30 UT, which was when our data set ended. The two GOES infrared images show the storm at 06:30UT and at 08:30 UT. Events associated with –CGs are indicated by green stars.

the Great Plains have shown that sprites tend to form in the trailing stratiform region ofan MCS [e.g., *Lyons*, 1996]. This is thought to be due, in part, to the fact that large negative lightning strokes tend to occur at the leading edge of the storm, while positive lightning strokes are more copious in the trailing regions, and these strokes are the main producers of sprites [*Lyons et al.*, 2008].

5.5. Halo Statistical Results

5.5.1. Altitude Range

Using the 85 halo events that were directly associated with WWLLN lightning events, the altitude of each event has been determined, using the method described in section 5.3. Figure 5.10 plots the distribution of altitudes for these events. Our measurements indicate a limited range of altitudes, from ~78-91 km, with a clear preference for events in the 80-84 km range (mean value, 82.7 ± 1 km). These results are in excellent agreement with the previous limited studies performed over the Midwestern U.S. by *Wescott et al*. [2001] and *Miyasato et al*. [2002]. Our statistical analysis, shown in Figure 5.10, also suggests that sprite-halos can occur at somewhat higher altitudes (> 90 km) than pure halos. More specifically, the results suggest that halos may be formed at a more limited altitude range (80-88 km), which could provide a distinction between these two types of halo events. However, our data set is limited for this analysis. It is also possible that some of the higher altitude events may be signatures of elves, that due to their rapid development (within 1 ms), were not fully resolved in the video data. This is not thought to be a significant factor in this analysis, as elves also have significantly larger diameters (as illustrated in Figure 1.18), and the events reported here were all <100 km in diameter.

5.5.2. Halo Diameters

Having established the geographical location and altitude of the halo events using the combined video and WWLLN data, the diameter of each event was determined from its geographic projection (as illustrated in Figure 5.6). A histogram distribution of these

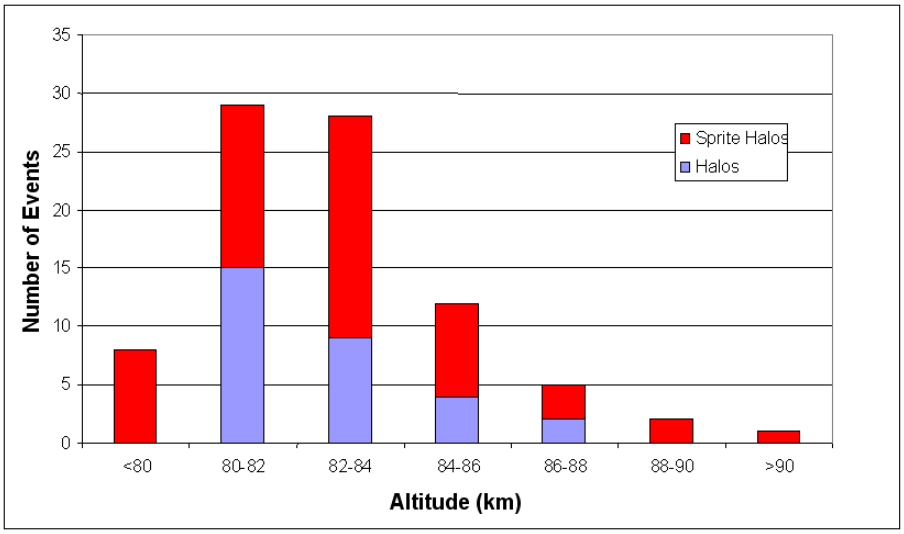


Figure 5.10. Altitude distribution (mean of 82.7 ± 1 km) of halos and sprite-halos, determined from 85 WWLLN lightning detections.

results is shown in Figure 5.11. The distribution indicates a distinct peak around 50-60 km (mean value 58 ± 5 km), but a relatively broad range from 31 – 93 km. These results also agree well with the studies of *Wescott et al.* [2001] and *Miyasato et al.* [2002] (mean diameters of ~66 km and 85.5 km, respectively). Estimating halo diameters is complicated by the fact that halos tend to be faint around their edges, and thus tracing their visual outline can produce errors. Indeed, some halos were captured simultaneously by both cameras that were operated at different gains, and measurements of these events indicated differences of up to 5 km in the diameter, which does not significantly affect our statistical results. Uncertainties in the WWLLN lightning location (± 10 km) were determined to have a minimal effect on these results. Figure 5.11 also suggests that sprite-halos exhibit the largest diameters (up to 100 km), although small diameter (30-40 km) sprite-halos were also observed.

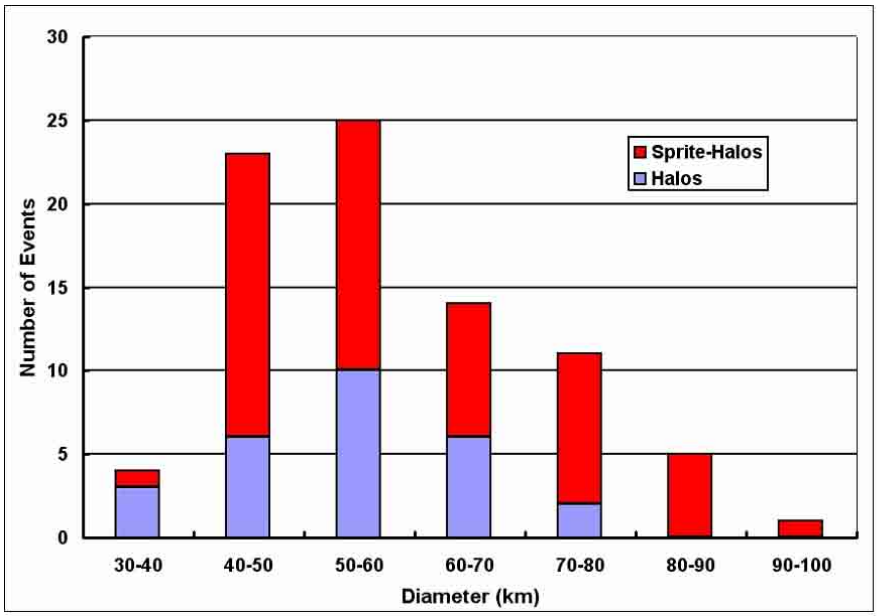


Figure 5.11. Distribution of diameters (mean of 58 ± 5 km) for halos and sprite-halos that were correlated with WWLLN lightning data.

5.5.3. Charge Moment Analysis

The Duke University ELF/VLF data were analyzed to determine the charge moments associated with 185 halo and sprite-halo events observed on Feb. 22-23. As the Duke sensors were sensitive to ELF/VLF sferic emissions originating from lightning all around the globe (see Appendices A and B), key information concerning the azimuth, range, and timing of each event was necessary to correctly identify the waveforms with our TLEs. This information was provided by a combination of WWLLN location data, image azimuth information, and GPS timing. Figure 5.12 shows the distribution of impulsive (2 ms) charge moment changes derived from the ELF/VLF data for the halo and sprite-halo events. The distribution shows a broad range of charge moments, from <100 to >600 C.km, with a distinct peak between 200-300 C.km (mean value of 255 C.km). This is a unique result, as there have been no such studies to date of charge

moments associated with halo events. The distribution also demonstrates well that the larger charge moments (>300 C.km) were essentially all associated with sprite-halo events.

While there are no measurements in the literature with which to directly compare our observations, we can contrast them with previous measurements during the Brazil 1 campaign (discussed in Chapter 3), and with a study by *Cummer and Lyons* [2005] where charge moments associated with sprite events over the Midwestern U.S were investigated. During the Brazil 1 measurements, 18 TLE events were identified, of which two (events 12 and 13 in Table 3.1) were pure halos. The impulsive charge moments using the University of Tohoku sferic measurements for these two events were 153 and 379 C.km. As discussed in Chapter 3, these values were thought to be too small when compared with the sprite results of *Cummer and Lyons* [2005]. One outcome of that study was the involvement of Duke University with the Brazil 2 campaign. The results of Figure 5.12 clearly demonstrate that all of the pure halo events and ~50% of the sprite-halo events imaged on Feb 22-23, exhibited charge moments of less than 300 C.km, and support our tentative finding that charge moments associated with TLEs were generally smaller than for those over the U.S. In general, *Cummer and Lyons* [2005] showed that charge moment changes of >600 C.km were associated with sprite production, yet Figure 5.12 shows that nearly all of the halos and sprite-halos observed from this large MCC over Argentina had charge moment changes significantly less than 600 C.km. This result is amplified by the study of *Hu et al*. [2002] who showed that the probability of sprite initiation is typically only 10% for charge moment changes less than 600 C.km (which is essentially the upper limit of our halo and sprite-halo observations). The reason for this

large discrepancy is not clear, as the same sensors and analysis method were utilized for this campaign as in the *Cummer and Lyons* [2005] study.

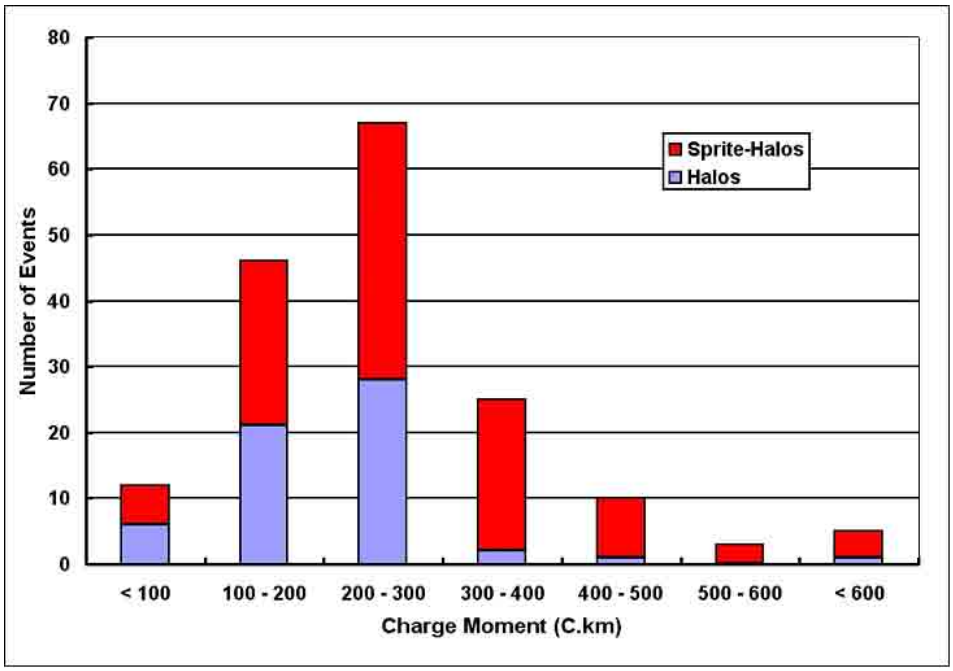


Figure 5.12. Impulsive (2ms) charge moment distribution (mean 255 C.km) for all 185 halo and sprite-halo events observed on Feb. 22-23.

5.6. Summary

Since their formal discovery in 2001, halos have only been studied sparingly. This is due, in part, to the early misidentification of halos as elves that was not corrected until modeling and high-speed video data revealed their distinction [*Barrington-Leigh et al.*, 2001]. The few studies of halos that have been made all took place over the Midwestern U.S., and in total were limited to <50 events. The large number of halo related events (185) from the MCC observed over Argentina has enabled a statistical study of their altitude and spatial characteristics, as well as a unique investigation of the charge moments associated with these events. The locale of South America used in this

study further enhances the interest and intrigue associated with these events, as it is also the first halo study performed outside of the continental U.S.

This statistical analysis has established that halos can frequently occur in South America, and that they have similar altitudes (~83 km) and diameters (~58 km) to those studied previously over the U.S. Great Plains [*Wescott et al.,* 2001; *Miyasato et al.,* 2002]. However, a novel investigation of the impulsive charge moment changes of these events (which included 121 sprite-halos), has revealed that they are significantly smaller than those associated sprites imaged over the U.S.A.

Also of great interest during this analysis was the detection of seven events associated with –CG strokes. Halos have previously been associated with –CGs, but apparently with a strong preference for their occurrence over open water [*Frey et al.,* 2007]. In contrast, the halo events reported here all occurred over the Argentinean Pampas region (over ~ 600 km to the nearest ocean). Furthermore, the detection of negative sprite-halo events was most surprising, as to date, there had only been two sprite events that have been accurately correlated with negative lightning events [*Williams et al.,* 2007]. A detailed investigation of these most unusual negative events is presented in Chapter 6.

CHAPTER 6

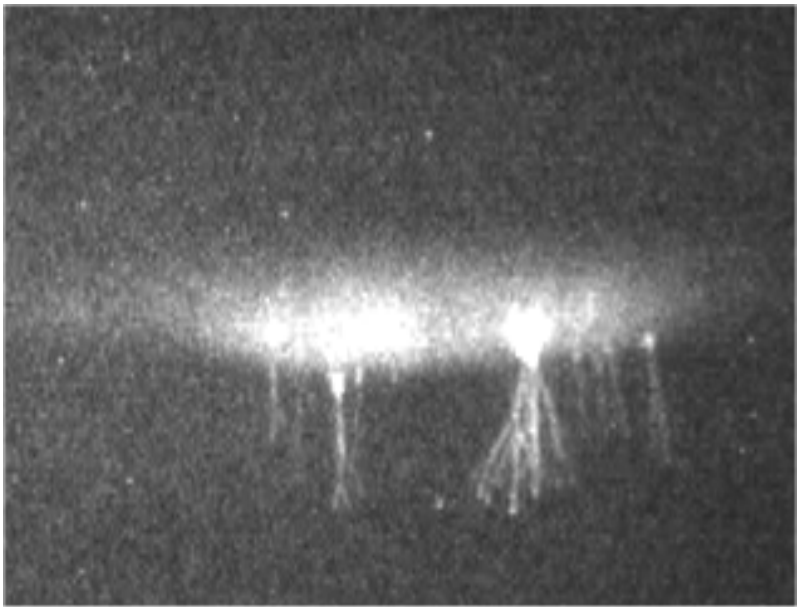
INVESTIGATING NEGATIVE CG EVENTS

"On August 28th I witnessed two sprites above a storm 100-150 miles due south of my location. I live in the edge of Phoenix, so there was a lot of background light.

The first Sprite was a series of vertical red streams from the top of the thunderstorm. It extended a considerable distance above the top of the cloud.

The second sprite was the mother of all Sprites. It was the largest and widest Sprite I have ever witnessed. It was in the shape of a funnel, with the small end at the top of the cloud. It was also red. It was so bright, my wife even saw it, and she can't see anything at night."

— Steve Schendel, amateur observer



Sprite-halo imaged at 06:32:06.085 UT on Feb 22-23, 2006, showing both a diffuse halo and well-developed tendril structure. This event has definitively been associated with a -CG discharge.

6.1. Introduction

The overwhelming association of sprites with +CG events [e.g., *Lyons*, 1996] appears enigmatic as the conventional quasi-static breakdown mechanism for sprites (discussed in Chapter 2) does not depend on the polarity of the parent CG discharge [*Pasko et al.*, 1997a]. In a recent paper by *Williams et al.* [2007], entitled, "Polarity asymmetry of sprite producing lightning: A paradox?," a summary is presented of all sprite measurements since 1995 where reference is made to their polarity. This is reproduced in Table 6.1, and shows that of the several thousand sprites reported in the literature only two (possibly three) events have been unambiguously associated with -CG discharges (indicated in the confident totals listed at the bottom of the table).

Several of the reports listed in Table 6.1 have associated sprite observations with possible -CG discharges (these reports include *Hardman et al.*, 2000; *Neubert et al.*, 2001; *São Sabbas*, 1999; *São Sabbas and Sentman*, 2003; *Winckler*, 1998; *Miyasato et al.*, 2002; *Barrington-Leigh et al*., 1999).

However, *Williams et al.* [2007] questioned the validity of many of these reports, mainly due to significant timing discrepancies (as listed in the right hand column of the table), and concluded that the ratio of positive to negative sprite production is at least 1000:1, leaving unambiguous identification of two (possibly three) negative events by *Barrington-Leigh et al.* [1999]. It is interesting to note that a significant number of events listed as negative TLEs were simple halos [*Bering et al.*, 2004 (17 events) and *Miyasato et al.*, 2002 (one event)]. But again, there was significant timing uncertainty with the *Bering et al.* measurements. As already discussed in Chapter 5, investigations of halos are relatively few [e.g., *Miyasato et al.*, 2002; *Wescott et al.*, 2001], and have only

Table 6.1. Table showing a summary of case studies of sprite parent lightning polarity [*Williams et al.*, 2007, Table 1]. Reprinted by Permission of the AGU.

Investigator	"Positive" Sprites	"Negative" Sprites	Time Window, ms
Adachi et al. [2005]	38	0	<10
Barrington-Leigh et al. [1999]	0	2	5
Bell et al. [1998]	17	0	
Bering et al. [2004]	26	17 (halos)	17
Boccippio et al. [1995]	81	0	16
Cummer and Inan [1997]	6	0	
Cummer and Lyons [2005]	87	0	16
Cummer et al. [2006]	2	0	<1
Frey et al. [2005]	2	0	30–70
Füllekrug et al. [1996]	18	0	140
Füllekrug et al. [1998]	92	0	
Füllekrug and Reising [1998]	5	0	
Gerken and Inan [2003]	5	0	16
Haldoupis et al. [2004]	28	0	20
Hardman et al. [2000]	36	6	16
Hayakawa et al. [2004]	4	0	20
Hobara et al. [2001]	3	0	
Hu et al. [2002]	76	0	
Huang et al. [1999]	40	0	16
Lyons [1996]	29	0	16
Lyons et al. [2003]	17	0	16
Lyons and Cummer [2004]	5	0	16
Lyons et al. [2006a]	33	0	16
Lyons et al. [2006b]	>1000	0	16
Mika et al. [2005]	131	0	12
Marshall and Inan [2005]	4	0	
Miyasato et al. [2002]	89	1 (halo)	1
Nelson [1997]	70	0	16
Neubert et al. [2001]	38	1	100
Neubert et al. [2005]	76	0	
Ohkubo et al. [2005]	3	0	16
Pinto et al. [2004]	14	0	14
Price et al. [2002]	15	0	16
Reising et al. [1996]	31	0	100
Reising et al. [1999]	82	0	200
Sao Sabbas [1999]	485	82	429
Sao Sabbas et al. [2003]	29	2	16
Stanley et al. [2000]	3	0	10–12
Wescott et al. [1998]	7	0	16
Winckler [1998]	35	3	1000
R. Boldi, personal communication, 4 Aug 1996	62	0	16
Confident totals	>3000	3	

recently been associated with both positive and negative CG discharges [*Frey et al.*, 2007], who also determined a clear predominance for -CG halos to occur over open water.

Due to their rarity, observations of sprites triggered by -CGs are of great interest and the measurements of *Barrington-Leigh et al.* [1999] remain exceptional to date. They reported high-speed photometric and ELF/VLF data on two discrete sprite

events observed over the Gulf of California, Mexico, that were closely associated (within 5 ms) with two large -CG lightning strokes (vertical charge moment changes $\Delta M_{Qv} \approx$ -1550 and -1380 C.km). Coincident low-light video data showed clear evidence of sprites with vertical (columnar) structure, despite intervening cloud cover and the large range (~695 km) to the storm. A third event (-1340 C.km) was also discussed, but no obvious sprite structure was identifiable through the clouds. Enlargements of the *Barrington-Leigh et al*. image data, along with an altitude scale, are shown in Figure 6.1.

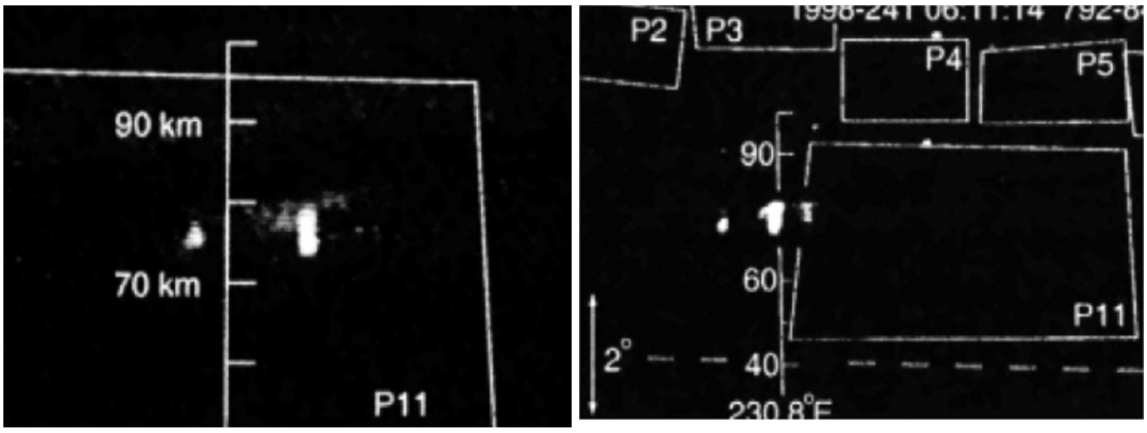


Figure 6.1. Sprite captured over the Gulf of California by low light level cameras operating at 60 Hz. These two events are the only substantiated sprites associated with -CGs up until the Brazil 2 campaign. Note the rectangular boxes indicate photometer fields of view [Adapted from *Barrington-Leigh et al*., 1999b, Figs. 2c and 3b]. Reprinted by Permission of the AGU.

In this chapter we report comprehensive new measurements of several well formed sprite-halo and halo events and establish their temporal and spatial association with a large -CG discharges. The first event (sprite-halo) was found serendipitously during analysis of the Feb. 22-23 storm data. This event is discussed in detail, comparing its optical and ELF/VLF signature [*Taylor et al.*, 2008]. Subsequently, six additional events have been identified in association with negative lightning discharges, and are

presented here for comparison. These data provide the first measurements of the spatial structure, altitudinal extent, and relative brightness of negative events and their associated electromagnetic properties.

6.2. The First Negative Event

In studying the data from the February 22-23 storm, we isolated each TLE and narrowed down initiation time to within 16.7 ms, which is the limit of our video data resolution. These times were then correlated with WWLLN events provided by the University of Washington. Originally, there were 42 lightning discharges located by WWLLN that correlated with TLEs (although later analysis using an improved WWLLN lightning detection algorithm increased the total number of correlated events to 144). Of the original 42 events, analysis of charge moment data by Duke University revealed that one of the TLEs was unambiguously associated with a –CG.

Figure 6.2 shows the observing geometry of the cameras from 05-06:00 UT encompassing the negative event. As discussed in Chapter 4, to capture the majority of the TLEs the two cameras were aimed W-SW with fields of view of ~15° and ~30° that overlapped by ~5°. The open/solid circles map the locations of 81 TLEs imaged during this one hour interval, all of which were found to be associated with +CGs. Furthermore, WWLLN identified 18 of these events (open circles) providing accurate information on their location. The positions of the remaining TLEs (solid circles) were estimated from their central azimuth and elevation in image data assuming an altitude of 86 km (the mean of 58 sprites identified by WWLLN during this night, as discussed in Chapter 4).

The resultant uncertainty in the location of these events was ~10-15 km, and had minimal effect on their overall spatial distribution.

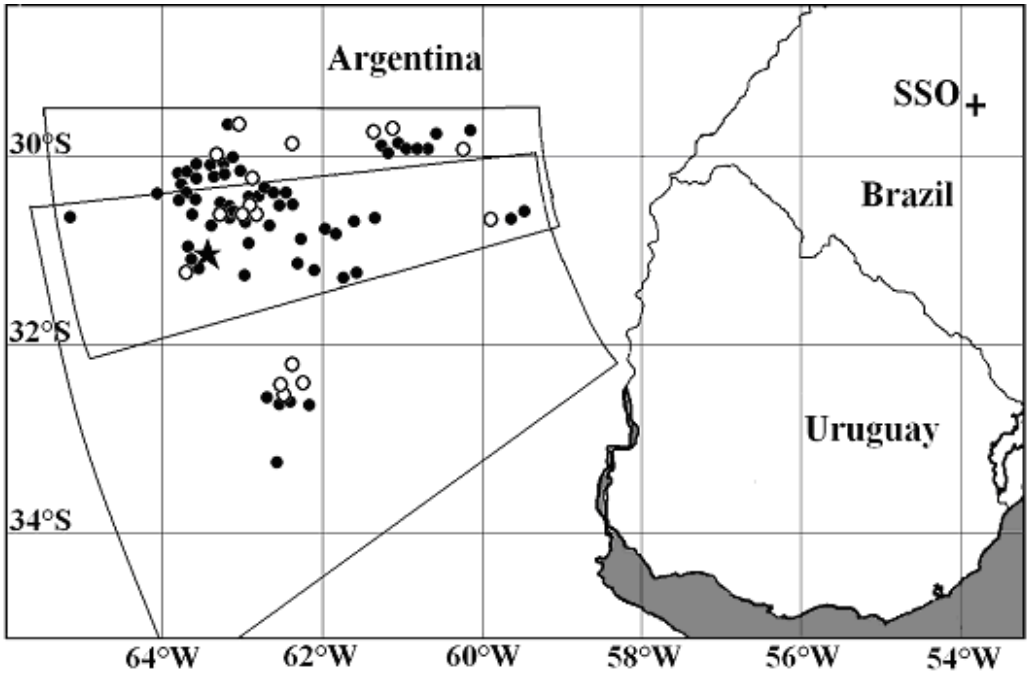


Figure 6.2. Map showing locations of 81 TLEs observed from 05-06:00 UT. The main storm activity was due west of SSO with a second, less active region to the ~WSW. Open circles denote 18 events identified by WWLLN. Solid circles depict estimated locations of remaining events. The star locates the negative sprite-halo event.

The star indicates the WWLLN location of the negative event (31.039°S, 63.457°W), which occurred at ~05:29:33 UT, and was clearly detected by both cameras (as it occurred in the overlapping region), and the ELF/VLF sensors. This TLE will hereafter be referred to as Event 1. Figure 6.3 shows a GOES infrared satellite image of the storm at 06:30 UT, approximately one hour after this negative event. Unfortunately, no satellite data were available from 04:00 – 06:30 UT. However, WWLLN lightning locations and rainfall data from the Tropical Rainfall Measuring Mission (TRMM) satellite [J. Thomas, private communication, 2007] indicate the events shown in Figure

6.2 occurred predominantly above the stratiform region of the MCS, rather than the convective core regions, in good agreement with previous U.S. High Plains TLE measurements [e.g., *Lyons*, 1996].

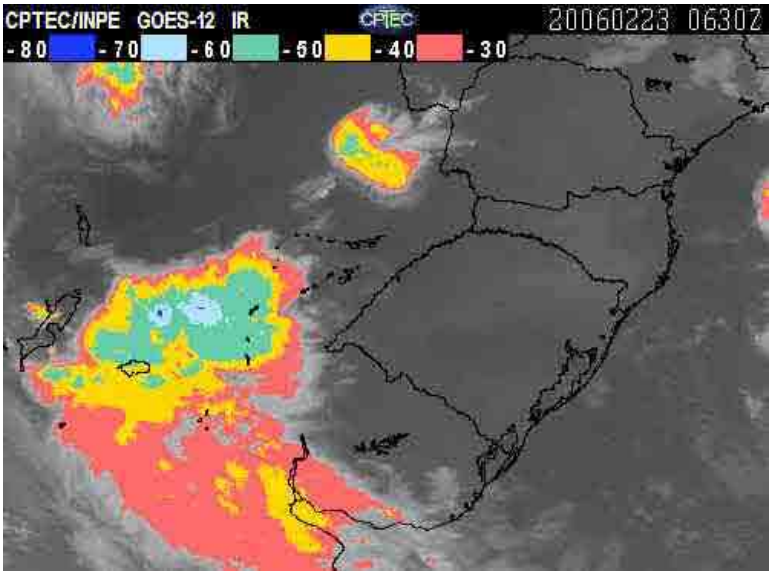


Figure 6.3. GOES 12 infrared satellite image showing the storm at 06:30 UT.

Figure 6.4 shows an enlarged (6° x 4°) image of the negative event as captured by the narrow angle camera at 05:29:33.522 UT. A well-developed sprite-halo is evident exhibiting a characteristic upper diffuse horizontal disk with several embedded, bright columnar forms and fainter tendrils extending downwards and branching at lower elevations. The event occurred at a central azimuth of 257.9° N and a range of 944 km. In the wider field image this event was observed in a single video field (16.7 ms duration) at 05:29:33.535 UT, whereas the narrow angle data (Figure 6.4) show development of the sprite-halo over two consecutive video fields. Together these data limit the sprite initiation time to between 05:29:33.515-519 UT (taking into account the ~3 ms

propagation time to SSO), with a maximum duration of <17 ms, which is in excellent agreement with the WWLLN time of 05:29:33.5162 UT.

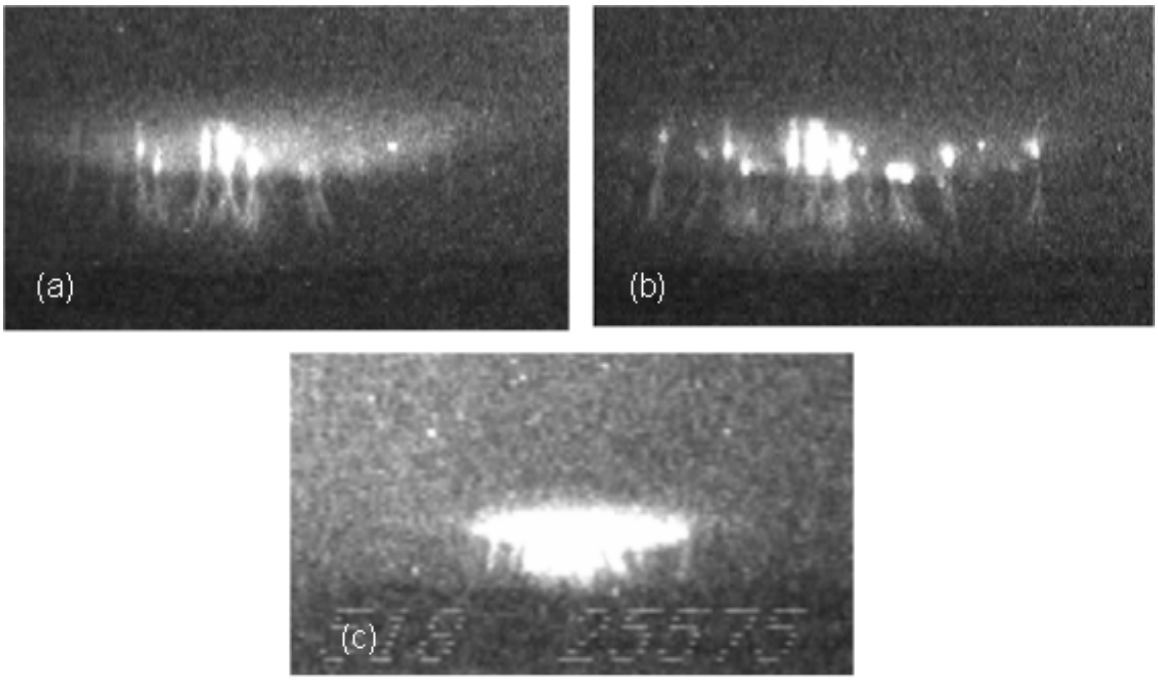


Figure 6.4. (a) Enlarged (6° x 4°) video image of the negative event imaged at 05:29:33.522 UT (azimuth ~257.9° N, range ~944 km) showing a well developed sprite-halo with streamers; (b) Same event with same camera 17 ms later, showing further streamer development as the halo slowly fades; (c) Same negative event imaged by the second camera with larger field of view and higher electronic gain. The event was only captured in one field with this camera, limiting its lifetime to less than 17 ms, and is temporarily overloaded in the image.

Coincident ELF/VLF measurements from SSO have been used to determine the polarity, current, and charge characteristics of the causative lightning stroke. Figure 6.5a shows its ELF/VLF azimuthal magnetic field (Bφ) waveform. The sferic onset time of 05:29:33.5193 UT matches the WWLLN data within 0.1 ms (taking the 3 ms travel time into account). The large upward pulse unmistakably shows that this TLE was produced by a -CG discharge with associated downward net charge transfer. In comparison, Figure 6.5b shows Bφ for a similar sprite-halo that occurred at the same azimuth (255.4°) ~1

hour earlier. The sharp downward pulse is typical for a TLE produced by a +CG (these two events are compared further later). The ΔM_{Qv} (first 2 ms) for the –CG (method of *Cummer and Inan* [2000]) was determined to be –503

C.km. Confirmation of the negative polarity of this event was also provided by simultaneous vertical electric field data from SSO (not shown), and by Y. Yair, University of Tel Aviv using ELF measurements from Israel and Hungary [*Taylor et al.*, 2008].

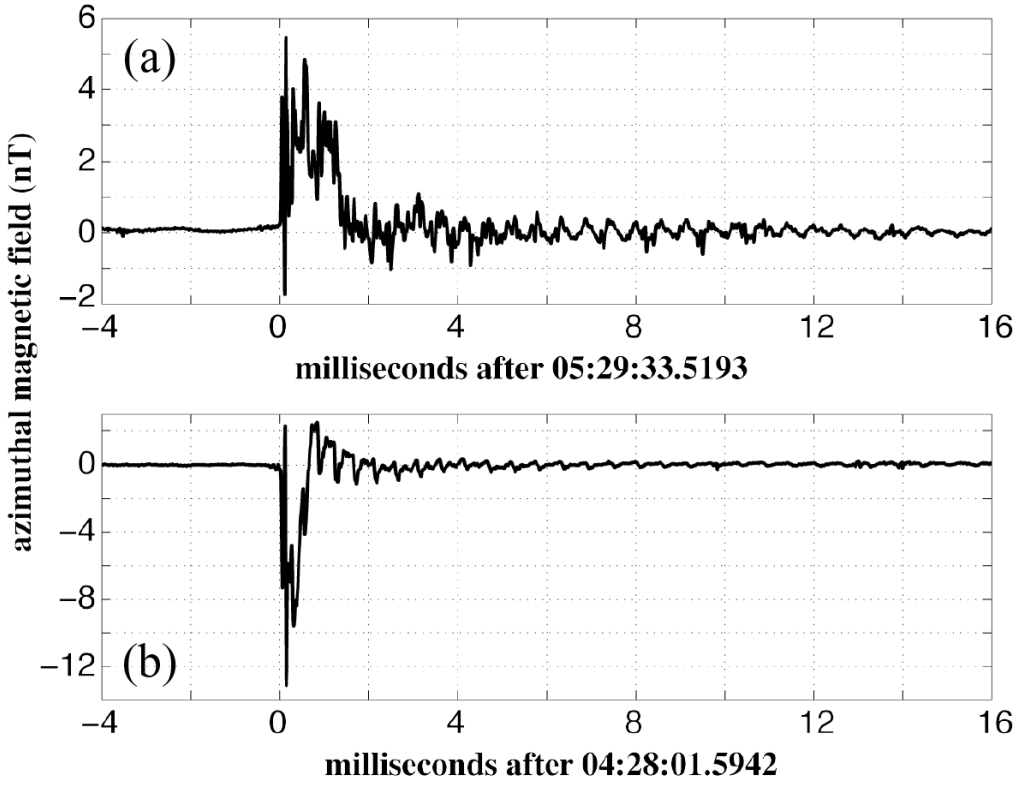


Figure 6.5. (a) The ELF/VLF azimuthal magnetic field (Bφ) waveform corresponding to Figure 6.3. The large positive pulse unambiguously identifies this TLE with a ` stroke. (b) The Bφ waveform of a sprite-halo (Figure 6.5c) produced by a positive CG of similar $\Delta M_{Qv.}$

By combining the WWLLN location of the negative event with its measured azimuth and elevation from the image data (determined using standard star field calibration and taking full account of refraction effects), the altitude of the halo was determined to be 83 ± 1 km, and its diameter 89 ± 5 km, using the analysis methods discussed in Chapter 5. These results are in good accord with previous halo observations [e.g., *Wescott et al.*, 2001] and provide further evidence for the accurate identification of this event.

6.2.1. Comparison with Previous Negative Results

Previously, only two negative events have been substantiated, both exhibiting exceptionally large ΔM_{Qv} (-1380 and -1550 C.km) as measured within the first 5 ms of the spheric. However, their video signatures were partially obscured by cloud and no estimates of their vertical extent were made [*Barrington-Leigh et al.*, 1999]. Both events originated from a thunderstorm system that was part of a MCS located over the Gulf of California. This storm was unusual as the sprites were produced from a region overly dominated by –CG lightning, with very few (~1.5%) +CG discharges detected during its lifetime, compared with the surrounding MCS that exhibited +CG occurrence rate of ~6% (of total lightning strokes) which is more typical of a spriting storm. In contrast, the negative event reported here originated from a large MCS over the Pampas of Argentina (~ 600 km to the nearest open water), that produced numerous TLEs (at least 445), within the stratiform region in close proximity to the observed negative event (Figure 6.2). The ΔM_{Qv} (-503 C.km in 2 ms) associated with this event was at least 30% larger than other TLEs observed within ±10 min and 100 km radius (total 6 events), all of which were

positive and had ΔM_{Qv} ranging from +32 to +383 C.km. For direct comparison with the *Barrington-Leigh et al*. results, Duke University further evaluated the ΔM_{Qv} of our negative event yielding -822 C.km (over a 5 ms interval) with a total of 843 C.km over the 8 ms duration of the charge moment change as determined from the spheric data. These are large values compared with typical sprite producing +CGs [e.g., *Cummer and Lyons*, 2005], but are significantly lower (~ 40%) than the negative ΔM_{Qv} reported by *Barrington-Leigh et al*.

6.2.2. Comparison with Positive Event

As discussed in Chapter 2, the conventional breakdown mechanism for initiating sprites and halos is largely independent of the electric field direction, and thus the lightning polarity [*Pasko et al.,* 1997a]. However, the critical field needed to maintain streamer propagation is approximately a factor of two larger for negative streamers when the field and propagation direction are anti-parallel [*Pasko et al.,* 2000; *Bazelyan and Raizer,* 2000]. Furthermore, simulations by *Pasko et al*. [2000] predict that although positive and negative sprites should be morphologically similar, positive sprites should extend approximately 10 km lower in altitude under otherwise identical conditions (e.g., charge moment change and atmospheric conductivity).

To investigate this, Figure 6.6 (a, b) shows the development of the negative sprite-halo as recorded by the narrow field camera over two consecutive video fields (total duration 33 ms). The data are shown as photographic negative images, after background subtraction, to enhance the sprite structures. As the halo (center altitude 83 km ± 1 km) faded during this interval, the sprite evolved with additional streamers and some limited

downward development of existing streamers. Using the WWLLN location, the lowest visible border of the streamers was determined to be ~ 63 km for the first field and ~ 61 km for a small part of the second field. However, the base of the streamers clearly remained above the horizon at SSO (as shown by the horizontal line). This indicates a relatively short vertical extent (~25 km) for the negative sprite with no obvious streamer penetration into the stratosphere. Figure 6.6c shows the optical signature of a sprite-halo that was produced by a +CG with a similar ΔM_{Qv} (480 C.km, shown in Figure 6.6c) to that of the negative event. This TLE was imaged by the narrow field camera at approximately the same azimuth (255.4°) as the negative event, but ~1-hour earlier (04:28:01 UT). The video data also show it occurred at almost the same geographic location as the negative sprite-halo (within 30 km) and exhibited a similar halo diameter (85 ± 5 km), assuming a central altitude of 83 km. The tendrils appear to be cut-off at the horizon (horizontal line) suggesting they extended to lower altitudes than ~60 km. Comparing these two events of different polarity suggests the positive sprite-halo exhibited streamers that were significantly longer, in agreement with predictions of *Pasko et al.* [2000].

As the Xybion camera was operated at the same electronic gain throughout the night, changes in relative brightness of the negative event as it developed have also been investigated. This is shown in Figure 6.6 (d, e) which plot the relative brightness of the sprite-halo as determined from a horizontal intensity scan through the middle of the halo centered at 83 km altitude. Significant development of both halo and sprite emissions are evident from one field (17 ms duration) to the next. Initially, several narrow sprite structures are evident (Plot d) imbedded in the diffuse halo emission, which appears as a

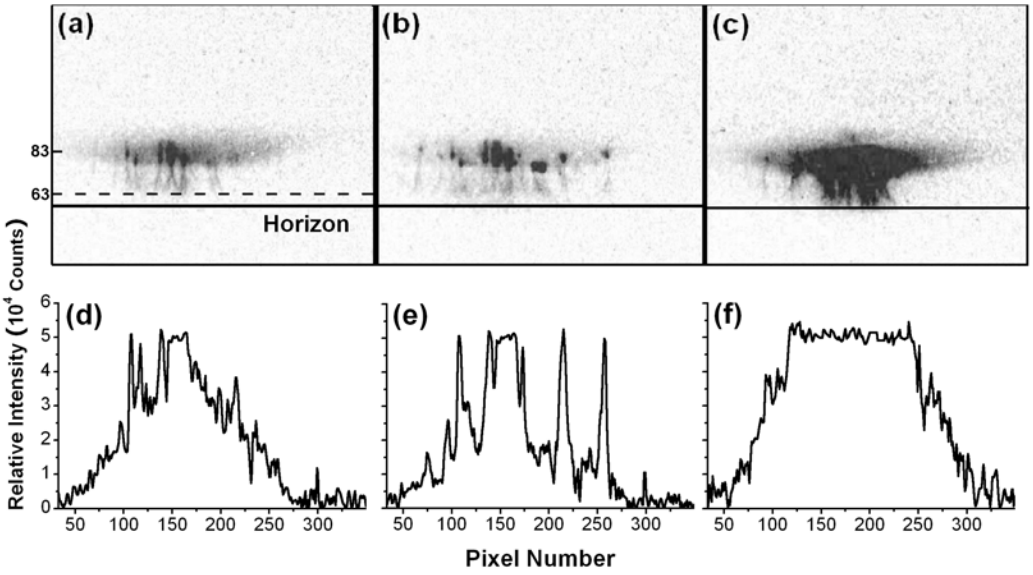


Figure 6.6. Images (a, b) showing the downward development of the negative event over two video fields (duration 33 ms). The data are shown as negative images, after background subtraction, to enhance the sprite structures (lower visible border ~61 km). Image (c) shows the positive sprite-halo, which occurred at approximately the same location 1-hr earlier. Panels (d, e, f) compare horizontal cross-sections of the relative brightness of the negative and positive events.

large symmetric bulge of peak relative brightness ~30,000 counts (or ~60% of maximum signal level). The subsequent field shows further intensification of the sprite's columnar-like structures (close to the video saturation level) and a significant decrease in the relative brightness of the halo emission by ~50%. Plot f shows a relative intensity scan through the halo region of the positive event, which exhibited comparable spatial dimensions to the negative event (but was only evident in one video field). Although the basic shape of the plot is similar, the combined sprite and halo emissions saturated the camera and the imbedded sprite structures are not discernable.

Together these results suggest that both the length and the apparent brightness of the downward negative streamers are more limited for this negative driven sprite-halo

event as compared with a positive event of similar location, morphology and ΔM_{Qv}. The shorter negative streamer lengths are consistent with the need for larger critical fields to maintain downward streamer propagation [*Bazelyan and Raizer*, 2000]. Furthermore, *Liu and Pasko* (2004) have shown that under identical conditions, positive sprite streamers should appear brighter, due to the larger expansion of their streamer heads as they propagate downwards into the higher electric field region, as compared with negative streamers which would appear dimmer when propagating over the same distance.

To summarize, there are many factors which ultimately control the development of a sprite, and the widely used phrase in the sprite community that no two sprites are the same underlines the inherent difficulties of comparing sprite events (even of similar charge moments). However, these data have provided the best opportunity to date to study a well-defined negative sprite event and to compare its optical properties with those of a similar sprite-halo generated by a +CG.

6.3. Other Negative Events

After discovering our first negative event, Duke University undertook a detailed investigation of their ELF/VLF lightning data examining waveforms associated with each of the 445 events observed on February 22-23, 2006. As WWLLN only measured lightning timing and location, the ELF/VLF data were the only way to determine TLE polarity. During this study an additional six negative events were found, all of which were associated with halos (2 sprite-halos and 4 halos). These events and their characteristics are now described.

6.3.1. Sprite-Halo Events

Two negative sprite-halo events of similar morphology to the event discussed in Section 6.2 were imaged from the storm during the next 1.5 hours as it moved northwards. Both events occurred at closer ranges of ~620 and ~650 km. Figure 6.7 shows a very clear sprite-halo event initiated between 06:32:06.085 - 06:32:06.099 UT, with a corresponding lightning time (as determined by the ELF/VLF sensor) of 06:32:06.091 UT. The sprite halo occurred at an azimuth of 266.1°, with an elevation of 4.31°. This event was also captured by both cameras, but in this instance the TLE was evident in only one field in each camera. This limited its lifetime, coupled with the lightning data, to < 8 ms. This event was not associated with a WWLLN lightning detection, and so a mean height of 83 km (based on the halo analysis of Chapter 5) was assumed for the spatial analysis. This event occurred at ~29.8°S, 60.5°W at a range of 647 km, and is indicated in Figure 6.8 as event 2. Using this result for the TLE location, the halo diameter was estimated to be 67 km, and the sprite tendrils were determined to extend down to ~61 km in altitude, which agrees well with the measured altitude from negative event studied in Section 6.2. The impulsive charge moment associated with this event was determined to be -317 C.km, somewhat lower than that of event 1.

The third negative sprite-halo is shown in Figure 6.9 and occurred at an azimuth of 265° and an elevation of 4.5°, in close proximity to event 2 (see Figure 6.8). The halo is very prominent in this TLE, which exhibited limited sprite structures. This event was initiated approximately 45 minutes after event 2, and was associated with WWLLN lightning detection at 07:17:17.143 UT. Event 3 was also captured in both cameras, and was seen in two fields of one camera, but only one field of the second camera, which

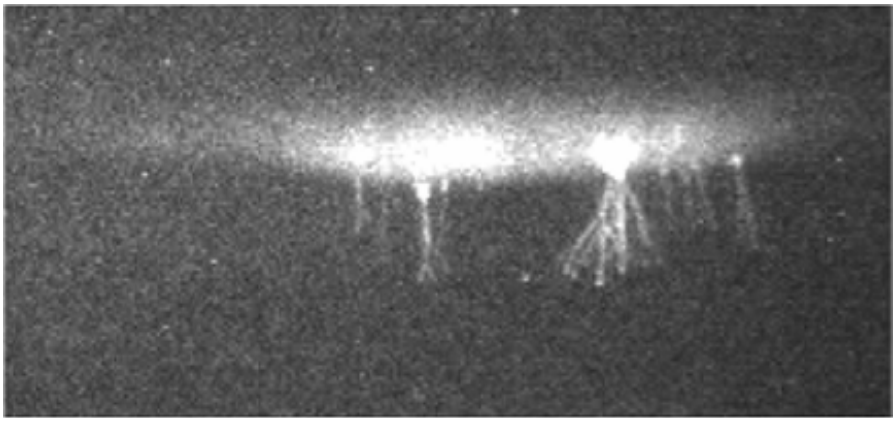


Figure 6.7. A sprite-halo associated with a negative event at 06:32:06.085 UT.

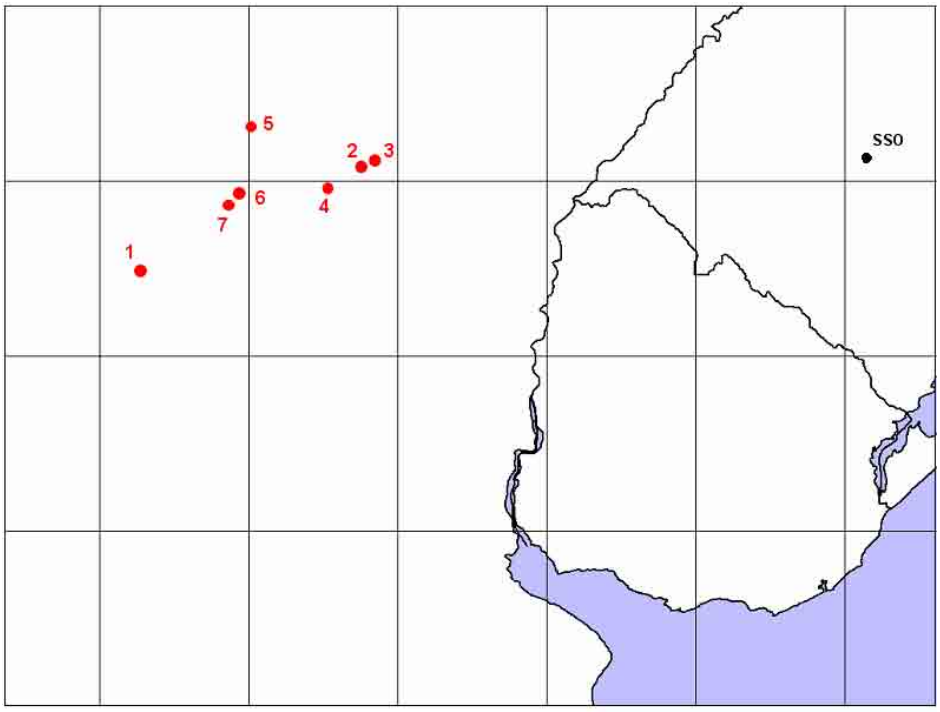


Figure 6.8. Map showing the locations of all TLEs associated with –CGs imaged on February 22-23. Also shown are identification numbers of these events.

limits its lifetime to <14 ms. Combining this information with the WWLLN data, indicates a TLE initiation time within 4 ms of the negative lightning stroke (between 07:17:17.143 and 07:17:17.147 UT). Using its WWLLN lightning location, the mean halo altitude was measured to be 81 km, and its diameter 64.5 km. This event occurred at a range of 623 km, and measurements of the tendrils show that they extended down to ~64 km. The impulsive charge moment associated with this event was -304 C.km, similar to event 2.

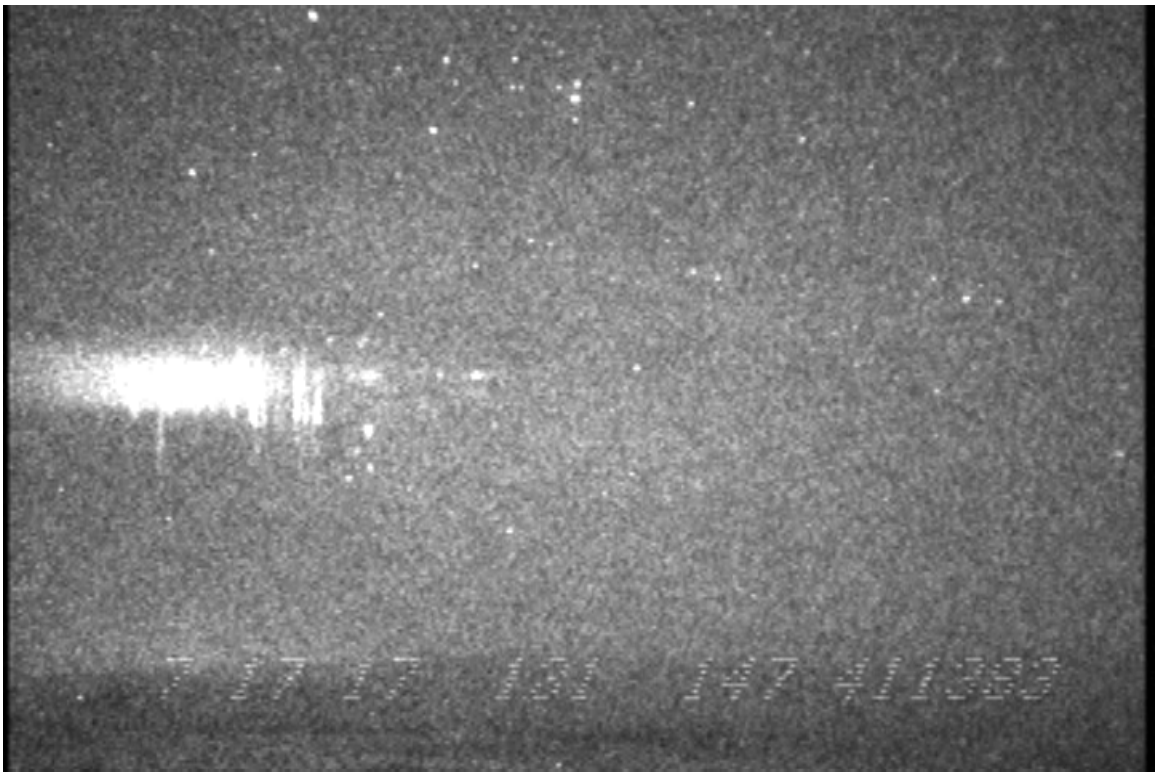


Figure 6.9. A sprite halo associated with a –CG at 07:17:17.131 UT.

As luck would have it, this negative event was immediately preceded by a large, long-lived, positive sprite-halo, which occurred in almost the same location. Figure 6.10 shows this positive event, which was clearly identified in WWLLN and had a charge

moment of 368 C.km. In comparison with event 3, this event had a similar range of 640 km, and a similar mean altitude of 83 km for its halo, but a somewhat larger halo diameter of 82 km. Figure 6.11 plots the location and apparent sizes of the halos associated with this positive and negative pair. The solid squares indicate the location of the WWLLN lightning for each event, which occurred within 0.9 s of each other. The map also shows that these two events are spatially overlapped, making this a very interesting pair of TLEs to study. The images of these two events, shown in Figures 6.9 and 6.10, were both taken by the same camera within a second of each other, and at the same electronic gain. Both events temporarily overloaded the camera, and it appears that the positive event is significantly brighter and more spatially extensive for both the halo and its associated sprite streamers.

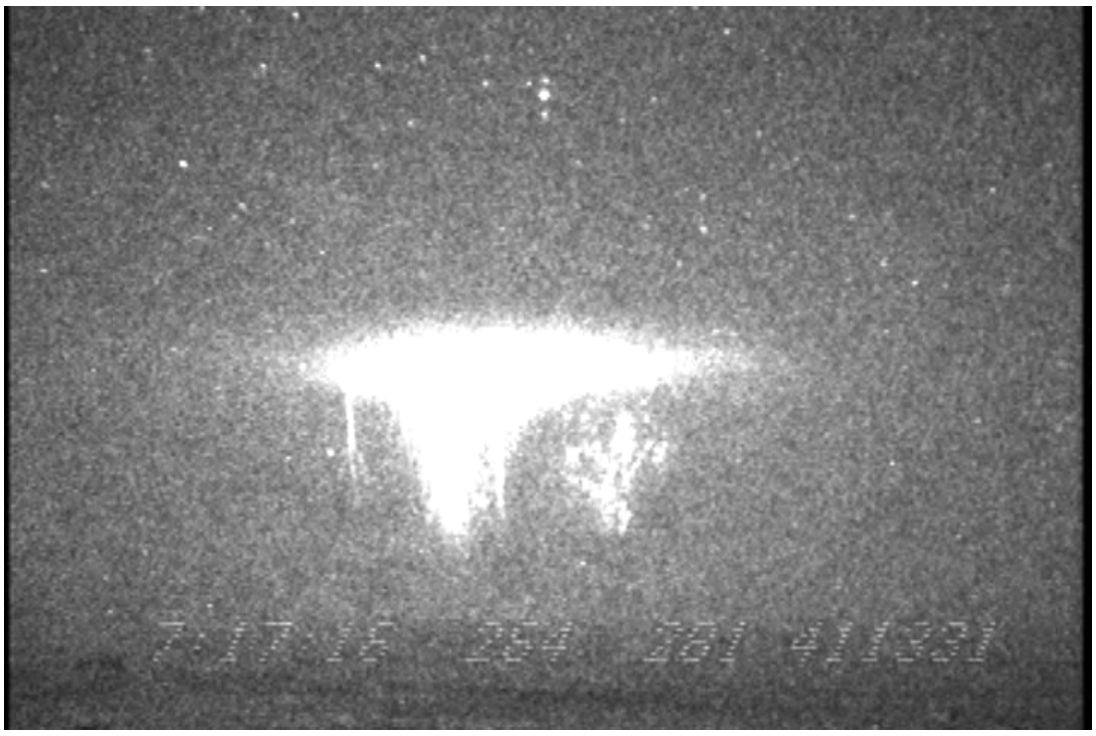


Figure 6.10. A sprite halo associated with a +CG occurring at 07:17:16.264, 867 ms just before the halo shown in Figure 6.9.

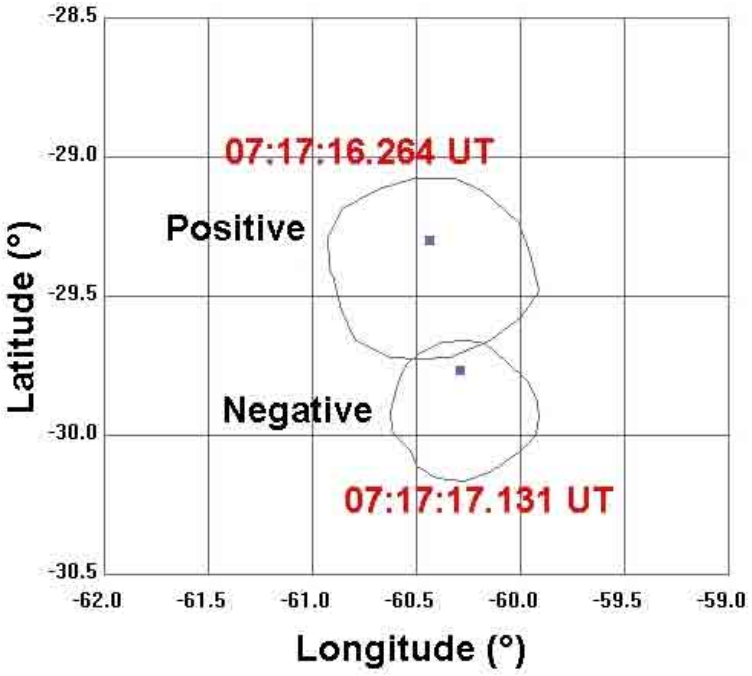


Figure 6.11. Map showing the locations of the positive and negative sprite-halos imaged at ~07:17:17 (within 1 second of each other).

This is qualitatively consistent with the measured charge moments, which were ~20% l00arger for the positive event. However, it is also expected that the brightness of the halo depends more on the impulsiveness of the charge moment than on its polarity. This point is illustrated earlier in Figure 6.5, which shows charge moments for event 1 compared with a similarly located positive event. The inspection of the waveform shows the charge moment change of the positive event was much more rapid than that of the negative event, yet it had a larger charge moment. To investigate this negative/positive pair further, we utilize image data of these two events from the second camera which, as mentioned earlier, had an overlapping field of view. This camera was operated at a lower electronic gain, and structure in these events is more easily discernable.

Figure 6.12 shows a composite image of these two distinct TLEs. The upper section shows the positive sprite-halo (left hand side only). In this image the halo and the associated sprite structures are quite distinct. The lower section shows the negative event in the correct lateral position, but displaced in altitude with respect to the positive event, so that we can compare their structures. This is illustrated in Figure 6.13 which shows intensity scans across each section, passing through the center of each halo. The negative event is plotted shown in red, and exhibits a well-formed bulge in emission intensity associated with the halo, with superposed fine-scale structure, due to the narrow c-sprites emanating from the halo and penetrating down to ~64 km. The black curve shows the intensity signature of the positive event, which appeared to exhibit similar halo emission brightness, but with significantly brighter embedded sprite structures that overloaded the camera near the edge of the field of view. Thus it is possible that it was the embedded sprite structures which cause the brighter TLE signature evident in Figure 6.9 (negative event) as compared with Fig 6.10 (positive event), rather than their associated halo signatures.

Also indicated on this plot is a strong signature of a unit sprite which is readily evident in the upper panel of Figure 6.12 (indicated by the arrow). Close inspection of the lower panel shows faint evidence of this structure in the negative event. This is remarkable as the negative event occurred ~0.9 s following the positive TLE, and suggests that the negative TLE, which has its own associated structure was also able to re-illuminate parts of this unit sprite structure that were closest to it. Such re-brightening has been observed in high speed imagery [*Stenbaek-Nielsen et al.,* 2000], but the rather

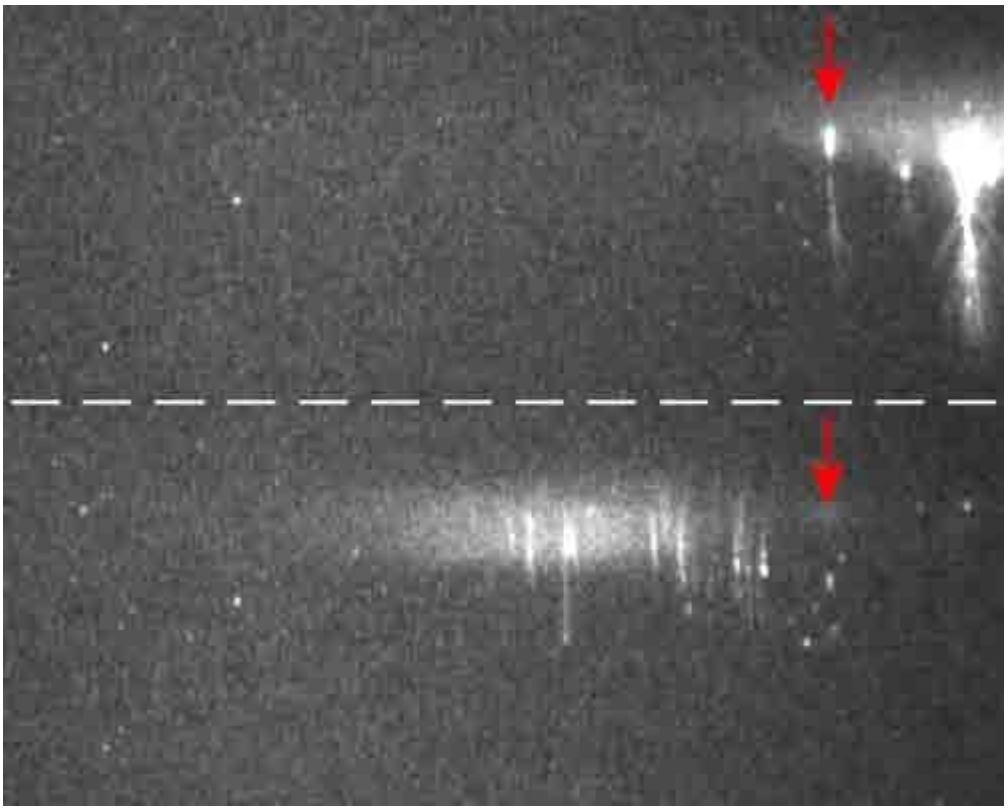


Figure 6.12. Composite image showing a positive sprite-halo (upper panel) and a nearby negative (bottom panel) event that occurred within 1 s of each other. Note both events are shown in their correct lateral position, but the negative event is displaced downwards in altitude to facilitate their comparison.

large time delay between these two events is unprecedented. This is because the relaxation time at sprite initiation altitudes (~70 km) is expected to be significantly <100 ms [*Pasko et al.,* 1997a]. Furthermore, it is interesting to note that the large sprite structure evident near the center of the positive halo extended down to ~50 km, approximately 14 km lower than the negative streamer structures, and that there is no evidence or re-brightening of this feature during the negative event (possibly due to its further lateral distance from the centroid of the negative event, ~20km, compared with the small unit sprite). This said, it also appears that the lightning stroke identified by WWLLN is offset, with respect to the estimated center of the optical signature, towards

the positive event, and therefore the electric field may have been stronger near the unit sprite. Further analysis of this complex pair and their continuing currents identified by the ELF/VLF data is ongoing.

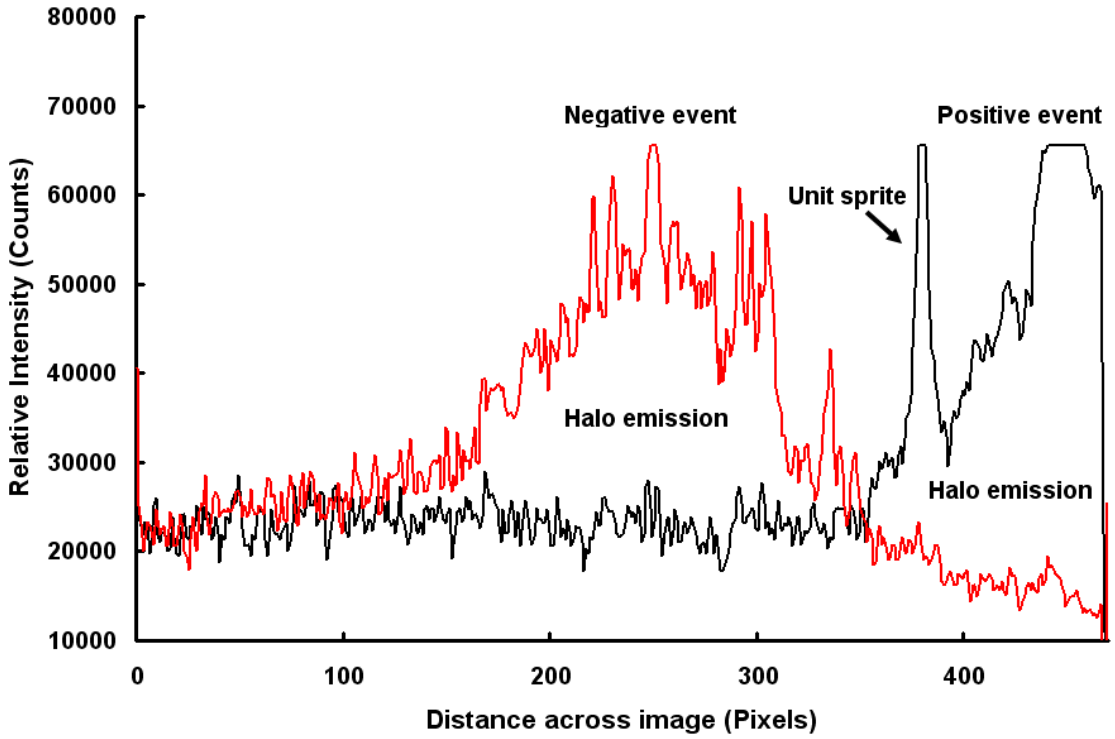


Figure 6.13. Horizontal scans across the TLE images shown in Figure 6.12 centered on the peak of the halo signatures. Note in these data the negative event is no longer overloaded.

6.3.2. Halo Events

As discussed earlier in this chapter, halos are mostly associated with +CG flashes (see Table 6.1), but recently they have been associated with negative lightning discharges, especially over open water [*Frey et al.*, 2007]. In addition to the three negative sprite halo events that were detected on this night, we have identified four simple halo events with no associated sprite streamers closely associated with –CGs.

These events occurred over the Pampas of Argentina, approximately 600 km to the nearest open water.

The two brightest halo events were observed over an hour apart at 05:59:43.467 UT and 07:00:10.581 UT. They were detected by WWLLN and by the ELF/VLF sensor and are designated as events 4 and 5. Figure 6.14 shows two images of halo event 4 as captured simultaneously by both cameras. The halo was evident for only one field in both data, and appears brighter in the left hand image due to the higher camera gain. The distinct form of the halo is clearly evident in both images. From these data, the halo initiated between 05:59:43.467 and 05:59:43.474UT, and its corresponding WWLLN lightning time was 05:59:43.470 UT. These data show that this event was very transient (<4 ms). The halo had an elevation of 3.66°, and occurred at an azimuth of 264.2°. From the mapping analysis, this event occurred at a range of 690 km, yielding an estimated altitude was ~85 km, and a diameter of ~50 km. Analysis of the image data shows that there were 27 TLE's within ±10 minutes of this event, of which two were halos, six were sprite halos, and 19 were sprites, all associated with +CGs. The impulsive charge moment of the parent lightning for this event was -279 C.km.

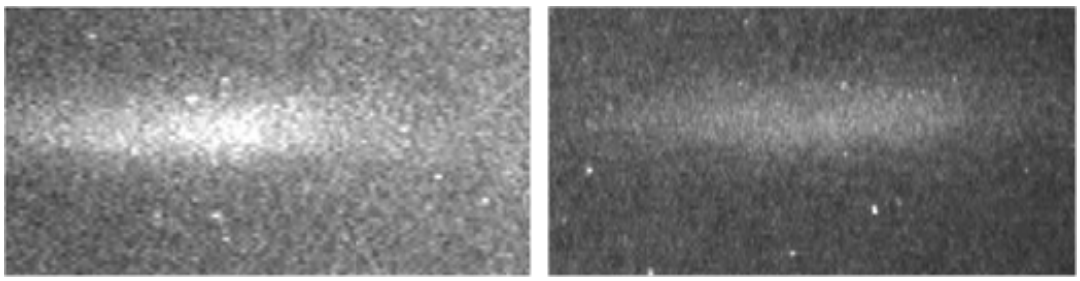


Figure 6.14. Two simultaneous images of a negative halo (event 4) imaged at 05:59:43 UT by separate cameras, each with different electronic gain settings.

Figure 6.15 shows a close up image of a second well-defined halo (event 5) which initiated between 07:00:10.587 and 07:00:10.598 UT. The corresponding lightning time was 07:00:10.596 UT. The halo occurred at an azimuth of ~270° and at an elevation of 2.4°, and at a range of 790 km, assuming an altitude of ~83 km, which yields a diameter of ~64 km. There were 21 TLE's associated with +CGs within ±10 minutes of this event, of which three were halos, eight were sprite-halos, and 10 were sprites. Figure 6.16 shows the ELF/VLF azimuthal magnetic field Bphi associated with negative halo. The impulsiveness of this lightning event is clearly evident, suggesting a duration of about 1 ms, comparable to waveform signatures of the sprite-halo event (shown in Figure 6.5). The associated charge moment for this halo event was determined to be -296 C.km, which is significantly less than that shown in Figure 6.5, due to the absence of continuing current in this case. For comparison with the sprite-halo data, the locations of these two halo events (4 and 5) are indicated on the map of Figure 6.8.

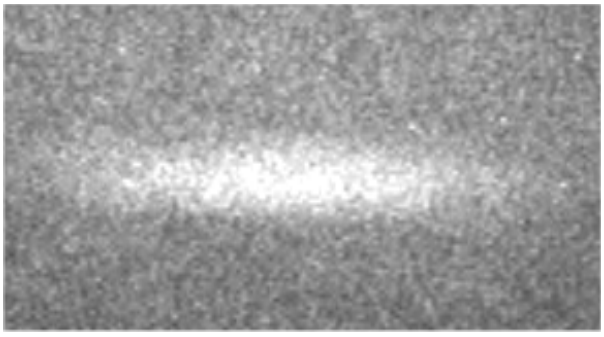


Figure 6.15. A negative halo captured at 07:00:10 UT on Feb. 22-23.

Two significantly fainter halo events were also identified during our image analysis and correlated well with –CGs. These events occurred somewhat earlier at 04:34:50.882 UT and 04:35:43.955 UT, within a minute of each other, and in geographic

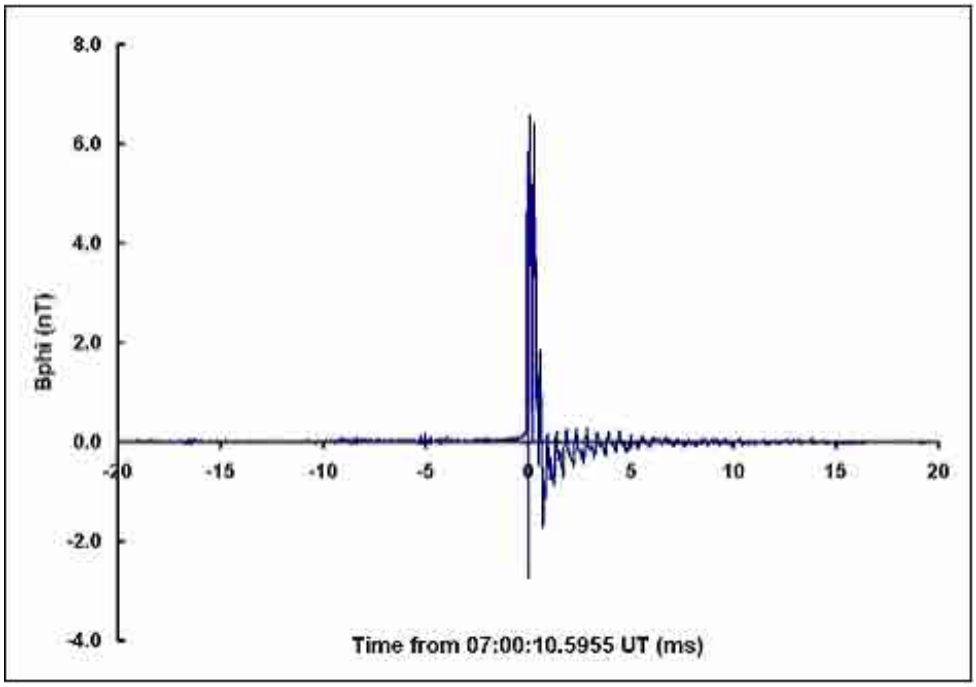


Figure 6.16. The ELF/VLF azimuthal magnetic field Bphi associated with a negative halo (event 5).

proximity. Their positions are indicated in Figure 6.8 as events 6 and 7. Although these halos were both very faint, they were visible to the eye as transient flashes during data analysis at standard video rates. Figure 6.17 shows a difference image of event 6 obtained by subtracting the halo image from an image immediately preceding the event. The ellipse indicates the location of the halo at an azimuth of ~263° and at an elevation of ~2°. This event occurred in a single field between 04:35:43.938 - 04:35:43.955 UT. It was detected by WWLLN at 04:35:43.943 UT, and its location was successfully correlated with the lightning data yielding an altitude of ~82 km. This event was also transient (<12ms) based on optical data coupled with the lightning data. It occurred at a large range of ~808 km, and had a diameter of ~42 km. Importantly, the impulsive

charge moment of the parent lightning associated with this event was only -97 C.km, significantly smaller than the brighter halo events 4 and 5.

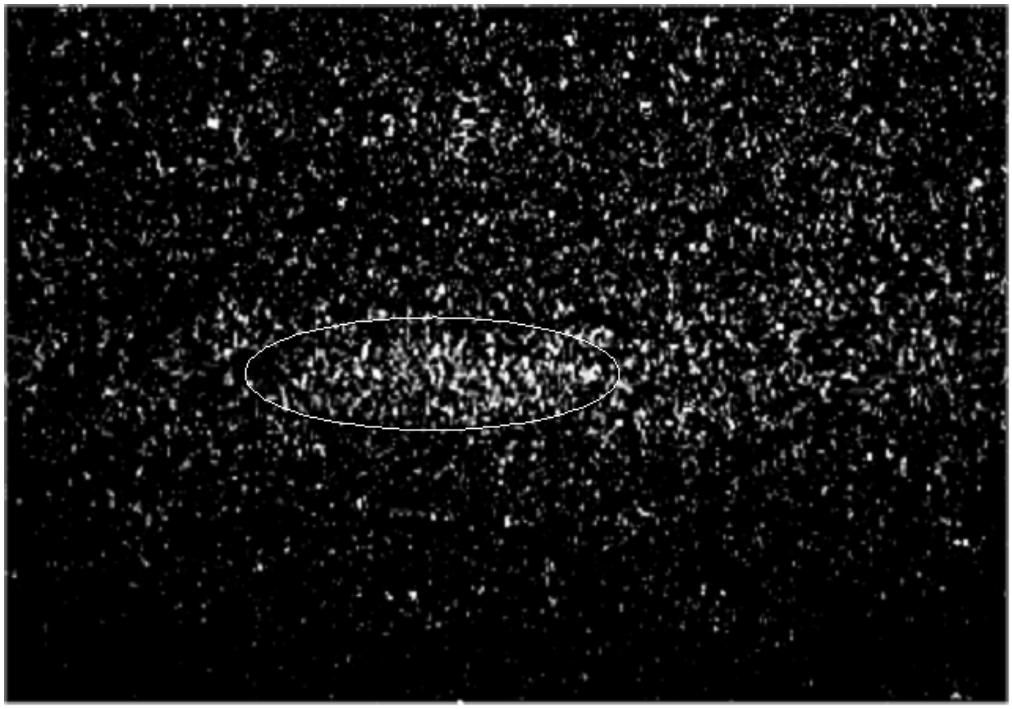


Figure 6.17. Contrast stretched difference image of a faint halo (event 6) that occurred at 04:35:43.955 UT on February 23, 2006. The oval indicates the location and approximate size of the halo.

The second faint halo (event 7) was initiated between 04:34:50.882 - 04:34:50.899 UT, with a corresponding sferic lightning time of 04:34:50.874 UT, indicating a lifetime of <10 ms. It was also only imaged in one field, with an estimated azimuth of ~263° and an elevation of ~2°. Using an assumed mean altitude of 83 km, this event was estimated to have occurred at a range of ~820 km, with an approximate diameter of 59 km. As with event 6, the impulsive charge moment of the parent lightning for this event was also quite small at -107 C.km.

6.3.2.1. Halo Discussion

Although evidence for sprites associated with –CGs is extremely rare, there are reports associating negative lightning strokes with halos. For example, studies by *Miyasato et al.* [2002] and *Bering et al.* [2004] associated at least 18 halo events to –CGs. In particular, *Bering et al*. [2004] detected 17 negative events which he associated with halos, using stratospheric balloon photometry measurements. Recent analysis of ISUAL satellite data suggests that the ratio of negative to positive lightning associated with halos was 2 to 1 [*Frey et al.*, 2007], with a majority of the events occurring over the ocean. The favored working hypothesis in present models suggests that the streamer-like structure of sprites requires a sustained electric field, whereas *Williams et al.* [2007] in their discussion on the polarity paradox suggest that an impulsive overvolting at mesospheric heights is all that is needed to create a simple halo. Evidence supporting this theory may be found in *Barrington-Leigh et al*. [2001] and *Bering et al*. [2004]. Both of these studies show measurements of halos with short time delays (~1ms) from the parent CG, indicating their impulsive nature. This result is supported in laboratory measurements where a fast overvolted electric field produced a uniform (diffuse) discharge in air at stratospheric pressures, whereas slower growing electric fields typically resulted in localized streamer-like discharges, of similar morphology to sprites [*Roth et al*., 2005].

Because the negative charge reservoir typically resides at a lower altitude in the thundercloud than the positive reservoir (as discussed in Chapter 1), sustained quasi-static fields are thought to be harder to produce with –CGs, as their impulsive charge moment changes are usually smaller, and not sustained for long periods of time. However, -CGs

as well as +CGs, are equally capable of producing large, very short-lived fields in the mesosphere, which are thought to be the driving force behind halo formation.

Ground-based observations using conventional video cameras have proven to be sensitive enough to capture halos, but available coordinated polarity measurements indicate that, like structured sprites, they are essentially associated with +CGs. Our observations of negative halos over northern Argentina provide conclusive evidence for negative driven halo events. These negative events represent only four out of a total of 183 halo related events (of which 61 were pure halos), indicating the prominent halos are indeed mainly driven by +CGs.

It has been speculated that there are many more negative halos than reported in the literature. This may be due to their lower brightness, especially when using cameras of limited sensitivity. Indeed, ISUAL satellite observations indicate that halos are typically less intense than sprites by usually an order of magnitude [*Williams et al.,* 2007]. However, there is no comparison to date between halo luminosities over ocean and land, or for positive and negative events. What is clear is that published reports from both ground-based and aircraft observations have yet to associate large numbers of halos with –CGs. Clearly sensitivity is a factor in this discrepancy, as two of the negative halo events reported here were associated with large negative charge moment changes, and were easily captured by our cameras (each of which was operated at a significantly different electronic gain). In contrast, the two faint halos were associated with much smaller negative charge moment changes. This said, the negative charge moments associated with our two highly visible halos were not unusually large, and therefore the

puzzle remains why there are so few examples of negative halos in ground-based data, especially given the preponderance for negative lightning in most thunderstorms.

6.4. Summary

Of the many thousands of sprites reported in the literature, clear images of a negative polarity sprite are extremely rare. This chapter presents detailed measurement of up to seven sprite-halo and halo events that were unambiguously associated with –CG lightning strokes originating from an MCC over Argentina. The identification of these TLEs were made using a combination of simultaneous video, ELF/VLF radio measurements, and WWLLN lightning data (when available) and provides further proof that sprites can be driven by upward as well as downward electric fields, as predicted by the conventional breakdown mechanism [e.g., *Pasko et al.*, 1997]. A summary of the properties of these unique events is given in Table 6.2.

Table 6.2. Summary of TLE events associated with negative CGs observed on February 23, 2006.

Time (UT)	TLE	Diameter	Range	Charge Moment	Latitude	Longitude	Altitude
04:34:50.882	Faint Halo	59 km	820 km	-107 C.km	~ -30.280	~ -62.269	
04:35:43.955	Faint Halo	42 km	808 km	-97 C.km	-30.143	-62.144	82 km
05:29:33.518	Sprite-Halo	89 km	944 km	-503 C.km	-31.039	-63.457	83 km
05:59:43.467	Halo	49 km	690 km	-279 C.km	-29.7	-61.15	85 km
06:32:06.085	Sprite-Halo	67 km	647 km	-317 C.km	~ -29.84	~ -60.495	
07:00:10.581	Halo	64 km	790 km	-296 C.km	~ -29.395	~ -61.971	
07:17:17.131	Sprite-Halo	63 km	623 km	-304 C.km	-29.774	-60.307	81 km
Mean		62 km	760 km	-272 C.km			~83 km

Each of these negative events was similar in morphology and duration to comparable positive polarity events observed from the same storm. However, detailed

analysis suggests that streamer brightness may be lower in the negative events and less vertically extensive, when compared with positive events of similar charge moments. The fact that we have detected several negative events from one storm is quite amazing, and at the same time puzzling. Many studies over the Midwestern U.S. have produced thousands of TLEs associated with positive lightning, yet no substantiated negative sprites and few halos have been reported. It is possible that this Argentinean storm was exceptional in both activity and strength of its lightning discharges. In a study by *Cummer and Lyons* [2005] that analyzed all lightning strokes from two MCSs over the U.S. Great Plains, no -CGs with charge moments over 300 C.km were detected using the same ELF/VLF instrument utilized in this campaign. However, in the South American storm analyzed here, the three negative sprite-halos exceeded this value. The characterization of these negative events is very important in trying to bridge the gap between observations and theory. Why we saw so many from one storm is not clear, especially considering the apparent lack of negative events over the U.S.A. Investigations to date of the March 3-4 storm have yielded no other negative events, although the analysis is still ongoing. Future studies in this part of the world, as well as other areas of high activity may answer the polarity paradox question, or at least help in improving our understanding.

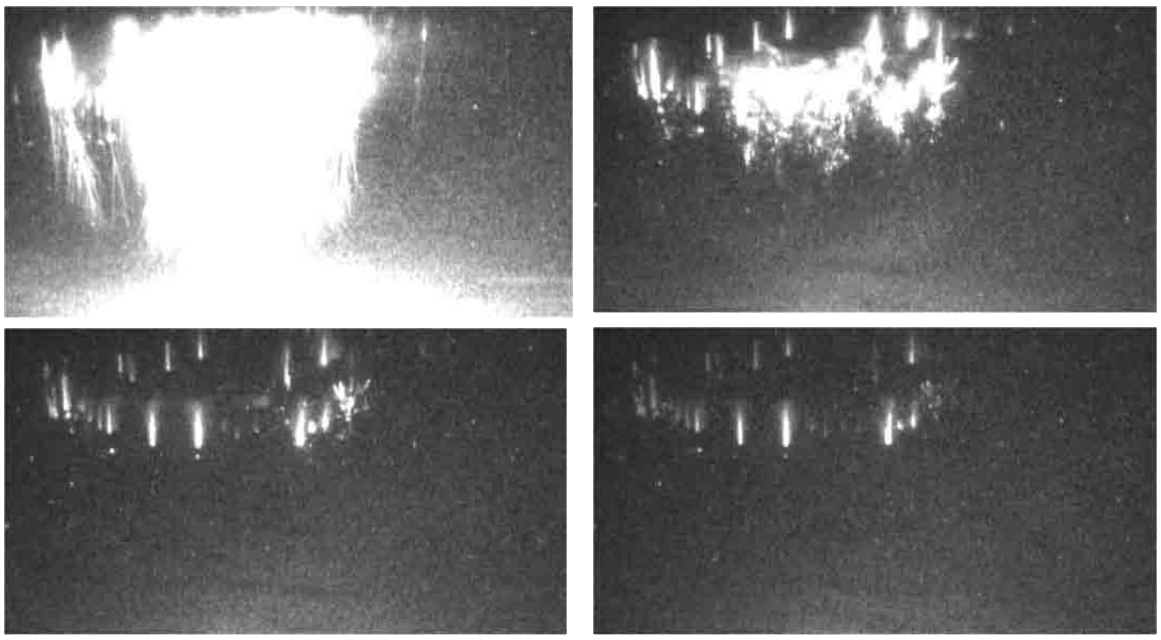
CHAPTER 7

SUMMARY AND FUTURE WORK

"… An American Airlines captain reported this event at approximately 0850GMT on 06/12/99 while flying near the coast of ***Costa Rica****. He said the anvil of a thunderstorm (located 40 nautical miles west-northwest of his aircraft) lit up with a very bright glow and then several discharges shot vertically to very high altitudes. He indicated the color of the event was white. The location of the aircraft was 09.423° N and 85.2° W.*

The pilot also indicated that he had read an article about Sprites and Jets!"

— Rob Hudson, meteorologist, American Airlines



Consecutive sequence of video images at 16.7 ms sample rate showing a remarkable ring-like cluster of sprites, recorded on February 23, over Northern Argentina.

7.1. Summary

Lightning-driven events in the middle atmosphere known as Transient Luminous Events (TLEs) have been discovered and characterized over the last two decades. These magnificent optical phenomena exhibit several different morphological forms, known as sprites, elves, halos, and jets, each characterized by differing horizontal and vertical structure and lifetimes. These events have been shown to be associated with terrestrial cloud-to-ground lightning, which temporarily provides large electric fields above active thunderstorms that can excite optical emissions by electron collision in the neutral upper atmosphere. Serendipitously discovered over the Midwestern U.S. in 1989, these beautiful phenomena have now been observed in many parts of the world, including Asia, Europe, and South America, in association with strong storm activity.

Previous studies of the low frequency waveforms generated by lightning discharges have indicated that the regions of southern Brazil and northern Argentina are prolific TLE producers. As part of a joint, collaborative Brazilian campaign with the University of Washington, INPE, and later Duke University, Utah State University deployed sensitive imagers on ground, aircraft, and balloon payloads to capture novel data of these transient events over South America. Two campaigns were conducted. During the Brazil 1 campaign, which was conducted from Cachoeira Paulista, SP, in 2002-2003, our exploratory measurements led to the first ground-based detection of sprites over Brazil, in association with large-scale storms driven by strong frontal activity. Planned coincident ground-based and balloon-borne measurements were not achieved. However, electric field measurements were successfully obtained above these

types of storms, using balloon-borne instrumentation, revealing the largest in-situ electric fields on record [*Holzworth et al.,* 2005].

Based on these successful, but limited measurements, a second campaign took place in 2006, this time from Santa Maria, in the southernmost part of Brazil. This site was chosen due to extremely large Mesoscale Convective Complexes, or MCCs, which occur frequently in this region of South America during the austral spring and fall seasons. On February 22-23, such a system formed over northern Argentina, several hundred km to the west of our observing site. This system was observed for over six hours as it developed throughout the night. However, its extreme range made it inaccessible to coordinated balloon-borne measurements. Our ground-based measurements were successful, and a total of 445 TLEs were recorded, making this the third largest spriting storm ever witnessed. Of these 445 TLEs, a high percentage were in the form of halos and sprite-halos, providing a unique opportunity to study the physical characteristics of these events over South America.

Halos are diffuse optical emissions which originate near 80 km altitude, and are primarily driven by the quasi-static electric field that occurs shortly after large cloud-to-ground lightning. Over 180 of these events were studied in detail, to determine their central altitude, mean diameters, and association with lightning charge moment changes. These measurements utilized ELF/VLF sferic data from Duke University, and lightning location information from the World Wide Lightning Location Network (WWLLN). The ELF/VLF sensors were co-located with our ground-based image measurements at the Southern Space Observatory (SSO) near Santa Maria, providing crucial information on the causative lightning. Key results of our investigation show that halo events occurred

at similar mean altitudes, and exhibited comparable scale-sizes and morphology to prior limited studies performed from the Midwestern U.S. Novel measurements of their associated charge moments were significantly smaller for almost all of the South American events as compared with similar North American sprite measurements.

Remarkably, seven of the halo and sprite-halo events were directly associated with –CGs, as confirmed by Duke University ELF/VLF data [*Taylor et al.*, 2008]. Negative sprite events are extremely rare, with only two (possibly three) out of many thousands of events reported in the literature. The absence of TLEs driven by negative lightning has puzzled many in the scientific community, because the prevailing quasi-static electric field theory is not polarity dependent. Our observations of seven negative events in a single storm are unprecedented. Detailed analysis of these data indicates that the three sprite-halo events were associated with relatively large charge moments, while the fainter pure halos exhibited smaller charge moments. Comparison of the sprite structures associated with the negative events with nearby positive events of similar charge moment changes suggest that the negative sprite streamers are significantly shorter and somewhat lower in luminosity. Our results, although limited in number, provide the first quantitative measurements of negative sprite morphology and scale sizes, and appear to agree well with theoretical expectations for negative driven TLEs [*Pasko et al.*, 2000].

These exploratory measurements have established the potential for large numbers of TLEs over South America. The events appear morphologically similar to those reported elsewhere, particularly over the Midwestern U.S. However, the MCC observed on February 22-23, 2006, appears to have been unusual in many ways, producing TLEs

with much lower charge moment changes, as well as several negative sprite events. Although not discussed in detail in this dissertation, a large number of events with unusual morphology and dynamics, such as dancing sprites, which are multiple sprites that appear to trigger in sequence, and remarkable ring-like clusters of sprites, as illustrated at the beginning of this chapter were also observed. These studies have raised the following questions:

- Why did this storm produce so many TLEs, and why did they occur throughout the storm complex, rather than in the trailing stratiform region as determined from previous measurements over the U.S.A?
- Why was this storm able to produce several negative sprite-halo events, and was this an anomaly or typical of storms in this geographical region?
- What are the relationships between halos (altitude, brightness, and diameter) and their associated charge moments?
- Why were the charge moments changes associated with the sprite-halo events at the lower limit of the expected ranges of charge moments for sprites observed in the U.S.?
- Is there a polarity difference between halo events produced over land versus oceans? If so, why did the MCC over Argentina produce at least four negative pure halos?
- What are the atmospheric dynamics associated with a negative event immediately following a positive event, as observed at 07:17:17 UT on Feb. 23, 2006, which revealed sprite re-brightening after ~1s and possible partial loss of halo signal?

- Given the apparent differences between TLEs produced in North and South America, what other regions of the world should be studied to further our understanding of their global characteristics?

7.2. Future Research

The coordinated measurements in Brazil were exploratory in nature and have raised new questions requiring continued data analysis, as well as new measurements. Important topics for future research are:

- To extend the charge moment analysis to shorter and longer time scales, to better quantify the impulsiveness and duration of the lightning and its relationship with the observed halo signatures (diameter, brightness, altitude).
- To compare and contrast the properties of the TLEs observed from the February storm with those of the March storm, focusing on halo characteristics.
- To compare charge moments associated with the sprites observed from both storms with published results from similar studies over the Midwestern U.S.
- To obtain new measurements from southern Brazil, to further characterize sprites from large MCCs, and to investigate occurrence of other negative events.

Finally, recent ISUAL satellite measurements and ground-based ELF/VLF data strongly suggest that the Central America is most likely the largest producer of TLE events. Yet, to date, there have been few ground-based observations from this region. Given the differences that we have determined between TLEs in North and South

America, new observations from this important region, in particular focused on detecting negative events over land and ocean, could provide crucial information for improving current theoretical and modeling studies.

REFERENCES

Adachi T., H. Fukunishi, Y. Takahashi, Y. Hiraki, R.-R. Hsu, H.-T. Su, A. B. Chen, S. B. Mende, H. U. Frey, and L. C. Lee (2006), Electric field transition between the diffuse and streamer regions of sprites estimated from ISUAL/array photometer measurements, *Geophys. Res. Lett., 33*, L17803, doi:10.1029/2006GL026495.

Ahrens, C. D. (2003), *Meteorology Today: An Introduction to Weather Climate, and the Environment, 7th ed.*, 624 pp., Thomson, Brooks & Cole, Pacific Grove, Calif.

Armstrong, R. A., J. A. Shorter, M. J. Taylor, D. M. Suszcynsky, W. A. Lyons, and L. S. Jeong (1998), Photometric measurements in the SPRITES '95 & '96 campaigns of nitrogen second positive (399.8 nm) and first negative (47.8 nm) emission, *J. Atmos. Sol. Terr. Phys., 60*, 787-799.

Barr, R. (1977), The effect of sporadic-E on the nocturnal propagation of ELF waves, *J. Atmos. Terr. Phys., 39*, 1379-1387.

Barrington-Leigh, C. P., and U. S. Inan (1999), Elves triggered by positive and negative lightning discharges, *Geophys. Res. Lett., 26*, 683-686.

Barrington-Leigh, C. P., U. S. Inan, M. Stanley and S. A. Cummer (1999), Sprites triggered by negative lightning discharges, *Geophys. Res. Lett., 26*, 3605-3608.

Barrington-Leigh, C. P., U. S. Inan, and M. Stanley (2001), Identification of sprites and elves with intensified video and broadband photometry, *J. Geophys. Res., 106*, 1741 – 1750.

Barrington-Leigh C. P., V. P. Pasko, and U. S. Inan (2002), Exponential relaxation of optical emissions in sprites, *J. Geophys. Res., 107*, A5, 1065, doi:10.1029/2001JA900117.

Bazelyan, E. M., and Y. P. Raizer (2000), *Lightning Physics and Protection*, 325 pp., Inst. of Phys., Philadelphia, Pa.

Bell, T. F., V. P. Pasko, and U. S. Inan (1995), Runaway electrons as a source of red sprites in the mesosphere, *Geophys. Res. Lett., 22*, 16, 2127-2130.

Berger, K. (1967), Novel observations on lightning discharges: results of research on Mount San Salvatore, *J. Franklin Inst., 283*, 478-525.

Bering, E. A., III, J. R. Benbrook, J. A. Garrett, A. M. Paredes, E. M. Wescott, D. R. Moudry, D. D. Sentman, H. C. Stenbaek-Nielsen, and W. A. Lyons (2002), The electrodynamics of sprites, *Geophys. Res. Lett., 29*, 5, 1064, doi:10.1029/2001GL013267.

Bering E. A. III, J. R. Benbrook, L. Bhusal, J. A. Garrett, A. M. Paredes, E. M. Wescott, D. R. Moudry, D. D. Sentman, H. C. Stenbaek-Nielsen, and W. A. Lyons (2004), Observations of transient luminous events (TLEs) associated with negative cloud to ground (−CG) lightning strokes, *Geophys. Res. Lett., 31*, L05104, doi:10.1029/2003GL018659.

Blanc, E., T. Farges, R. Roche, D. Brebion, T. Hua, A. Labartha, and V. Melnikov (2004), Nadir observations of sprites from the International Space Station, *J. Geophys. Res., 109*, A02306, doi:10:1029/2003JA009972.

Boccippio, D. J., E. R. Williams, W. A. Lyons, I. Baker, and R. Boldi (1995), Sprites, ELF transients and positive ground strokes, *Science, 169*, 1088-1091.

Boeck, W. L., O. H. Vaughan, Jr., R. Blakeslee, B. Vonnegut, M. Brook, and J. M. McKue (1992), Lightning induced brightening in the airglow layer, *Geophys. Res.. Lett., 19*, 99-102.

Boeck, W. L., O. H. Vaughan Jr., R. J. Blakeslee, B. Vonnegut, M. Brook, and J. McKune (1995), Observations of lightning in the stratosphere, *J. Geoophys. Res., 100*(D1), 1465-1475.

Boeck, W. L., O. H. Vaughan Jr., R. J. Blakeslee, B. Vonnegut, and M. Brook (1998), The role of the space shuttle video tapes in the discovery of sprites, jets, and elves, *J. Atmos. Sol. Terr. Phys., 60*, 669-677.

Bracewell, R. N. (1986), *The Fourier Transform and Its Applications*, 486 pp., McGraw-Hill, New York.

Budden, K. G. (1961), *The Wave-Guide Mode Theory of Wave Propagation*, 325 pp., Logos Press, London.

Casper, P. W., and R. B. Bent (1992), Results from the LPATS USA national lightning detection and tracking system for the 1991 lightning season, *Proc. 21st Int. Conf. on Lightning Protection, Berlin German*, pp. 339-342.

Cho, M., and M. J. Rycroft (1998), Computer simulation of electric field structure and optical emission from cloud top to the ionosphere, *J. Atmos. Sol. Terr. Phys., 60*, 871-878.

Cliverd, M. A., C. J. Rodger, and D. Nunn (2004), Radiation belt electron precipitation fluxes associated with lightning, *J. Geophys. Res., 109*, A122208, doi:10.1029/2004JA010644.

Cummer, S. A., and U. S. Inan (1997), Measurement of charge transfer in sprite-producing lightning using ELF radio atmospherics, *Geophys. Res. Lett., 24*, 1731-1734.

Cummer, S. A., and U. S. Inan (2000), Modeling ELF radio atmospheric propagation and extracting lightning currents from ELF observations, *Radio Sci., 35*(2), 385-394, doi:10.1029/1999RS002184.

Cummer, S. A., and W. A. Lyons (2005), Implications of lightning charge moment changes for sprite initiation, *J. Geophys. Res., 110*, A04304, doi: 10.1029/2004JA010812.

Cummer, S. A., U. S. Inan, T. F. Bell, and C. P. Barrington-Leigh (1998), ELF radiation produced by electrical currents in sprites, *Geophys. Res. Lett., 25*, 1281.

Cummer, S. A., N. Jaugey, J. Li, W. A. Lyons, T. E. Nelson, and E. A. Gerken (2006), Sub-millisecond imaging of sprite development and structure, *Geophys. Res. Lett., 33*, L04104, doi:10.1029/2005GL024969.

Engholm, C. D., E. R. Williams, and R. M. Dole (1990), Meteorological and electrical conditions associated with positive cloud-to-ground lightning, *Mon. Wea. Rev., 118*, 470-487.

Enell, C. –F., E. Arnore, O. Chanrion, T. Adachi, P. T. Verronen, A. Sepala, T. Neubert, T. Ulich, E. Turunen, Y. Takanahashi, and R. -R. Hsu (2008), Parameterization of the chemical effects of sprites in the middle atmosphere, *Ann. Geophys., 26*, 13-17.

Fernsler, R. F., and H. L. Rowland (1996), Models of lightning produced sprites and elves, *J. Geophys. Res., 101*, 29, 653-662.

Finkelstein, D., and J. Rubinstein (1964), Ball lightning, *Phys. Rev. A, 135*, 390-396.

Fleagle, R. G., and J. A. Businger (1980), *An Introduction to Atmospheric Physics*, 42 pp., Academic Press, New York.

Franz, R. C., J. Nemzak, and J. R. Winckler (1990), Television image of a large upward electrical discharge above a thunderstorm system, *Science, 249*, 48-51.

Frey, H. U., S. B. Mende, S. A. Cummer, J. Li, T. Adachi, H. Fukunishi, Y. Takahashi, A. B. Chen, R.-R. Hsu, H.-T. Su, and Y.-S. Chang (2007), Halos generated by negative cloud-to-ground lightning, *Geophys. Res. Lett., 34*, L18801, doi: 10.1029/2007GL030908.

Fukunishi, H., Y. Takahashi, M. Kubota, and K. Sakanoi (1995) Low ionosphere flashes induced by lightning discharges, *Eos Supplement, 76*(46), F114.

Fukunishi, H., Y. Takahashi, M. Kubota, K. Sakanoi, U. S. Inan, and W. A. Lyons (1996), Elves: Lightning-induced transient luminous events in the lower ionosphere, *Geophys. Res. Lett., 23*, 2157-2160.

Gerken, E. A., U. S. Inan, and C. P. Barrington-Leigh (2000), Telescopic imaging of sprites, *Geophys. Res. Lett., 27*, 2637-2640.

Glukhov, V. S., and U. S. Inan (1996), Particle simulation of the time-dependent interaction with the ionosphere of rapidly varying lightning EMP, *Geophys. Res. Lett., 23*, 2193-2196.

Gomes, C., and V. Cooray (1998), Long impulse currents associated with positive return strokes, *J. Atmos. Sol. Terr. Phys., 60*, 693-699.

Gurevich, A. V., G. M. Milikh, and R. Roussel-Dupre (1992), Runaway electron mechanism of air breakdown and preconditioning during a thunderstorm, *Phys. Lett. A, 165*, 463-468.

Gurevich, A. V., K. P. Zybin, and R. A. Roussel-Dupre (1999), Lightning initiation by simultaneous effects of runaway breakdown and cosmic ray showers, *Phys. Lett. A, 254*, 79–87.

Hampton, D. L., M. J. Heavner, E. M. Wescott, and D. D. Sentman (1996), Optical spectral characteristics of sprites, *Geophys. Res. Lett., 23*(1), 89-92.

Hardman, S. F., R. L. Dowden, J. B. Brundell, J. L. Bahr, Z. -I. Kawasaki, and C. J. Rodger (2000), Sprite observations in the Northern Territory of Australia, *J. Geophys. Res., 105*, 4689-4697.

Heavner, M. J. (2000), Optical spectroscopic observations of sprites, blue jets, and elves: inferred microphysical processes and their macrophysical implications, Ph.D. dissertation, University of Alaska, Fairbanks.

Hiraki, Y., T. Lizhu, H. Fukunishi, K. Nanbu, and H. Fujiwara (2002), Development of a new numerical model for investigating the energetics of sprites, *Eos Trans. AGU, 83*(47): Fall Meet. Suppl., Abstract A11C-0105.

Hojo, J., M. Ishii, T. Kawamura, F. Suzuki, H. Komuro, and M. Shiogama (1989), Seasonal variation of cloud-to-ground lightning flash characteristics in the coastal area of the Sea of Japan, *J. Geophys. Res. 95*, 13, 207-212.

Holzworth, R. H., and E. A. Bering (1998), Ionospheric electric fields from stratospheric balloon-borne probes, *Measurment Techniques in Space Plasmas: Fields, Geophysical Monograph, 103*, AGU.

Holzworth, R. H., M. C. Kelley, C. L. Siefring, L. C. Hale, and J. D. Mitchell (1985), Electrical measurements in the atmosphere and the ionosphere over an active thunderstorm. 2. Direct current electric fields and conductivity, *J. Geophys. Res., 90*(A10), 9824-9830.

Holzworth, R. H., M. P. McCarthy, J. N. Thomas, J. Chin, T. M. Chinowsky, M. J. Taylor, and O. Pinto Jr. (2005), Strong electric fields from positive lightning strokes in the stratosphere, *Geophys. Res. Lett.*, 32, L04809, doi:10.1029/2004GL021554.

Hu W., S. A. Cummer, W. A. Lyons, and T. Nelson (2002), Lightning charge moment changes for the initiation of sprites, *Geophys. Res. Lett., 29*(8), 1279, doi:10.1029/2001GL014593.

Hubert, P., P. Laroche, A. Eybert-Berard, and L. Barret (1984), Triggered lightning in New Mexico, J. Geophys. Res., 89, D2, doi:10.1029/JD089iD02p02511.

Inan, U. S., T. F. Bell, and J. V. Rodriguez (1991), Heating and ionization of the lower ionosphere by lightning, *Geophys. Res. Lett., 18*, 705-708.

Inan, U. S., S. C. Reising, G. J. Fishman, and J.M. Horack (1996), On the association of terrestrial gamma-ray bursts with lightning discharges and sprites, *Geophys. Res. Lett., 23*, 1017-1020.

Inan, U. S., C. Barrington-Leigh, S. Hansen, V. S. Glukhov, T. F. Bell, and R. Rairden (1997), Rapid lateral expansion of optical luminosity in lightning-induced ionospheric flashes referred to as ‘elves,’ Geophys. Res. Lett., *24*(5), 583-586.

Jayaratne, E. R. (1998), Possible laboratory evidence for multipole electric charge structures in thunderstorms, *J. Geophys. Res., 103*: 1878.

Jayaratne, E. R., C. P. R. Saunders, and J. Hallet (1983), Laboratory studies of the charging of soft-hail during ice crystal interactions, *Q. J. R. Meteorol. Soc., 109.*

Kelley, M. C., C. L. Siefring, R. F. Pfaff, P. M. Kintner, M. Larsen, R. Green, R. H. Holzworth, L. C. Hale, J. D. Mitchell, and C. Le Vine (1985), Electrical measurements in the atmosphere and the ionosphere over an active thunderstorm, 1. Campaign overview and itnitial ionospheric results, *Geophys. Res. Lett., 90*, 9815-9823.

Kelley, M. C., J. G. Ding, and R. H. Holzworth (1990), Intense ionospheric electric and magnetic pulses generated by lightning. *Geophys. Res. Lett., 17*, 2221-2224.

Kelley, M. C., S. D. Baker, R. H. Holzworth, P. Argo, and S. A. Cummer (1997), LF and MF observations of the lightning electromagnetic pulse at ionospheric altitudes, *Geophys. Res. Lett., 24*, 1111-1114.

Krehbiel, P. R., M. Brook, and R. A. McCrory (1979), An analysis of the charge structure of lightning discharges to ground. *J. Geophys. Res.*, 84(C5):2432–2456.

Krider, E. (1992), On the electromagnetic fields, poynting vector, and peak power radiated by lightning return strokes, *J. Geophys. Res., 97*(D14), 15913-15917.

Krider, E. P, R. C. Noggle, and M. A. Uman (1976), A gated wideband magnetic direction finder for lightning return strokes, *J. Appl. Meteor, 15*, 301–306.

Kuo, C. -L., R. R. Hsu, A. B. Chen, H. T. Su, L. C. Lee, S. B. Mende, H. U. Frey, H. Fukunishi, and Y. Takahashi (2005), Electric fields and electron energies inferred from the ISUAL recorded sprites, *Geophys. Res. Lett., 32*, L19103, doi:10.1029/2005GL023389.

Lay E. H., R. H. Holzworth, C. J. Rodger, J. N. Thomas, O. Pinto Jr., and R. L. Dowden (2004), WWLL global lightning detection system: Regional validation study in Brazil, *Geophys. Res. Lett., 31*, L03102, doi:10.1029/2003GL018882.

Lehtinen, N. G., T. F. Bell, V. P. Pasko, and U. S. Inan (1997), A two-dimensional model of runaway electron beams driven by quasi-electrostatic thundercloud fields, *Geophys. Res. Lett., 24*, 2639-2642.

Lehtinen, N. G., T. F. Bell, and U. S. Inan (1999), Monte Carlo simulation of runaway MeV electron breakdown with application to red sprites and terrestrial gamma ray flashes, *J. Geophys. Res.*, *104*(A11), 24,699–24,712.

Lehtinen, N., U. Inan, and T. Bell (2001), Effects of thunderstorm-driven runaway electrons in the conjugate hemisphere: Purple sprites, ionization enhancements, and gamma rays, *J. Geophys. Res., 106*(A12), 28841-28856.

Le Vine, D., and J. Willett (1992), Comment on the transmission-line model for computing radiation From lightning, *J. Geophys. Res., 97*(D2), 2601-2610.

Li, Y. Q., R. H. Holzworth, H. Hu, M. McCarthy, R. D. Massey, P. M. Kintner, J. V. Rodrigues, U. S. Inan, and W. C. Armstrong (1991), Anomalaous optical events detected by rocket-borne sensor in the WIPP campaign, *J. Geophys. Res.*, *96*(AS), 13115-1326.

Liu, N., and V. P. Pasko (2004), Effects of photoionization on propagation and branching of positive and negative streamers in sprite, *J. Geophys. Res*., *109*, A04301, doi:10.1029/2003JA010064.

Lyons, W. A. (1994), Characteristics of luminous structures in the stratosphere above thunderstorms as imaged by low-light video, *Geophys. Res. Lett., 21*, 875-878.

Lyons, W. A. (1996), Sprite observations above the U.S. High Plains in relation to their parent thunderstorm systems, *J. Geophys. Res., 101*, 29,641-29,652.

Lyons, W. A., and T. E. Nelson (1995), The Colorado SPRITES '95 campaign: Initial results, *Eos Supplement 76*(46), 113.

Lyons, W. A., and E. R. Williams (1993), Preliminary investigations of cloud-to-stratosphere lightning discharges, paper presented at *Conf. Atmospheric Electricity*, St. Louis, MO, 4-8 Oct.

Lyons, W. A., T. E. Nelson, E. R. Williams, J. A. Cramer, and T. R. Turner (1998), Enhanced positive cloud-to-ground lightning in thunderstorms ingesting smoke from fires, *Science, 282*, 77-80.

Lyons, W. A., R. A. Armstrong, E. A. Gering, and E. R. Williams (2000), The hundred year hunt for the sprite, *Eos Trans. AGU, 81*(33), 373-377.

Lyons, W. A., L. Andersen, T. E. Nelson, and G. R. Huffines (2006), Characteristics of sprite producing electrical storms in the steps 2000 campaign, paper presented at Second Conference on Meteorological Applications of Lightning Data, AM. Meteorol. Soc, Atlanta, Ga., 30 Jan.- 2 Feb.

Lyons, W. A., M. Stanley, J. Meyer, T. Nelson, S. A. Cummer, N. Jaugey, S. A. Rutledge, and T. Lang (2008), Real time detection of sprite producing storms using RF techniques, paper presented at Coupling., Energetics and Dynamics of Atm. Regions workshop, Midway, Utah, 16-21 June.

MacGorman, D. R., and D. W. Burgess (1994), Positive cloud-to-ground lightning in tornadic storms and hailstorms, *Mon. Wea. Rev., 126*, 1671-1697.

Marshall, T. C., M. P. McCarthy, and W. D. Rust (1995), Electric-field magnitudes and lightning initiation in thunderstorms, *J. Geophys. Res., 100*:7097-7103.

Mayes, J., and K. Hughes (2004), *Understanding Weather*, 202 pp., Oxford University Press, New York.

McHarg, M. G., H. C. Stenbaek-Nielsen, and T. Kammae (2007), Observations of streamer formation in sprites, *Geophys. Res. Lett., 34*, L06804, doi:10.1029/2006GL027854.

Mende, S. B., R. L. Rairden, and G. R. Swenson (1995), Sprite spectra: $N_2$1PG band identification, *Geophys. Res. Lett., 22*, 2633-2636.

Mende, S. B., H. U. Frey, R. R. Hsu, H. T. Su, A. B. Chen, L. C. Lee, D. D. Sentman, Y. Takahashi, and H. Fukunishi (2005), D region ionization by lightning-induced electromagnetic pulses, *J. Geophys. Res., 110*, A11312, doi:10.1029/2005JA011064.

Mikaye, K., T. Suzuki, and K. Shinjoy (1992) Characteristics of winter lightning current on Japan Sea Coast, *IEE Trans. Pow. Del., 7*, 1450-1456.

Milikh, G. M., K. Papadopoulos, and C. L. Chang, (1995), On the physics of high altitude lightning, *Geophys. Res. Lett., 22*, 85-88.

Milikh, G. M., D. A. Usikov, and J. A. Valdivia (1998a), Model of infrared emission from sprites, *J. Atmos. Sol. Terr. Phys., 60*, 895-906.

Milikh, G. M., J. A. Valdivia, and K. Papadopoulos (1998b), Spectrum of red sprites, *J. Atmos. Sol. Terr. Phys., 60*, 907-916.

Miyasato, R., M. J. Taylor, H. Fukunishi, and H. C. Stenbaek-Nielsen (2002), Statistical characteristics of sprite halo events using coincident photometric and imaging data, *Geophys. Res. Lett., 29*(21), 2033, doi:10.1029/2001GL014480.

Neubert, T., T. Allin, H. Stenbaek-Nielsen, and E. Blanc (2001), Sprites over Europe, *Geophys. Res. Lett., 28*, 3585-3588.

Nishino, M., A. Iwai, and M. Kahiwagi (1973), Location of the sources of atmospherics in and around Japan, *Proc. Res. Inst. Atmospherics, Nagoya Univ., Japan, 20*: 9-21.

Norinder, H., and E. Knudsen (1956), Pre-discharges in relation to subsequent lightning strokes, *Arkiv För Geofysik, 2*(27), 551–571.

Orville, R. E., R. W. Henderson, and L. F. Bosart (1983), An East Coast lightning detection network, *Bull. Am. Meteor. Soc., 64*, 1029-1037.

Papadopoulos, K., G. Milikh, and J. Valdivia (1996), Comment on "Can gamma radiation be produced in the electrical environment above thunderstorms," *Geophys. Res. Lett., 23*, 2283-2284.

Pappert, R . A., and J. A. Ferguson (1986), VLF/LF mode conversion model calculations for air to air transmissions in the Earth-ionosphere waveguide, *Radio Sci., 21*, 551-558.

Pasko, V. P., U. S. Inan, Y. N. Taranenko, and T. F. Bell (1995), Heating, ionization and upward discharges in the mesosphere due to intense quasi-electrostatic thundercloud fields, *Geophys. Res. Lett., 22*, 365-368.

Pasko, V. P., U. S. Inan, and T. F. Bell (1996a), Blue jets produced by quasi-electrostatic pre-discharge thundercloud fields, *Geophys. Res. Lett., 23*, 301-304.

Pasko, V. P., U. S. Inan, and T. F. Bell (1996b), Sprites as luminous columns of ionization produced by quasi-electrostatic thundercloud fields, *Geophys. Res. Lett., 23*, 649-652.

Pasko, V. P., U. S. Inan, T. F. Bell, and Y. N. Taranenko (1997a), Sprites produced by quasi-electrostatic heating and ionization in the lower ionosphere, *J. Geophys. Res., 102*, 529-4561.

Pasko, V. P, U. S. Inan, and T. F. Bell (1997b), Sprites as evidence of vertical gravity wave structures above mesoscale thunderstorms, *Geophys. Res. Lett., 24*, 1735-1738.

Pasko, V. P., U. S. Inan, and T. F. Bell (1998), Spatial structure of sprites, *Geophys. Res. Lett., 25*, 2123-2126.

Pasko, V. P., U. S. Inan, and T. F. Bell (2000), Fractal structure of sprites, *Geophys. Res. Lett., 27*, pp. 497-500.

Pasko, V. P, M. A. Stanley, J. D. Matthews, U. S. Inan, and T. G. Woods (2002), Electrical discharge from a thundercloud top to the lower ionosphere, *Nature, 416*, 152-154.

Pessi, A. T., S. Businger, K. L. Cummins, N. W. S. Demetriades, M. Murphy, and B. Pifer (2008), Development of a long-range lightning detection network for the pacific: construction, calibration, and performance, *J. Atmos. Oceanic Tech.*, doi: 10.1175/2008JTECHA1132.1.

Pinto, O. Jr., M. M. F. Saba, I. R. C. A. Pinto, F. S. S. Tavares, K. P. Naccarato, N. N. Solorzano, M. J. Taylor, P. D. Pautet, and R. H. Holzworth (2004), Thunderstorm and lightning characteristics associated with sprites in Brazil, *Geophys. Res. Lett., 31*, L13103, doi:10.1029/2004GL020264.

Press, W. H., S. A. Teukolsky, W. T. Vetterling, and B. P. Flannery (1992), *Numerical Recipes in FORTRAN*, 2nd ed., 500 pp., Cambridge Univ. Press, New York.

Raizer, Y. P, G. M. Milikh, M. N. Shneider, and S. V. Novakovski (1998), Long streamers in the atmosphere above thunderclouds, *J. Phys. D. Appl. Phys., 31*, 3255-3264.

Rakov, V. A., and M. A. Uman (2003), *Lightning: Physics and Affects*, 687 pp., Cambridge University Press, Cambridge, UK.

Rawer, K., D. Bilitza, and S. Ramakrishnan (1978), Goals and status of the International Reference Ionosphere, *Rev. Geophys., 16*, 177-181.

Reising, S. C., U. S. Inan, T. F. Bell, and W. A. Lyons (1996), Evidence for continuing current in sprite-producing cloud-to-ground lightning, *Geophys. Res. Lett., 23*(24), 3639-3642.

Rodger, C. J. (1999), Red sprites, upward lighting and VLF perturbations, *Rev. Geophys., 37*(3), 317-336.

Rodriguez, J., U. Inan, and T. Bell (1992), D region disturbances caused by electromagnetic pulses from lightning, *Geophys. Res. Lett., 19*(20), 2067-2070.

Roth, J. R., J. Rahel, X. Dai, and D. M. Sherman (2005), The physics and phenomenology of One Atmosphere Uniform Glow Discharge Plasma (OAUGDP) reactors for surface treatment applications, *J. Phys. D. Appl. Phys.*, 38, 555–567.

Rousell-Dupre, R. A., and A. V. Gurevich (1996), On run-away breakdown and upward-propagating discharges, *J. Geophys. Res., 101*, 2297-2311.

Rousell-Dupre, R. A., A. V. Gurevich, T. Turnell, and M. Milikh (1994), Kinetic theory for runaway breakdown, *Phys. Rev. E, 49*, 2257-2271.

Rowland, H. L. (1998), Theories and simulations of elves, sprites, and blue jets, *J. Atmos. Sol. Terr. Phys., 60*, 831-844.

Rowland, H. L., R. F. Fernsler, J. D. Huba, and P. A. Bernhardt (1995), Lightning driven EMP in the upper atmosphere, *Geophys. Res. Lett., 22*, 361-364.

Rowland, H. L, R. F. Fernsler, and P. A. Bernhardt (1996), Breakdown of the neutral atmosphere in the D region due to lightning-driven electromagnetic pulses, *J. Geophys. Res., 101*, 7935-7945.

Rycroft, M. J., and M. Cho (1998), Modeling electric and magnetic fields due to thunderclouds and lightning from cloud tops to the ionosphere, *J. Atmos. Sol. Terr. Phys., 60,* 889-894.

São Sabbas, F. T. (1999), Estudo da relação entre sprite e os relâmpagos das tempestades associadas (Study of the relationship between sprites and lightning from the associated storms), M.S. Thesis, Inst. Nac. De Pesqui. Especiais, São José dos Campos, Brazil.

São Sabbas, F. T., and D. D. Sentman (2003), Dynamical relationship of infrared cloudtop temperatures with occurrence rates of cloud-to-ground lightning and sprites, *Geophys. Res. Lett., 30* (5), 1236, doi:10.1029/2002GL015382.

Sato, M. and H. Fukunishi (2003), Global sprite occurrence locations and rates derived from triangulation of transient Schumann resonance events, *Geophys. Res. Lett., 30*(16), 1859, doi:10:1029/2003GLO017291.

Sentman, D. D., and E. M. Wescott (1993), Observations of upper atmospheric optical flashes recorded from an aircraft, *Geophys. Res. Lett., 20,* 2857-2860.

Sentman, D. D., E. M. Wescott, D. L. Osborne, D. L. Hampton, and M. J. Heavner (1995), Preliminary results from the Sprites94 aircraft campaign: 1. Red Sprites, *Geophys. Res. Lett., 22,* 1205-1208.

Sentman, D. D., E. M. Wescott, M. J. Hevner, and D. R. Moudry (1996), Observations of sprite beads and balls, *Eos Supplement, 77*(406), F61.

Shellman, C. H. (1986), A new version of MODESRCH using interpolated values of the magnetoionic reflection coeificients, *Tech. Rep. 1473*, Nav. Ocean Sys. Cent., San Diego, CA.

Solorzano, N. N., J. N. Thomas, M. J. Taylor, P. D. Pautet, M. A. Bailey, R. H. Holzworth, F. T. São Sabbas, O. Pinto Jr., S. A Cummer, N. Jaugey, N. J. Schuch, and P. L. da Silva Dias (2006), Meteorological aspects of TLE-producing thunderstorms over northeastern Argentina: Two case studies, paper presented at Annual AGU fall meeting, San Francisco, CA, 11-15 Dec.

Stanley, M., P. Krehbiel, M. Brook, C. Moore, W. Rison, and B. Abrahams (1999), High speed video of initial sprite development, *Geophys. Res. Lett., 26*(20), 3201-3204.

Stenbaek-Nielsen, H. C., D. R. Moudry, E. M. Wescott, D. D. Sentman, and F. T. São Sabbas (2000), Sprites and possible mesospheric effects, *Geophys. Res. Lett., 27,* 3829-3832.

Stolzenburg, M., W. D. Rust, and T. C. Marshall (1998), Electrical structure in thunderstorm convective regions 3. Synthesis, *J. Geophys Res., 103*(D12): 14097-14108, 10.1029/97JD03545.

Su, H. T., R. R. Hsu, A. B. Chen, Y. C. Wang, W. S. Hsiao, W. C. Lai, L. C. Lee, M. Sato, and H. Fukunishi (2003), Gigantic jets between a thundercloud and the ionosphere, *Nature, 423,* 974-976, doi:10.1038/nature01759.

Sukhorukov, A. I., E. V. Mishin, P. Stubbe, and M. J. Rycroft (1996a), On blue jet dynamics, *Geophys. Res. Lett., 23,* 1625-1628.

Sukhorukov, A. I., E. A. Rubenchik, and P. Stubbe (1996b), Simulation of strong lightning pulse penetration into the lower ionosphere, *Geophys. Res. Lett., 23,* 2911-2914.

Taranenko, Y. N., and R. A. Roussel-Dupre (1996), High altitude discharges and gamma-ray flashes: a manifestation of runaway air breakdown, *Geophys. Res. Lett., 23,* 571-574.

Taranenko, Y. N., U. S. Inana, and T. F. Bell (1993a), Interaction with the lower ionosphere of electromagnetic pulses from lightning: Heating, attachment, and ionization, *Geophys. Res. Lett., 20*, 1539-1542.

Taranenko, Y. N., U. S. Inan, and T. F. Bell (1993b), Interaction with the lower ionosphere of electromagnetic pulses from lightning: Excitation of optical emissions, *Geophys. Res. Lett., 20*, 2675-2678.

Taylor, M. J., and S. Clark (1996), High resolution CCD and video imaging of sprites and elves in the N_2 first positive emission, *Eos Supplement, vol. 77,* P. F135, AGU Fall Meeting Abstracts.

Taylor, W. L., and K. Sao (1970), ELF attenuation rates and phase velocities observed from slow-tail components of atmospherics, *Radio Sci., 5,* 1453-1460.

Taylor, M. J., M. A. Bailey, P. D. Pautet, S. A. Cummer, N. Jaugey, J. N. Thomas, N. N. Solorzano, F. São Sabbas, R. H. Holzworth, O. Pinto, and N. J. Schuch (2008), Rare measurements of a sprite with halo event driven by a negative lightning discharge over Argentina, *Geophys. Res. Lett., 35,* L14812, doi:10.1029/2008GL033984.

Thomas, J. N. (2005), Lightning-driven electric and magnetic field measured in the stratosphere: Implications for sprites, Ph.D. Dissertation, University of Washington.

Thomas, J. N., R. H. Holzworth, M. P. McCarthy, and O. Pinto Jr. (2005), Predicting lightning-driven quasi-electrostatic fields at sprite altitudes using in-situ measurements and a numerical model, *Geophys. Res. Lett., 32*(L10809), doi:10.1029/2005GLO022693.

Thomas, J. N., M. J. Taylor, D. Pautet, M. Bailey, N. N. Solorzano, R. H. Holzworth, M. P. McCarthy, M. Kokorowski, F. São Sabbas, O. Pinto Jr., S. A. Cummer, N. Jaugey, J. Li, and N. J. Schuch (2007), A very active sprite-producing storm observed over Argentina, *Eos Trans. AGU, 88*(10), 117, doi:10.1029.

Valdivia, J. A. (1997*),* The physics of high altitude lightning, Ph.D. dissertation, University of Maryland at College Park.

Valdivia, J. A., G. M. Milikh, and K. Papadopoulos (1997), Red sprite: Lightning as a fractal antenna, *Geophys. Res. Lett., 24,* 3169-3172.

Valdivia, J. A., G. M. Milikh, and K. Papadopoulos (1998), Lightning to the ionosphere, *Weatherwise, 35,* 70-71.

Vaughan Jr., O. H., and B. Vonnegut (1989), Recent observations of lighting discharges from the top of a thundercloud into the clear air above. *J. Geophys. Res., 94*(13), 179-182.

Vaughan Jr., O. H., R. J. Blakeslee, W. L. Boeck, B. Vonnegut, M. Brook, and J. McKune, Jr. (1992), A cloud to space lightning recorded by the space shuttle payload bay TV cameras, *Mon. Weather. Rev., 120*, 1459.

Veronis, G., V. P. Pasko, and U. S. Inan (1999), Characteristics of mesospheric optical emissions produced by lightning discharges, *J. Geophys. Res., 104*(12), 645-656.

Voss, H. D., M. Walt, W. L. Imhof, J. Moblilia, and U. S. Inan (1998), Satellite observations of lightning-induced electron precipitation, *J. Geophys. Res., 103* (11), 725-744.

Wescott, E. M., D. D. Sentman, D. L. Osborne, S. L. Hampton, and M. J. Heavner (1995), Preliminary results from the Sprites94 aircraft campaign: 2. Blue jets, *Geophys. Res. Lett., 22*, 1209-1212.

Wescott, E. M., D. D. Sentman, M. J. Heavner, D. L. Hampton, and O. H. Vaughan, Jr. (1998a), Blue jets: their relationship to lightning and very large hailfall, and their physical mechanisms for their production, *J. Atmos. Sol. Terr. Phys., 60*, 713-724.

Wescott, E. M., D. D. Sentman, M.J . Heavner, D. L. Hampton, W. A. Lyons, and T. Nelson (1998b), Observations of 'columniform' sprites, *J. Atmos. Sol. Terr. Phys., 60*, 733-740.

Wescott, E. M., H. C. Stenbaek-Nielsen, D. D. Sentman, M. J. Heavner, D. R. Moudry, and F. T. S. Sabbas (2001), Triangulation of sprites, associated halos and their possible relation to causative lightning and micrometeors, *J. Geophys. Res*., *106*(A6), 10,467-10,478, 10.1029/2000JA000182.

Williams, E. R., E. Downes, R. Boldi, W. Lyons, and S. Heckman (2007), Polarity asymmetry of sprite producing lightning: A paradox?, *Radio Sci*., *42*, RS2S17, doi:10:1029/2006RS003488.

Williams, E. R. (2001), Sprites, elves, and glow discharge tubes, *Physics Today*, November, 41-47.

Wilson, C. T. R. (1956), A theory of thundercloud electricity, *Proc. Roy. Meteor. Soc*., *236*, 297-317.

Winckler, J. R. (1995), Further observations of cloud-ionosphere electrical discharges above thunderstorms, *J. Geophys. Res., 100*, 14335.

Winckler, J. R., (1998), Optical and VLF radio observations of sprites over a frontal storm views from O'Brien Observatory of the University of Minnesota, *J. Atmos. Sol. Terr. Phys., 60*, 679-688.

Yukhimuk, V., R. Roussel−Dupre, E. Symbalisty, and Y. Taranenko (1998), Optical characteristics of Red Sprites produced by runaway air breakdown, *J. Geophys. Res.,* 103(D10), 11473-11482.

Yukhimuk, V., R. A. Roussel-Dupre, and E. M. D. Simbalisty (1999), On the temporal evolution of red sprites: Runaway theory versus data, *Geophys. Res. Lett., 26,* 679-682.

APPENDICES

APPENDIX A: LIGHTNING DETECTION NETWORKS

A.1. Introduction

Many individual physical processes take place during the formation of a lightning stroke. Each of these processes has characteristic electric and magnetic fields associated with them. These fields also may be related to electromagnetic waves emitted by the formation lightning strokes. This Appendix contains a brief summary of how this type of electromagnetic radiation can be used to determine the location of the source lightning. The following discussion of lightning detection sensors is condensed from a study by *Rakov and Uman* [2003].

Mathematically, it can be shown that any waveform or wave pulse may be constructed by superimposing sinusoidal waves of different amplitudes and frequencies. Similarly, one may think of a lightning stroke as a very impulsive antenna, which radiates electromagnetic waves with a multitude of frequencies. In fact, lightning is known to emit significant electromagnetic energy in the frequency range from below 1 Hz to 300 MHz, with a peak in the frequency spectrum near 5 to 10 kHz for lightning at distances beyond ~50 km [*Rakov and Uman*, 2003]. There are other frequencies which lightning emits as well, such as in the microwave range (300 MHz to 300 GHz), as well as in the visible spectrum (10^{14} to 10^{15} Hz), although electromagnetic waves with frequencies in these ranges have limited energies. Any of these observable signals can be used to detect and calculate the location of the lightning process which produced it.

The three most common electromagnetic radio-frequency locating techniques are known as magnetic direction finding (MDF), time of arrival (TOA), and interferometry

where the type of locating information depends on the wavelength (or the frequency) of the radiation detected. If the detected signals wavelength is very short compared with the length of the radiating lightning channel (very high frequency), the whole lightning channel can be imaged in three dimensions. For lower frequency detections, generally only a single location can be obtained by these detectors.

Single-station sensors can detect lightning occurrence, but are not designed to determine the location of the lightning stroke (there are many single-station detectors that are sold which claim to be able to provide lightning locations, using the amplitude of radio static to approximate distances, intrinsically causing large errors). However, a single-station detector can be used to assign groups of flashes to approximate distance ranges if data are accumulated and averaged over a period of time. Accurate lightning locating networks utilize multiple locator sensors to determine where lightning occurs.

A.2 Magnetic Field Direction Finding (MDF)

Two vertical and orthogonal loops, each measuring the magnetic field from a given vertical radiating source, can be used to obtain the direction of that source. For example, two loops oriented in the North-South (NS) and the East-West (EW) directions will measure different magnetic fields due to a lightning stroke. Faradays Law shows us that the output voltage from a loop is proportional to the direction of the magnetic field emitted by the source compared with the normal vector of that loop. For two orthogonal loops, the signal in one of the loops will be proportional to the cosine of the angle between the loop and the source, while the other loop's signal will be proportional to the

sine of the angle between the loop and the source. When comparing the two signals, the ratio is proportional to the tangent of the angle between the source and the sensor.

These types of direction finders (DFs) for lightning location can be divided into narrowband and gated wideband DFs. Narrowband DFs have been used for decades to detect distant lightning, and generally operated in a narrow frequency band (with a center frequency of 5 to 10 kHz), where lightning signal is relatively high. These types of sensors were used to identify and map thunderstorms at large ranges before the development of weather radars in the mid 1900's [*Rakov and Uman*, 2003]. Two such sensors at known locations are sufficient to approximate the location of a lightning stroke. A major disadvantage of narrowband DFs is that if the lightning range is over 200 km, inherent errors in the calculated azimuth occur, known as polarization errors, which can be as large as 10° [*Nishino et al.*, 1973]. These errors are caused by detection of non-vertical lightning channels and the reflection of the electromagnetic signals from the ionosphere (see Figure A.1). Additionally, variations in the topography near the sensors, as well as nearby conducting mediums may cause uncertainty in the analysis of the sensor data.

To deal with the polarization errors associated with narrowband DFs, gated wideband DFs were developed in the 1970's. These sensors sample the orthogonal components of the return stroke's magnetic field, this field originating from the bottom part of the lightning channel, which is typically vertical. Additionally, this type of DF does not record reflections of the signal from the ionosphere, as this signal arrives after the direct signal is sampled. The operating bandwidth of the gated wideband DF ranges

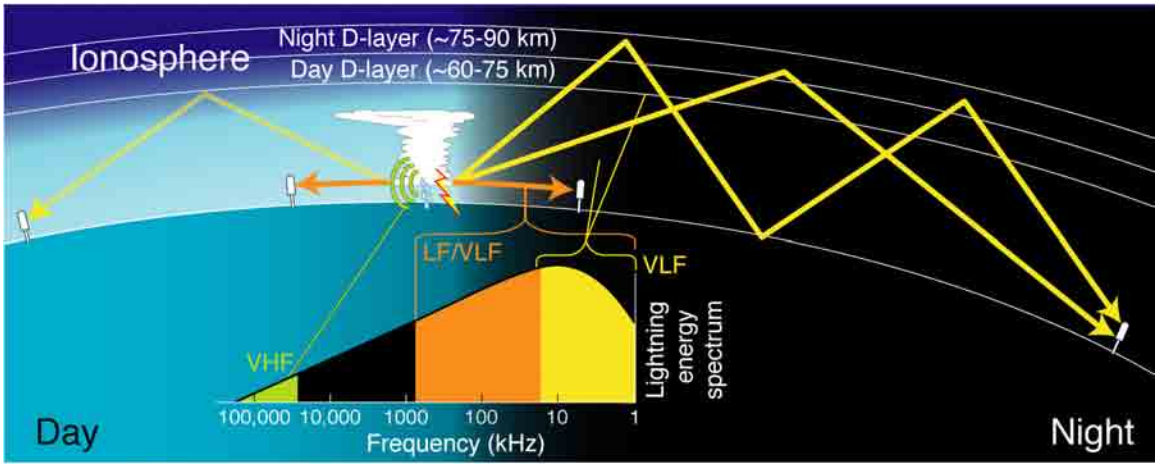


Figure A.1. Illustration showing the Earth-Ionosphere wave guide, which allows VLF (3– 30 kHz) sferics to propagate over large distances (100s – 1000s km) through reflection off the ionosphere. [*Pessi et al.*, 2008: Figure 1]. © American Meteorological Society. Reprinted with permission.

from a few kHz to about 500 kHz [*Rakov and Uman*, 2003]. Early studies of the accuracy of these systems showed that these sensors individually located lightning strokes to ± 1° [*Krider et al.*, 1976]. Gated wideband DF sensors were originally designed to detect only –CGs, but were configured in the late 1980s to measure both positive and negative CGs, by also measuring the electric field associated with the lightning stroke.

Gated wideband DFs, like their narrowband counterparts, are vulnerable to site errors, which are typically a function of direction, but not of time. These errors arise from non-horizontal terrain near the sensors, as well as nearby conducting objects. Since field sites with a totally flat surrounding area and no conducting mediums in the nearby vicinity are not common, it is often easier to measure the site errors and then compensate for them in the data analysis.

Although only two detectors are necessary to determine the location for a lightning stroke, when three or more sensors detect the same lightning signature, the accuracy in the calculated lightning stroke location is increased. When multiple sensors are used, each with a known uncertainty, a minimization technique can be performed using the azimuthal direction provided by each sensor.

A.3. Time of Arrival (TOA) Sensors

A single time-of-arrival sensor provides the time at which some component of the electromagnetic signal produced by a lightning stroke arrives at the sensor. TOA sensors typically are derived into three categories, based upon the wavelengths (or the frequencies) of the signal detected. These three types are: (1) very-short-baseline (wavelengths typically 10s to 100s of meters); (2) short-baseline (10s of km's); and (3) long-baseline (hundreds to thousands of km). The first two types are typically used to study the development of the lightning channel, while the third (long-baseline) type of TOA sensors are utilized to determine the geographical coordinates of the lightning strike.

Long-baseline TOA sensors were first operated at a bandwidth of 4 to 45 kHz using four stations with a total separation distance of 100 km. Since all electromagnetic radiation propagates through a vacuum (and very near that speed in air) at 3×10^8 m/s, by measuring the time of arrival at different sensors, and coordinating that information between all sensors, the location of the lightning stroke can be determined. In theory, four sensors are needed to accurately locate a lightning stroke, while two such sensors would give a direction, similar to one DF sensor.

There are difficulties with this type of sensor. It does not differentiate between a cloud-to-cloud flash from a cloud-to-ground flash, and errors in locations arise when anything changes the arrival time of an ideal signal, such as topography, or stations receiving different parts of the lightning signal. In fact, the early versions of these sensors were shown to be only about 50% accurate [*Casper and Bent*, 1992].

A.4. Lightning Detection Networks

The first commercial venture for lightning detectors using orthogonal magnetic direction finders (DFs) was started in the mid 1970s, when E.P. Krider, M.A. Uman, and A.E. Pifer formed the company Lightning Location and Protection, Inc. [*Rakov and Uman*, 2003]. These networks needed operators at each station to report the calculated azimuth from each sensor to determine locations of lightning strokes. Original studies using the Lightning Location and Protection (LLP) network were performed in Florida, in Alaska, and along the U.S. Gulf Coast. These early programs relied on three stations communicating with a central command by telephone.

Meanwhile, larger networks were being developed. The United States Bureau of Land Management developed an LLP DF system to cover 11 western states and Alaska, originally using the data to predict forest fires. In the early 1980's, networks covering Oklahoma and the U.S. East Coast were developed. The efficiency of these types of networks was studied by many during the 1980's and early 1990's, and it was found that lightning detection was approximately 70% efficient if the stroke occurred within 400 km of three sensors. The polarity of the lightning and season of the year were found to effect this efficiency [*Hojo et al.*, 1989].

In 1989, the United States National Lightning Detection Network (NLDN) was created, mainly by combining multiple LLP gated wideband magnetic DFs. Today, this network utilizes both DFs and TOA sensors, which provides increased detection efficiency to ~ 90%, and almost an order of magnitude improvement in locating accuracy (from ~ 12 km to ~ 3 km). This network now employs 106 lightning sensors throughout the U.S.

A.5. World Wide Lightning Location Network

The World Wide Lightning Location Network (WWLLN) consists of a series of VLF (3 - 30 kHz) sensors located at a number of distributed sites around the globe. This network is made of TOA sensors, with readings from four or more sensors needed to determine a lightning location. This is a cooperative network that has been operated by the University of Washington since 2003. In this type of network, geographical location of the lightning as compared to the network's sensors is pivotal in locating the stroke. For example, if a lightning strike is enclosed by network sensors, the probability of the network picking up that lightning stroke is improved. Because the Earth is spherical, every lightning stroke is technically enclosed by the network, but as of 2008, there are not as many sensors placed around the world as would be ideal to detect lightning flashes. The WWLLN is currently looking for host sites to improve the networks accuracy. This is especially true in less-developed areas of the world. A satellite image, showing an example of WWLLN data are shown in Figure A.2.

WWLLN currently picks up ~ 50% of all lightning strokes worldwide, but only 15 – 20% of lightning in South America. It is believed (although not technically proven)

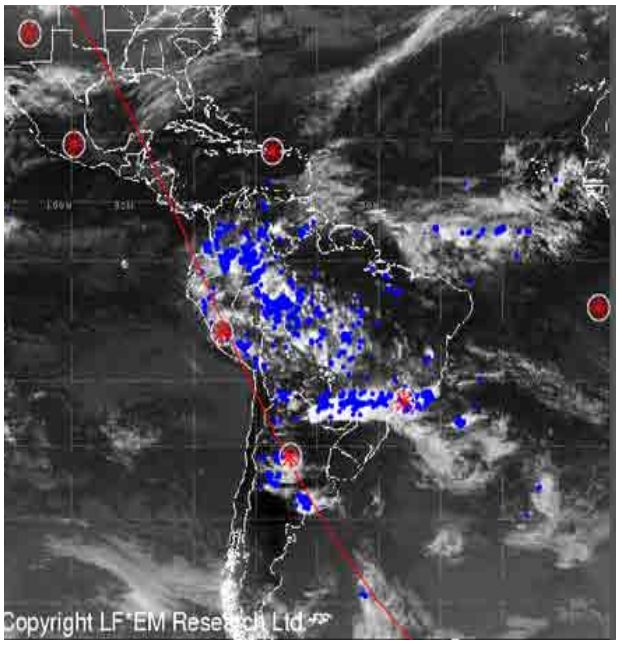


Figure A.2. Map of South America, with overlaying WWLLN lightning stroke locations. The blue dots depict lightning detection, while the red dots show the locations of the WWLLN sensors.

that large, impulsive lightning strokes are detected at a higher rate than smaller strokes (an example of this is that the causative lightning of halos seen during the February 22-23, 2006 storm had a much higher WWLLN detection rate than its normal detection efficiency, see Chapter 5). WWLLN has a timing accuracy of 30μs, and a spatial accuracy of 10 km. Due to the type of sensors within this network, lightning polarity cannot be measured. WWLLN data are available online and are updated every 10 minutes. They were used through our South American programs to first identify the general location(s) of distant thunderstorms to help aim our cameras, and later to determine the location of the individual TLE events used in this analysis.

APPENDIX B: CHARGE MOMENT CALCULATION

B.1. Introduction

Direct measurements of charge transfer during lightning strokes have been made in the past using electrically grounded rockets [*Hubert et al.,* 1984], from chance instances when lightning strikes an instrument tower [*Berger,* 1967], and from multi-site electrostatic field measurements [*Krehbiel et al*., 1979]. These types of measurements are difficult to perform because of the unpredictability of where (and when) a lightning stroke will actually occur, and the proximity at which the sensors must be placed.

As lightning strokes inherently produce electromagnetic radiation, new methods have been devised to use remote detection of this radiation to estimate the amount of charge transferred during a lightning event. This Appendix gives a brief overview of a method developed and utilized by Steven Cummer and U.S. Inan, used to calculate charge moment changes of sprite-producing lightning over the Midwestern United States [*Cummer and Inan*, 1997; *Cummer et al*., 2006; *Cummer and Lyons*, 2005]. Although other similar techniques are being employed by research groups around the globe, this was the method used to calculate charge moments during our collaborative TLE campaign in South America. This appendix does not contain detailed discussion of such techniques, but provides essential background information for the reader to show how the charge-moments used in this dissertation were calculated. This summary is derived almost exclusively from a paper outlying the method [*Cummer and Inan*, 2000]. The reader is encouraged to study the method in its entirety in the above mentioned publication.

Lightning emits electromagnetic (E-M) radiation over a wide range of frequencies (see Appendix A), but most of the energy is radiated in the very low frequency (VLF) and extremely low frequency (ELF) range (3 Hz to 30,000 Hz). E-M waves in these bandwidths have large enough wavelengths that they can reflect multiple times off the ionosphere and Earth's (conducting) surface which forms a natural waveguide (see Figure A.1). This wave proliferation has low attenuation rates [*Taylor and Sao*, 1970], enabling waves to propagate over large distances. Various sensors around the globe can therefore make measurements of lightning-induced ELF/VLF radio atmospheric waves (or sferics, for short). Since the sensors do not need to be in close proximity to a lightning source(s), using ELF/VLF radiation to determine the amount of charge removed during a lightning flash is a very powerful tool for remotely studying lightning and its effects. The particular sensors used by Duke University to detect and measure these ELF/VLF lightning signatures during the South American campaigns are discussed in Chapter 4.

B.2. QTEM Modes in the Ionosphere

When modeling how low frequency waves behave as they propagate within the Earth-ionosphere waveguide, natural changes in the ionosphere must also be included. Early studies of ELF sferic wave propagations were based on simple representations of the ionosphere and do not reproduce some of the details evident in sferic signatures reported in later studies. University of Stanford researchers used a well-validated ionospheric program (MODEFNDR) [*Shellman,* 1986] to model the ionosphere, successfully reproducing some of the fine sferic features observed by sensors [*Cummer*

and Inan, 1997]. Their work compared measured sferic waveforms with differing theoretical results selecting different electron densities in the E and F region ionosphere in the MODEFNDR model. Thus, the proper ionospheric conditions (electron densities, as well as height) can be investigated, and included in their model of propagating sferic waves.

To simplify the determination of the source lightning's current moment from the sferic signature, only the quasi-transverse electromagnetic (QTEM) propagation in a horizontally homogeneous Earth-ionosphere waveguide is used. This assumption is valid at night in the mid-latitude region, where the ionosphere is relatively stable. The QTEM mode is predominantly produced by vertical current discharges, and therefore, horizontal current sources (such as intra-cloud lightning) will not provide similar waveforms. A low-pass (~1.5 kHz) filtering system is utilized to extract the QTEM mode, which on arrival at the sensor composes superposition of many modes. This filtering limits the bandwidth of the extracted waveforms to frequencies above 1.5 kHz, and although some of the waveform's characteristics are lost, the determination of the total charge moment change of the discharge (important for TLE production) is not significantly affected.

B.3. ELF Sferic Modeling

A lightning stroke can be treated as an electrically short antenna having a time-varying current that is constant along the channel length. This approximation is valid due to the fact that for frequencies below 1.5 kHz, the E-M wavelengths will be greater than 200 km (which is much larger than the actual lightning channel length, typically several km), and because the radiated fields are nearly independent of source altitude for

propagation in QTEM mode [*Cummer et al.*, 1998; *Cummer and Inan*, 2000]. The magnitude of the radiated fields depends primarily on the charge moment of the lightning stroke (see Chapter 2), but the propagation of these fields is time invariant, so it is sufficient to consider the fields produced by an impulsive current.

The model developed by *Cummer and Inan* [2000] is based upon a single frequency LWPC ELF/VLF propagation model originally developed by *Pappert and Ferguson* [1986]. For ELF propagation, this model solves the time harmonic propagation using mode theory [*Budden*, 1961], in which the E-M field at the distance from the source are produced by the QTEM waveguide mode. This mode is composed of a horizontal magnetic field perpendicular to the propagation direction and a vertical electric field.

The linearity and time invariance of the sferic propagation means the fields can be related to any given current waveform by a simple convolution operation [see *Bracewell*, 1986, p. 24], when considering fields produced by an impulsive current source. Such fields can be mathematically represented by the Green's function for a known distance between the receiver and the source. This propagation can be readily modeled using Fourier transform methods, from which a time domain waveform can be computed from the inverse transform of the frequency domain solution, which works well in a horizontal waveguide [*Cummer and Inan*, 2000].

The shape of the observed ELF waveform is also strongly related to the bandwidth of the receiver instrument. Therefore, filters must be applied to effectively model any ELF waveform or impulse response so that it is directly comparable with the ELF sferics. *Cummer and Inan* [2000] applied a single-pole high-pass filter to the

observed spectra, as well as to their modeled spectra. It is also possible to digitally filter the data after observation. In general, it is desired to keep the lower frequency cutoff as low as possible, but not so low that other (Schuman) resonances contribute to the observed signal.

As already mentioned, the *Cummer and Inan* [2000] method utilizes a single-frequency LWPC ELF/VLF propagation mode, initially proposed by *Pappert and Ferguson* [1986]. This mode is composed primarily of a horizontal magnetic field perpendicular to the propagation direction and a vertical electric field. It allows for arbitrary altitude profiles of ionspheric electron density, an arbitrary orientation of the magnetic field, and arbitrary homogeneous ground permittivity and conductivity.

For example, the transverse horizontal magnetic field B_y at a distance x along the ground from a vertical electric dipole source as a function of frequency is:

$$B_y(\omega, x) = -\mu_0 k^{1/2} M_e(\omega) \left[R_E \sin\left(\frac{x}{R_E}\right) \right]^{1/2} * \left(\frac{\pi}{2}\right)^{-1/2} e^{i\pi/4} \Lambda_t(\omega) \Lambda_r(\omega) e^{-ikx\sin\theta(\omega)}, \quad (1)$$

where the wave number k is given by $k = 2\pi/\omega$, $M_e(\omega)$ is the vertical electric dipole moment of the source (which is related to the source current moment by $M_e(\omega) = -i M_i(\omega)/\omega$, and M_i is the source current moment amplitude). The term $[R_E \sin(x/R_E)]^{-1/2}$ accounts for the spreading of the fields over a spherical Earth of Radius R_E. The eigenangle θ is related to the index of refraction for the QTEM mode, and the excitation and receiver factors, Λ_t and Λ_r correlate the coupling between the transmitting and receiving antennas and the fields of the waveguide mode. The terms θ, Λ_t, and Λ_r are functions of frequency and depend on the ionospheric electron density and the collision

frequency profiles inputted into the model. These profiles are site and time dependent and are calculated numerically, as discussed in detail by *Pappert and Ferguson* [1986].

Figure B.1 shows the ELF sferic amplitude spectra calculated with this model using representative nighttime and daytime electron density (Ne) altitude profiles. These profiles are for mid-latitude local midnight and midday and were calculated using the 1995 International Reference Ionosphere [*Rawer et al.*, 1978]. The positive ion density is taken to be equal to the electron density except where N_e, 100 cm^{-3}, at which altitudes the positive and negative ion densities are both set to 100 cm^{-3}. The spectra shown in Figure 1 are the amplitude of the transverse horizontal magnetic field B_y as a function of the frequency observed at different distances from the source, specifically, at x = 1000, 2000, and 3000 km. The source current for each is an impulse with a total charge moment change of 10 C·km. The secondary peaks in the nighttime spectral amplitudes are a consequence of the nighttime ionosphere. These types of resonance effects have been seen in theoretical studies of ELF propagation in the presence of narrow sporadic E layers [*Barr*, 1977]. This suggests that electron densities at high altitudes can strongly influence ELF propagation.

The sferic spectrum of Figure B.1 can be converted to a time domain waveform using an inverse Fourier transform operation. However, this operation must be approximated since the spectrum is only a sampled version of the continuous spectrum. *Cummer and Inan* [2000] use a fast Fourier transform (FFT) to do this calculation. The

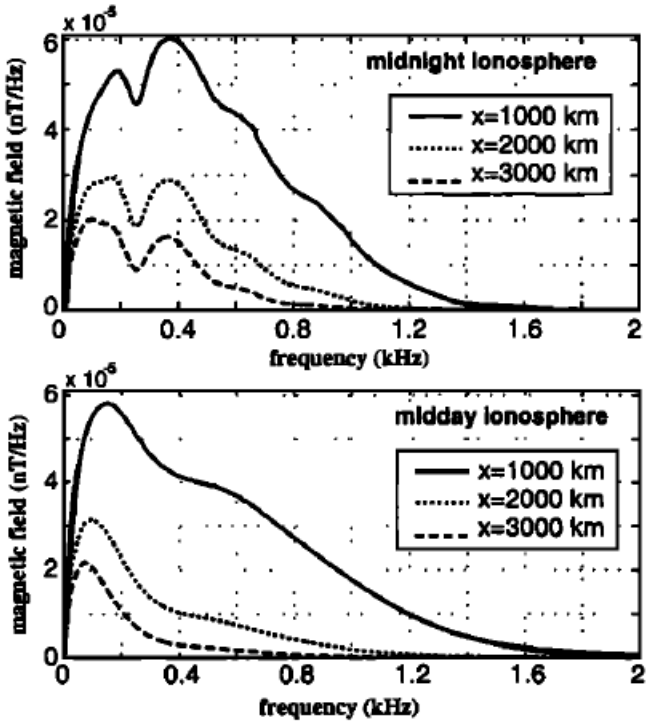


Figure B.1. Calculated ELF sferic spectra for propagation distances of 1000, 2000, and 3000 km under nighttime and daytime ionospheres. The source is an impulsive discharge with a charge moment change of 10 C*km [*Cummer and Inan*, 2000, Figure 2]. Reprinted by permission of the AGU.

continuous time domain waveform *f(t)* is defined by the inverse Fourier transform:

$$f(t) = \frac{1}{2\pi}\int_{-\infty}^{\infty} F(\omega)\exp(i\omega t)d\omega\,, \tag{2}$$

where $F(\omega)$ is the continuous sferic spectrum for positive ω. This inverse transform can be approximated by:

$$F(t) \approx \mathrm{Re}\left[\frac{\Delta\omega}{\pi}\sum_{m=0}^{N-1} F(m\Delta\omega)\exp(im\Delta\omega t)\right], \tag{3}$$

which utilizes the fact that $f(t)$ must be causal, and therefore $F(\omega)$ must have Hermitian

symmetry. In Equation (2) $\Delta\omega$ is the difference between frequency samples and N is the number of samples of $F(\omega)$ calculated through (1). Using the definition of the inverse FFT, namely:

$$IFFT(X) = x_n = \frac{1}{N}\sum_{m=0}^{N-1} X_m wzp(i2\pi mn/N), \tag{4}$$

$f(t)$ can be written as

$$f(n\Delta t) \approx \frac{N\Delta\omega}{\pi}\mathrm{Re}\{IFFT[F(m\Delta\omega)]\}, \tag{5}$$

where $\Delta t = \frac{2\pi}{N\Delta\omega}$. A frequency of $\Delta\omega = 2\pi\cdot 5$ Hz is small enough to capture the fine spectral variations. A relatively smooth waveform results from a sampling period of $\Delta t = 10^{-4}$ s, which is justified since the signal strength is essentially zero for frequencies greater than 2.0 kHz. Together, these two values require a sample set of $N = 2000$, which corresponds to a maximum calculated frequency of $\omega_{max} = 2\pi\cdot 10$ Hz. Since the sferic spectrum is approximately zero for frequencies above 2 kHz, $F(\omega)$ need only be calculated up to this frequency. In fact, applying a 1-kHz low-pass filter can eliminate any contributions to the signal from the QTM or QTE modes, ensuring that $|F(\omega)| \approx 0$ for f > 2 kHz. Figure B.2 shows the calculated B_y waveforms for the three propagation distance under daytime and night-time ionospheric conditions for the spectra shown in Figure B.1.

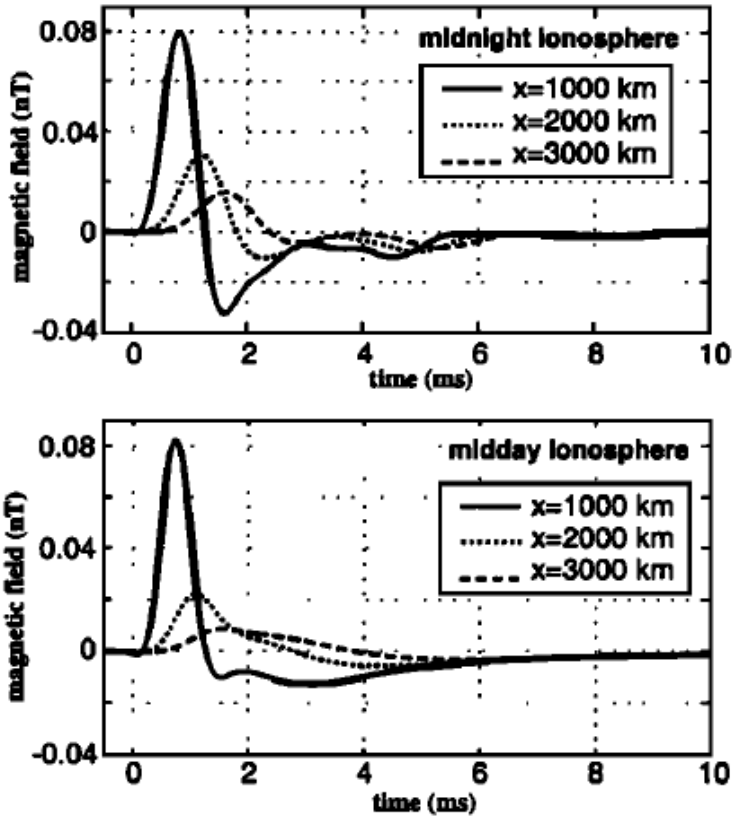


Figure B.2. Calculated ELF B_y waveforms for the ELF sferic spectra of Figure 1, [*Cummer and Inan*, 2000, Figure 3]. Reproduced by permission of the AGU.

B.4. Source Current Extraction

Due to the time invariance and linearity of the propagation problem, the relationship between the sferic waveform, current moment waveform, and propagation impulse response is a simple convolution, namely:

$$f(t) = \int_{-\infty}^{\infty} m_i(\tau) h(t-\tau) d\tau \,, \tag{6}$$

where $h(t)$ is the propagation impulse response, $m_i(t)$ is the source current moment, and $f(t)$ is the observed electric or magnetic field waveform. If an observed sferic has a

known propagation distance from the discharge to the receiver, the ELF propagation impulse response $h(t)$ can be modeled. After this, the source current moment can be extracted by solving the inverse convolution (or deconvolution) problem. Deconvolution methods can be problematic, due to the non-unique nature of the problem. In particular, convolution removes information contained in higher frequencies of $m_i(t)$. This information cannot be recovered and there are many waveforms that satisfy the forward convolution problem nearly as well as each other. A deconvolution technique must therefore be used to handle the non-uniqueness of the situation. *Cummer and Inan* [2000] discuss that different techniques have been used in past studies, but that linear regularization has proved to be the most effective method (as considered by *Press et al*. [1992, p. 799]).

Solutions from the linear regularization must be physically reasonable; the solution must be causal (the current must be zero before the sferic starts), and it must be positive (because the vertical current in a single lightning discharge does not change direction). The linear regularization technique itself does not guarantee these conditions and *Cummer and Inan* [2000] uses an additional technique to implement these conditions in the solution. This solution is known as the method of Projections Onto Convex Sets (POCS) [*Press et al*., 1992, p. 804].

Cummer and Inan [2000] tested their techniques using a modeled sferic, and showed that the current moment (and thus the charge moment for a given time interval) can be accurately extracted from the sferic information. However, it should be mentioned that a significant deviation in the extracted charge moment change from the actual charge moment change occurred around 10 ms after the discharge onset, when the

background noise began to dominate the signal. Therefore, although the method works well, it is limited when the signal-to-noise ratio is low. *Cummer and Inan* [2000] has successfully applied this technique to observed sferic, providing quantitative information about the causative lightning stroke.

B.5 Conclusion

Lightning discharges generate electromagnetic waves at very low frequencies, known as radio atmospherics or sferics. A method using these sferics to extract information about the lightning discharge, namely, the current moment (and thus the charge moment), has been developed and described in *Cummer and Inan* [2000]. This method consists of two components. The first is a model which deals with the propagation of the low frequency energy from the lightning source to the receiver, and the second is a deconvolution technique in which the source current moment can be extracted from the observed sferic signature. This method has been used to quantify charge-moments of lightning in many studies, and was used extensively during the South American campaign discussed in this dissertation.

APPENDIX C: PERMISSION FOR PUBLICATION FORMS

AGU

22 February 2010

Matthew Bailey
832 Prospect Street
Wethersfield, CT 06109

We are pleased to grant permission for the use of the material requested for inclusion in your thesis. The following non-exclusive rights are granted to AGU authors:

- All proprietary rights other than copyright (such as patent rights).
- The right to present the material orally.
- The right to reproduce figures, tables, and extracts, appropriately cited.
- The right to make hard paper copies of all or part of the paper for classroom use.
- The right to deny subsequent commercial use of the paper.

Further reproduction or distribution is not permitted beyond that stipulated. The copyright credit line should appear on the first page of the article or book chapter. The following must also be included, "Reproduced by permission of American Geophysical Union." To ensure that credit is given to the original source(s) and that authors receive full credit through appropriate citation to their papers, we recommend that the full bibliographic reference be cited in the reference list. The standard credit line for journal articles is: "Author(s), title of work, publication title, volume number, issue number, citation number (or page number(s) prior to 2002), year. Copyright [year] American Geophysical Union."

If an article was placed in the public domain, in which case the words "Not subject to U.S. copyright" appear on the bottom of the first page or screen of the article, please substitute "published" for the word "copyright" in the credit line mentioned above.

Copyright information is provided on the inside cover of our journals. For permission for any other use, please contact the AGU Publications Office at AGU, 2000 Florida Ave., N.W., Washington, DC 20009.

Sincerely,

Michael Connolly
Journals Publications Specialist

OXFORD
UNIVERSITY PRESS

Academic Division
Rights Department
Great Clarendon Street
Oxford OX2 6DP
United Kingdom
+ 44 (0) 1865 556767 *telephone*
+ 44 (0) 1865 353 429 *fax*
www.oup.co.uk/rights/academic_permissions/

Matt Bailey
832 Prospect Street
Wethersfield
CT 06109
USA

Dear Matthew,

Thank you for your enquiry. You have our permission to use the OUP Material you list in your email below in your thesis for submission to Utah State University. A maximum of 20 copies to be made for distribution only to the University Library, the Physics Department for their library, your PhD committee, and yourself and your family and colleagues.

If at some future date your thesis is published it will be necessary to re-clear this permission.
Please also note that if the material to be used is acknowledged to any other source, you will need to clear permission with the rights holder.

Best wishes,

Ben Kennedy
Permissions Assistant
Academic Rights & Journals
Oxford University Press
Great Clarendon Street
Oxford
OX2 6DP
Direct tel. +44 (0)1865 354728
Direct fax +44 (0)1865 353429
e mail: ben.kennedy@oup.com<mailto:ben.kennedy@oup.com>

PERMISSION INVOICE

Inv. # P03B 17789

January 26, 2010

CAMBRIDGE UNIVERSITY PRESS
32 Avenue of the Americas
New York, NY 10013-2473, USA
www.cambridge.org
Telephone 212 924 3900
Fax 212 691 3239

Matthew Bailey
832 Prospect
Weathersfield, CT
06109

REFERENCE

ISBN:	HB	PB 9780521035415	Other
Author:	Vladamir A. Rakov and Martin A. Uman		
Title:	LIGHTNING, PHYSICS AND EFFECTS, 3RD EDITION		
Selection/pp.:	Figure 3.1, Figure 4.2		

Additional:

USE

Reprint Title:	INVESTIGATING CHARACTERISTICS OF LIGHTNING INDUCED TRANSIENT LUMINOUS EVENTS OVER SOUTH AMERICA
Publisher:	Utah State University
Format:	dissertation / thesis
Quantity (Limit*):	20
Avail. Date:	2/10

RIGHTS/ACKNOWLEDGEMENT

Permission is granted for nonexclusive rights throughout the World in the English language for interior text editorial use in the format described above only, including non-profit editions for the blind and handicapped. Please fully acknowledge our material and indicate the copyright notice as it appears in our publication, followed by the phrase "Reprinted with the permission of Cambridge University Press."
All requests from third parties to reproduce this material must be forwarded to Cambridge University Press.

FEES/RESTRICTIONS

$0.00

*You must re-apply for permission if this print run is exceeded. This permission is restricted to the indicated format and excludes reproduction in any other medium; for additional use, you must apply for permission separately. This permission does not allow reprinting of any material copyrighted by or credited in our publication to another source; Cambridge disclaims all liability in connection with the use of such material without proper consent. A COPY OF THIS INVOICE MUST ACCOMPANY PAYMENT. Payment is due upon publication or within 12 months, whichever is sooner. Make check payable to Cambridge University Press, Attn: Rights and Permissions. (CUP Fed. I.D. #: 13 -1599108.)

This permission does not supersede permission that may be required from the original source indicated in our publication.

This permission requires that you send zero (0) copies of your publication directly to our author and zero (0) copy of your publication to this office upon availability.

Authorization: Adam Hirschberg

Adam Hirschberg
Rights and Permissions Associate

Feb 27, 2010

Matthew Bailey
Center for Atmospheric and Space Sciences
Department of Physics
4405 Old main Hill
Logan, UT 84322-4405
(860) 297 5103

Dear Dr. Mayes

I am in the process of preparing my dissertation in the physics Department at Utah State University. I hope to complete it in the Spring of 2010.

I am requesting your permission to include the attached material as shown. I will include acknowledgements and/or appropriate citations to your work as shown and copyright and reprint rights information in a special appendix. The bibliographical citation will appear at the end of the manuscript as shown. Please advise me on any changes you require.

Please indicate your approval of this request by signing in the space provided, attaching any other form or instruction necessary to confirm permission. If you charge a reprint fee for use of your material, please indicate this as well. If you have any questions, please contact me at the number above.

I hope you will be able to reply immediately. If you are not the copyright holder, please forward my request to the appropriate position or institution.

Thank you for your cooperation.

Matthew Bailey

I hereby give permission to Matthew Bailey to reprint the following material in his dissertation.

Mayes, J., and K. Hughes (2004), *Understanding Weather*, Oxford University Press, New York: Figure 1.1.

Name: Julian Mayes Date: 4—3—10.

March 5, 2010

Matthew Bailey
Center for Atmospheric and Space Sciences
Department of Physics
4405 Old main Hill
Logan, UT 84322-4405
(860) 297 5103

Dear Lina

I am in the process of preparing my dissertation in the physics Department at Utah State University. I hope to complete it in the Spring of 2010.

I am requesting your permission to include the attached material as shown. I will include acknowledgements and/or appropriate citations to your work as shown and copyright and reprint rights information in a special appendix. The bibliographical citation will appear at the end of the manuscript as shown. Please advise me on any changes you require.

Please indicate your approval of this request by signing in the space provided, attaching any other form or instruction necessary to confirm permission. If you charge a reprint fee for use of your material, please indicate this as well. If you have any questions, please contact me at the number above.

I hope you will be able to reply immediately. If you are not the copyright holder, please forward my request to the appropriate position or institution.

Thank you for your cooperation.

Matthew Bailey

I hereby give permission to Matthew Bailey to reprint the following material in his dissertation.

Miyasato, R., M. J. Taylor, H. Fukunishi, and H. C. Stenbaek-Nielsen (2002), Statistical Characteristics of Sprite Halo Events Using Coincident Photometric and Imaging Data, *Geophys. Res. Lett.*, *29*(21), 2033, doi:10.1029/2001GL014480: Figure1, Figure 3.

Name: Rina Oro Date: 3/9/2010

March 8, 2010

Matthew Bailey
Center for Atmospheric and Space Sciences
Department of Physics
4405 Old main Hill
Logan, UT 84322-4405
(860) 297 5103

Dear Dr. Nemzek

I am in the process of preparing my dissertation in the physics Department at Utah State University. I hope to complete it in the Spring of 2010.

I am requesting your permission to include the attached material as shown. I will include acknowledgements and/or appropriate citations to your work as shown and copyright and reprint rights information in a special appendix. The bibliographical citation will appear at the end of the manuscript as shown. Please advise me on any changes you require.

Please indicate your approval of this request by signing in the space provided, attaching any other form or instruction necessary to confirm permission. If you charge a reprint fee for use of your material, please indicate this as well. If you have any questions, please contact me at the number above.

I hope you will be able to reply immediately. If you are not the copyright holder, please forward my request to the appropriate position or institution.

Thank you for your cooperation.

Matthew Bailey

I hereby give permission to Matthew Bailey to reprint the following material in his dissertation.

Franz, R. C., J. Nemzek, and J. R. Winckler (1990), Television image of a large upward electrical discharge above a thunderstorm system, *Science*, *249*, 48-51: Figure 1.

Name:  Date: 10 March 2010

Feb 27, 2010

Matthew Bailey
Center for Atmospheric and Space Sciences
Department of Physics
4405 Old main Hill
Logan, UT 84322-4405
(860) 297 5103

Dear Dr. Pasko:

I am in the process of preparing my dissertation in the physics Department at Utah State University. I hope to complete it in the Spring of 2010.

I am requesting your permission to include the attached material as shown. I will include acknowledgements and/or appropriate citations to your work as shown and copyright and reprint rights information in a special appendix. The bibliographical citation will appear at the end of the manuscript as shown. Please advise me on any changes you require.

Please indicate your approval of this request by signing in the space provided, attaching any other form or instruction necessary to confirm permission. If you charge a reprint fee for use of your material, please indicate this as well. If you have any questions, please contact me at the number above.

I hope you will be able to reply immediately. If you are not the copyright holder, please forward my request to the appropriate position or institution.

Thank you for your cooperation.

Matthew Bailey

I hereby give permission to Matthew Bailey to reprint the following material in his dissertation.

Pasko, V.P, M.A. Stanley, J.D. Matthews, U.S. Inan, and T.G Woods (2002), Electrical discharge from a thundercloud top to the lower ionosphere, *Nature, 416*, 152-154: Figures. 2a, 2b, 2c.

Pasko, V. P., U. S. Inan, T. F. Bell, and Y. N. Taranenko (1997), Sprites produced by quasi-electrostatic heating and ionization in the lower ionosphere, *J. Geophys. Res., 102*, 529-4561: Figures. 1.

Pasko, V.P., U.S. Inan, Y.N. Taranenko, and T.F. Bell (1995), Heating, ionization and upward discharges in the mesosphere due to intense quasi-electrostatic thundercloud fields, *Geophys. Res. Lett., 22*, 365-368: Figure 4.

Name: Victor Pasko Date: March 1, 2010

Feb 27, 2010

Matthew Bailey
Center for Atmospheric and Space Sciences
Department of Physics
4405 Old main Hill
Logan, UT 84322-4405
(860) 297 5103

Dear Dr. Rakov:

I am in the process of preparing my dissertation in the physics Department at Utah State University. I hope to complete it in the Spring of 2010.

I am requesting your permission to include the attached material as shown. I will include acknowledgements and/or appropriate citations to your work as shown and copyright and reprint rights information in a special appendix. The bibliographical citation will appear at the end of the manuscript as shown. Please advise me on any changes you require.

Please indicate your approval of this request by signing in the space provided, attaching any other form or instruction necessary to confirm permission. If you charge a reprint fee for use of your material, please indicate this as well. If you have any questions, please contact me at the number above.

I hope you will be able to reply immediately. If you are not the copyright holder, please forward my request to the appropriate position or institution.

Thank you for your cooperation.

Matthew Bailey

I hereby give permission to Matthew Bailey to reprint the following material in his dissertation.

Rakov, V.A and M.A. Uman (2003), *Lightning: Physics and Effects*, Cambridge University Press, Cambridge, UK: Figures 3.1, 4.2.

Name: _____ Date: 03/01/10

VLADIMIR A. RAKOV

Feb 27, 2010

Matthew Bailey
Center for Atmospheric and Space Sciences
Department of Physics
4405 Old main Hill
Logan, UT 84322-4405
(860) 297 5103

Dear Dr. Rodger:

I am in the process of preparing my dissertation in the physics Department at Utah State University. I hope to complete it in the Spring of 2010.

I am requesting your permission to include the attached material as shown. I will include acknowledgements and/or appropriate citations to your work as shown and copyright and reprint rights information in a special appendix. The bibliographical citation will appear at the end of the manuscript as shown. Please advise me on any changes you require.

Please indicate your approval of this request by signing in the space provided, attaching any other form or instruction necessary to confirm permission. If you charge a reprint fee for use of your material, please indicate this as well. If you have any questions, please contact me at the number above.

I hope you will be able to reply immediately. If you are not the copyright holder, please forward my request to the appropriate position or institution.

Thank you for your cooperation.

Matthew Bailey

I hereby give permission to Matthew Bailey to reprint the following material in his dissertation.

Rodger, C.J., Red sprites, upward lighting and VLF perturbations (1999), *Review of Geophysics*, *37*(3), pp. 317-336: Figure 7.

Name: _____ Craig Rodger _____ Date: _____2 March 2010_____

Feb 27, 2010

Matthew Bailey
Center for Atmospheric and Space Sciences
Department of Physics
4405 Old main Hill
Logan, UT 84322-4405
(860) 297 5103

Dear Dr. Rodriguez:

I am in the process of preparing my dissertation in the physics Department at Utah State University. I hope to complete it in the Spring of 2010.

I am requesting your permission to include the attached material as shown. I will include acknowledgements and/or appropriate citations to your work as shown and copyright and reprint rights information in a special appendix. The bibliographical citation will appear at the end of the manuscript as shown. Please advise me on any changes you require.

Please indicate your approval of this request by signing in the space provided, attaching any other form or instruction necessary to confirm permission. If you charge a reprint fee for use of your material, please indicate this as well. If you have any questions, please contact me at the number above.

I hope you will be able to reply immediately. If you are not the copyright holder, please forward my request to the appropriate position or institution.

Thank you for your cooperation.

Matthew Bailey

I hereby give permission to Matthew Bailey to reprint the following material in his dissertation.

Rodriguez, J., U. Inan, and T. Bell (1992), D region disturbances caused by electromagnetic pulses from lightning, *Geophys. Res. Lett., 19*(20), 2067-2070: Figure 4b.

You will need to secure permission from AGU as well.

Name: Juan V. Rodriguez Date: 3/1/10

203-413-5643

Feb 27, 2010

Matthew Bailey
Center for Atmospheric and Space Sciences
Department of Physics
4405 Old main Hill
Logan, UT 84322-4405
(860) 297 5103

Dear Dr. Williams:

I am in the process of preparing my dissertation in the physics Department at Utah State University. I hope to complete it in the Spring of 2010.

I am requesting your permission to include the attached material as shown. I will include acknowledgements and/or appropriate citations to your work as shown and copyright and reprint rights information in a special appendix. The bibliographical citation will appear at the end of the manuscript as shown. Please advise me on any changes you require.

Please indicate your approval of this request by signing in the space provided, attaching any other form or instruction necessary to confirm permission. If you charge a reprint fee for use of your material, please indicate this as well. If you have any questions, please contact me at the number above.

I hope you will be able to reply immediately. If you are not the copyright holder, please forward my request to the appropriate position or institution.

Thank you for your cooperation.

Matthew Bailey

I hereby give permission to Matthew Bailey to reprint the following material in his dissertation.

Williams, E., E. Downes, Ro. Boldi, W. Lyons, and S. Heckman (2007), Polarity asymmetry of sprite producing lightning: A paradox?, *Radio Sci.*, 42, RS2S17, doi:10:1029/2006RS003488: Table 1.

Name: Earle R Williams Date: March 3/2010

Feb 27, 2010

Matthew Bailey
Center for Atmospheric and Space Sciences
Department of Physics
4405 Old main Hill
Logan, UT 84322-4405
(860) 297 5103

Dear Dr. Stenbaek-Nielsen:

I am in the process of preparing my dissertation in the physics Department at Utah State University. I hope to complete it in the Spring of 2010.

I am requesting your permission to include the attached material as shown. I will include acknowledgements and/or appropriate citations to your work as shown and copyright and reprint rights information in a special appendix. The bibliographical citation will appear at the end of the manuscript as shown. Please advise me on any changes you require.

Please indicate your approval of this request by signing in the space provided, attaching any other form or instruction necessary to confirm permission. If you charge a reprint fee for use of your material, please indicate this as well. If you have any questions, please contact me at the number above.

I hope you will be able to reply immediately. If you are not the copyright holder, please forward my request to the appropriate position or institution.

Thank you for your cooperation.

Matthew Bailey

I hereby give permission to Matthew Bailey to reprint the following material in his dissertation.

Stenbaek-Nielsen, H. C., D. R. Moudry, E. M. Wescott, D. D. Sentman, and F. T. Sao Sabbas (2000), Sprites and Possible Mesospheric Effects, *Geophys. Res. Lett.*, *27*, 3829-3832: Figure 1.

Name: _____ Date: March 1, 2010

Feb 27, 2010

Matthew Bailey
Center for Atmospheric and Space Sciences
Department of Physics
4405 Old main Hill
Logan, UT 84322-4405
(860) 297 5103

Dear Dr. Hampton:

I am in the process of preparing my dissertation in the physics Department at Utah State University. I hope to complete it in the Spring of 2010.

I am requesting your permission to include the attached material as shown. I will include acknowledgements and/or appropriate citations to your work as shown and copyright and reprint rights information in a special appendix. The bibliographical citation will appear at the end of the manuscript as shown. Please advise me on any changes you require.

Please indicate your approval of this request by signing in the space provided, attaching any other form or instruction necessary to confirm permission. If you charge a reprint fee for use of your material, please indicate this as well. If you have any questions, please contact me at the number above.

I hope you will be able to reply immediately. If you are not the copyright holder, please forward my request to the appropriate position or institution.

Thank you for your cooperation.

Matthew Bailey

I hereby give permission to Matthew Bailey to reprint the following material in his dissertation.

Hampton, D.L., M.J. Heavner, E.M. Wescott, and D.D. Sentman (1996), Optical spectral characteristics of sprites, *Geophys. Res. Lett, 23*(1), 89-92: Figure 2, Figure 3.

Name: [signature] Date: 3-1-2010

Feb 27, 2010

Matthew Bailey
Center for Atmospheric and Space Sciences
Department of Physics
4405 Old main Hill
Logan, UT 84322-4405
(860) 297 5103

Dear Dr. Wescott:

I am in the process of preparing my dissertation in the physics Department at Utah State University. I hope to complete it in the Spring of 2010.

I am requesting your permission to include the attached material as shown. I will include acknowledgements and/or appropriate citations to your work as shown and copyright and reprint rights information in a special appendix. The bibliographical citation will appear at the end of the manuscript as shown. Please advise me on any changes you require.

Please indicate your approval of this request by signing in the space provided, attaching any other form or instruction necessary to confirm permission. If you charge a reprint fee for use of your material, please indicate this as well. If you have any questions, please contact me at the number above.

I hope you will be able to reply immediately. If you are not the copyright holder, please forward my request to the appropriate position or institution.

Thank you for your cooperation.

Matthew Bailey

I hereby give permission to Matthew Bailey to reprint the following material in his dissertation.

Wescott, E. M., H. C. Stenbaek-Nielsen, D. D. Sentman, M. J. Heavner, D. R. Moudry, F. T. S. Sabbas (2001), Triangulation of sprites, associated halos and their possible relation to causative lightning and micrometeors, *J. Geophys. Res.*, *106*(A6), 10467-10478, 10.1029/2000JA000182: Figures 5, 9.

Name: _____ Date: MAR 26, 2010

March 5, 2010

Matthew Bailey
Center for Atmospheric and Space Sciences
Department of Physics
4405 Old main Hill
Logan, UT 84322-4405
(860) 297 5103

Dear Dr. Rousell-Dupre

I am in the process of preparing my dissertation in the physics Department at Utah State University. I hope to complete it in the Spring of 2010.

I am requesting your permission to include the attached material as shown. I will include acknowledgements and/or appropriate citations to your work as shown and copyright and reprint rights information in a special appendix. The bibliographical citation will appear at the end of the manuscript as shown. Please advise me on any changes you require.

Please indicate your approval of this request by signing in the space provided, attaching any other form or instruction necessary to confirm permission. If you charge a reprint fee for use of your material, please indicate this as well. If you have any questions, please contact me at the number above.

I hope you will be able to reply immediately. If you are not the copyright holder, please forward my request to the appropriate position or institution.

Thank you for your cooperation.

Matthew Bailey

I hereby give permission to Matthew Bailey to reprint the following material in his dissertation.

Rousell-Dupre, R.A., and A.V. Gurevich (1996), On run-away breakdown and upward-propagating discharges, *J. Geophys. Res., 101*, 2297-2311: Figure 7.

Name: Robert Roussel-Dupre Date: 3/14/2010

Powered by RIGHTSLINK
COPYRIGHT CLEARANCE CENTER, INC.
Home | Account Info | Help

nature publishing group

Title: Electrical discharge from a thundercloud top to the lower ionosphere

Author: Victor P. Pasko, Mark A. Stanley, John D. Mathews, Umran S. Inan and Troy G. Wood

Publication: Nature

Publisher: Nature Publishing Group

Date: Mar 14, 2002

Copyright © 2002, Nature Publishing Group

Logged in as:
matthew bailey
Account #:
3000286282
LOGOUT

Order Completed

Thank you very much for your order.

This is a License Agreement between matthew bailey ("You") and Nature Publishing Group ("Nature Publishing Group"). The license consists of your order details, the terms and conditions provided by Nature Publishing Group, and the payment terms and conditions.

Get the printable license.

License Number	2380291016937
License date	Mar 01, 2010
Licensed content publisher	Nature Publishing Group
Licensed content publication	Nature
Licensed content title	Electrical discharge from a thundercloud top to the lower ionosphere
Licensed content author	Victor P. Pasko, Mark A. Stanley, John D. Mathews, Umran S. Inan and Troy G. Wood
Volume number	416
Issue number	6877
Pages	pp152-154
Year of publication	2002
Portion used	Figures / tables
Number of figures / tables	1
Requestor type	Student
Type of Use	Thesis / Dissertation
Billing type	Invoice
Company	matthew bailey
Billing address	832 Prospect Wethersfield, CT 06109 United States
Customer reference info	
Total	0.00 USD

ORDER MORE... CLOSE WINDOW

Copyright © 2010 Copyright Clearance Center, Inc. All Rights Reserved. Privacy statement.
Comments? We would like to hear from you. E-mail us at customercare@copyright.com

McAfee SECURE
TESTED DAILY 01-MAR

THE AMERICAN ASSOCIATION FOR THE ADVANCEMENT OF SCIENCE LICENSE TERMS AND CONDITIONS

Mar 01, 2010

This is a License Agreement between matthew bailey ("You") and The American Association for the Advancement of Science ("The American Association for the Advancement of Science") provided by Copyright Clearance Center ("CCC"). The license consists of your order details, the terms and conditions provided by The American Association for the Advancement of Science, and the payment terms and conditions.

All payments must be made in full to CCC. For payment instructions, please see information listed at the bottom of this form.

License Number	2380281481207
License date	Mar 01, 2010
Licensed content publisher	The American Association for the Advancement of Science
Licensed content publication	Science
Licensed content title	Television Image of a Large Upward Electrical Discharge Above a Thunderstorm System
Licensed content author	R. C. Franz, R. J. Nemzek, J. R. Winckler
Licensed content date	Jul 6, 1990
Type of Use	Thesis / Dissertation
Requestor type	Other Individual
Format	Print
Portion	Text Excerpt
Number of pages requested	1
Order reference number	
Title of your thesis / dissertation	INVESTIGATING CHARACTERISTICS OF LIGHTNING INDUCED TRANSIENT LUMINOUS EVENTS OVER SOUTH AMERICA
Expected completion date	May 2010
Estimated size(pages)	200
Total	0.00 USD
Terms and Conditions	

American Association for the Advancement of Science TERMS AND CONDITIONS

Regarding your request, we are pleased to grant you non-exclusive, non-transferable permission, to republish the AAAS material identified above in your work identified above, subject to the terms and conditions herein. We must be contacted for permission for any uses other than those specifically identified in your request above.

The following credit line must be printed along with the AAAS material: "From [Full Reference Citation]. Reprinted with permission from AAAS."

March 4, 2010

Hi, Matthew--

Apologies for not replying to your email and thank you for pinging me with a voicemail. I had somehow archived your message without responding.

You may reprint the figure with the following conditions:

+ please include the complete bibliographic citation of the original source, and
+ please include the following statement with that citation:
(c)American Meteorological Society. Reprinted with permission.

That should take care of the permission, but if you have any additional questions, please get in touch. My contact information is below.

Jinny Nathans
AMS Permissions

jnathans@ametsoc.org
617 227-2426 x213

Feb 27, 2010

Matthew Bailey
Center for Atmospheric and Space Sciences
Department of Physics
4405 Old main Hill
Logan, UT 84322-4405
(860) 297 5103

Dear Dr. Fukunishi:

I am in the process of preparing my dissertation in the physics Department at Utah State University. I hope to complete it in the Spring of 2010.

I am requesting your permission to include the attached material as shown. I will include acknowledgements and/or appropriate citations to your work as shown and copyright and reprint rights information in a special appendix. The bibliographical citation will appear at the end of the manuscript as shown. Please advise me on any changes you require.

Please indicate your approval of this request by signing in the space provided, attaching any other form or instruction necessary to confirm permission. If you charge a reprint fee for use of your material, please indicate this as well. If you have any questions, please contact me at the number above.

I hope you will be able to reply immediately. If you are not the copyright holder, please forward my request to the appropriate position or institution.

Thank you for your cooperation.

Matthew Bailey

I hereby give permission to Matthew Bailey to reprint the following material in his dissertation.

Sato, M. and H. Fukinish (2003), Global sprite occurrence locations and rates derived from triangulation of transient Schumann resonance events, *Geophys. Res. Lett., 30*(16), 1859, doi:10:1029/2003GLO017291: Figure 4c.

Fukunish, H., Y. Takahashi, M. Kubota, K. Sakanoi, U.S. Inan, and W.A. Lyons (1996), Elves: Lightning-induced transient luminous events in the lower ionosphere, *Geophys. Res. Lett., 23*, 2157-2160: Figures 1a, 2a, 2d.

Name: Hiroshi Fukunishi Date: March 2, 2010

March 2, 2010

Matthew Bailey
Center for Atmospheric and Space Sciences
Department of Physics
4405 Old main Hill
Logan, UT 84322-4405
(860) 297 5103

Dear Dr. Blanc,

I am in the process of preparing my dissertation in the physics Department at Utah State University. I hope to complete it in the Spring of 2010.

I am requesting your permission to include the attached material as shown. I will include acknowledgements and/or appropriate citations to your work as shown and copyright and reprint rights information in a special appendix. The bibliographical citation will appear at the end of the manuscript as shown. Please advise me on any changes you require.

Please indicate your approval of this request by signing in the space provided, attaching any other form or instruction necessary to confirm permission. If you charge a reprint fee for use of your material, please indicate this as well. If you have any questions, please contact me at the number above.

I hope you will be able to reply immediately. If you are not the copyright holder, please forward my request to the appropriate position or institution.

Thank you for your cooperation.

Matthew Bailey

I hereby give permission to Matthew Bailey to reprint the following material in his dissertation.

Blanc, E., T. Farges, R. Roche, D. Brebion, T. Hua, A. Labartha, and V. Melnikov (2004), Nadir observations of sprites from the International Space Station, J. *Geophys. Res.*, *109*, A02306, doi:10:1029/2003JA009972: Figure 3.

Name: _____Elisabeth Blanc_____ Date: _____March, 4th, 2010_____



Feb 27, 2010

Matthew Bailey
Center for Atmospheric and Space Sciences
Department of Physics
4405 Old main Hill
Logan, UT 84322-4405
(860) 297 5103

Dear Dr. Boeck:

I am in the process of preparing my dissertation in the physics Department at Utah State University. I hope to complete it in the Spring of 2010.

I am requesting your permission to include the attached material as shown. I will include acknowledgements and/or appropriate citations to your work as shown and copyright and reprint rights information in a special appendix. The bibliographical citation will appear at the end of the manuscript as shown. Please advise me on any changes you require.

Please indicate your approval of this request by signing in the space provided, attaching any other form or instruction necessary to confirm permission. If you charge a reprint fee for use of your material, please indicate this as well. If you have any questions, please contact me at the number above.

I hope you will be able to reply immediately. If you are not the copyright holder, please forward my request to the appropriate position or institution.

Thank you for your cooperation.

Matthew Bailey

I hereby give permission to Matthew Bailey to reprint the following material in his dissertation.

Boeck, W.L., O.H. Vaughan Jr., R.J. Blakeslee, B. Vonegut, M. Brook, and J. McKune (1995), Observations of lightning in the stratosphere, *J. Geoophys. Res., 100*(D1), 1465-1475: Figure 1g.

Name: William T Boeck Date: 3/1/2010

Feb 27, 2010

Matthew Bailey
Center for Atmospheric and Space Sciences
Department of Physics
4405 Old main Hill
Logan, UT 84322-4405
(860) 297 5103

Dear Dr. Cummer:

I am in the process of preparing my dissertation in the physics Department at Utah State University. I hope to complete it in the Spring of 2010.

I am requesting your permission to include the attached material as shown. I will include acknowledgements and/or appropriate citations to your work as shown and copyright and reprint rights information in a special appendix. The bibliographical citation will appear at the end of the manuscript as shown. Please advise me on any changes you require.

Please indicate your approval of this request by signing in the space provided, attaching any other form or instruction necessary to confirm permission. If you charge a reprint fee for use of your material, please indicate this as well. If you have any questions, please contact me at the number above.

I hope you will be able to reply immediately. If you are not the copyright holder, please forward my request to the appropriate position or institution.

Thank you for your cooperation.

Matthew Bailey

I hereby give permission to Matthew Bailey to reprint the following material in his dissertation.

Cummer, S. A., N. Jaugey, J. Li, W. A. Lyons, T. E. Nelson, and E. A. Gerken (2006), Sub-millisecond imaging of sprite development and structure, *Geophys. Res. Lett., 33*, L04104, doi:10.1029/2005GL024969: Figure 2.

Cummer, S. A., U. S. Inan (2000), Modeling ELF radio atmospheric propagation and extracting lightning currents from ELF observations, *Radio Sci., 35*(2), 385-394, 10.1029/1999RS002184: Figure 2, Figure 3.

Name:  Date: March 2, 2010

Feb 27, 2010

Matthew Bailey
Center for Atmospheric and Space Sciences
Department of Physics
4405 Old main Hill
Logan, UT 84322-4405
(860) 297 5103

Dear Dr. Sentman:

I am in the process of preparing my dissertation in the physics Department at Utah State University. I hope to complete it in the Spring of 2010.

I am requesting your permission to include the attached material as shown. I will include acknowledgements and/or appropriate citations to your work as shown and copyright and reprint rights information in a special appendix. The bibliographical citation will appear at the end of the manuscript as shown. Please advise me on any changes you require.

Please indicate your approval of this request by signing in the space provided, attaching any other form or instruction necessary to confirm permission. If you charge a reprint fee for use of your material, please indicate this as well. If you have any questions, please contact me at the number above.

I hope you will be able to reply immediately. If you are not the copyright holder, please forward my request to the appropriate position or institution.

Thank you for your cooperation.

Matthew Bailey

I hereby give permission to Matthew Bailey to reprint the following material in his dissertation.

Sentman, D.D., E.M. Wescott, D.L. Osborne, D.L. Hampton, and M.J. Heavner (1995b), Preliminary results from the Sprites94 aircraft campaign: 1. Red Sprites, *Geophys. Res. Lett., 22*, 1205-1208: Figure 1.

Name: D.D. Sentman Date: 1 Mar 2010

Feb 27, 2010

Matthew Bailey
Center for Atmospheric and Space Sciences
Department of Physics
4405 Old main Hill
Logan, UT 84322-4405
(860) 297 5103

Dear Dr. Gerken:

I am in the process of preparing my dissertation in the physics Department at Utah State University. I hope to complete it in the Spring of 2010.

I am requesting your permission to include the attached material as shown. I will include acknowledgements and/or appropriate citations to your work as shown and copyright and reprint rights information in a special appendix. The bibliographical citation will appear at the end of the manuscript as shown. Please advise me on any changes you require.

Please indicate your approval of this request by signing in the space provided, attaching any other form or instruction necessary to confirm permission. If you charge a reprint fee for use of your material, please indicate this as well. If you have any questions, please contact me at the number above.

I hope you will be able to reply immediately. If you are not the copyright holder, please forward my request to the appropriate position or institution.

Thank you for your cooperation.

Matthew Bailey

I hereby give permission to Matthew Bailey to reprint the following material in his dissertation.

Gerken, E.A., Inan, U.S., and Barrington-Leigh, C.P. (2000), Telescopic imaging of sprites, *Geophys. Res. Lett., 27*, 2637-2640: Figure 1.

Name: _____ Date: 3-2-10

Elizabeth Kendall (nee Gerken)

March 2, 2010

Matthew Bailey
Center for Atmospheric and Space Sciences
Department of Physics
4405 Old main Hill
Logan, UT 84322-4405
(860) 297 5103

Dear Dr. Hu,

I am in the process of preparing my dissertation in the physics Department at Utah State University. I hope to complete it in the Spring of 2010.

I am requesting your permission to include the attached material as shown. I will include acknowledgements and/or appropriate citations to your work as shown and copyright and reprint rights information in a special appendix. The bibliographical citation will appear at the end of the manuscript as shown. Please advise me on any changes you require.

Please indicate your approval of this request by signing in the space provided, attaching any other form or instruction necessary to confirm permission. If you charge a reprint fee for use of your material, please indicate this as well. If you have any questions, please contact me at the number above.

I hope you will be able to reply immediately. If you are not the copyright holder, please forward my request to the appropriate position or institution.

Thank you for your cooperation.

Matthew Bailey

I hereby give permission to Matthew Bailey to reprint the following material in his dissertation.

Hu W., S.A. Cummer, W.A. Lyons, and T. Nelson (2002), Lightning charge moment changes for the initiation of sprites, *Geophys. Res. Lett., 29*(8), 1279, doi:10.1029/2001GL014593: Figure 6.

Name: Wenyi Hu Date: 03/04/2010

I hereby give permission to Matthew Bailey to reprint the following material in his dissertation.

Barrington-Leigh, C. P., U. S. Inan, and M. Stanley (2001), Identification of sprites and elves with intensified video and broadband photometry, *J. Geophys. Res.*, *106*, 1741 – 1750: Figure 1, Plate 6c.

Barrington-Leigh, C. P., U. S. Inan, M. Stanley and S. A. Cummer (1999), Sprites triggered by negative lightning discharges, *Geophys. Res. Lett., 26*, 3605-3608: Figures 2c, 3b.

Name: ___C P Barrington-Leigh _____ Date: _____ 04 March 2010

C P Barrington-Leigh

March 26, 2010

Matthew Bailey
Center for Atmospheric and Space Sciences
Department of Physics
4405 Old main Hill
Logan, UT 84322-4405
(860) 297 5103

Dear Dr. Pessi

I am in the process of preparing my dissertation in the physics Department at Utah State University. I hope to complete it in the Spring of 2010.

I am requesting your permission to include the attached material as shown. I will include acknowledgements and/or appropriate citations to your work as shown and copyright and reprint rights information in a special appendix. The bibliographical citation will appear at the end of the manuscript as shown. Please advise me on any changes you require.

Please indicate your approval of this request by signing in the space provided, attaching any other form or instruction necessary to confirm permission. If you charge a reprint fee for use of your material, please indicate this as well. If you have any questions, please contact me at the number above.

I hope you will be able to reply immediately. If you are not the copyright holder, please forward my request to the appropriate position or institution.

Thank you for your cooperation.

Matthew Bailey

I hereby give permission to Matthew Bailey to reprint the following material in his dissertation.

Pessi, A.T., S. Businger, K.L Cummins, N.W.S. Demetriades, M. Murphy, and B. Pifer (2008), Development of a long-range lightning detection network for the pacific: construction, calibration, and performance, *Journal of Atmospheric and Oceanic Technology,* doi: 10.1175/2008JTECHA1132.1: Figure 1.

Name: Antti Pessi Date: 4/1/10

Antti Pessi

CURRICULUM VITAE

Matthew A. Bailey
832 Prospect Street
Wethersfield, CT 06109
matthew.bailey@trincoll.edu
Work Phone (860) 297-5103

EDUCATION

Utah State University, Logan, UT

Doctor of Philosophy, Physics, May, 2010

- Dissertation: Investigating Characteristics of Lightning-Induced Transient Luminous Events over South America

Bachelor of Science, Civil Engineering, May 1998

PROFESSIONAL ORGANIZATIONS

American Geophysical Union

American Association of Physics Teachers

PROFESSIONAL EXPERIENCE

Teaching

Trinity College, Hartford, Connecticut

Visiting Assistant Professor, July 1, 2008 – June 15, 2010

- *Phys 101* (Principles of Physics 1), Fall 2008, Fall 2009. Algebra-based course covering basic mechanics, geared toward Life Science majors. Class includes lab component. Responsible for designing syllabus, preparing lectures, assigning and grading homework, creating and grading exams, designing and teaching labs, office hours, and review sessions. Textbooks: "Physics", Walker, 3rd Edition (2008); "College Physics, a Strategic Approach", Knight, Jones, and Field, 1st. Edition (2009).

- Phys *102* (Principles of Physics 2), Spring 2009, Spring 2010. Second part of algebra-based course covering thermodynamics, electromagnetism, optics, and modern physics, geared toward life science majors. Class includes lab component. Responsible for designing syllabus, preparing lectures, assigning and grading homework, creating and grading exams, designing and teaching labs, office hours, and review sessions. Textbooks: "Physics", Walker, 3rd Edition (2008); "College Physics, a Strategic Approach", Knight, Jones, and Field, 1st. Edition (2009).

- Physics 108, (Energy and Society), Spring 2010. One-term general science course geared toward non-science majors. Textbook: "Energy, its Use and the Environment", Hinrichs and Kleinbach, 4th Edition.

- Physics 490 (Research Assistantship), Fall 2009, Spring 2010. Oversee student research dealing with Transient Luminous Events, and using video data and computer programming to quantify the location and extent of these events.

Utah State University, Logan, UT

- *SCI 4300* (Science and Technology in Society), taught Spring 2006, Spring 2007, and Fall, 2007. Course geared toward Secondary Education Science Majors. Responsible for: Designing syllabus, choosing textbook, preparing lectures, evaluating course design, grading homework, creating and grading exams, helping students with individual projects, and overseeing class project.
    - Individual projects consisted of students picking a topic that is "controversial" in our society, related to science or technology (Examples: Global Warming, Abortion, Space Exploration), doing research, writing a paper, and giving a presentation in class.
    - Class project consisted of class picking a topic related to science and technology in society (Example, Fall 2007 class picked bio-fuels), then working in groups to do research on the subject. The students were encouraged to interview local experts in the community. Class periods were set aside to debate points and discuss what students had learned, and to plan new aspects of research. At the end of the project each class member was required to write a letter to a public figure or official related to the topic, expressing their views on the subject.
    - Textbook: "Taking Sides; Clashing Views on Controversial Issues in Science, Technology, and Society", *Thomas A. Easton*, Sixth Edition.

- *PHYS 2100* (Physics of Life Science), Fall 2005. Algebra-based course for Life Sciences Majors. Class included lectures, labs, and recitations. Responsible for: Overseeing large class (180 students), preparing lectures, assigning homework, creating and grading exams, conducting office hours, working with and managing graduate teaching assistants. Textbook: "Physics", *Cutnell and Johnson*, Seventh Edition.

- *PHYS 2200/2210* (Elements of Mechanics). Spring 2004. Calculus-based course for Engineers/Physical Scientists/Pre-Med. Class included lectures, labs, and recitations. Responsible for: Overseeing large class (160 students), preparing lectures, assigning homework, creating and grading exams, conducting office hours, working with and managing graduate teaching assistants. Textbook: "Principles of Physics", *Serway and Jewett*, Third Edition.

- *PHYS 2220* (Elements of Mechanics II). Summer 2002, Summer 2003. Calculus-based course designed for Engineers. Class included lectures, labs, and recitations. Responsible for: Preparing lectures, assigning and grading homework, creating and grading exams, conducting office hours. Textbook: "Principles of Physics", *Serway and Jewett*, Third Edition.

Teaching Assistant

- *PHYS 2200/2210* (Elements of Mechanics), assisted for seven semesters. Responsible for: Teaching laboratories, holding weekly recitation sessions to help with homework, grading homework, tests, and being available for optional study hall.

- *USU 1800* (Study of Energy), assisted for one semester. Responsible for: Meeting with students to discuss class projects, grading projects, teaching class when professor absent, grading exams.

Research

Trinity College (Hartford, CT)

- Video Analysis of Transient Luminous Events (TLEs). This includes video calibration, and data processing to determine location, azimuth, size and height of TLEs.

- Coordination of coincident radio data from Duke University, and satellite data from the University of Washington.

- Working with undergraduates to do this type of video analysis (starting Fall, 2009). Two data sets are being investigated, one over South America, and one over Colorado.

Utah State University, (Logan, UT),

- Participation in USU collaboration with University of Washington, Duke University, Brazilian Institute of Space Sciences (INPE) field campaigns in Brazil, Fall 2003, Spring 2006; Colorado, Summer 2005.

- Responsibilities:
  - Using Low Light Level Video Cameras for night observations TLEs that occur over large thunderstorms.
  - After video capture, image calibration and data processing to determine location, azimuth, size, and height of TLEs.
  - Detailed coordination with ULF/VLF data from Duke University, and satellite data from University of Washington, to determine TLE relationships with causative lightning and parent thunderstorms.

- Working with undergraduate researchers at USU.
  - Responsibilities include overseeing students work, coordinating weekly work schedules, and overseeing analysis and publication of results.

PUBLICATIONS AND PRESENTATIONS

Refereed Publications

- "Rare Measurements of a Sprite-Halo Driven by a Negative Lightning Discharge over Argentina", M.J. Taylor, ***M.A. Bailey***, P.D. Pautet, S.A. Cummer, N. Jaugey, J.N. Thomas, N.N. Solorzano, F. Sao Sabbas, R.H. Holzworth, O. Pinto, and N.J. Schuch, *Geophys. Res. Lett., 35,* L14812, doi:10.1029/2008GL033984.

- "A very active sprite-producing storm observed over Argentina", J.N. Thomas, M.J. Taylor, P.D. Pautet, ***M.Bailey***, N.N. Solorzano, R.H. Holzworth, M.P. McCarthy, M.Kokorowski, F. Sao Sabbas, O.Pinto Jr., S. A. Cummer, N. Jaugey, J. Li, and N.J. Schuch, *EOS*, 88(10), 117 - 119, 2007.

Manuscripts in Review

- "Sprites2006 campaign in Brazil: Some convective characteristics of the third worldwide most prolific TLE producing convective system", F.T. Sao Sabbas, M.J.Taylor, P.D. P.D. Pautet, ***M.A. Bailey***, R.H. Holzworth, S.A.Cummer, R.R. Azambuja, J.N. Thomas, O. Pinto, N.N. Solrzano, and N.J. Schuch, *Journal of Geophysical Research*, submitted March, 2010.

- Two, first author papers in preparation, "Negative Sprite-Halo events seen over South America" (*Journal of Geophysical Research*) and "Measured Halo Characteristics over an Argentinean Storm" (*Geophysical Research Letters*), submissions May. 2010/June. 2010.

Conference Presentations

- "Investigating Halo Optical Signatures and Associated Lightning Parameters from a Large MCS over Argentina" ***M.A. Bailey***, M.J. Taylor, P.D. Pautet, S.A. Cummer, J.N. Thomas, R.W. Holzworth, American Geophysical Union (AGU) Chapman Conference, State College, PA, May 2009.

- "Characterizing lightning-driven negative transient luminous events over an intense South America storm", ***M.A. Bailey***, M. J. Taylor, P.D. Pautet, S.A. Cummer, N. Jaugey, J.N. Thomas, Oral Presentation, American Geophysical Union (AGU) Meeting, San Francisco, CA, Dec. 2008.

- "Quantifying positive and negative sprite-halo events over Northern Argentina", ***M.A. Bailey***, M. J. Taylor, P.D. Pautet, S.A. Cummer, N. Jaugey, J.N. Thomas, R.H. Holzworth, poster and presentation, CEDAR (Coupling, Energetics and Dynamics of Atmospheric Regions) meeting, Midway, UT, June, 2008.

- "Very active sprite-producing thunderstorms observed over Argentina and Brazil", J.N. Thomas, M.J. Taylor, ***M.A. Bailey***, S.A. Cummer, N.N. Solorzano, F. Sao Sabbas, P.D. Pautet, R.H. Holzworth, N. Jaugey, J. Li, M.P. McCarthy, M. Kokorowski, O. Pinto Jr., and N.J. Schuch, invited talk, URSI (Union Radio-Scientifique Internaionale), Boulder Colorado, January 2008.

- "Sprite Halos and Associated Lightning Characteristics over South America", Poster Presentation, ***M*.A. Bailey**, M.J. Taylor, S.A. Cummer, N. Jaugey, J.N. Thomas, R.H. Holzworth, American Geophysical Union (AGU) meeting, San Francisco, CA, Dec 2007.

- "Very active sprite-producing thunderstorms observed over Argentina and Brazil", J.N. Thomas, M.J. Taylor, ***M.A. Bailey***, S.A. Cummer, N.N. Solorzano, F. Sao Sabbas, P.D. Pautet, R.H. Holzworth, N. Jaugey, J. Li, M.P. McCarthy, M. Kokorowski, O. Pinto Jr., and N.J. Schuch, talk, URSI North American Radio Science Meeting, Ottowa, Canada, July 2007.

- "Investigating Sprite Halo Optical Signatures and Associated Lightning Characteristics over South America", ***M.A. Bailey***, M.J. Taylor, P.D. Pautet, S.Cummer, N. Jaugey, and J.N. Thomas, presented poster, CEDAR (Coupling, Energetics and Dynamics of Atmospheric Regions) meeting, Santa Fe, New Mexico, June, 2007.

- "Infrared Imaging of Transient Luminous Events (1 - 1.5 micrometers) Over the Midwestern US and Comparison with Their Visible Wavelength signatures", ***M.A. Bailey***, M.J. Taylor, P.D. Pautet, W. Lyons, and S.A. Cummer, presented poster, CEDAR meeting, Santa Fe, NM, June, 2006.

AWARDS AND RECOGNITIONS

- First Place, student poster presentation, Atmospheric and Space Electricity section, American Geophysical Union Conference, San Francisco, CA, 2007.
- First Place, Oral Presentation, Graduate Research Symposium, science section, Utah State University, Oct., 2007.
- Graduate Teacher of the Year, Utah State University College of Science, 2007.
- Robins Award Nominee (Utah State University), Graduate Teacher of the year, 2007.
- Teaching Assistant of the Year, Utah State University Physics Department, 2005.